Interactions between the Nrf2 antioxidant response and mammalian iron homeostasis

Pei Jin Lim

Lincoln College
&
MRC Weatherall Institute of Molecular Medicine

Supervisor: Professor Hal Drakesmith



Thesis submitted for the degree of
Doctor of Philosophy
University of Oxford
Trinity Term 2017

Acknowledgements

I am extremely grateful to the following people and organisations, without which my DPhil journey would not be such a memorable, enlightening and mostly enjoyable one:

My supervisor **Professor Hal Drakesmith**: for his guidance in science, enlightenment in life, encouragement in tough times, provision of many opportunities and critical review of this thesis.

Dr Tiago Duarte: for the fantastic collaboration and his contribution to many parts of this thesis, enthusiasm in science, and impartment of knowledge on Nrf2 and oxidative stress.

My lab colleagues – **Dr Andrew Armitage**: for his scientific inputs, help with performing and guidance with analysis of experiments, advice on life and exposure to many sporting events; **Dr Sant-Rayn Pasricha**: for constructive criticism and guidance in science, help with conducting experiments and sharing his life experiences; **Dr Sarah Gooding**: for sharing her perspectives from a clinical point of view; **Kate Wray**: for always motivating me to stay fit; **Joe Frost**: for his infectious enthusiasm in Biology, help with experiments and for proof-reading parts of this thesis; **Dr João Arezes**: for his scientific inputs, help with experiments, introduction to Lab Wars and supply of Port wine; **Dr Kirsty McHugh**: for her bubbly and straightforward personality and advice on life; **Dr Kinda Al-Hourani**: for helping me settle into Oxford, her family for their warm welcome during my first Christmas away from home, her positivity in life and her life-long friendship.

Professor Graça Porto: for her expertise and help with the Hfe-haemochromatosis patient experiment.

Dr Jodie Babitt and **Dr Chia-Yu Wang**: for their help in performing LSEC experiments.

Dr Liz Soilleux: for her assistance in imaging histology slides.

Prof Jim Hughes, **Ron Schwessinger** and **Matt Gosden**: for their help with chromosome biology experiments and computational biology.

Prof Alain Townsend: for his insights and feedback at thesis committee meetings, and his encouragement in doing hypothesis-driven science.

The support staff – the BMS staff for animal husbandry and technical help; the WIMM canteen staff who are the fuel of cutting edge science by making the best lunches in the world; the WIMM IT staff for making our computers run smoothly.

Radcliffe Department of Medicine: for funding my studies.

Lincoln College: for providing a platform through which I met people from all walks of life and made many wonderful memories with friends from around the world, and the generosity with the annual funding to attend conferences; my college friends with whom I share memorable road trips around the UK and pub crawls.

My Singaporean buddies for being my source of emotional support away from home and being ever-ready to gastronomically indulge ourselves together.

Dr Michael Brand: for his constant encouragement and reassurance every day, and for taking this roller coaster ride with me.

My dearest family: who I love and miss every day, especially **Daddy** who quietly offers his utmost support and **Mummy** who was the first to show me the world of Biology. Thank you for showing me the principles of life and providing me with a well-rounded education.

Declaration of authorship

The majority of the work presented in this thesis was developed and performed by myself under the supervision of Professor Hal Drakesmith at the Weatherall Institute of Molecular Medicine, University of Oxford. Experiments performed by our collaborators were conceptualised and analysed as a joint effort and are clearly indicated in the thesis. No part of this thesis has been submitted for examination for a degree at this or any other university.

Pei Jin Lim

5th September 2017

Abstract

Iron is an essential micronutrient as it contributes to the oxygen-carrying capacity of blood and is a cofactor for many enzymes. However, excess iron is toxic as it promotes the formation of reactive oxygen species (ROS), which react with and alter the functions of biomolecules. Moreover, there is no regulated iron excretion mechanism from our body. Hence, iron homeostasis is tightly regulated by the hormone hepcidin that restricts iron absorption and controls iron distribution in the body. Accumulation of iron in the liver increases the expression of bone morphogenetic protein-6 (*Bmp6*), which induces hepcidin synthesis via Bmp responsive elements in the hepcidin promoter. The mechanism by which excess iron is 'sensed', leading to increased *Bmp6*, is unknown. Since excess iron induces oxidative stress, we hypothesized that *Bmp6* expression is upregulated during iron-overload via the Nrf2-driven antioxidant response pathway. Nrf2 is a transcriptional activator that is activated by oxidative stimuli and binds to antioxidant responsive elements (AREs) to induce the expression of a battery of ARE-regulated antioxidant genes. Bach1 is a transcriptional repressor that binds AREs and suppresses gene expression. Haem can induce the degradation of Bach1 and derepress the expression of ARE-regulated genes. In this thesis, we demonstrated the simultaneous induction of *Bmp6* and classical Nrf2/ARE-driven genes in mice and cell lines by iron and hemin (haem-chloride). ChIP-sequencing analyses showed binding of Nrf2 to a conserved ARE within intron 1 of *Bmp6*. The antioxidant mitoTEMPO blunted the activation of Nrf2 and upregulation of *Bmp6* by iron. Furthermore, siRNA-mediated knockdown of *Nrf2* decreased basal *Bmp6* expression and inhibited the upregulation of *Bmp6* by iron *in vitro*, whereas knockdown of *Bach1* increased *Bmp6* expression. Similarly, the upregulation of *Bmp6* and hepcidin expression was blunted or completely abrogated in several models of iron overloading in *Nrf2*-knockout mice. *Nrf2*-knockout mice were more prone to iron accumulation and susceptible to oxidative stress-induced liver damage. Deletion of *Nrf2* in *Hfe*-knockout haemochromatosis mice, and a SNP associated with reduced *NRF2* expression in *HFE*-hereditary haemochromatosis patients, worsened the iron accumulation phenotype; conversely, pharmacological activation of Nrf2 upregulated the *Bmp6*/hepcidin axis and alleviated iron accumulation and oxidative stress in *Hfe*-knockout mice. In summary, Nrf2 links cellular and systemic iron homeostasis, is required for the upregulation of *Bmp6* by iron, and is an important modifier and therapeutic target for iron overload disorders.

Abbreviations

ARE	Antioxidant Response Element
BMP/Bmp	Bone Morphogenetic Protein
CDDO-Im	1-(2-cyano-3,12-dioxooleana-1,9-dien-28-oyl) imidazole
ChIP-seq	Chromatin Immunoprecipitation-sequencing
CI	Carbonyl iron
DMEM	Dulbecco's Modified Eagles' Medium
FAC	Ferric Ammonium Citrate
FBS	Fetal Bovine Serum
FeDx	Iron-dextran
Gclc	Glutamate-cysteine ligase catalytic subunit
Hamp1/*HAMP*	Hepcidin
Hmox1	Heme oxygenase 1
Id1	Inhibitor of DNA binding 1
IRE	Iron Regulatory Element
IRP	Iron Regulatory Protein
LSEC	Liver Sinusoidal Endothelial Cell
mRNA	Messenger ribonucleic acid
Nfe2l2/Nrf2	Nuclear factor (erythroid-derived 2)-like 2
Nqo1	NAD(P)H dehydrogenase, quinone 1
NTC	Non-targeting control
ppm	Parts per million
qRT-PCR	Quantitative reverse transcription real-time polymerase chain reaction
ROS	Reactive Oxygen Species
siRNA	Short interfering ribonucleic acid
Slc40a1	Ferroportin
SMAD/Smad	Sons of mothers against decapentapleg

Table of content

Acknowledgements ..... **i – ii**

Declaration of authorship ..... **iii**

Abstract ..... **iv**

Abbreviations ..... **v**

Table of content ..... **vi – ix**

1 Introduction ..... **1 – 32**

1.1 The importance of iron homeostasis ..... **2 – 19**

1.1.1 Systemic iron homeostasis is regulated by the hepcidin-ferroportin axis ..... 3 – 6

1.1.2 Non-systemic roles of hepcidin-ferroportin axis ..... 7 – 8

1.1.3 Regulation of hepcidin expression ..... 8 – 13

1.1.4 Control of intracellular iron homeostasis ..... 14 – 16

1.1.5 Iron disorders ..... 17 – 19

1.2 The Nrf2 antioxidant response system ..... **20 – 30**

1.2.1 Regulation of Nrf2 activity in response to oxidative stress ..... 21 – 25

1.2.2 Nrf2 in cellular protection and health ..... 25 – 27

1.2.3 Nrf2 in intracellular iron homeostasis 27

1.2.4 NF-E2, Nrf1 and Nrf3 transcriptional activators ..... 28 – 29

1.2.5 Bach1 and Bach2 transcriptional repressors ..... 29 – 30

1.3 Aims of project ..... **31 – 32**

2 Materials and Methods ..... **33 – 43**

2.1 Mice breeding and husbandry ..... **34 – 35**

2.2 Mice genotyping ..... **35 – 37**

2.2.1 *Nrf2*-knockout mice genotyping 36

2.2.2 *iNOS*-knockout mice genotyping 36

2.2.3 i*Hamp1*-knockout mice genotyping 37

2.3 *In vivo* treatments ..... **37 – 38**

2.4 Cell cultures and *in vitro* treatments ..... **38 – 39**

2.5 Gene expression analysis by quantitative real time PCR (qRT-PCR) ..... **39 – 42**

2.6 Western blot **42**

2.7 Tissue non-haem iron measurement **42**

2.8 Tissue histology ..... **42 – 43**

2.9 Liver malondialdehyde (MDA) 43
2.10 Serum measurements 43
2.11 Statistics 43

3 Iron and hemin alter the Bmp6/hepcidin axis and activate Nrf2 ..... 44 – 67
3.1 Background ..... 45 – 50
3.1.1 Hepatic *Bmp6* expression fluctuates with alterations in iron status 45
3.1.2 Iron and haem activates the Nrf2 antioxidant response pathway ..... 45 – 47
3.1.3 Chapter aims 47
3.1.4 Methodology ..... 48 – 50
3.2 Results ..... 51 – 63
3.2.1 Dietary iron upregulates *Bmp6* expression and activates Nrf2 in purified liver sinusoidal endothelial cells 51
3.2.2 Iron upregulates *Bmp6* expression and Nrf2 activity simultaneously *in vitro* in L929 cells ..... 52 – 54
3.2.3 Hepatic iron accumulation simultaneously upregulates *Bmp6* and hepcidin and enhances Nrf2 activity *in vivo* ..... 55 – 58
3.2.4 Hemin upregulates *Bmp6* expression, degrades Bach1 and activates Nrf2 ..... 59 – 61
3.2.5 Effects of iron and hemin on the endogenous expression of *Bmp2* and *Bmp4* ..... 62 - 63
3.3 Discussion ..... 64 – 67

4 Nrf2 regulates *Bmp6* expression in response to iron and haem ..... 68 – 109
4.1 Background ..... 69 – 76
4.1.1 *Bmp6* induction is associated with Nrf2 activation in response to iron 69
4.1.2 Regulation of Nrf2 in response to physiological perturbations ..... 69 – 71
4.1.3 Chapter aims 72
4.1.4 Methodology ..... 73 – 76
4.2 Results ..... 77 – 104
4.2.1 Nrf2 binds in proximity to the *Bmp6* promoter 77
4.2.1.1 Nrf2 ChIP-sequencing ..... 77 – 79
4.2.1.2 C2C12 and MEF induce *Bmp6* expression in response to ferric ammonium citrate ..... 79 – 80
4.2.2 Alterations in the Nrf2/Bach1 axis affects baseline *Bmp6* expression 80
4.2.2.1 siRNA-mediated knockdown of *Nrf2*, *Keap1* and *Bach1* alters *Bmp6* expression ..... 80 – 87

4.2.2.2 Small molecule Nrf2 agonists upregulate *Bmp6* expression *in vitro*...87 – 89
4.2.2.3 CDDO-Im upregulates *Bmp6* expression in an Nrf2-dependent manner *in vivo* ..... 89 – 90
4.2.3 Nrf2 controls the upregulation of *Bmp6* in response to iron 90
4.2.3.1 siRNA-mediated knockdown of *Nrf2* blocks the induction of *Bmp6* by iron ..... 90 – 93
4.2.3.2 Induction of *Bmp6* by iron and hemin is blunted in *Nrf2*-knockout mice .... 93 – 98
4.2.4 Mechanism of Nrf2 activation by iron 98
4.2.4.1 Nrf2 mRNA is not consistently upregulated in response to iron and hemin .. .. 98 – 99
4.2.4.2 Iron activates Nrf2 and upregulates *Bmp6* via induction of oxidative stress .. .. 99 – 101
4.2.4.3 Activation of Nrf2 by iron is independent of inducible nitric oxide synthase .....102 – 104
4.3 Discussion ..... 105 – 109

5 Regulation of iron homeostasis and haemochromatosis by Nrf2 ..... 110 – 142
5.1 Background ..... 111 – 117
5.1.1 Disruption of hepcidin synthesis causes dysregulation of iron homeostasis and iron disorders ..... 111 – 112
5.1.2 Hepcidin as a therapeutic target for ameliorating HFE-haemochromatosis .... 112 – 113
5.1.3 Chapter aims 113
5.1.4 Methodology..... 113 – 117
5.2 Results ..... 118 – 137
5.2.1 *Nrf2*-knockout mice have dampened iron-induced hepcidin response, enhanced iron accumulation and more oxidative damage ..... 118 – 121
5.2.2 Hepcidin is not a direct target of Nrf2 ..... 121 – 124
5.2.3 Nrf2 deficiency worsens haemochromatosis ..... 125 – 129
5.2.4 Pharmacological Nrf2 activation protects *Hfe*-knockout haemochromatosis mice against iron loading .....130 – 137
5.3 Discussion ..... 137 – 143

6 Summary and future perspectives ..... 144 – 152
6.1 Summary ..... 145 – 148
6.2 Future perspectives ..... 148 – 152

6.2.1 Therapeutic potential of Nrf2 activation in iron overload disorders ..... 148 – 149
6.2.2 The role of Nrf2 and Bach1 in non-hepatic tissues in regulating iron homeostasis ..... 149 – 151
6.2.3 The role of Nrf2 in microbial infections ..... 151 – 152
6.3 Final statement 152

Supplementary data ..... 153 – 155
References ..... 156 – 169

Chapter 1

Introduction

1.1 The importance of iron homeostasis

Iron is an essential micronutrient for life. It facilitates the oxygen-carrying capacity of erythrocytes in blood and serves as a cofactor for enzymes involved in many processes in cellular physiology, such as cytochrome c reductase in oxidative phosphorylation and ribonucleotide reductase in the synthesis of deoxyribonucleotides for DNA replication. The ability of iron to act as an enzymatic cofactor by facilitating the transfer of electrons and to associate with oxygen molecules stems from its ability to exist in two oxidation states. However, this exact same property contributes to the toxicity of iron as it makes iron highly redox-active and allows free iron to catalyse the formation of reactive oxygen species (ROS) and reactive nitrogen species (RNS) when in excess. ROS and RNS in turn causes DNA oxidative damage and lipid peroxidation, leading to aberrant changes to their structure and functions (Jomova and Valko, 2011; Koskenkorva-Frank et al., 2013). In addition, iron overload has been associated with increased infection risk since iron is also required for the survival and growth of microorganisms (reviewed by Drakesmith and Prentice, 2012; Weinberg, 1999). Infections by microorganisms, such as *Vibrio vulnificus*, *Yersinia enterocolitica* and *Salmonella typhimurium*, also lead to poorer clinical outcomes in iron-overloaded haemochromatosis patients (reviewed by Khan et al., 2007). On the contrary, restricting microorganism's access to iron results in diminished microbial growth and improved survival of host (Arezes et al., 2015; Nairz et al., 2013).

Since iron is necessary for most forms of life, yet too much iron can present problems to the body, the amount and distribution of iron in our body must be tightly regulated in order to strike a favourable balance. This is achieved at the cellular level via mechanisms involving the iron regulatory proteins and iron response element (IRP/IRE) system (Muckenthaler et al., 2008) and systemically by the liver-expressed hormone hepcidin (Ganz, 2013). In fact, due to the demand for iron by both hosts and pathogens, hepcidin is a micronutrient hormone that responds to both infection and iron status of an organism.

1.1.1 Systemic iron homeostasis is regulated by the hepcidin-ferroportin axis

The average human adult body contains three to four grams of iron. Systemic iron homeostasis is regulated through the control of dietary iron absorption, iron recycling from erythrocytes by red pulp macrophages in the spleen and iron export from the liver. Each day, approximately one milligram of iron is absorbed from our diet as haem or non-haem inorganic iron.

Dietary non-haem iron exists as ferric Fe^{3+} iron, and is reduced to ferrous Fe^{2+} iron by the duodenal cytochrome B DCYTB (McKie et al., 2001) before being taken up by the enterocyte via the divalent metal transporter 1 (DMT1, also known as divalent cation transporter 1 DCT1, encoded by *SLC11A2* gene) at the apical membrane (Gunshin et al., 1997). Within enterocytes, iron is trafficked via currently undefined mechanisms from the apical to the basolateral membrane, where it is exported out of the enterocytes into the plasma circulation via ferroportin (also known as iron-regulated transporter 1 IREG1, encoded by *SLC40A1*), the only known mammalian iron export protein (McKie et al., 2000). The iron is then oxidised to Fe^{3+} ferric iron by hephaestin (Vulpe et al., 1999), bound by plasma transferrin and circulates around the body to deliver iron to other tissues, such as the bone marrow for erythropoiesis. Iron that is not exported from enterocytes into the plasma via ferroportin is stored safely as a catalytically inactive form intracellularly within ferritin proteins (Vanoaica et al., 2010) until it is lost through duodenal epithelial shedding.

The absorption of haem by enterocytes is poorly understood and was thought to be facilitated through haem carrier protein 1 HCP1 (Le Blanc et al., 2012; Shayeghi et al., 2005). HCP1 was subsequently found to have a much higher affinity for folate and was renamed proton coupled folate transporter PCFT. Loss of function mutation in HCP1/PCFT led to folate malabsorption in humans and *HCP1*/*PCFT*-knockout mice have folate deficiency but normal levels of serum haem and iron content (Qiu et al., 2006; Salojin et al., 2011). Thus, the physiological relevance of HCP1 in regulating haem absorption remains controversial, and the mechanism of dietary haem uptake remains to be studied. Intracellular haem can either be converted to iron, bilirubin and carbon monoxide via heme oxygenase 1, where the iron is exported out of enterocytes via ferroportin, or

possibly exported out of the cell into the plasma via the Feline Leukemia Virus subgroup C Receptor FLVCR1a (Keel et al., 2008), where it is bound by hemopexin.

In addition to dietary iron absorption, our body recycles about 25mg of iron from erythrocytes per day. In fact, majority of our systemic demand for iron is met through iron recycling. Macrophages phagocytose damaged or senescent erythrocytes and break down haemoglobin to release iron (Ganz, 2012). The iron can be recycled back into plasma circulation via ferroportin (Zhang et al., 2012) and the ferroxidase ceruloplasmin (Harris et al., 1999), which is then used for erythropoiesis to make new red blood cells.

The liver is the major storage site of iron in our body. Iron sequestered in the liver can be mobilized via ferroportin when the demand arises (Ramey et al., 2010; Zhang et al., 2012), such as to cope with increased erythropoiesis after excessive bleeding (Barton, 2007; Beguin et al., 1989).

Since there is no known mechanism of iron excretion in our body that is physiologically regulated, dietary iron absorption at the enterocytes must be regulated to ensure a tight balance in the amount of iron in our body. The distribution of iron within the body must also be tightly regulated to ensure sufficient levels for erythropoiesis at the bone marrow yet avoiding the toxicity of excess iron in circulation. Hepcidin, encoded by *HAMP* gene in humans and *Hamp1* in mice, is the hormone that controls iron levels and distribution in our body. It was first discovered in the blood ultrafiltrate and urine by three independent groups of researchers (Krause et al., 2000; Park et al., 2001; Pigeon et al., 2001). The term hepcidin was coined as it is predominantly expressed in the liver (hep-) and appeared to have bactericidal and fungicidal activity (-cidin). It was previously also known as liver-expressed antimicrobial peptide (LEAP-1) although it is now more commonly known as hepcidin. Notably, Pigeon and colleagues were the first to identify hepcidin as an iron-induced gene in the liver of mice fed a high iron diet by performing subtractive hybridisation. An increase in hepatic iron content upregulates the expression of Bone Morphogenetic Protein-6 (BMP6) which then activates the BMP/SMAD signalling pathway to enhance hepcidin expression. In addition, the liver also senses

an increase in transferrin saturation via the transferrin receptor TFR2 and haemochromatosis protein HFE to activate the BMP/SMAD signalling pathway and enhance hepcidin expression (see Chapter 1.1.3 for details on regulation of hepcidin expression). Hepcidin is secreted from the liver into the plasma circulation, then binds to ferroportin on enterocytes, macrophages and hepatocytes. Hepcidin induces the internalisation and degradation of ferroportin (Nemeth et al., 2004a), thereby restricting dietary iron absorption by the enterocytes and iron recycling by the macrophages, and retains iron storage in the liver. This regulation of systemic iron homeostasis is summarised in Figure 1.1.

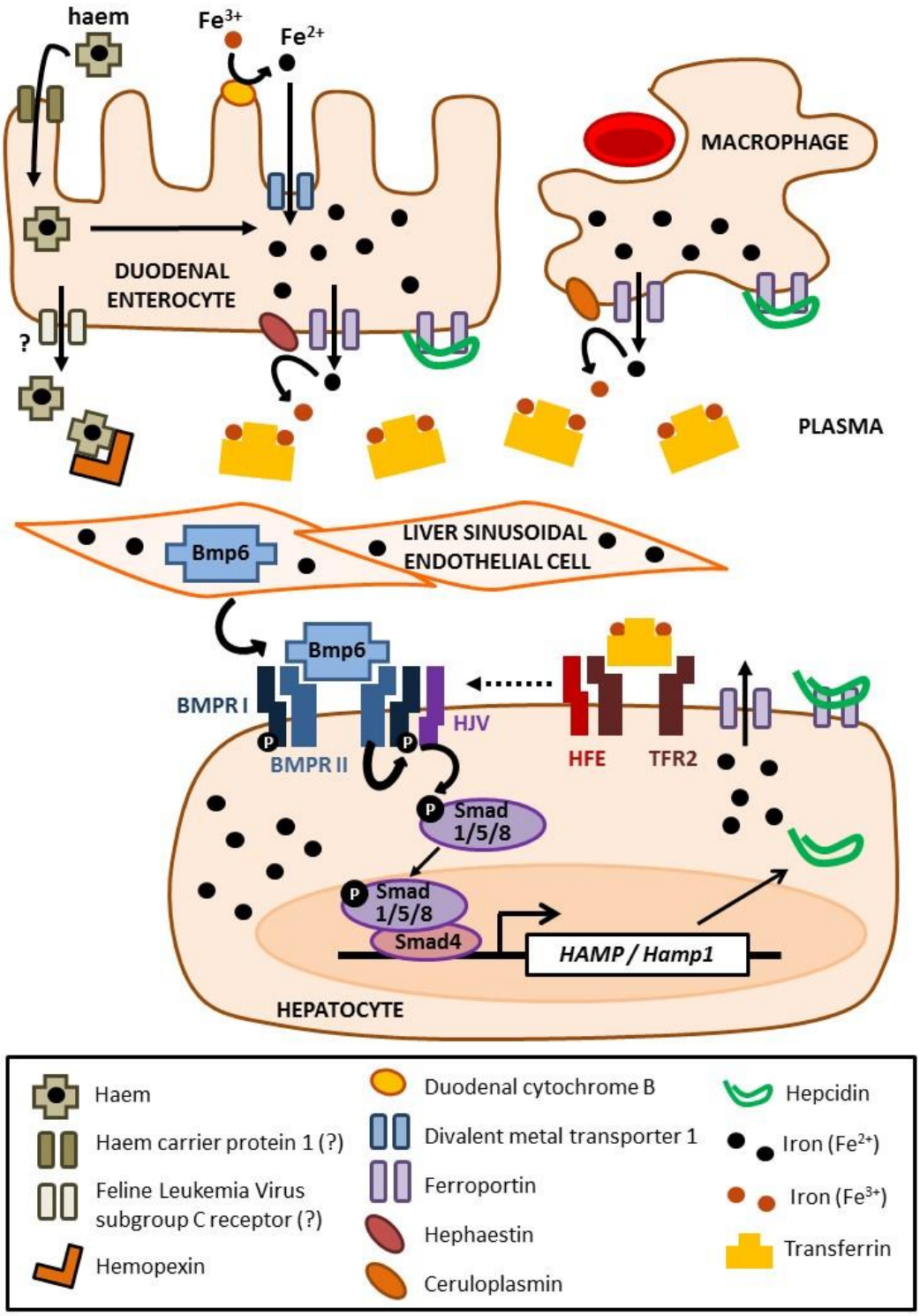


Figure 1.1: Graphical summary of systemic iron homeostasis. At the enterocytes, haem iron is absorbed from our diet, possibly via haem carrier protein 1 and exported via Feline Leukemia Virus subgroup C Receptor or degraded by heme oxygenase 1 to release iron. Dietary non-haem iron is reduced by duodenal cytochrome B and taken up by the enterocytes via divalent metal transporter 1. Iron is exported from the enterocytes into plasma via ferroportin and oxidised to the ferric form by hephaestin. Macrophages engulf damaged or senescent erythrocytes to recycle iron from haemoglobin back to the plasma via ferroportin. In the plasma, haem is bound by hemopexin while iron is bound by transferrin and delivered to other tissues. Hepatocytes sense increases in tissue iron and transferrin saturation and upregulate hepcidin expression via BMP/SMAD signalling pathway. Hepcidin induces the degradation of ferroportin to block dietary iron uptake and iron recycling.

1.1.2 Non-systemic roles of hepcidin-ferroportin axis

In systemic iron homeostasis, ferroportin regulates iron export from duodenal enterocytes, splenic red pulp macrophages and the liver for dietary absorption, recycling and mobilisation. However, ferroportin is also expressed in other tissues such as the lung and the heart. In addition, hepcidin can also be expressed in these tissues, albeit in much lower levels compared to the liver, suggesting that the hepcidin-ferroportin axis may have a non-systemic role by regulating local tissue iron homeostasis.

In a mouse model of cardiomyocyte-specific ferroportin deletion, iron accumulation was observed in the cardiomyocytes and associated with cardiac dysfunction and increased mortality (Lakhal-Littleton et al., 2015). On the opposite end of the spectrum, cardiomyocyte-specific deletion of hepcidin led to iron depletion in cardiomyocytes, enhanced apoptosis and a loss of cardiac function (Lakhal-Littleton et al., 2016). In addition, a single amino acid substitution in ferroportin from cysteine to either tyrosine (C326Y) (Viprakasit et al., 2004) or serine (C326S) (Sham et al., 2005) may cause iron overload due to expression of mutant ferroportin that is resistant to hepcidin-induced internalisation and degradation (Drakesmith et al., 2005; Fernandes et al., 2009). Transgenic mice expressing C326Y-mutant ferroportin specifically in cardiomyocytes displayed characteristics similar to that observed in mice with cardiomyocyte-specific hepcidin deficient mice (Lakhal-Littleton et al., 2016). Collectively, these data demonstrate a tissue-specific iron-regulatory role of hepcidin and ferroportin, which is essential for maintaining a fine balance in cardiomyocyte iron content necessary for cardiac function.

Within the lung, shRNA-mediated knockdown of hepcidin in airway epithelial cells led to increased mortality in response to acute lung injury induced by polymicrobial sepsis via cecal ligation and puncture surgery in mice. This observation was paralleled with an increase in ferroportin expression in the lung, and reduction in iron content and phagocytic function of alveolar macrophages (Chen et al., 2014). More recently, researchers have also shown that mice homozygous

for the hepcidin-resistant ferroportin (*Slc40a1* C326S) experience pulmonary iron accumulation, alongside a reduction in total lung capacity and blood oxygen saturation. Oddly, alveolar macrophages isolated from these mice have a higher iron content, unlike splenic macrophages and liver Kupffer cells which are iron-depleted (Neves et al., 2017). The ubiquitous expression of hepcidin-resistant ferroportin in this particular model makes it difficult to conclude the role of hepcidin and ferroportin specifically in the lungs, and the data may be confounded by the fact that systemic iron levels in these mice are elevated. As such, the pulmonary role of the hepcidin-ferroportin axis remains to be explored using tissue-specific transgenic models.

1.1.3 Regulation of hepcidin expression

Hepcidin expression is controlled at the transcriptional level via various signalling mechanisms in response to physiological stimuli in our body, including changes in liver iron content and transferrin saturation, inflammation, and erythropoiesis (summarised in Figure 1.2).

Since hepcidin inhibits dietary iron absorption and iron recycling by macrophages, the appropriate regulation of hepcidin synthesis in response to changes in serum and tissue iron levels is crucial for the maintenance of systemic iron homeostasis. The control of hepcidin in response to iron status occurs via the bone morphogenetic protein / sons of mothers against decapentaplegic (BMP/SMAD) signalling pathway. The BMP receptor complex consists of a pair of type I and type II BMP receptor dimers (BMPRI and BMPRII). When a BMP ligand binds to its receptors, the constitutively active intracellular kinase domain of BMPRII phosphorylates BMPRI, thus activating the intracellular kinase domain of BMPRI. Consequentially, BMPR I phosphorylates the receptor-regulated SMAD1, SMAD5 and SMAD8 proteins (collectively termed SMAD1/5/8), allowing SMAD1/5/8 to associate with the co-SMAD (SMAD4) and translocate into the nucleus. Within the nucleus, SMAD1/5/8 and SMAD4 function as transcription factors and bind BMP responsive elements (BMP-RE) to induce the expression of their downstream target genes, including hepcidin (Casanovas et al., 2009).

The BMP/SMAD signalling pathway was first found to be associated with hepcidin regulation and iron homeostasis in patients with juvenile haemochromatosis carrying mutations in hemojuvelin, a co-receptor for BMPs (Papanikolaou et al., 2004). Subsequently, liver-specific deletion of Smad4 was shown to reduce hepcidin expression and cause iron accumulation in mice, further demonstrating that BMP/SMAD signalling is crucial in maintaining iron homeostasis (Wang et al., 2005). *In vitro* studies have identified two BMP-REs in the hepcidin promoter (Truksa et al., 2009). Additionally, exogenous addition of BMP2, BMP4, BMP5, BMP6, BMP7 and BMP9 recombinant proteins enhances hepcidin expression *in vitro* (Babitt et al., 2007). Amongst these, Bmp6 was thought to be a critical, non-redundant endogenous regulator of hepcidin in response to hepatic iron accumulation. Dietary iron loading upregulated the expression of *Bmp6* and *Bmp2*, while iron deficiency suppressed only *Bmp6* expression without altering the expression of other Bmps (Kautz et al., 2008). Additionally, *Bmp6*-deficient mice displayed suppressed hepcidin expression, coupled with rapid and massive iron accumulation in the liver (Andriopoulos et al., 2009; Meynard et al., 2009). *BMP6* expression was also found to be enhanced in hereditary haemochromatosis patients with hepatic and systemic iron-overloading, suggesting an important role for BMP6 in iron homeostasis in humans (Ryan et al., 2010). Moreover, missense mutations in *BMP6* cause a reduction in hepcidin synthesis and is associated with iron overload in humans (Daher et al., 2016; Piubelli et al., 2017).

More recently, conditional knockout of *Bmp6* in different cell populations within the liver demonstrated that endothelial cells are the predominant source of Bmp6 in the liver. Liver sinusoidal endothelial cell (LSEC)-specific deletion of *Bmp6* resulted in hepcidin deficiency and massive iron accumulation similar to that seen in *Bmp6*-knockout mice, whereas deletion of *Bmp6* in hepatocytes or Kupffer cells did not alter hepcidin and iron status, suggesting a paracrine Bmp6 signalling from the endothelial cells to the neighbouring hepatocytes to upregulate hepcidin expression (Canali et al., 2017). At the same time, a separate group of researchers independently showed that LSEC-specific deletion of *Bmp2* also reduced hepcidin expression and resulted in severe iron overload (Koch et al., 2017), once again highlighting a paracrine Bmp/Smad signalling pathway from LSEC to hepatocytes to regulate hepcidin and iron status. Notably, whilst *Bmp2* and *Bmp6* are both essential in maintaining

basal hepcidin expression and iron homeostasis at resting conditions, only *Bmp6* expression is downregulated by iron deficiency and upregulated by overloading.

The control of hepcidin expression in response to fluctuating serum iron levels is also mediated by the BMP/SMAD signalling pathway, but without major alterations in *Bmp6* expression as with hepatic iron accumulation. Instead, it involves the haemochromatosis protein (HFE), transferrin receptors 1 and 2 (Tfr1 and Tfr2), BMP co-receptor hemojuvelin (HJV) and type I BMP receptor ALK3 located on the hepatocyte cellular membrane. Tfr1 is ubiquitously expressed and has a higher affinity for holotransferrin than Tfr2, and its expression fluctuates in response to intracellular iron status. In comparison, Tfr2 expression is restricted to specific tissues and is not altered by intracellular iron levels (Kawabata et al., 2000). The liver expresses high levels of Tfr2 and low levels of Tfr1 (Kawabata et al., 2001). HFE can interact with both Tfr1 and Tfr2, but with contrasting effects on hepcidin expression. The interaction of HFE with Tfr1 is associated with a decrease in hepcidin expression, whilst mutations inhibiting the HFE-Tfr1 interaction increase hepcidin expression (Schmidt et al., 2008). Conversely, the interaction between HFE and Tfr2 is necessary for the induction of hepcidin expression in response to iron-loaded holotransferrin (Gao et al., 2009). In addition, HFE interacts with Tfr1 at its transferrin binding site (Bennett et al., 2000; West et al., 2001), whilst HFE and transferrin binds to different sites on Tfr2 and do not compete for binding to Tfr2 (Chen et al., 2007). HFE and Tfr2 have been proposed to stabilise the BMP/SMAD signalling pathway, since mutations in *HFE* and *Tfr2* causes an impairment in BMP/SMAD signalling in both mice (Corradini et al., 2009, 2011a; Kautz et al., 2009) and humans (Bolondi et al., 2010; Ryan et al., 2010). These data collectively suggest that increased serum iron levels, and thus transferrin saturation, causes more holotransferrin to bind Tfr1 and release HFE for binding with Tfr2, which then stabilises or enhances BMP/SMAD signalling to increase hepcidin expression. The exact mechanism how HFE-Tfr2 enhances the BMP/SMAD signalling pathway is unclear. *In vitro* overexpression assays have shown that HFE interacts and stabilises the type I BMP receptor ALK3 (Wu et al., 2014b), and that HFE-Tfr2 forms a complex with the BMP co-receptor HJV (D'Alessio

et al., 2012), thereby mediating BMP/SMAD signalling. However, the physiological interactions between HFE, Tfr2, HJV and ALK3 remains to be explored *in vivo*.

Inflammation also drives hepcidin synthesis through inflammatory cytokines such as interleukin-6 (Nemeth et al., 2004b) and interleukin-22 (Armitage et al., 2011). The binding of interleukin-6 and interleukin-22 to their receptors activates Janus kinases (JAK), which phosphorylates signal transducers and activators of transcription-3 (STAT3) protein. Phosphorylated STAT3 then translocates into the nucleus and binds to STAT responsive elements to upregulate the expression of its target genes, including hepcidin (Verga Falzacappa et al., 2007). The induction of hepcidin by inflammatory cytokines via the JAK/STAT signalling pathway is thought to synergise with the BMP/SMAD signalling pathway, since deletion of BMP-RE in the hepcidin promoter blocks interleukin-6-mediated hepcidin upregulation (Verga Falzacappa et al., 2008). Chronic upregulation of hepcidin expression in response to inflammation contributes to the anaemia of inflammation, which is characterised by low serum iron levels due to hepcidin-mediated ferroportin degradation causing impaired iron recycling and absorption, so less iron is available for erythropoiesis.

Erythropoiesis also regulates systemic iron homeostasis via altering hepcidin expression, which is unsurprising since the majority of iron is contained within erythrocytes to deliver oxygen throughout the body. Hepcidin expression is suppressed in pathologies associated with elevated erythropoietic demand for iron, such as in ß-thalassemia where a reduction or complete absence of ß-globin synthesis causes ineffective haemoglobin synthesis and anaemia (Jones et al., 2015; Origa et al., 2007; Wray et al., 2017). In addition, hypoxic conditions also enhance erythropoiesis that is paralleled with a downregulation in hepcidin synthesis (Talbot et al., 2012). Researchers initially suggested direct binding of hypoxia inducible factors (HIFs) to the hepcidin promoter to block hepcidin expression (Peyssonnaux et al., 2007). However, later investigations showed that the suppression of hepcidin is not directly regulated by HIF in the liver; instead, it occurs via erythropoietin (EPO)-mediated erythropoiesis since liver-specific *Hif2α*-knockout mice can mount the same kidney EPO induction and liver hepcidin suppression in response to iron-deficiency

anaemia as wildtype mice, and anti-EPO antibodies block hepcidin suppression and erythropoiesis in a mouse model of hepatocyte-specific constitutively active Hif2α (Mastrogiannaki et al., 2012). Moreover, ablation of the bone marrow by irradiation (Vokurka et al., 2006) or chemotherapy using carboplatin or doxorubicin (Pak et al., 2006) blocks the suppression of hepcidin in response to phlebotomy or recombinant EPO administration, suggesting the presence of an erythroid-derived regulator that controls hepcidin expression in response to changes in erythropoietic demand. More recently, the erythroblast-derived hormone erythroferrone (ERFE, encoded by *Fam132b* gene) was identified as the long sought-for regulator of hepcidin expression in response to elevated erythropoietic demand. ERFE production is elevated in response to exogenous EPO administration, erythropoietic stimulation by phlebotomy, and in a β-thalassemia mouse model. Furthermore, genetic ablation of *Fam132b* blocked the suppression of hepcidin and alleviated the iron overload phenotype in β-thalassemia mice, confirming the involvement of ERFE in downregulating hepcidin expression and regulating iron availability in response to erythropoietic demand. The upregulation of *Fam132b* expression in response to recombinant EPO occurs via the JAK/STAT5 signalling pathway (Kautz et al., 2014, 2015). However, the exact mechanism as to how ERFE suppresses hepcidin is currently unknown and remains of great interest in the field.

Prior to the identification of the role of ERFE in regulating hepcidin expression in response to increased erythropoietic demand, other regulators of hepcidin have been proposed. These include Growth Differentiation Factor 15 (GDF15), Twisted Gastrulation (TWSG1) and Platelet Derived Growth Factor (PDGF)-BB. Expression and secretion of GDF15 and TWSG1 were upregulated upon erythroblasts maturation *in vitro*. Serum GDF15 concentration was significantly elevated in β-thalassaemia patients and correlated positively with serum EPO levels. In Huh7 cells, *HAMP* expression was suppressed by supraphysiological doses of GDF15, yet surprisingly, low doses of GDF15 below physiological concentrations also suppressed *HAMP* expression (Tanno et al., 2007). The same group of researchers also demonstrated that TWSG1 suppressed *Hamp1* expression in murine primary hepatocytes *in vitro*. TWSG1 did not reduce *HAMP* expression in Huh7 cells, but blocked the induction of *HAMP* expression by recombinant BMP2 and BMP4 (Tanno et al., 2009).

However, the expression of *Gdf15* and *Twsg1* was not upregulated in the bone marrow of mice upon phlebotomy and in β-thalassaemic mice; in the spleen of β-thalassaemic mice, the expression of *Gdf15* was upregulated less than 2-fold while *Twsg1* expression was unaltered (Kautz et al., 2014, 2015). Moreover, *Gdf15*-knockout mice were able to suppress hepcidin expression to the same degree as wildtype mice in response to phlebotomy (Casanovas et al., 2013), suggesting Gdf15 is unlikely a regulator of hepcidin expression in response to increased erythropoietic demand. The role of TWSG1 in erythropoiesis-induced hepcidin suppression remains to be clarified, perhaps by measuring hepcidin expression in *Twsg1*-knockout mice in response to EPO or phlebotomy. Lastly, the serum protein concentration of PDGF-BB was elevated in healthy volunteers and wildtype mice in response to 6 hours of hypoxia using a hypoxic chamber. The suppression of hepatic *Hamp1* expression in response to hypoxic conditions was abrogated by administration of either a PDGF receptor kinase antagonist or anti-PDGF-BB antibodies. However, the authors mentioned that serum PDGF-BB levels were unaltered by a week of EPO administration, suggesting that hypoxia itself, rather than elevated erythropoietic demand, caused the induction of PDGF-BB (Sonnweber et al., 2014). Whether ablation of PDGF-BB affects the rate of erythropoiesis remains to be characterised.

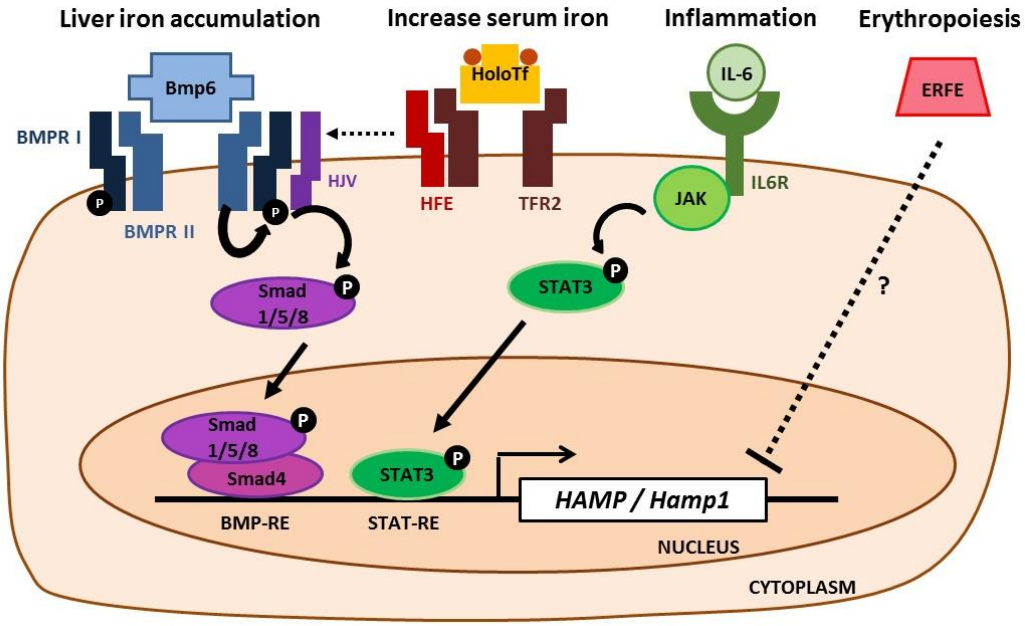


Figure 1.2: Transcriptional control of hepcidin expression. Hepcidin is upregulated in response to elevated liver iron and serum iron via the BMP/SMAD signalling pathway, and in response to inflammatory cytokines via the JAK/STAT signalling pathway. Enhanced erythropoiesis increases ERFE production by erythroblasts, which inhibits hepcidin expression via mechanisms that are currently poorly defined.

1.1.4 Control of intracellular iron homeostasis

Intracellular iron homeostasis is achieved by regulating the uptake, storage and export of iron. In most cells, transferrin receptor 1 (encoded by *TFR1*) mediates cellular iron uptake by binding and internalising holotransferrin via endocytosis. Acidification of the endosome triggers the release of ferric iron from transferrin, and iron is then reduced to ferrous iron by the ferrireductase six-transmembrane epithelial antigen of the prostate 3 (STEAP3) (Ohgami et al., 2005) and transported into the cytosol via DMT1 (Touret et al., 2003). Within the cell, iron can be used as a cofactor in enzymatic processes or for haem synthesis mediated by the δ-aminolevulinic acid synthases 1 and 2 (*ALAS1* and *ALAS2*). Excess intracellular iron can either be stored in a safe, redox-inactive manner within polymers of ferritin heavy and light chains (encoded by *FTH* and *FTL*), or exported out of the cell via ferroportin.

Iron regulatory proteins 1 and 2 (IRP1 and IRP2) are RNA-binding proteins that bind to a conserved nucleotide sequence that forms a stem and loop structure, which is known as the iron response elements (IREs) located in the 5' or 3' untranslated regions (UTRs) of mRNA. Under iron replete conditions, iron-sulfur clusters [4Fe-4S] form within the cell and bind directly to IRP1, thereby interfering with its ability to bind IREs on mRNAs. In addition, the F-box and leucine-rich repeat protein 5 (FBXL5) is stabilised in iron replete cells, and FBXL5 acts as an adaptor protein to recruit an E3 ubiquitin ligase complex consisting of Skp, Cullin and F-box protein (SCF complex) to IRP2, thereby inducing ubiquitin-mediated proteosomal degradation of IRP2 (Salahudeen et al., 2009; Vashisht et al., 2009). Thus, the binding of IRP1 and IRP2 to mRNA IREs is hindered in iron replete cells. When cells become iron deficient, IRP1 is not bound by [4Fe-4S] clusters and IRP2 protein is stabilised. Hence, IRP1 and IRP2 proteins bind to IREs in iron depleted cells.

IRP1 and IRP2 maintain intracellular iron homeostasis by binding to IREs in the 5' or 3' UTRs of mRNA encoding proteins involved in cellular iron trafficking, utilisation and storage. These include the above-mentioned *TFR1*, *ALAS2*, *FTH*, *FTL* and *SLC40A1* (Figure 1.3). The *TFR1* mRNA

contains IREs in the 3' UTR and is protected against degradation by nucleases when bound by IRP1 and IRP2. In comparison, IREs are located in the 5' UTR of *ALAS2*, *FTH*, *FTL* and *SLC40A1* mRNA. Binding of IRP1 and IRP2 to these 5'UTR IREs block translation and expression of the encoded proteins. Under iron-deficient conditions, IRP1 and IRP2 stabilises the *TFR1* mRNA and enhances the translation and expression of transferrin receptor 1, thus enhancing transferrin iron uptake by the cells. Simultaneously, the translation of *SLC40A1* is blocked, thus allowing iron retention. In iron replete cells, the absence of IRP1 and IRP2 allow efficient translation of *FTH* and *FTL* to synthesize ferritin for safe intracellular iron storage, as well as *ALAS2* for the utilisation of iron for haem synthesis (reviewed in Hentze et al., 2010).

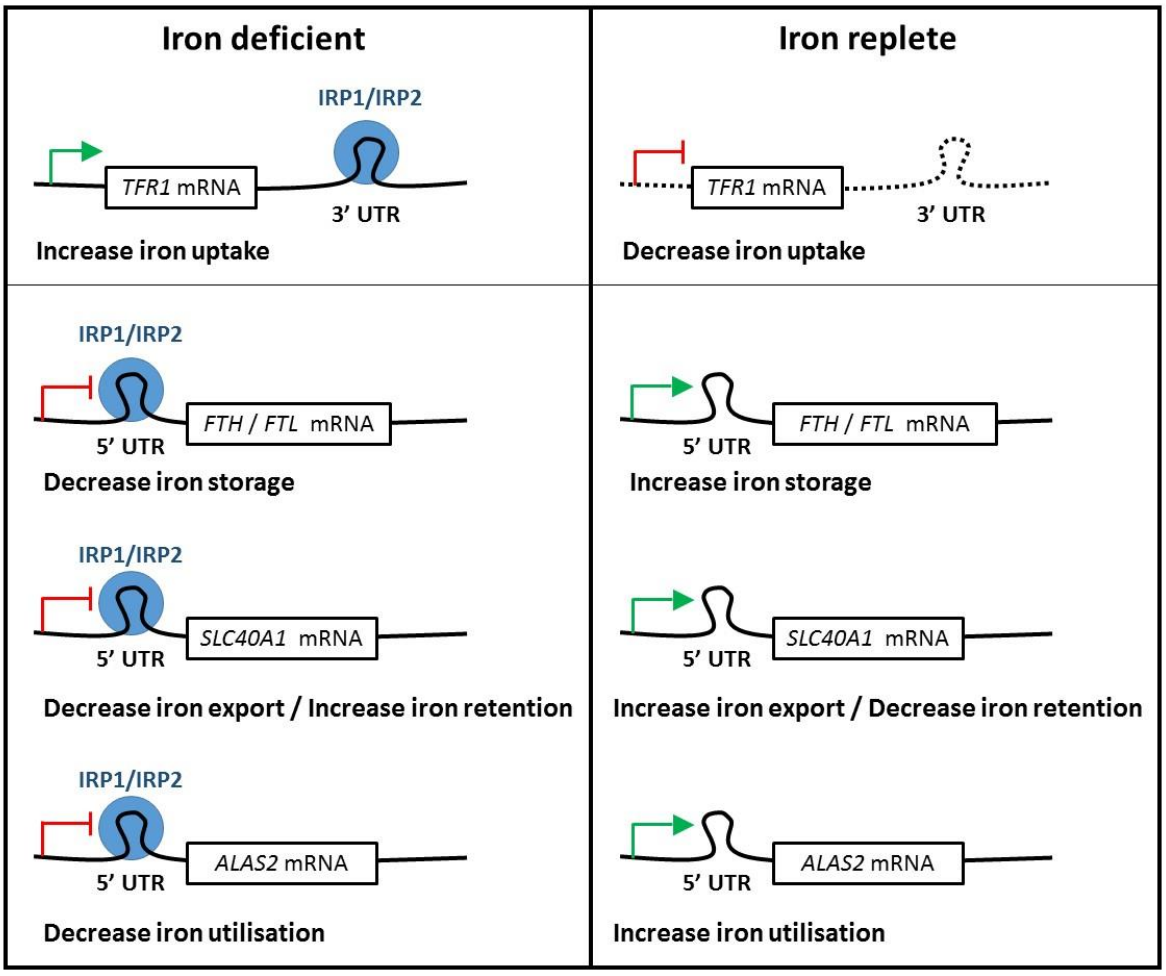


Figure 1.3: Intracellular iron homeostasis is controlled by IRP/IRE. In iron deficient cells, IRP1 and IRP2 binds to IRE on 5' UTR of *TFR1* mRNA to stabilise it, thus increasing transferrin receptor 1 expression and iron uptake. IRP1 and IRP2 binds to IREs on 3' UTR of *FTH*, *FTL*, *SLC40A1* and *ALAS2* mRNA to block translation and decrease iron storage and utilisation, and increase iron retention. In iron replete cells, IREs are not bound by IRP1 and IRP2, causing reduced *TFR1* expression and increased *FTH*, *FTL*, *SLC40A1* and *ALAS2* expression to enhance iron storage, export or utilisation.

In addition to post-transcriptional control, intracellular ferritin protein levels are also regulated by iron availability within the cell. *In vitro,* iron deprivation achieved by either reducing iron content in the culture medium or adding iron chelators induced lysosomal degradation of ferritin proteins and release of iron. (Kidane et al., 2006; Zhang et al., 2010). More recently, the nuclear receptor coactivator 4 (NCOA4) was identified as a cargo receptor that associates with ferritin proteins. Under iron-deplete conditions, NCOA4 facilitates the autophagic delivery of ferritin to lysosomes for degradation thereby releasing iron from ferritin stores. In contrary, in iron-replete conditions, NCOA4 is targeted for ubiquitin-mediated degradation, thus stabilising ferritin proteins (Mancias et al., 2014, 2015).

Intracellular iron trafficking to organelles, iron-requiring enzymes or proteins is aided by cytosolic chaperones. For example, the poly (rC)-binding protein 1 (PCBP1) interacts with iron and ferritin directly and facilitates the loading of ferritin with cytosolic iron (Shi et al., 2008). Subsequently, PCBP1 and its homologue PCBP2 were shown to deliver iron to prolyl hydroxylases which in turn targets HIF1α for degradation in normoxic conditions (Nandal et al., 2011). In addition, 2,5-dihydroxybenzoic acid (2,5-DHBA) acts as a chaperone to deliver iron from the cytosol to mitochondria; knockdown of *BDH2*, which encodes a dehydrogenase that mediates formation of 2,5-DHBA, causes iron accumulation in the cytosol, iron deficiency in mitochondria and reduction in haem biogenesis (Devireddy et al., 2010). *Bdh2*-knockout mice are mildly anaemic, likely a result of impaired haem synthesis at the mitochondria (Liu et al., 2014b). Within mitochondria, frataxin functions as an iron chaperone for the synthesis of iron-sulphur clusters required by proteins in the electron transport chain for energy generation and for haem synthesis. Frataxin deficiency, the genetic cause of Friedreich's ataxia, causes a reduction in mitochondria ferritin, accumulation of mitochondrial iron and elevation of oxidative stress levels (reviewed in Richardson et al., 2010).

1.1.5 Iron disorders

According to the World Health Organisation and other reports, iron deficiency is the most common nutritional disorder and causes iron deficiency anaemia in about 30% of the world population. Whilst iron deficiency can be partly accounted for by malnutrition, it can also occur in populations that are well nourished due to dysregulated hepcidin levels. For example, inflammation caused by infections and diseases raise hepcidin levels which block iron absorption and recycling. In a condition termed iron refractory iron deficiency anaemia (IRIDA), the BMP/SMAD signalling pathway is overactive due to loss of function mutations in transmembrane protease serine 6 (*TMPRSS6*), which is a protease that cleaves the BMP co-receptor HJV and downregulates the BMP/SMAD signalling pathway. Thus, patients with mutated *TMPRSS6* have inappropriately high levels of hepcidin driven by enhanced the BMP/SMAD signalling pathway, and fail to absorb sufficient iron from the diet.

At the opposite end of the spectrum, iron overload diseases are also common. The iron overload disease, haemochromatosis, is one of the most common genetic disorders in Europeans. Haemochromatosis is genetically heterogenous and can be caused by mutations in several genes involved in regulating iron homeostasis. In particular, a single nucleotide mutation in *HFE* causing a cysteine to tyrosine substitution at amino acid position 282 (HFE C282Y) was the first to be associated with hereditary haemochromatosis and is the most common cause of haemochromatosis in patients with European ancestry (Feder et al., 1996). Other mutations in *HFE* were found to be more rarely associated with iron overload, including the HFE H63D mutation where histidine is substituted by aspartic acid at amino acid position 63 (Merryweather-Clarke et al., 1997). In HFE-associated haemochromatosis, hepatic *HAMP* expression was significantly suppressed (Bridle et al., 2003), likely due to disruption in HFE-TFR2-mediated BMP/SMAD signalling as discussed above. This results in gradual iron loading due to excessive dietary iron absorption, elevated transferrin saturation, and adult-onset of parenchymal iron deposition and hepatic damage from the fourth decade of life. Subsequently, a mutation in *TFR2* resulting in a premature stop codon at amino acid position 250 was also found to be associated with adult-onset haemochromatosis, where phenotypes

were similar to HFE-associated haemochromatosis (Camaschella et al., 2000). Hepatic hepcidin expression was suppressed in a murine model encoding a premature stop codon in *Tfr2* corresponding to the *TFR2* mutation in haemochromatosis patients (Kawabata et al., 2005). In addition, mutations in *HAMP* (Roetto et al., 2003, 2004) and the BMP coreceptor *HJV* are associated with juvenile haemochromatosis, where symptoms of iron overload present before the age of 30 (Niederkofler et al., 2005; Papanikolaou et al., 2004); in the latter case, mutations in *HJV* led to an impairment in BMP/SMAD signalling and hence suppression in hepcidin expression. These highlight that genetic defects associated with haemochromatosis converge on hepcidin deficiency causing dysregulated iron homeostasis. As discussed earlier, a single amino acid substitution at position 326 in ferroportin from cysteine to tyrosine (C326Y) (Viprakasit et al., 2004) or serine (C326S) (Sham et al., 2005) is also associated with iron accumulation as the mutations encode hepcidin-resistant ferroportin. Notably, mutations in *HFE*, *TFR2*, *HJV* and *HAMP* are autosomal recessive loss-of-function mutations while mutations in *SLC40A1* are gain-of-function mutations that are inherited in an autosomal dominant manner.

The symptoms of hereditary haemochromatosis include lethargy, weight loss and arthralgia at early stages, and skin pigmentation, liver cirrhosis, diabetes, arthritis and cardiomyopathy with advancement of the disease. These symptoms are, however, not specific to haemochromatosis. Thus, haemochromatosis is usually diagnosed by elevated transferrin saturation and serum ferritin levels, and carriage of known haemochromatosis-associated mutations. Patients with consistently high transferrin saturation and serum ferritin levels and/or have a family history are suspected to have hereditary haemochromatosis and referred for genetic testing for HFE C282Y mutation. Subsequently, patients who do not have the HFE C282Y mutation but are iron overloaded based on magnetic resonance imaging of the liver, iron quantification from liver biopsies or quantitative phlebotomies are referred for genetic testing for other haemochromatosis-associated variants by sequencing of *HFE, HJV, HAMP, TFR2, SLC40A1* (Porto et al., 2016).

Haemochromatosis patients are predisposed to cirrhotic liver, diabetes, cardiomyopathy and infections by siderophilic microbes (Jomova and Valko, 2011; Pietrangelo, 2015). In particular, elevated serum ferritin levels are used as a non-invasive indicator of a possibility of liver fibrosis in homozygous HFE C282Y patients (Guyader et al., 1998; Wood et al., 2017). Despite the prevalence of haemochromatosis and its contribution to several diseases, treatment options are limited, but usually effective; patients usually rely on regular phlebotomy throughout their life to remove excess iron. At the first instance, haemochromatosis patients are phlebotomised weekly until serum ferritin is reduced to 50ng/ml. Thereafter, phlebotomies are performed less frequently to maintain serum ferritin at normal levels. Phlebotomy treatment reduces mortality, improves cardiac function (Niederau et al., 1994) and alleviates liver fibrosis (Falize et al., 2006) in haemochromatosis patients. While effective for most patients, phlebotomy treatment is lifelong and puts a time and financial strain on patients and healthcare services, and may cause side effects such as soreness, fatigue and heart palpitations (Adams and Barton, 2010; Assi and Baz, 2014). Moreover, phlebotomy may be unsuitable for certain patients, including those with insufficient venous access or with certain religious beliefs against venesection. These highlight the need to explore other therapeutic strategies to manage haemochromatosis.

1.2 The Nrf2 antioxidant response system

Our body is inevitably and constantly exposed to reactive radical species. Reactive radical species are formed as byproducts of metabolic processes in our body, such as during the production of ATP where the transfer of electrons down the electron transport chain occasionally leads to partial reduction of oxygen to form superoxides $O_2^{\bullet-}$ (Jastroch et al., 2010). They can also be endogenously synthesized as signal transducers. Examples include the formation of nitric oxide $^{\bullet}NO$ by endothelial nitric oxide synthase eNOS for smooth muscle relaxation and vasodilation (Zhao et al., 2015), and the formation of the antimicrobial $^{\bullet}NO$ by inducible nitric oxide synthase iNOS in phagocytes in response to bacterial infections as an immune response (Bogdan, 2015). Whilst these ROS and RNS serve as important signalling molecules in physiology, ROS and RNS can also interact with DNA, lipids and proteins when present in excess, causing damage to these biological materials and disrupting their functions. As such, the careful maintenance of an optimal amount of ROS and RNS is necessary.

The cellular antioxidant responses are orchestrated by Nrf2 (also known as nuclear factor erythroid-derived 2-like 2, encoded by the gene *Nfe2l2*) (Suzuki and Yamamoto, 2015). Nrf2 is a member of the Cap'n'Collar (CNC) family of basic leucine zipper (bZIP) transcription factors. Other members of the CNC family include nuclear factor erythroid-derived 2 (NF-E2), NF-E2 related factors Nrf1 and Nrf3, and BTB and CNC homology Bach1 and Bach2 proteins. These CNC transcription factors form heterodimers with small Maf proteins mafG, mafK and mafF, which also contain a bZIP domain that facilitates the binding of the CNC-small Maf heterodimers to antioxidant response elements (AREs) on promoter and enhancer regions of DNA. In most cases, NF-E2, Nrf1, Nrf2 and Nrf3 function as transcriptional activators whilst Bach1 and Bach2 are transcription repressors.

Nrf2 was first identified in a screen for transcription factors that can bind to the NF-E2 and activating protein 1 (AP1) transcription factors binding site present within the locus control region of β-globin gene. In a screening assay, the authors co-expressed proteins synthesized from a hemin-

induced K562 cell cDNA library fused to β-galactosidase with a plasmid containing the NF-E2/AP1 binding site upstream of *lacZ* in *Escherichia coli*. The cDNA from one of the positive clones was subsequently found to encode a protein containing a bZIP domain that displayed a high degree of homology with the other CNC transcription factors and hence named NF-E2-like 2 (*NFE2L2*). *In vitro* transcription and translation of the cDNA produced a protein with a molecular mass of 96kDa (Moi et al., 1994). NF-E2 is erythroid-specific and essential for the development of haematopoietic cells; NF-E2 null mice succumb to bleeding due to a blockage in megakaryocyte maturation causing lack of platelets and mice that survive are mildly anaemic. In contrast, Nrf2 is expressed widely expressed in many tissues and mice lacking functional Nrf2 grow to adulthood without developing anaemia, suggesting its role in haematopoiesis is not crucial (Chan et al., 1996).

1.2.1 Regulation of Nrf2 activity in response to oxidative stress

Of the CNC family of transcription factors, Nrf2 is the most extensively studied and characterised. Nrf2 is ubiquitously expressed in all tissues and serves as the master regulator of redox balance by controlling a battery of antioxidant and cytoprotective genes under the control of ARE. At basal condition, Nrf2 protein has a short half-life of less than 20 minutes (Itoh et al., 2003; Kobayashi et al., 2004a). It is sequestered in the cytoplasm by its inhibitor protein Keap1 (Kelch-like ECH-associated protein 1). Keap1 recruits the Cullin3 E3 ubiquitin ligase at its bric-à-brac, tramtrack and broad complex transcription regulators (BTB) and intervening region (IVR) domains and targets Nrf2 for ubiquitin-mediated degradation (Cullinan et al., 2004; Kobayashi et al., 2004a). The BTB domain of Keap1 also facilitates the homodimerisation of Keap1 (Zipper and Timothy Mulcahy, 2002). In addition, Keap1 contains six Kelch domains that form a ß-barrel structure that binds to Nrf2. The Nrf2 protein contains seven Neh (Nrf2-Ech homology) domains, of which Neh2 contains two Keap1-binding motifs – the DLG motif with a low affinity for Keap1, and the ETGE motif with a high affinity for Keap1 (Tong et al., 2006). As such, one molecule of Nrf2 binds to two molecules of Keap1 (as a homodimer) in a hinge-and-latch mechanism. To date, site directed mutagenesis of Keap1 has identified several cysteine residues that are involved in sensing oxidative stress and triggering the activation of Nrf2. Substitution of cysteine C273 and C288 with serine on Keap1

renders it unable to facilitate the ubiquitination of Nrf2 in the absence of electrophiles, resulting in hyperactivity of Nrf2 at basal state. In contrast, substitution of C151 with serine causes a constitutive repression of Nrf2 (Zhang and Hannink, 2003). Additionally, cysteine residues C226 and C613 senses the redox-active elements Zn^{2+}, Cd^{2+}, Se^{4+} and As^{3+} (McMahon et al., 2010). Due to its cysteine-rich nature, the Keap1 protein contains several thiol groups that are highly reactive with electrophilic agents, including ROS and RNS. These electrophilic agents cause a reduction in the thiol groups, resulting in formation of disulphide bonds and conformational changes in Keap1 that destabilizes the Nrf2-Keap1-Cullin3 complex (Figure 1.4). As a consequence, the ubiquitin ligase Cullin3 and/or the low affinity DLG motif of Nrf2 dissociates from Keap1 and inhibits Nrf2 degradation, allowing *de novo* synthesized Nrf2 to translocate into the nucleus and induce the expression of ARE-dependent antioxidant genes (Figure 1.5). By responding to toxic stimuli and controlling the expression of enzymes with detoxification and antioxidant activity, Nrf2 is critical for maintaining the redox balance and thus cellular integrity in response to intracellular and environmental stresses.

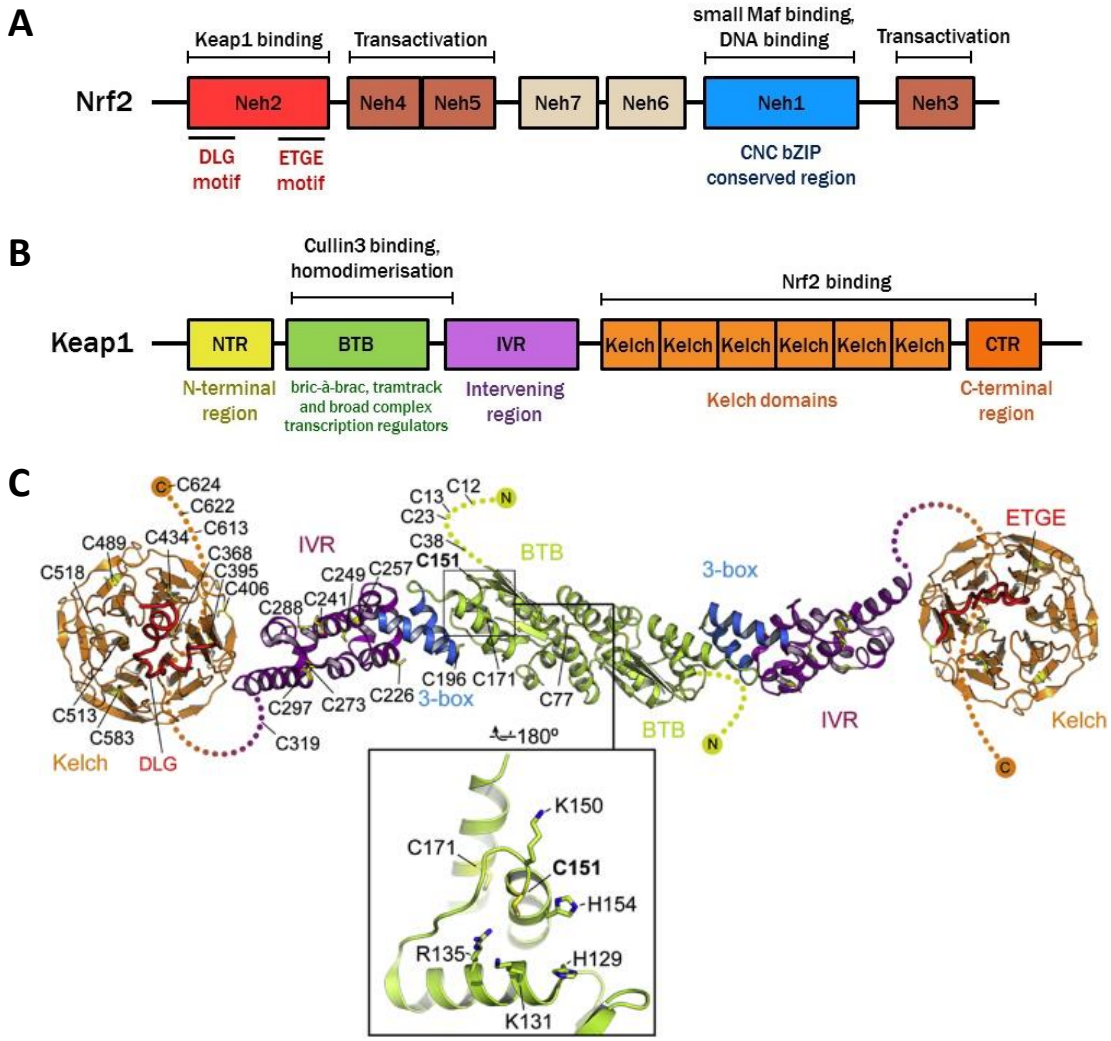


Figure 1.4: (A) Domain structure of Nrf2 showing the seven Neh domains. The Neh2 domain contains the low affinity DLG motif and high affinity ETGE motif that binds to Keap1. Neh4, Neh5 and Neh3 function as transactivation domains to recruit other proteins in the transcription machinery. The Neh1 domain is the highly conserved CNC bZIP region that associates with small Maf protein and binds to ARE sites on DNA. **(B)** Domain structure of Keap1. The BTB and IVR regions are involved in Keap1 homodimerisation and the recruitment of Cullin3 ubiquitin ligase. The six Kelch domain repeats and CTR interacts with the DLG and ETGE motifs of Nrf2. **(C)** Model of Keap1 and Nrf2 interactions (adapted from Dinkova-Kostova et al., 2017). Two molecules of Keap1 interact via the BTB domain (green) to form a homodimer. The six Kelch domains form a ß-barrel structure (orange) that interacts with the DLG and ETGE motifs of Nrf2 (red). The 27 cysteine residues of Keap1 are highlighted, demonstrating the thiol-rich nature of this protein.

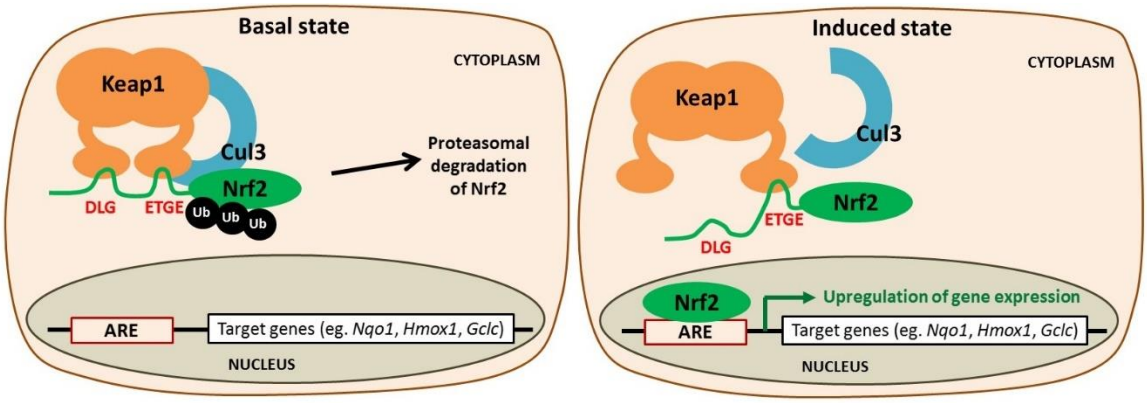


Figure 1.5: Hinge and latch mechanism of Nrf2 activation. At basal state, Keap1 sequesters Nrf2 in the cytoplasm and recruits the Cullin 3 (Cul3) ubiquitin ligase to mediate the ubiquitination and proteosomal degradation of Nrf2. Oxidative stress induces conformational changes in Keap1 and causes the dissociation of Cul3 and the low affinity DLG motif of Nrf2 (latch) but not the ETGE motif (hinge), allowing Nrf2 protein stabilisation. Nrf2 translocates into the nucleus to bind ARE sites on DNA and induces the expression of its target genes.

Nrf2 interacts with its obligatory dimerization partner small Maf protein and binds to DNA via its Neh1 domain (Itoh et al., 1995; Moi et al., 1994). It also recruits other proteins that form the transcription machinery, such as the histone acetyltransferase cAMP-responsive element binding protein CBP via Neh4 and Neh5 (Katoh et al., 2001) and chromodomain helicase DNA binding protein CHD6 via Neh3 (Nioi et al., 2005).

The role of Nrf2 as a transcriptional activator that upregulates the expression of antioxidant and cytoprotective genes has been well-defined. For example, transgenic mice expressing constitutively active Nrf2 lacking the Keap1 binding domain in the skin express higher levels of ARE-driven genes glutamate cysteine ligase catalytic and modifier subunits (*Gclc* and *Gclm*) and *Nqo1* (Schäfer et al., 2012). In the lungs, cigarette smoke exposure induces an Nrf2-dependent upregulation of antioxidant genes *Nqo1*, *Hmox1*, *Gclc* and *Gclm* (Yageta et al., 2011). Small molecule activators of Nrf2 and genetic deletion of Keap1 (Yates et al., 2007, 2009), as well as hepatotoxic drugs such as acetaminophen (Chan et al., 2001b) also activate Nrf2 and induce the expression of cytoprotective genes in the liver. However, the ability of Nrf2 to repress the expression of downstream target genes have also been demonstrated in a limited number of scenarios. The binding of Nrf2 at the promoter of Recepteur d' origine nantais (RON) tyrosine kinase receptor has

been associated with repression of RON expression in breast cancer cells (Thangasamy et al., 2011). In bone marrow derived macrophages exposed to lipopolysaccharide, the binding of Nrf2 to the proximal enhancers upstream of interleukin 6 (*Il-6*) and interleukin 1b (*Il-1b*) was associated with a block in RNA polymerase II recruitment to the promoter and reduced expression of these pro-inflammatory cytokine genes, thereby contributing to Nrf2's anti-inflammatory role (Kobayashi et al., 2016). These studies challenge the view of Nrf2 being an inducer of gene expression in all circumstances. Nevertheless, the general role of Nrf2 in upregulating the expression of its target genes is widely accepted.

1.2.2 Nrf2 in cellular protection and health

Nrf2 activates a variety of target genes that encode proteins involved in multiple cellular protection processes in response to environmental stresses. These processes include the synthesis of the antioxidant glutathione, and the detoxification and export of metabolites via glutathione S-transferases and multidrug resistance proteins. As such, Nrf2 deficiency increases susceptibility to a variety of environmental stressors. For example, deletion of *Nrf2* is associated with increased mortality in response to acetaminophen-induced toxicity (Chan et al., 2001b), LPS-induced sepsis (Thimmulappa et al., 2006), 1-methyl-4-phenyl-1,2,3,6-tetrahydropyridine-induced Parkinson's disease (Burton et al., 2006) and liver fibrosis in haemochromatosis mice (Duarte et al., 2017). *Nrf2*-knockout mice also display elevated levels of inflammatory cytokines, immune cell recruitment and mortality rate in response to Influenza virus infection (Yageta et al., 2011). Conversely, pharmacological activation of Nrf2 by sulforaphane improves bacterial clearance in a murine model of chronic obstructive pulmonary disease. In humans, *NRF2* single nucleotide polymorphisms (SNPs) predicted to reduce *NRF2* expression have also been associated with elevated systolic and diastolic blood pressure (Shimoyama et al., 2014).

Due to its role in maintaining cellular health, the Nrf2/ARE antioxidant and cytoprotective system became an attractive drug target for many diseases. Dimethyl fumarate, under the trade name Tecfidera, is approved for the treatment of relapsing multiple sclerosis. The exact mechanism by

which dimethyl fumarate reduces the relapse of multiple sclerosis is not entirely clear. In a murine model of experimental autoimmune encephalomyelitis, dimethyl fumarate reduced demyelination and axon loss in wildtype but not *Nrf2*-knockout mice (Linker et al., 2011), suggesting that the protective effects of dimethyl fumarate in multiple sclerosis is mediated, at least in part, through Nrf2 activation. In addition, the potent Nrf2 activator methyl 2-cyano-3,12-dioxooleana-1,9(11)-dien-28-oate (CDDO-Me) is under phase 2 and 3 clinical trials for chronic kidney disease and pulmonary hypertension.

In addition to Nrf2-activating drugs, Nrf2 inhibitors have also come under the spotlight in more recent years due to studies pointing towards the dual role of Nrf2 in oncogenesis. In earlier studies, Nrf2 was thought to be protective against carcinogenesis. *Nrf2*-knockout mice are more susceptible to Benzo[a]pyrene-induced gastric neoplasia (Ramos-Gomez et al., 2001) and N-nitrosobutyl(4-hydroxybutyl)amine-induced bladder carcinoma (Iida et al., 2004); the Nrf2 activator Oltipraz reduced tumour incidences in an Nrf2-dependent manner in these scenarios. The incidences of dextran sulfate sodium-induced colitis and colorectal cancer (Khor et al., 2008) and 4-nitroquinoline-1-oxide-induced tongue and oesophageal cancer (Ohkoshi et al., 2013) are also higher in *Nrf2*-knockout mice. In humans, an *NRF2* SNP that suppressed *NRF2* gene expression was associated with an elevated risk of lung cancer in smokers (Suzuki et al., 2013).

More recent studies demonstrated that while Nrf2 prevents the initiation of carcinogenesis, over-activation of Nrf2 in tumour cells can then accelerate tumour progression. Primary cells and tissues isolated from mice expressing the oncogene K-Ras^{G12D} or B-Raf^{V619E} had elevated Nrf2 gene expression, enhanced Nrf2 activity and lower intracellular ROS levels. In addition, siRNA-mediated knockdown of *KRAS* oncogene in human pancreatic ductal adenocarcinoma cells reduced NRF2 activity, suggesting that oncogenes upregulate Nrf2 expression. In a murine model of pancreatic cancer, deletion of Nrf2 led to a reduction in the total number of pre-invasive pancreatic intraepithelial neoplasia (PanIN). Moreover, PanIN from *Nrf2*-knockout mice were less proliferative than PanIN from *Nrf2*-expressing mice (DeNicola et al., 2011). In another study, *Nrf2*-knockout mice

develop more tumour nodules in the lung in response to urethane in early stages, but observations at a later time point showed that the tumours in *Nrf2*-knockout mice were smaller than in wildtype mice. Moreover, transplantation of tumours from wildtype mice into nude mice led to progressive tumour growth while tumours originating from *Nrf2*-knockout mice failed in engraft in nude mice. Microarray and pathway analyses demonstrated higher expression of genes related to cell growth and proliferation in tumours from wildtype mice (Satoh et al., 2013). The findings from DeNicola and Satoh consistently suggest that the lack of Nrf2 in the tumour is beneficial for the host by limiting tumour growth. Additionally, elevated levels of Nrf2 expression have also been associated with chemoresistance both *in vitro* (Cho et al., 2008; Jiang et al., 2010) and from *ex vivo* patient specimens (Kim et al., 2008; Solis et al., 2010) possibly due to the upregulation of drug-metabolising enzymes and drug efflux proteins (reviewed in Bai et al., 2016). Investigations of Nrf2 inhibitors as potential therapeutics have been studied in *in vitro* models (reviewed in No et al., 2014). Examples include naturally-occurring flavonoid luteolin and chrysin; luteolin sensitized human lung carcinoma A549 cells to several anticancer drugs (Tang et al., 2011) and chrysin restores the chemosensitivity of doxorubicin-resistant hepatocellular carcinoma BEL-7402/ADM cells (Gao et al., 2013). The efficacy of Nrf2 inhibitors in suppressing tumour progression and preventing chemoresistance remains to be characterised *in vivo*.

1.2.3 Nrf2 in intracellular iron homeostasis

Nrf2 has been shown to be involved in intracellular iron homeostasis. *Fth* and *Ftl* were found to be associated with AREs and transcriptionally regulated by Nrf2 (Tsuji et al., 2000; Wasserman and Fahl, 1997). The authors highlighted the coordinated transcriptional control of ferritin by Nrf2 and post-transcriptional regulation by the IRP/IRE system, allowing cells to respond to iron stimuli and safely store iron in the catalytically inactive ferric form. In addition, Nrf2 also controls the transcription of *Slc40a1* to enhance cellular iron export. This facilitates iron recycling by macrophages (also see Chapter 1.2.5), and also confers protection to macrophages during infections via nitric oxide-mediated Nrf2 activation whereby iron depletion restricts *Salmonella* growth (Nairz et al., 2013).

1.2.4 NF-E2, Nrf1 and Nrf3 transcriptional activators

In addition to NRF2, the CNC family of transcriptional activators also include NF-E2, NRF1 and NRF3, each with a distinct pattern of tissue expression and regulation.

NF-E2 is an erythroid-specific transcription factor that is involved in the development of haematopoietic cells. NF-E2 deficient mice have defective megakaryocyte differentiation and lack functional platelets, causing increased bleeding and a high mortality rate of 90% within the first week after birth due to severe thrombocytopenia. NF-E2 deficient mice that live to adulthood experience mild anaemia associated with elevated oxidative stress and reduced survival of erythrocytes (Chan et al., 2001a; Lecine et al., 1998; Shivdasani, 1996).

Nrf1 is ubiquitously expressed in all tissues, with higher levels of expression in the heart, muscle, liver and kidney (Biswas and Chan, 2010). Deletion of Nrf1 leads to impaired fetal liver erythropoiesis and embryonic lethality in mice, highlighting its essential role in development (Chan et al., 1998). Intracellularly, Nrf1 is a transmembrane protein located in the endoplasmic reticulum (ER) at rest and translocates to the nucleus upon activation, suggesting that Nrf1 could function as a sensor of ER stress. In addition, fibroblasts derived from Nrf1-knockout mice have increased susceptibility to oxidative stress due to reduced expression of genes involved in glutathione biosynthesis, demonstrating the Nrf1 is involved in maintaining a redox balance within the cell (Kwong et al., 1999). However, studies on fibroblasts isolated from Nrf1-knockout and Nrf2-knockout mice suggest that the defect in oxidative stress is more pronounced in the absence of Nrf2 due to a greater reduction in expression of the antioxidant response genes *Gclc*, *Hmox1* and *Fth*. Yet, double deletion of Nrf1 and Nrf2 showed higher levels of oxidative stress and greater extent of suppression in the expression of antioxidant response genes compared to single deletion of Nrf1 or Nrf2, suggesting that Nrf1 and Nrf2 may play overlapping but non-redundant roles in regulating redox levels (Leung et al., 2003). Due to the greater sensitivity of Nrf2 in mediating the antioxidant response, and the ease of working with Nrf2-knockout mice which are viable and live to adulthood, this thesis focuses on the role of Nrf2 in response to iron-induced oxidative stress.

The expression of NRF3 in humans is restricted mainly to the placenta, with very low levels of expression in the heart, brain, lung, kidney, pancreas, thymus, spleen, intestine, B cells and haematopoietic cells from monocyte lineages (Kobayashi et al., 1999). In contrast, mice express high levels of Nrf3 in the placenta, brain, thymus and testis, but not in the heart, spleen and liver (Derjuga et al., 2004). Nrf3-knockout mice develop normally without obvious phenotypic abnormalities in terms of haematological indices (red blood cell count, white blood cell count, haemoglobin levels) and plasma biochemical parameters including glucose, cholesterol, triglyceride, iron, alanine transaminase levels (Derjuga et al., 2004). In a mouse model of acute pulmonary injury induced by the administration of butylated hydroxytoluene, increased number of lesions and infiltration of alveolar macrophages were observed in the lungs of Nrf3 deficient mice compared to wildtype mice (Chevillard et al., 2010). In contrast, administration of butylated hydroxyanisole resulted to similar levels of induction of the classical antioxidant response gene *Nqo1* in the livers of wildtype and Nrf3-knockout mice (Kobayashi et al., 2004b). This observation, together with gene expression data demonstrating minimal Nrf3 expression in the liver, suggests that Nrf3 does not play a critical role in the regulation of gene expression in the liver, which is the main iron storage site in the body and site of Bmp/Smad-signalling and hepcidin production.

1.2.5 Bach1 and Bach2 transcriptional repressors

In an effort to identify novel binding partners to small Maf using the yeast two hybrid system, the BTB and CNC homology proteins Bach1 and Bach2 were discovered (Oyake et al., 1996). Bach1 is expressed ubiquitously, with the highest levels of expression in the small intestine, whilst the expression of Bach2 seemed more restricted. Of the two, Bach1 is generally better studied.

Bach1 contains four dipeptide cysteine-proline (CP) motifs that function as haem-binding domains (Ogawa et al., 2001). The binding of haem to Bach1 triggers chromosome region maintenance 1 (Crm1)-mediated nuclear export of Bach1 (Suzuki et al., 2004). In the cytoplasm, the ubiquitin ligase HOIL-1 (haem-oxidised IRP2 ubiquitin ligase 1) associates with haem-bound Bach1

and induces its ubiquinitation and proteasomal degradation (Zenke-Kawasaki et al., 2007). As such, accumulation of haem causes a reduction in Bach1 protein levels and derepression of its target genes. The control of Bach1 activity by haem is an important mechanism in erythroid cells as it leads to the derepression of ARE-regulated alpha- and beta-globin genes and thus allow erythroid cells to increase their haemoglobin content to carry oxygen (Tahara et al., 2004a, 2004b).

Nrf2 and Bach1 also facilitate haem-recycling in macrophages in a coordinated fashion. Haem-induced Bach1 degradation causes the derepression of *Spic*, which encodes the Spi-C transcription factor involved in the differentiation of monocytes to iron-recycling red pulp macrophages (Haldar et al., 2014). Haem-mediated Bach1 degradation also increases *Hmox1* expression to catalyse the breakdown of haem into iron, biliverdin and carbon monoxide in macrophages. At the same time, the inhibition of Bach1 and binding of Nrf2 to an ARE 7kb upstream of the promoter of *Slc40a1* upregulates the expression of ferroportin to enhance iron recycling for haematopoiesis (Haldar et al., 2014; Marro et al., 2010). This enables the body to adapt to the increase demand to recycle iron during haemolysis by increasing red pulp macrophage content, and efficiently recycle iron and detoxify haem from damaged or senescent erythrocytes.

Bach2 has been implicated in the differentiation of B and T cells. Antigenic stimulation induces Akt-mediated phosphorylation and nuclear export of Bach2, causing the derepression of genes involved in effector differentiation, including Blimp1 which drives the differentiation of germinal center cells into antibody-secreting plasma cells (Sidwell and Kallies, 2016).

1.3 Aims of project

As discussed above, the liver BMP/SMAD signalling pathway evidently plays a crucial role in maintaining iron homeostasis by controlling hepcidin expression. Notably, *Bmp6* was shown to be a non-redundant endogenous regulator of iron-induced hepcidin response via the BMP/SMAD signalling pathway, since it was the only Bmp whose expression responds to changes in liver iron concentration (Kautz et al., 2008). However, the molecular mechanism as to how iron accumulation is sensed by our body and turned into a signal to upregulate *Bmp6* is unknown. Whilst the IRP/IRE system has been demonstrated to control the expression of many genes involved in iron homeostasis, the *Bmp6* mRNA does not contain IREs and is not regulated by IRPs (Sanchez et al., 2011). Therefore, the fundamental aim of this thesis is to identify an alternative iron-sensing mechanism that controls hepatic *Bmp6* expression, and thus maintains systemic iron homeostasis.

The Nrf2 antioxidant response system can be activated by excess iron. Bach1, which plays an opposing role to Nrf2, is also directly targeted for degradation by haem. The derepression of Bach1 and activation of Nrf2 has been shown to be involved in intracellular iron homeostasis, such as the control of ferritin heavy and light chains expression for intracellular iron storage and the regulation of ferroportin and haem oxygenase 1 expression for erythrocytes iron recycling by macrophages. However, Nrf2's involvement in the regulation of hepcidin and systemic iron homeostasis is not well-characterised. Earlier studies have shown that *Nrf2*-knockout mice on either a normal iron diet or high iron diet have a trend towards, albeit non-significant, lower levels of hepcidin expression (Silva-Gomes et al., 2014). Another group of investigators independently demonstrated elevated liver iron and reduced serum hepcidin levels in 13-week old but not 6-week old *Nrf2*-knockout mice on a normal iron diet (Okada et al., 2012), suggesting that the absence of Nrf2 is associated with progressive accumulation of iron with age. Yet, how Nrf2 affects iron homeostasis is not mechanistically well-defined. *In vitro* studies have claimed that NRF2 directly controls *HAMP1* expression (Bayele et al., 2015), but the lack of well-controlled experiments questions the plausibility of the data (see Chapter 5) and warrants more efforts in dissecting the molecular mechanism as to how Nrf2 controls iron homeostasis.

The first aim of this thesis is to elucidate the molecular mechanism as to how *Bmp6* expression is induced in response to iron. We hypothesize that Nrf2 acts as a molecular sensor for iron- or haem-induced oxidative stress, and converts this toxic signal into a mechanism to influence systemic iron levels via hepcidin. Specifically, we investigated whether the upregulation of *Bmp6* expression in response to iron is Nrf2-dependent by performing a series of experiments involving knockdown of *Nrf2 in vitro* and knockout of *Nrf2 in vivo*. The effects of pharmacological Nrf2 inducers on *Bmp6* expression were also studied both *in vitro* and *in vivo*.

Upon demonstrating that *Bmp6* is an Nrf2-dependent gene, the second aim of this thesis is to study whether the loss of Nrf2 hinders the regulation of hepcidin and alters iron status. This was investigated by comparing hepcidin expression and hepatic iron concentration in *Nrf2*-deficient and wildtype mice. The toxicity of iron in *Nrf2*-deficient and wildtype mice was also accessed by measuring hepatic lipid peroxidation levels as a marker of oxidative stress levels. The role of Nrf2 was also studied in the context of haemochromatosis through characterising iron phenotypes in *Hfe*/*Nrf2* double knockout mice, and by assessing the effects of *NRF2* single nucleotide polymorphisms in *HFE*-C282Y haemochromatosis patients.

Lastly, we aimed to determine whether pharmacological activation of Nrf2 confers protection against the iron overload disease haemochromatosis by enhancing the Bmp/hepcidin axis and by exerting general antioxidant and cytoprotective effects. *Hfe*-knockout haemochromatosis mice and *Hamp1*-knockout mice were given a small molecule pharmacological activator of Nrf2, and hepatic iron and gene expression of *Bmp6*, hepcidin, and other Nrf2 target genes were assayed.

Chapter 2

Materials and Methods

2.1 Mice breeding and husbandry

Unless otherwise stated, animal procedures were performed under the authority of UK Home Office project and personal licenses in accordance with the Animals (Scientific Procedures) Act 1986, and were approved by the University of Oxford ethical review committee. Mice were housed in individually ventilated cages and fed ad-libitum with standard diet containing 188 ppm iron (SDS Dietex Services, diet 801161).

Wildtype C57BL6 mice were purchased from Envigo. C57BL6 mice were used for dietary iron loading (2ppm, 200ppm or 1% carbonyl iron diets), intraperitoneal iron-dextran (FeDx), intraperitoneal hemin, oral ferrous sulphate and intraperitoneal mitoTEMPO experiments.

Nrf2-knockout mice (RIKEN) were generated as described previously by replacing the genomic sequence encoding DNA-binding Neh1 domain in exon 5 of *Nrf2* with ß-galactosidase *lacZ* gene (Itoh et al., 1997) and bred by crossing heterozygotes. *Nrf2*-knockout mice and wildtype littermates were used for iron-loading ($FeSO_4$ oral gavage, 1 week or 4 weeks 1% carbonyl iron diet), intraperitoneal injections of hemin, and pharmacological Nrf2 activation with oral gavage of a small molecule Nrf2 agonist CDDO-Imidazole (CDDO-Im).

Inducible hepcidin-knockout (i*Hamp1*-knockout) mice were generated in our lab as described (Armitage et al., 2016). Briefly, mice with LoxP sites flanking exons 2 and 3 of *Hamp1* were crossed with Rosa-CreERT2 mice which express Cre recombinase fused to a modified oestrogen receptor (allowing nuclear translocation and activation by tamoxifen) under the control of the ubiquitous Gt(ROSA)26Sor promoter. i*Hamp1*-knockout mice were bred by crossing homozygous floxed-*Hamp1* mice and either heterozygous or wildtype Rosa-CreERT2 mice to obtain Cre-positive floxed-*Hamp1* (i*Hamp1*-knockout) mice or Cre-negative floxed-*Hamp1* (i*Hamp1*-control) mice.

iNOS-knockout mice (Jackson Laboratory) were a gift from Prof Keith Channon and Dr Eileen McNeill (University of Oxford) and bred by crossing heterozygotes. *iNOS*-knockout and wildtype littermates were used for intraperitoneal FeDx experiments.

The following experimental procedures were approved by the *Instituto de Biologia Molecular e Celular* Animal Ethics Committee and were done in collaboration with Dr Tiago L. Duarte:

(i) *Nrf2* wildtype, heterozygous knockout and homozygous knockout mice treated with 4mg FeDx or dextran control for 24 hours

(ii) *Nrf2* wildtype, heterozygous knockout and homozygous knockout mice treated with 2 doses of 50µmol/kg hemin or saline control for 24 hours

(iii) *Nrf2*-knockout and wildtype littermate mice fed 2 weeks of 2% carbonyl iron diet or 200ppm iron diet control

(iv) *Hfe/Nrf2*-knockout mice bred to up to 24 months of age

(v) *Hfe*-knockout mice treated with 1 or 10 doses of 30µmol/kg CDDO-Im or vehicle control

(vi) *Hamp1*-knockout mice treated with 10 doses of 30µmol/kg CDDO-Im or vehicle control

Mice were bred and received humane care according to the EU Directive 2010/63/EU. The mice were fed ad-libitum with standard diet containing 200 ppm iron (Envigo, Teklad 2018S).

Liver sinusoidal endothelial cells (LSECs) isolation studies were performed by Dr Jodie L. Babitt and Dr Chia-Yu Wang (Boston, MGH). Protocols were approved by the Institutional Animal Care and Use Committee at Massachusetts General Hospital.

2.2 Mice genotyping

Transgenic mice were genotyped by performing PCR on ear tissues. Ear tissues were lysed in 75µl alkaline lysis buffer (25mM NaOH / 0.2mM EDTA, pH=12) at 95ºC for 2 hours, then neutralised with 75µl 40mM Tris HCl (pH=5.5). 5µl lysate was used for PCR genotyping using MyTaq Red mix (Bioline, BIO-25044) and 0.2µM primers in a final volume of 25µl.

2.2.1 *Nrf2*-knockout mice genotyping

Primers for *Nrf2*-knockout mice genotyping PCR are:

(i) Primer Nrf2-5 (5'- TGGACGGGACTATTGAAGGCTG -3')

(ii) Primer Nrf2-AS (5'- GCCGCCTTTTCAGTAGATGGAGG -3')

(iii) Primer LacZ (5'- GCGGATTGACCGTAATGGGATAGG -3')

PCR cycling conditions are:

1. Initial denaturation: 2 minutes at 94ºC
2. Denaturation: 30 seconds at 94ºC
3. Annealing: 30 seconds at 60ºC
4. Extension: 30 seconds at 72ºC
5. Repeat steps 2 to 4 for 30 cycles.
6. Final extension: 10 minutes at 72ºC

Amplicons are 734bp (*Nrf2*-wildtype allele) and 400bp (*Nrf2*-knockout allele)

2.2.2 *iNOS*-knockout mice genotyping

Primers for *iNOS*-knockout mice genotyping PCR are:

(i) Primer iNOS-WT-Forward (5'- TCCGATTTAGAGTCTTGGTGA -3')

(ii) Primer iNOS-KO-Forward (5'- CCTTCTATCGCCTTCTTGACG -3')

(iii) Primer iNOS-Reverse (5'- TCACCACCAGCAGTAGTTGC -3')

PCR cycling conditions are:

1. Initial denaturation: 5 minutes at 94ºC
2. Denaturation: 40 seconds at 94ºC
3. Annealing: 40 seconds at 56ºC
4. Extension: 30 seconds at 72ºC
5. Repeat steps 2 to 4 for a total of 40 cycles.
6. Final extension: 10 minutes at 72ºC

Amplicons are 640bp (*iNOS*-wildtype allele) and 200bp (*iNOS*-knockout allele)

2.2.3 i*Hamp1*-knockout mice genotyping

Primers for *iHamp1*-knockout mice genotyping PCR are:

(i) Primer Cre-Forward (5'- CGTTTTCTGAGCATACCTGGA -3')

(ii) Primer Cre-Reverse (5'- ATTCTCCCACCGTCAGTACG -3')

PCR cycling conditions are:

1. Initial denaturation: 5 minutes at 95ºC
2. Denaturation: 30 seconds at 95ºC
3. Annealing: 30 seconds at 60ºC
4. Extension: 45 seconds at 72ºC
5. Repeat steps 2 to 4 for a total of 35 cycles.
6. Final extension: 10 minutes at 72ºC

Amplicon is 472bp (Cre-positive i*Hamp1*-knockout).

2.3 *In vivo* treatments

Dietary iron loading: Mice were fed 2ppm iron diet (Harlan, TD.99397), 200ppm iron control diet (Harlan, TD.07801) or 1% carbonyl iron diets *ad-libitum* (Harlan, TD.09077, equivalent to 10,000ppm iron) for 1, 3 or 4 weeks; diets were matched for other constituents. For 2% carbonyl iron loading experiment, *Nrf2*-knockout and wildtype mice were fed control 200ppm iron control diet or 2% carbonyl iron diet (Harlan, 2018S) for 2 weeks. For LSEC experiments, wildtype male 129S6/SvEvTac mice were fed control 37ppm iron or 1% carbonyl iron diets (Research Diets) for 4 weeks.

Iron-dextran (FeDx) treatment: Mice were given intraperitoneal (i.p.) injections of FeDx (1mg, 2mg, 4mg; Sigma, D8517) or dextran (Dx) control (Sigma, D9260) for 6 or 24 hours.

Genetic deletion of hepcidin: i*Hamp1*-control and i*Hamp1*-knockout mice were given 1mg tamoxifen (Sigma, T5648) in 90% corn oil / 10% ethanol i.p. for 4 consecutive days.

Ferrous sulphate treatment: Mice were fed 2ppm iron diet ad-libitum for 3 weeks, followed by oral gavage with 2mg/kg elemental iron as ferrous sulphate (Sigma, F7002) or water control and culled 6 hours later.

Hemin treatment: Hemin (Sigma, 512800) was reconstituted in 0.2M sodium hydroxide and pH adjusted to 7.4 with hydrochloric acid. Mice were administered two i.p. doses of 50µmol/kg hemin or saline 12-hours apart and culled 12 hours after the last hemin dose.

Neutralisation of oxidative stress with free radical scavenger mitoTEMPO: 0.25mg mitoTEMPO (Sigma, SML0737) dissolved in saline was administered i.p. 1 hour after gavage with 2mg/kg elemental iron (as $FeSO_4$) and culled 6 hours later.

Pharmacological activation of Nrf2 with CDDO-Imidazole (CDDO-Im): Mice were given CDDO-Im (Tocris Bioscience, 4737) dissolved in DMSO and reconstituted in PBS / 5% Tween80 / 5% PEG300 or vehicle control (equivalent volume of DMSO in PBS / 5% Tween80 / 5% PEG300) by oral gavage. Each dose of CDDO-Im was 30µmol/kg. For repeated dosing, mice were gavaged on Mondays, Wednesdays and Fridays each week and culled 6 hours after the last dose.

Mice were euthanized in increasing CO_2 concentrations. Livers and spleens were harvested in RNAlater for RNA extraction and gene expression quantification, and/or snap-frozen for non-haem iron measurement, Nrf2 protein detection, malondialdehyde quantification, and fixed in formalin for histology analysis. Serum was collected for iron and hepcidin measurements. Heart and pancreas from *Hfe*/*Nrf2*-knockout mice were also harvested for histology analysis. Duodenal enterocytes were isolated by agitating 3cm duodenum in DMEM / 5mM EDTA / 5% FCS at 37ºC for 20 minutes, followed by centrifugation to collect the dissociated epithelial cells for gene expression analysis.

2.4 Cell cultures and *in vitro* treatments

Mouse L929 fibroblast, mouse embryonic fibroblasts (MEF), mouse C2C12 myoblast cells and human hepatoma-derived HepG2 cells were maintained in Dulbecco's modified Eagle's medium (DMEM*)* supplemented with 10% fetal bovine serum (FBS), 2mM glutamine, 100U/ml penicillin and 0.1mg/ml streptomycin.

Cells were treated with 0.1 to 1mg/ml FeDx (Sigma, D8517), 2 to 10µM hemin (Sigma, 51280), 200µg/ml ferric ammonium citrate (FAC) (Sigma, F5879) and/or mitoTEMPO (Sigma,

SML0737) for 6 hours. siRNA-mediated gene knockdown experiments were performed using Lipofectamine RNAiMAX reagent with Dharmacon siGENOME SMARTpool siRNA targeting mouse *Nrf2* (M-040766-01-0005), mouse *Bach1* (M-042956-01-0005), mouse *Keap1* (M-041104-01-0005) or human NRF2 (M-003755-02-0005) in antibiotics-free medium for 24hours (*Nrf2*/*NRF2*) or 48hours (*Bach1* and *Keap1*).

In collaboration with Dr Jodie L. Babitt and Dr Chia-Yu Wang (MGH, Boston), CD1 mouse primary liver sinusoidal endothelial cells (Cell Biologics) were maintained in complete mouse endothelial cell medium with growth factor supplement. CD1 cells were treated with either 100nM CDDO-Im or 200µg/ml FAC for 6 hours.

2.5 Gene expression analysis by quantitative real time PCR (qRT-PCR)

Total RNA was extracted from liver and spleen explants, duodenal enterocytes and *in vitro* experiments with RNeasy plus (Qiagen, 74136) and reverse transcribed to cDNA (Life Technologies, 4387406) according to the manufacturers' protocols. Quantitative real time PCR was performed using 1 to 5ng/µl cDNA on the Applied Biosystems 6500 Fast Real-Time PCR system machine using TaqMan assays listed in Table 1, except for *Hfe/Nrf2*-knockout mice and LSECs experiments.

In *Hfe/Nrf2*-knockout experiment (performed by Tiago Duarte), RNA was extracted using TriZol, DNase-treated, and reverse transcribed to cDNA (ThermoScript RT-PCR System). Relative gene expression levels were quantified with iQ SYBR Green Supermix, with primers listed in Table 2 using iQ5 Real-Time PCR Detection System. The quantity of each transcript was estimated against the respective standard curve and normalized against the quantity of the endogenous control gene Hypoxanthine phosphoribosyltransferase 1 (*Hprt1*).

In LSECs experiments (performed by Chia-Yu Wang), livers were dissected after cardiac perfusion with 25ml sterile PBS. Single cell suspension was made by incubating 200mg liver 10minutes at 37°C in 1ml cocktail containing 450U/ml collagenase I, 125U/ml collagenase XI,

60U/ml Dnase I, 60U/ml Hyaluronidase and 20mM HEPES (Sigma). After cell suspension was filtered through 40µm cell strainer, non-parenchymal cells were pelleted at 750 X g for 7minutes at 4°C and resuspended in PBS containing 1% FBS and 0.5% BSA. Endothelial cells were isolated by fluorescence-activated cell sorting on a FACSAria II (BD Biosciences) as CD45-, CD31+, Lin-, MHCII-, CD64-, CD146+ cells. Total RNA was isolated from purified LSECs using PicoPure RNA Isolation Kit (Thermo Scientific). cDNA was synthesized using the SuperScript VILO cDNA Synthesis Kit (Invitrogen). PCR reactions were carried out by using the PowerUp SYBR Green Master Mix (Applied Biosystems) on the QuantStudio3 Real-Time PCR system (Applied Biosystems), with primers listed in Table 3.

Table 1: List of TaqMan Gene Expression assays (Applied Biosystems)

Protein	**Gene**	**Assay code**
Mouse		
Hypoxanthine-guanine phosphoribosyltransferase	*Hprt1*	Mm01545399_m1
Bone morphogenetic protein 6	*Bmp6*	Mm01332882_m1
NAD(P)H dehydrogenase, quinone 1	*Nqo1*	Mm01253561_m1
Heme oxygenase 1	*Hmox1*	Mm00516005_m1
Glutamate-cysteine ligase catalytic subunit	*Gclc*	Mm00802655_m1
Hepcidin	*Hamp1*	Mm04231240_s1
Nuclear factor (erythroid-derived 2)-like 2	*Nfe2l2 (Nrf2)*	Mm00477784_m1
Kelch-like ECH associated protein 1	*Keap1*	Mm00497268_m1
BTB And CNC Homology 1	*Bach1*	Mm01344527_m1
Inhibitor of DNA-binding protein 1	*Id1*	Mm00775963_g1
Sons of mothers against decapentaplegic 6	*Smad6*	Mm00484738_m1
Sons of mothers against decapentaplegic 7	*Smad7*	Mm00484742_m1
Atonal bHLH transcription factor 8	*Atoh8*	Mm00464055_m1
Bone morphogenetic protein 2	*Bmp2*	Mm01340178_m1
Ferritin heavy chain	*Fth1*	Mm00850707_g1
Ferritin light chain	*Ftl1*	Mm03030144_g1
Collagen type I alpha I chain	*Col1a1*	Mm00801666_g1
Transgelin	*Tagln*	Mm00441661_g1
Human		
Glyceraldehyde 3-phosphate dehydrogenase	*GAPDH*	Hs99999905_m1
Nuclear factor (erythroid-derived 2)-like 2	*NFE2L2 (NRF2)*	Hs00975961_g1
Bone morphogenetic protein 6	*BMP6*	Hs01099594_m1
Heme oxygenase 1	*HMOX1*	Hs01110250_m1
NAD(P)H dehydrogenase, quinone 1	*NQO1*	Hs01045993_g1
Hepcidin	*HAMP*	Hs00221783_m1

Table 2: List of primers for *Hfe/Nrf2*-knockout liver qRT-PCR

Gene	**Forward primer sequence (5'-3')**	**Reverse primer sequence (5'-3')**
Hprt1	AGATGGGAGGCCATCACATTGT	ATGTCCCCCGTTGACTGATCAT
Bmp6	TCCCCACATCAACGACACCA	TCCCCACCACACAGTCCTTG
Nqo1	GTGCAGAAGCGAGCTGGAAATACTC	CGAATCTTGATGGAGGACTGGATGC
Hamp1	CCTATCTCCATCAACAGATG	AACAGATACCACACTGGGAA

Table 3: List of primers for LSECs qRT-PCR

Gene	Forward primer sequence (5'-3')	Reverse primer sequence (5'-3')
Rpl19	AGGCATATGGGCATAGGGAAGAG	TTGACCTTCAGGTACAGGTGTG
Bmp6	AGCACAGAGACTCTGACCTATTTTT	CCACAGATTCTAGTTGCTGTGA
Nqo1	GCCCGCATGCAGATCCT	GGTCTCCTCCCAGACGGTTT
Hmox1	CAGCCCCACCAAGTTCAAA	TCAGGTGTCATCTCCAGAGTGTTC

2.6 Western blot

Cells were pelleted for nuclear and cytoplasmic fractionation using NEPER protein extraction kit (Thermo Scientific, 78833). Whole cell extracts were harvested using the RIPA lysis buffer (ThermoFisher, 89900) with protease and phosphatase inhibitor cocktail. Liver tissues were agitated with glass beads (Sigma, G8772) and lysed in RIPA buffer (ThermoFisher, 89900). Proteins were separated by 10% SDS-polyacrylamide gel electrophoresis, transferred onto 0.2µm nitrocellulose membrane, and probed with antibodies against Nrf2 (Cell Signaling Technology, C1Z9C), Bach1 (R&D systems, AF5777), lamin A (Abcam, ab8980), and GAPDH (Proteintech, 60004).

2.7 Tissue non-haem iron measurement

Tissues were dried for 3 hours at 100ºC, weighed and digested in 10% tricholoroacetic acid / 30% hydrochloric acid for 20 hours at 65ºC. Non-haem iron content was determined colourimetrically by measuring absorbance at 535nm immediately following reaction with chromogen reagent containing 0.1% (w/v) bathophenanthrolinedisulphonic acid (Sigma, 146617) / 0.8% thioglycolic acid (Sigma, 88652) against a standard curve using titrating concentrations of FAC.

2.8 Tissue histology

Liver tissues from wildtype and *Nrf2*-knockout mice fed 1% carbonyl iron diet for 4 weeks were fixed in 10% neutral-buffered formalin and processed to paraffin. 4µm-thick sections were stained with Perls' Prussian blue stain using standard techniques at the Oxford Centre for

Histopathology Research. Sections were examined by a pathologist (Dr Elizabeth Soilleux, Oxford JR Hospita, UKl) and photographed using a Nikon DS-FI1 camera with a Nikon DS-L2 control unit (Nikon UK Limited) and Olympus BX40 microscope (Olympus UK Limited).

Liver and spleen samples from *Hfe*-knockout mice given CDDO-Im, and liver, heart and pancreas tissues from *Hfe*/*Nrf2*-knockout mice were fixed in 10% neutral-buffered formalin and embedded in paraffin. 3µm-thick sections were stained with Perls' Prussian blue for ferric iron using standard procedures at Ipatimup Diagnostics (Ipatimup, Porto, Portugal).

2.9 Liver malondialdehyde (MDA)

Liver tissues were agitated with glass beads (Sigma, G8772) and lysed in RIPA buffer (ThermoFisher, 89900). Lysates were used for quantification of malondialdehyde (MDA) using the thiobarbaturic acid reactive substance (TBARS) kit according to the manufacturer's protocols (Cayman Chemical, 700870). Briefly, liver lysates were allowed to react with thiobarbaturic acid at 95ºC for 1hour, and absorbance of the solution was measured at 530nm.

2.10 Serum measurements

Blood was taken by cardiac puncture immediately after euthanising mice. Serum was prepared by centrifugation of clotted blood at 8000 x g for 5 minutes in BD Microtainer SST tubes (Beckton Dickinson). Serum hepcidin was quantified by competitive ELISA using the Hepcidin-Murine Compete Kit (Intrinsic Lifesciences) according to the manufacturer's protocol. For mice given $FeSO_4$ gavage, serum iron was quantified using the MULTIGENT Iron Kit on the Abbott Architect c16000 automated analyzer (Abbott Laboratories) at Oxford John Radcliffe Hospital, UK. For *Hfe*-knockout and *Hamp1*-knockout mice given 10 doses of CDDO-Im, serum iron was quantified in a Cobas C8000 analyzer (Roche Diagnostics, Mannheim, Germany) at *Centro Hospitalar do Porto*.

2.11 Statistics

Statistical analyzes were performed using Prism 6 (GraphPad Software).

Chapter 3

Iron and hemin alter the Bmp6/hepcidin axis and activate Nrf2

3.1 Background

3.1.1 Hepatic *Bmp6* expression fluctuates with alterations in iron status

The BMP/SMAD signalling pathway plays a crucial role in regulating iron homeostasis via the control of hepcidin synthesis; it was first found to be associated with iron homeostasis in juvenile haemochromatosis patients carrying mutations in the BMP coreceptor hemojuvelin (Papanikolaou et al., 2004). Although recombinant BMP2, BMP4, BMP5, BMP6, BMP7 and BMP9 proteins can upregulate hepcidin expression *in vitro* (Babitt et al., 2007), *Bmp6* and *Bmp2* appear to be the most physiologically relevant to iron homeostasis. Both *Bmp2* and *Bmp6* expression are necessary for controlling iron homeostasis in mice, since LSEC-specific deletion of either *Bmp2* or *Bmp6* led to a blunted hepcidin expression and consequentially elevated iron status (Canali et al., 2017; Koch et al., 2017). In response to perturbations in iron status by feeding mice diets with altered iron content, *Bmp6* appeared to be the only BMP that is endogenously induced in response to dietary iron accumulation and suppressed during iron deficiency in mice. In the same *in vivo* dietary iron model, *Bmp2* expression was elevated upon iron accumulation but unaltered in iron deficiency (Kautz et al., 2008). Additionally, elevated hepatic iron content was paralleled by increased gene expression of *Bmp6* in an *Hfe*-knockout haemochromatosis mouse model, although *Bmp2* expression was unaltered (Corradini et al., 2009). In humans, an upregulation of *BMP6* expression is also observed in iron-loaded hereditary haemochromatosis patients (Ryan et al., 2010). Collectively, these point towards *Bmp6* as an endogenous regulator that fluctuates with iron status and plays a critical role in controlling hepcidin and so iron homeostasis. Nonetheless, the molecular mechanism as to how iron is sensed to generate a signal to control *Bmp6* expression has not been elucidated. Understanding this mechanism is the fundamental aim of this thesis.

3.1.2 Iron and haem activates the Nrf2 antioxidant response pathway

The antioxidant response pathway is controlled by a balance between the transcriptional activator Nrf2 and transcriptional repressor Bach1, both of which bind to antioxidant response elements (AREs) and control the expression of ARE-regulated genes. The classical ARE-driven genes encode proteins with antioxidant and cytoprotective functions, such as *Nqo1*, *Hmox1* and *Gclc*.

Nqo1 encodes a 2-electron reductase that prevents the formation of free radicals by ensuring complete oxidation of quinones. *Hmox1* controls the catabolism of the pro-apoptotic free haem as a cytoprotective mechanism. *Gclc* encodes the rate-limiting enzyme in synthesis of glutathione, a tripeptide that carries a thiol group and functions as an antioxidant by donating electrons to neutralise reactive radicals. The expression of these antioxidant genes is controlled in a complex manner, despite the fact that they are all ARE-regulated. In a series of siRNA-mediated knockdown of Keap1, Bach1 or Nrf2 in keratinocytes (Macleod et al., 2009), *Hmox1* was shown to be heavily Bach1-repressed as the knockdown of Bach1 led to more than a 100-fold induction of *Hmox1*. Bach1 knockdown upregulated the expression of *Gclc* by only 1.5-fold and did not alter *Nqo1* expression. Knockdown of Nrf2 led to similar magnitudes of repression in *Nqo1*, *Hmox1* and *Gclc*. In comparison, knockdown of Keap1 (the inhibitor of Nrf2) led to an upregulation of these 3 genes, with the largest effect observed for *Gclc*. These demonstrated that ARE-regulated genes have different sensitivities to Nrf2 activation and Bach1 derepression.

Redox-active metals, including iron, catalyse the formation of free radicals that in turn react with and disrupt biological molecules. Oral and intravenous iron supplementation is associated with elevated levels of free radicals and lipid peroxidation in humans and rat models (reviewed in Koskenkorva-Frank et al., 2013). In addition, elevated hepatic iron content in mice fed modified diets containing trimethyl-hexanoyl-ferrocene was associated with increased Nrf2 activity based on induction of phase I/II detoxification enzymes (Moon et al., 2012), demonstrating that iron-induced oxidative stress can trigger the Nrf2 antioxidant response pathway as a cytoprotective mechanism. Moreover, the role of Nrf2 in cellular iron homeostasis has been well-documented. Elevation in cellular iron content leads to an Nrf2-dependent transcriptional upregulation of *Fth* and *Ftl*, allowing cells to store iron in the catalytically inactive form within ferritin (Tsuji et al., 2000; Wasserman and Fahl, 1997). Nrf2 also facilitates the recycling of iron from senescent erythrocytes by controlling the transcription of *Hmox1* to release iron from haem and of *Slc40a1* to mediate cellular iron export via ferroportin (Marro et al., 2010).

Free haem is a pro-oxidant and pro-apoptotic compound and its levels can be elevated during haemolytic events. When cells experience excess haem, the antioxidant response pathway is de-repressed via haem-mediated proteosomal degradation of Bach1. Haem may also directly activate Nrf2 by inducing oxidative stress via several mechanisms. Haem elevates the levels of ROS in macrophages but this effect is abrogated with the iron chelator deferoxamine, suggesting that the iron molecule in haem can cause oxidative stress (Fortes et al., 2012). Additionally, haem may contribute directly to the formation of superoxides by serving as a prosthetic group for NADPH oxidase, since haem-induced superoxide production can be blocked by an NADPH oxidase inhibitor (Graça-Souza et al., 2002). These free radicals generated in response to haem can then directly activate Nrf2 by destabilising the Nrf2-Keap1-Cullin3 complex. The derepression of Bach1 and activation of Nrf2 in response to haem upregulates *Hmox1*, which exerts its cytoprotective effects by catabolising haem (Gozzelino et al., 2010).

3.1.3 Chapter aims

The upregulation of *Bmp6* expression and Nrf2 activity in response to iron accumulation has been independently demonstrated by various groups of researchers as described above. There are however no studies to date detailing concurrent activation of Nrf2 and upregulation of *Bmp6* by iron, or by haem, within a single system. Hence, the first aim of this Chapter is to investigate whether iron and haem triggers the antioxidant response via altering the Nrf2/Bach1 axis and upregulates *Bmp6* in parallel, and whether this was generalizable across several models of iron overload.

Secondly, we assessed the effects of iron on expression of two other Bmps. *Bmp2* can be upregulated by iron accumulation (Kautz et al., 2008) and has been shown to be involved in iron homeostasis through controlling basal hepcidin expression (Koch et al., 2017). Moreover, soluble hemojuvelin proteins can block the induction of hepcidin by recombinant BMP2 and BMP4 *in vitro* (Babitt et al., 2007). Thus, changes in hepatic *Bmp2* and *Bmp4* expression were also quantified in the *in vivo* iron and haem-treatment models.

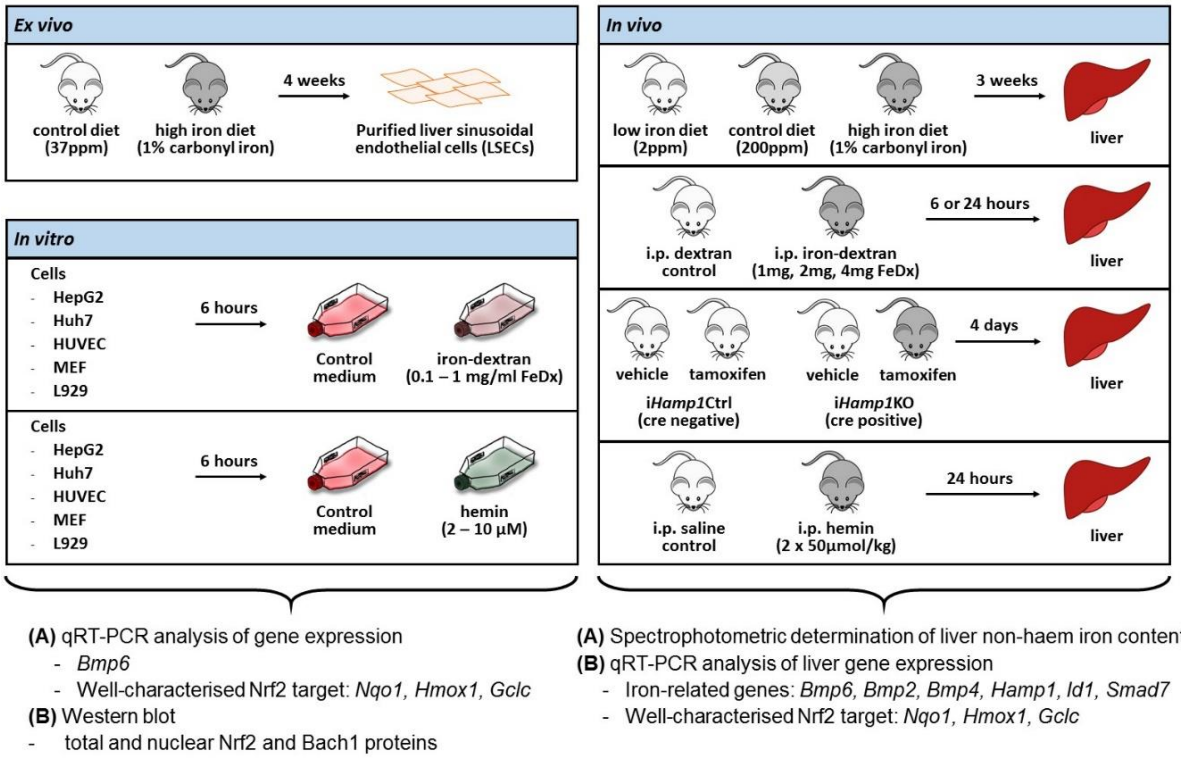
3.1.4 Methodology

We established *ex vivo*, *in vitro* and *in vivo* models of iron accumulation and exposure to haem and looked for concurrent activation of Nrf2 and upregulation of *Bmp6* expression in these models (summarised in Figure 3.1). Details on cell culture, animal husbandry and reconstitution of chemicals are documented in Chapter 2.

Ex vivo: Since iron accumulation causes the upregulation of *Bmp6* in LSECs, which then activates the Bmp/Smad signalling pathway in neighbouring hepatocytes via paracrine signal, we performed *ex vivo* studies on LSECs isolated from iron-loaded mice in collaboration with Dr Jodie L. Babitt and Chia-Yu Wang (MGH, Boston). Wildtype 129S6/SvEvTac male mice were fed control diet containing 37ppm iron or a high iron diet containing 1% carbonyl iron for 4 weeks, after which, LSECs were purified from the liver. 200mg of PBS-perfused livers were incubated at 37 °C in 1 ml cocktail containing 450U/ml collagenase I, 125 U/ml collagenase XI, 60 U/ml Dnase I, 60 U/ml Hyaluronidase and 20 mM HEPES (Sigma-Aldrich) to obtain a single cell suspension. The cell suspension was filtered through 40 µm cell strainer and centrifuged at 750 x g for 7 minutes at 4 °C to obtain a pellet containing non-parenchymal cells. The cells were then resuspended in PBS containing 1% FBS and 0.5% BSA. The cells were sorted on a FACSAria II (BD Biosciences) using the following monoclonal antibodies: anti-Ly-6C (clone AL-21, BD Biosciences), anti-CD45.2 (clone 104, BD Biosciences), anti-CD3e (clone 145-2C11, ebioscience), anti-CD90.2 (clone 53-2.1, BD Biosciences), anti-CD19 (clone 6D5, Biolegend), anti-MHC-II (clone AF6-120.1, BD Biosciences), anti-F4/80 (clone BM8, Biolegend), anti-NK1.1 (clone PK136, BD Biosciences), anti-Ly-6G (clone 1A8, BD Biosciences), anti-CD11b (clone M1/70, BD Biosciences), anti-CD146 (clone ME-9F1, BioLegend), anti-CD31 (clone 390, BioLegend), anti-CD326 (clone G8.8, BioLegend), anti-CD64 (clone X54-5/7.1, BioLegend). LSECs were identified as CD45-, CD31+, Lin-, MHCII-, CD64-, CD146+. mRNA was extracted from purified LSECs and reverse transcribed into cDNA for qRT-PCR of *Bmp6*, as well as classical Nrf2 target genes *Nqo1*, *Hmox1* and *Gclc*.

In vitro: Human hepatoma-derived cell lines HepG2 and Huh7, primary human umbilical vein endothelial cells (HUVEC), mouse embryonic fibroblasts (MEF), and L929 mouse fibroblast cells were treated with 0.1mg/ml or 1mg/ml iron-dextran (FeDx), or with 2μM or 10μM hemin for 6 hours. qRT-PCR was performed to determine whether *Bmp6* is upregulated in response to iron and hemin. Nrf2 activity was determined by qRT-PCR of *Nqo1*, *Hmox1* and/or *Gclc*, and by performing Western blot on nuclear and cytoplasmic fractions as well as whole cell extract for Nrf2 and Bach1 proteins.

In vivo: Mouse models of iron accumulation were established via altering dietary iron content, intraperitoneal administration of iron, or by inducing the genetic deletion of hepcidin in mice. In the dietary loading model, 3-week old C57BL6 male mice were given diets containing 2ppm iron (low), 200ppm iron (control) or 1% carbonyl iron (high) for 3 weeks *ad libitum*. 6-week old male and female C57BL6 mice were also challenged with iron by intraperitoneal injections of 1mg, 2mg or 4mg of FeDx and sacrificed 6 hours or 24 hours later. Iron accumulation by genetic intervention was also performed by deleting hepcidin in an inducible i*Hamp1*-knockout mouse model (Armitage et al., 2016). Mice that express Rosa-CreERT2 recombinase (i*Hamp1*KO) and have LoxP sites flanking exons 2 and 3 of *Hamp1* were injected with vehicle or 1mg tamoxifen in 90% corn oil / 10% ethanol intraperitoneally daily for 4 consecutive days to activate the Cre recombinase ubiquitously and excise exons2 and 3 of *Hamp1*. Floxed-*Hamp1* mice that do not express Rosa-CreERT2 (i*Hamp1*Ctrl) mice were also given the same tamoxifen treatment regimen to control for off-target effects of tamoxifen, since they cannot excise *Hamp1* without the Cre recombinase. The *in vivo* effects of haem were also investigated by intraperitoneal administration of 50μmol/kg hemin in mice, two doses 12 hours apart. Mice were sacrificed 12 hours after the second dose of hemin. Liver non-haem iron was quantified colourimetrically from these mice. mRNA was also extracted from the livers for qRT-PCR to measure *Bmp6*, *Bmp2*, *Bmp4* and Bmp pathway target genes *Hamp1*, *Id1* and *Smad7* in response to iron and hemin, as well as *Nqo1*, *Hmox1* and *Gclc* as a proxy for Nrf2 activation.



(A) qRT-PCR analysis of gene expression
- *Bmp6*
- Well-characterised Nrf2 target: *Nqo1, Hmox1, Gclc*

(B) Western blot
- total and nuclear Nrf2 and Bach1 proteins

(A) Spectrophotometric determination of liver non-haem iron content

(B) qRT-PCR analysis of liver gene expression
- Iron-related genes: *Bmp6, Bmp2, Bmp4, Hamp1, Id1, Smad7*
- Well-characterised Nrf2 target: *Nqo1, Hmox1, Gclc*

Figure 3.1: *Ex vivo*, *in vitro* and *in vivo* models of iron and haem challenge. Nrf2 activity was assayed by quantification of Nrf2 target genes *Nqo1*, *Hmox1* and *Gclc* and/or by measuring Nrf2 and Bach1 protein levels in nuclear fractions and whole cell lysates. *Bmp6* expression was quantified by qRT-PCR. *In vivo*, hepatic *Bmp2*, *Bmp4* and Bmp pathway target genes *Hamp1*, *Id1* and *Smad7* expression were also quantified by qRT-PCR, and liver non-haem iron content was measured.

3.2 Results

3.2.1 Dietary iron upregulates *Bmp6* expression and activates Nrf2 in purified liver sinusoidal endothelial cells

The spatial regulation of *Bmp6* expression within the liver has been characterised in recent years. Gene expression quantification in various populations of cells in the liver demonstrated that *Bmp6* is upregulated in non-parenchymal cells but not hepatocytes in response to dietary iron loading (Enns et al., 2013). Moreover, conditional knockout of *Bmp6* specifically in liver sinusoidal endothelial cells (LSECs) mirrors the iron loading phenotype observed in global *Bmp6*-knockout mice; in contrast, deletion of *Bmp6* in hepatocytes and macrophages did not cause iron accumulation (Canali et al., 2017), suggesting that *Bmp6* is predominantly induced in LSECs and signals to neighbouring hepatocytes to upregulate hepcidin expression via paracrine signalling. Thus, we purified LSECs from 129S6/SvEvTac mice fed either control diet containing 37ppm iron or high iron diet containing 1% carbonyl iron (CI) for 4 weeks. Gene expression analysis by qRT-PCR demonstrated parallel upregulation of *Bmp6* and the classical Nrf2 antioxidant genes *Nqo1*, *Hmox1* and *Gclc* in purified LSECs following *in vivo* iron loading (Figure 3.2).

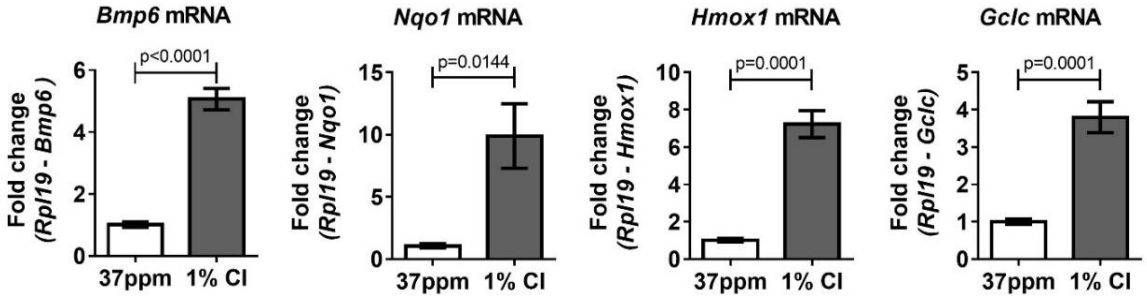


Figure 3.2: qRT-PCR was performed on purified LSECs from mice fed a diet containing either 37ppm iron or 1% carbonyl iron (1% CI) for 4 weeks. Dietary iron loading increased gene expression of *Bmp6* and classical Nrf2-dependent antioxidant genes *Nqo1*, *Hmox1* and *Gclc* in parallel (n=4, paired t-test).

3.2.2 Iron upregulates *Bmp6* expression and Nrf2 activity simultaneously *in vitro* in L929 cells

The purification of LSECs from mouse livers is technically complicated and the cells are difficult to culture *in vitro* for use in downstream assays such as siRNA-mediated gene knockdown. As such, we aimed to establish an *in vitro* model using an immortalised cell line that responds to iron by increasing *Bmp6* expression. In a preliminary screen, human hepatoma-derived cells Huh7 and Hep3B, and human umbilical vein endothelial cells (HUVEC) were treated with 0.1mg/ml or 1mg/ml iron-dextran (FeDx) for 6 hours and gene expression of *BMP6* and *HMOX1* were quantified by qRT-PCR. In agreement with literature demonstrating that hepatocytes have low levels of *Bmp6* expression, *BMP6* mRNA levels in Huh7 (Figure 3.3) and HepG2 (Figure 3.4) were in the order of 1 copy per 100,000 copies of *GAPDH*, in comparison to 1 copy per 100 copies of *GAPDH* in HUVEC endothelial cells (Figure 3.5). FeDx increased the expression of *HMOX1* but *BMP6* expression was not convincingly upregulated in Huh7 and HepG2 (Figure 3.3, Figure 3.4), in line with previously published data that hepatocytes do not induce *Bmp6* expression in response to iron. FeDx also increased *HMOX1* but decreased *BMP6* expression in HUVEC, which is in contrary to purified LSEC cells, suggesting that upregulation of *BMP6* by iron is a tissue specific response (Figure 3.5).

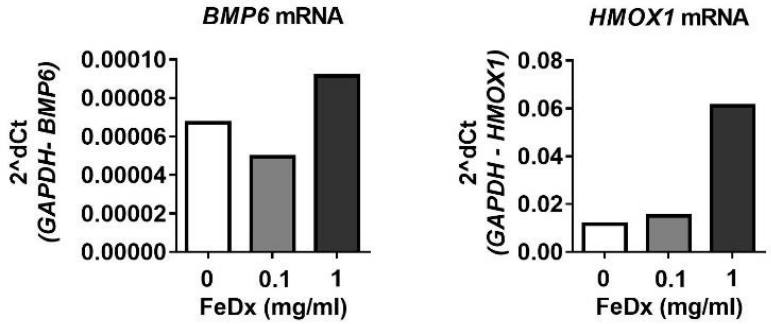


Figure 3.3: Huh7 cells were treated with 0.1mg/ml or 1mg/ml iron-dextran (FeDx) for 6 hours and qRT-PCR was performed. FeDx upregulated the expression of *HMOX1* but did not alter *BMP6* expression (n=1).

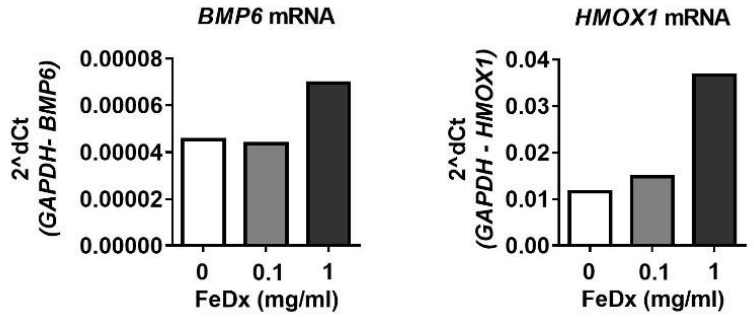


Figure 3.4: HepG2 cells were treated with 0.1mg/ml or 1mg/ml iron-dextran (FeDx) for 6 hours and qRT-PCR was performed. FeDx upregulated the expression of *HMOX1* but did not alter *BMP6* expression (n=1).

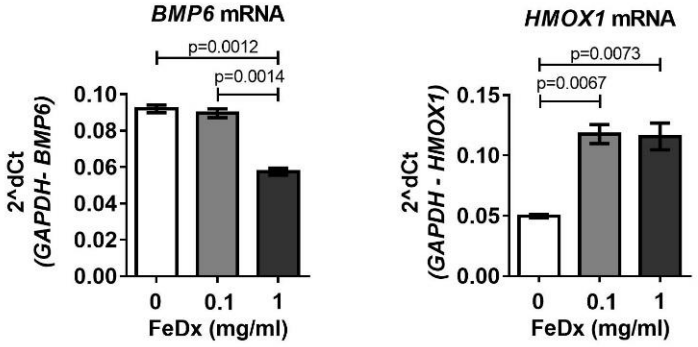


Figure 3.5: HUVEC cells were treated with 0.1mg/ml or 1mg/ml iron-dextran (FeDx) for 6 hours and qRT-PCR was performed. FeDx upregulated the expression of *HMOX1* but did not alter *BMP6* expression (n=2, ANOVA).

Subsequently, we treated mouse embryonic fibroblasts (MEF) and mouse L929 fibroblast cells with 0.1mg/ml or 1mg/ml FeDx for 6 hours. In MEF cells, *Bmp6* expression was significantly higher in cells treated with 1mg/ml FeDx compared to 0.1mg/ml FeDx, although the magnitude of difference is small. *Nqo1* expression was also significantly upregulated, albeit with a small magnitude induction, in response to FeDx. *Hmox1* and *Gclc* expression was not significantly altered (Figure 3.6). Interestingly, FeDx upregulated *Bmp6* expression in L929 cells and concurrently increased the expression of Nrf2-dependent detoxification genes *Nqo1, Hmox1* and *Gclc* (Figure 3.7A). Western blot was also performed on whole cell lysates as well as nuclear and cytoplasmic fractions of L929 cells, with lamin A as a nuclear marker and GAPDH as a cytoplasmic marker; nuclear accumulation of Nrf2 proteins was observed upon FeDx treatment in a dose-dependent manner (Figure 3.7B). Collectively, these data demonstrate the parallel upregulation of *Bmp6* expression and induction of Nrf2 activity by iron in L929 cells.

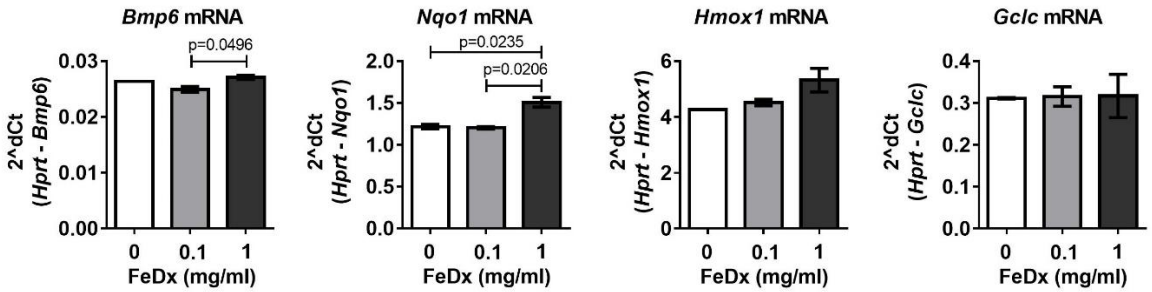


Figure 3.6: MEF cells were treated with 0.1mg/ml or 1mg/ml iron-dextran (FeDx) for 6 hours and qRT-PCR was performed. FeDx significantly altered *Bmp6* and *Nqo1* expression, although the magnitude of induction was small, and did not alter *Hmox1* and *Gclc* expression (n=2, ANOVA).

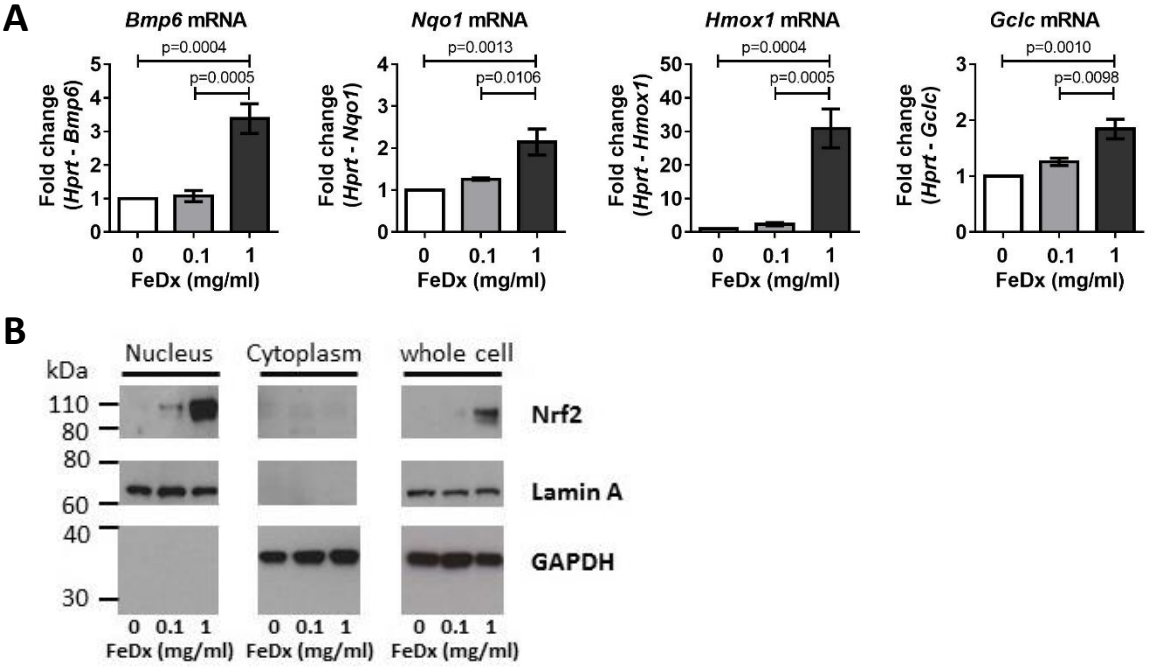


Figure 3.7: **(A)** qRT-PCR and **(B)** Western blot was performed on L929 cells 6 hours after treatment with 0.1mg/ml or 1mg/ml iron-dextran (FeDx). FeDx upregulated the expression of *Bmp6* and Nrf2-dependent genes *Nqo1, Hmox1* and *Gclc* simultaneously (n=4, ANOVA). FeDx also induced nuclear accumulation of Nrf2 proteins.

3.2.3 Hepatic iron accumulation simultaneously upregulates *Bmp6* and hepcidin and enhances Nrf2 activity *in vivo*

In addition to *in vitro* experiments, we wanted to investigate how altering hepatic iron *in vivo* via chronic or acute iron challenges affects the expression of *Bmp6*, downstream Bmp-target genes including hepcidin, and Nrf2-target genes.

Firstly, 3-week old C57BL6 male mice were fed a low iron diet containing 2ppm iron, normal diet containing 200ppm iron or a high iron diet containing 1% CI for 3 weeks *ad libitum*. Dietary iron loading increased liver non-haem iron content and increased the expression of *Bmp6* and Bmp-target genes *Hamp1*, *Id1* and *Smad7*. Concurrently, upregulation of *Nqo1, Hmox1* and *Gclc* was observed, consistent with activation of Nrf2 (Figure 3.8).

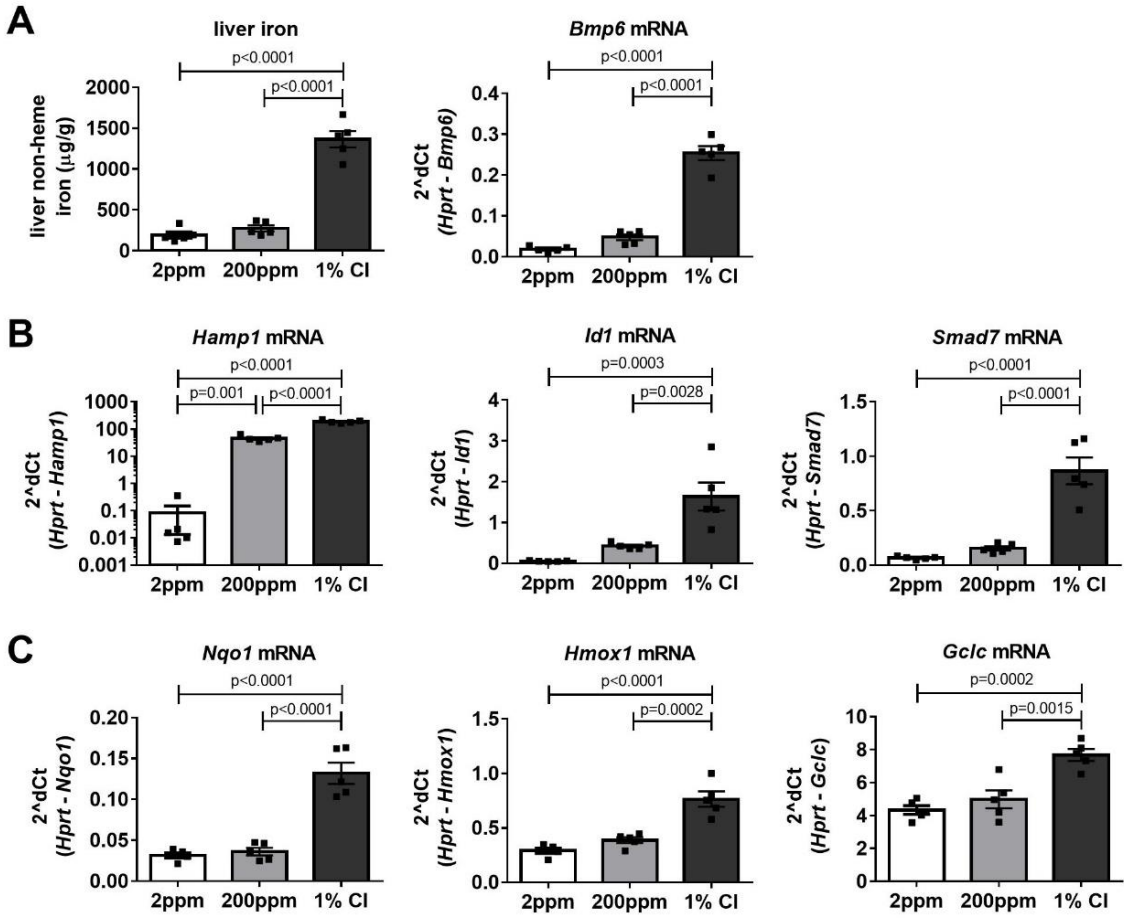


Figure 3.8: C57BL6 mice were fed *ad libitum* with diets containing either 2ppm iron, 200ppm iron or 1% carbonyl iron (1% CI) for 3 weeks. **(A)** Dietary iron loading increased hepatic iron concentration and *Bmp6* expression in a dose-dependent manner. **(B)** Expression of Bmp-target genes *Hamp1*, *Id1* and *Smad7* were also elevated in iron-loaded mice. **(C)** Nrf2-dependent antioxidant genes *Nqo1*, *Hmox1* and *Gclc* were also upregulated in response to iron accumulation (n=5, ANOVA).

In a second *in vivo* model of iron loading, 6-week old male C57BL6 mice were injected intraperitoneally with dextran (Dx) control or various doses of iron-dextran (FeDx) at 1mg, 2mg or 4mg. 24 hours later, hepatic iron was quantified and gene expression was measured by qRT-PCR. Injection with FeDx increased liver non-haem iron content and upregulated the expression of *Bmp6* and the downstream Bmp pathway target genes *Hamp1* and *Id1* in a dose-dependent manner. FeDx also activated the Nrf2 antioxidant response pathway, as demonstrated by increased *Nqo1*, *Hmox1* and *Gclc* gene expression (Figure 3.9). Intraperitoneal injection of 4mg FeDx gave the most robust induction of *Bmp6* expression, Bmp signalling and Nrf2 activity and did not lead to observable adverse effects in mice, thus we chose this dose for subsequent experiments.

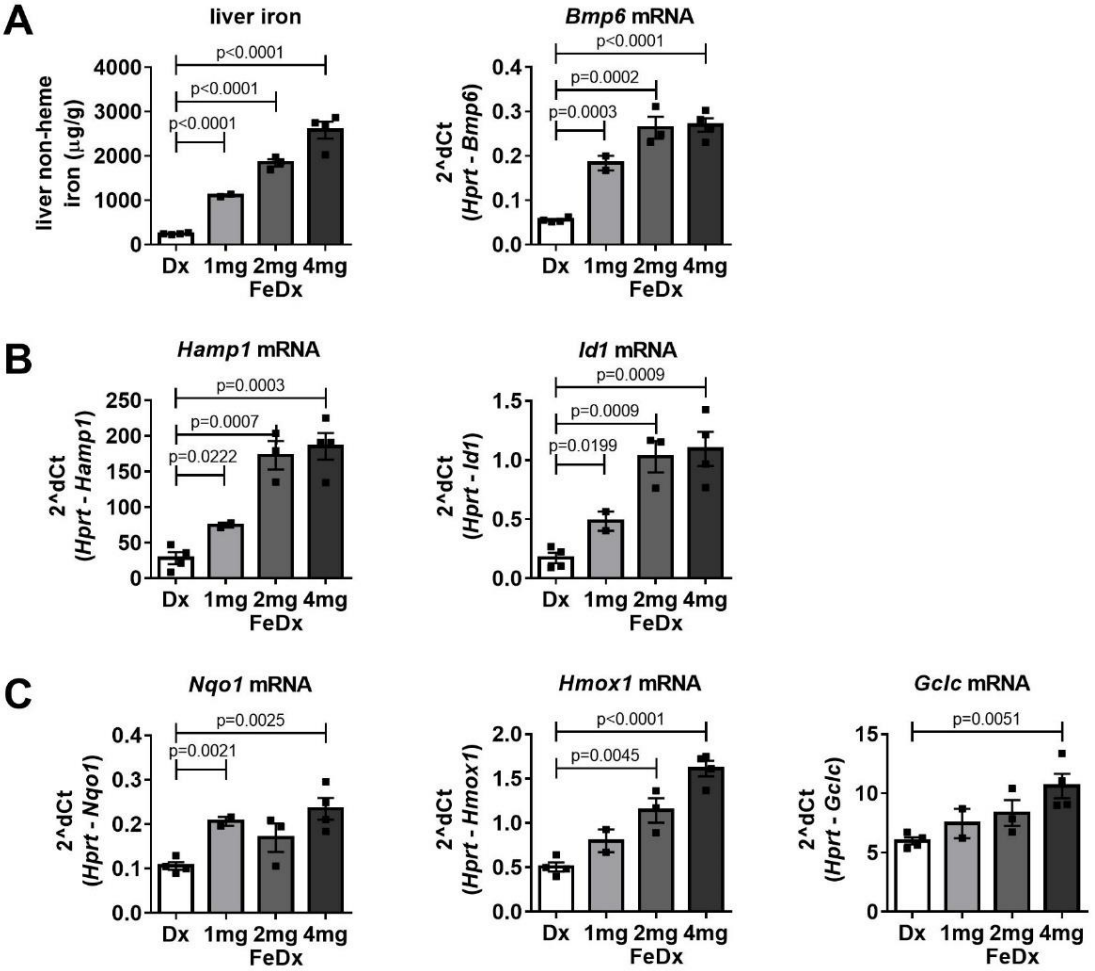


Figure 3.9: C57BL6 mice were injected with 1mg, 2mg or 4mg iron-dextran (FeDx, grey bars) or dextran control (Dx, white bar) and sacrificed 24 hours later. **(A)** FeDx injection increased liver non-heme iron and upregulated *Bmp6* expression in a dose-dependent manner. **(B)** Bmp-target genes *Hamp1* and *Id1* were also upregulated by FeDx dose-dependently. **(C)** Expression of Nrf2-target genes *Nqo1*, *Hmox1* and *Gclc* were also enhanced in response to FeDx (n=2 to 4, t-test).

Subsequently, 6-week old male and female C57BL6 mice were injected with 4mg FeDx or Dx control intraperitoneally and sacrificed 24 hours later for tissue iron quantification and gene expression analysis to determine whether iron overload causes similar changes in males and females. FeDx increased liver non-heme iron content in both male and female mice. Expression of *Bmp6* and downstream BMP pathway target genes *Hamp1* and *Id1* were also upregulated in response to FeDx. Concurrently, FeDx activated the Nrf2 antioxidant response as evident from increased *Nqo1*, *Hmox1* and *Gclc* expression (Figure 3.10). Notably, the baseline expression of *Nqo1* and *Hmox1* in mice given Dx, and the extent of hepcidin induction in response to FeDx were different in male and female mice, highlighting the need to use the block design with sex as a blocking factor for statistical analyses of experiments involving both males and females. Nevertheless, *Bmp6* expression and Nrf2 activity was consistently upregulated in response to hepatic iron accumulation in both males and females.

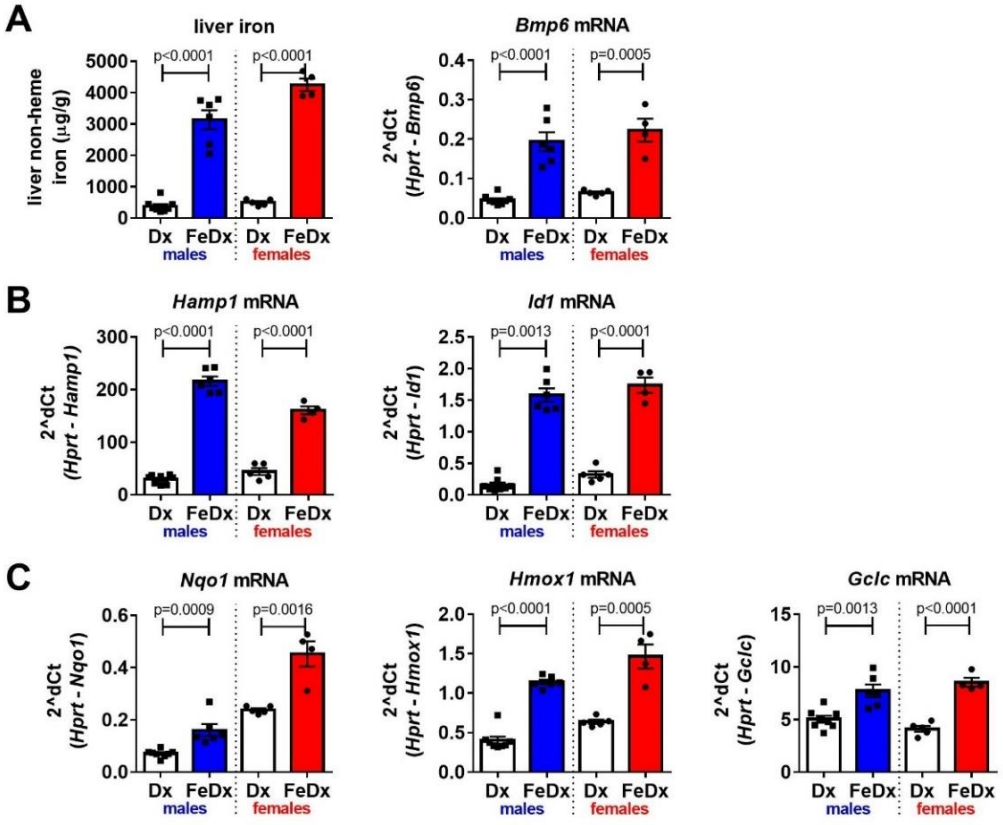


Figure 3.10: C57BL6 mice were injected with 4mg iron-dextran (FeDx) or dextran (Dx) control and sacrificed 24 hours later. The left columns depict male mice injected with Dx (white) or FeDx (blue) while the right columns depict female mice injected with Dx (white) or FeDx (red). **(A)** FeDx injection increased liver non-heme iron and upregulated *Bmp6* expression. **(B)** Bmp-target genes *Hamp1* and *Id1* were also upregulated in FeDx-treated mice. **(C)** Expression of Nrf2-dependent antioxidant genes *Nqo1*, *Hmox1* and *Gclc* were also enhanced in response to FeDx (n=5 to 8, t-test).

To cause iron accumulation by genetic intervention, we deleted hepcidin in an inducible *Hamp1*-knockout mouse model. Mice that express Rosa-CreERT2 recombinase (i*Hamp1*KO) and have LoxP sites flanking exons 2 and 3 of *Hamp1* were injected with vehicle or tamoxifen daily for 4 days to activate the Cre recombinase ubiquitously and excise exons2 and 3 of *Hamp1*. Floxed-*Hamp1* mice that do not express Rosa-CreERT2 (i*Hamp1*Ctrl) mice were also given the same tamoxifen treatment regimen to control for off-target effects of tamoxifen, since they cannot excise *Hamp1* without the Cre recombinase. Deletion of hepcidin disrupted the iron homeostatic feedback loop, resulting in hepatic iron accumulation and upregulation of *Bmp6* expression and Bmp pathway target gene *Id1*. The expression of *Nqo1*, *Hmox1* and *Gclc* were also upregulated in iron-loaded tamoxifen-treated i*Hamp1*KO mice, suggesting concurrent Nrf2 activation and *Bmp6* induction in this inducible hepcidin deletion mouse model (Figure 3.11).

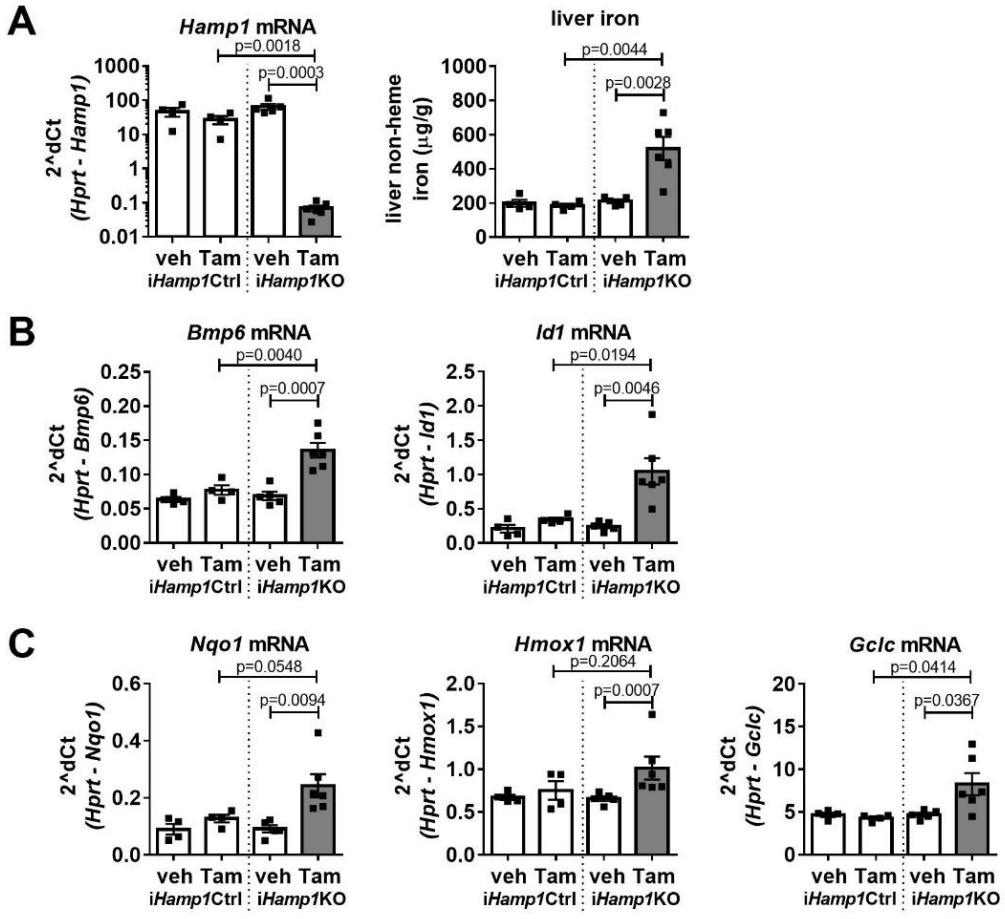


Figure 3.11: Cre-positive (i*Hamp1*KO) and Cre-negative (i*Hamp1*Ctrl) mice were injected with vehicle (veh) or 1mg tamoxifen (Tam) daily for 4 days. **(A)** Deletion of hepcidin causes liver non-heme iron accumulation and **(B)** upregulation of *Bmp6* and Bmp-target gene *Id1* compared to vehicle treated mice. **(C)** Expression of Nrf2-dependent genes *Nqo1*, *Hmox1* and *Gclc* were also induced in response to iron accumulation caused by hepcidin deletion (n=4 to 6, t-test).

3.2.4 Hemin upregulates *Bmp6* expression, degrades Bach1 and activates Nrf2

The Bach1 transcriptional repressor binds to AREs and suppresses the expression of ARE-associated genes, such as α- and ß-globin (Tahara et al., 2004a, 2004b), *Hmox1* (Reichard et al., 2007) and ferroportin (Marro et al., 2010). Haem induces Bach1 degradation and leads to the derepression of ARE-associated genes (Zenke-Kawasaki et al., 2007). This consequentially alters physiology, such as increasing haemoglobin synthesis in erythrocytes, and haem degradation and iron recycling in macrophages (Igarashi and Watanabe-Matsui, 2013; Marro et al., 2010). Hence, we investigated if haem-mediated Bach1 degradation and derepression of ARE-driven genes alters *Bmp6* expression.

L929 cells were treated with 2µM or 10µM hemin for 6 hours. Western blot was performed to measure Bach1 protein in the nuclear fraction and whole cell lysates of L929 cells. Hemin treatment resulted in reduction of Bach1 protein levels in the nuclear fraction as well as the whole cell lysate. In addition, stabilisation and nuclear accumulation of Nrf2 was observed. qRT-PCR analysis also showed upregulation of *Bmp6*, *Nqo1*, *Hmox1* and *Gclc* expression in L929 cells in response to hemin (Figure 3.12). Collectively, these data demonstrate that the derepression of Bach1 and activation of Nrf2 occurs in parallel with the upregulation of *Bmp6* expression upon hemin treatment *in vitro*.

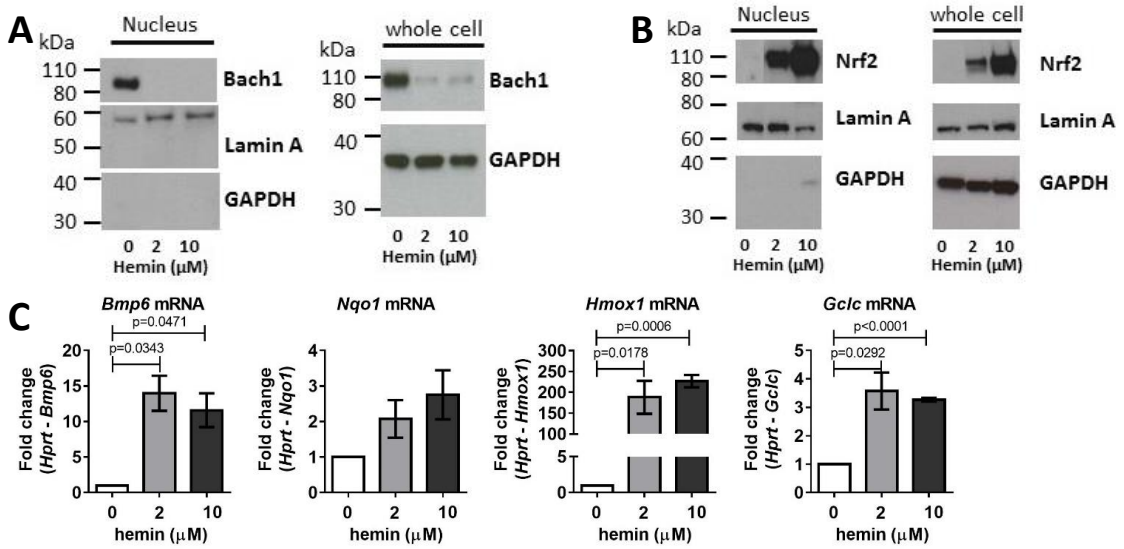


Figure 3.12: **(A)** Western blot for Bach1 protein and **(B)** Nrf2 protein was performed on L929 cells 6 hours after treatment with hemin. Hemin induced Bach1 nuclear export and degradation and Nrf2 stabilisation and nuclear accumulation. [Note: image has been cropped between 0µM and 2µM hemin treatment. The original blot has samples in the order of untreated, 0.1mg/ml FeDx, 1mg/ml FeDx, 2µM hemin and 10µM hemin. Please see Supplementary Figure 1 for full image.] **(C)** qRT-PCR analysis demonstrated parallel upregulation of *Bmp6*, *Nqo1*, *Hmox1* and *Gclc* by hemin (n=4, ANOVA).

In addition, hepatoma-derived Huh7 and HepG2 cells, HUVEC cells and MEF cells were also treated with 2µM or 10µM hemin for 6 hours. qRT-PCR analysis showed robust upregulation of *HMOX1* in Huh7, HepG2 and HUVEC cells in response to hemin. Hemin also caused induction of *BMP6* expression in a dose-dependent manner in Huh7 and HepG2 cells, although the magnitude of induction is much smaller compared to that of *HMOX1* (Figure 3.13A–B). *BMP6* was not upregulated by hemin in HUVEC cells (Figure 3.13C). In addition, treatment with hemin led to an induction in *Hmox1* and *Gclc* expression, but did not upregulate *Nqo1* or *Bmp6* expression in MEF cells (Figure 3.13D). The lack of robust *Bmp6* induction by hemin mirrors the trend observed in response to FeDx in these cells.

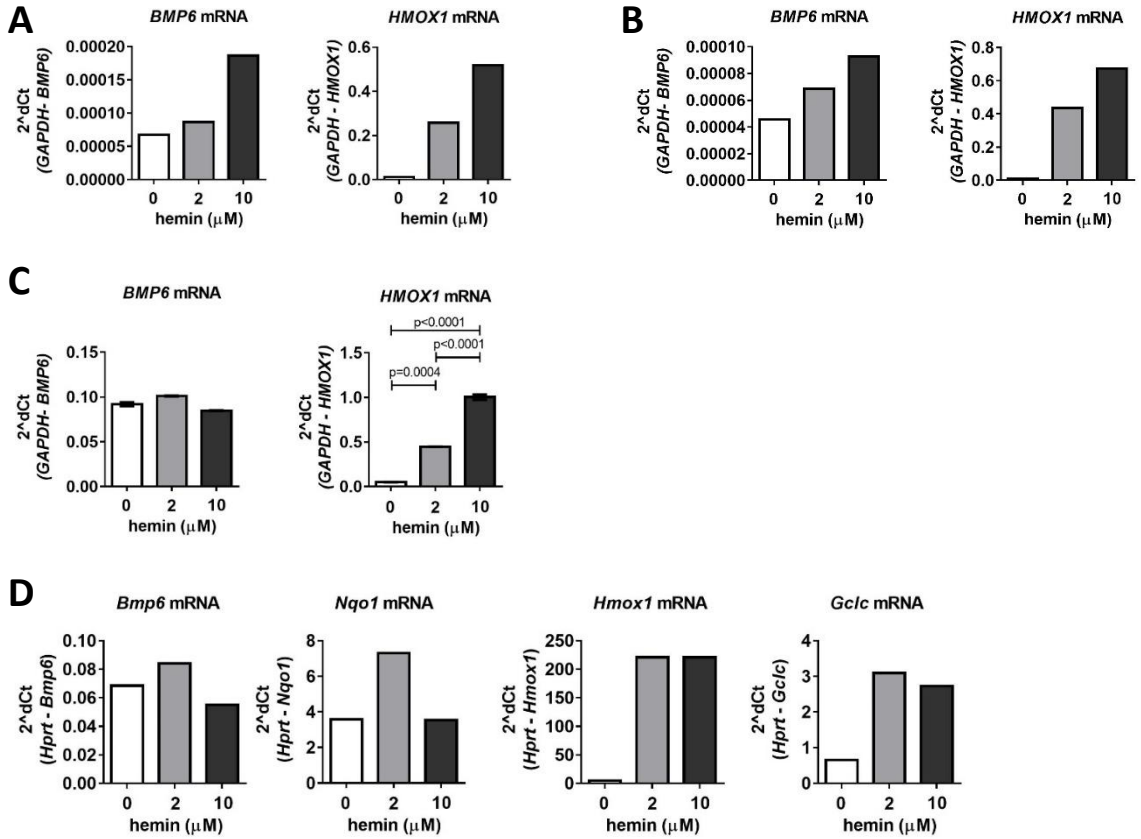


Figure 3.13: (A) Huh7 cells, **(B)** HepG2 cells, **(C)** HUVEC cells and **(D)** MEF cells were treated with 2µM and 10µM hemin for 6 hours. qRT-PCR analysis demonstrated robust induction of *HMOX1* expression but marginal or no increase in *BMP6* expression in Huh7, HepG2 and HUVEC cells in response to hemin. Hemin treatment also increased *Hmox1* and *Gclc*, but not *Bmp6* expression in MEF cells.

To study the effects of haem on *Bmp6* expression and Nrf2 activation *in vivo*, we injected C57BL6 mice with two doses of 50µmol/kg hemin or saline 12 hours apart intraperitoneally, and measured gene expression 12 hours after the second dose. Hemin did not lead to detectable changes in liver non-haem iron content, but led to increased hepatic *Bmp6* expression and a trend towards elevated Bmp signalling based on *Hamp1*, *Id1* and *Smad7* expression. Concurrently, Nrf2 activation was observed in hemin-treated mice, as demonstrated by increased *Nqo1*, *Hmox1* and *Gclc* expression (Figure 3.14).

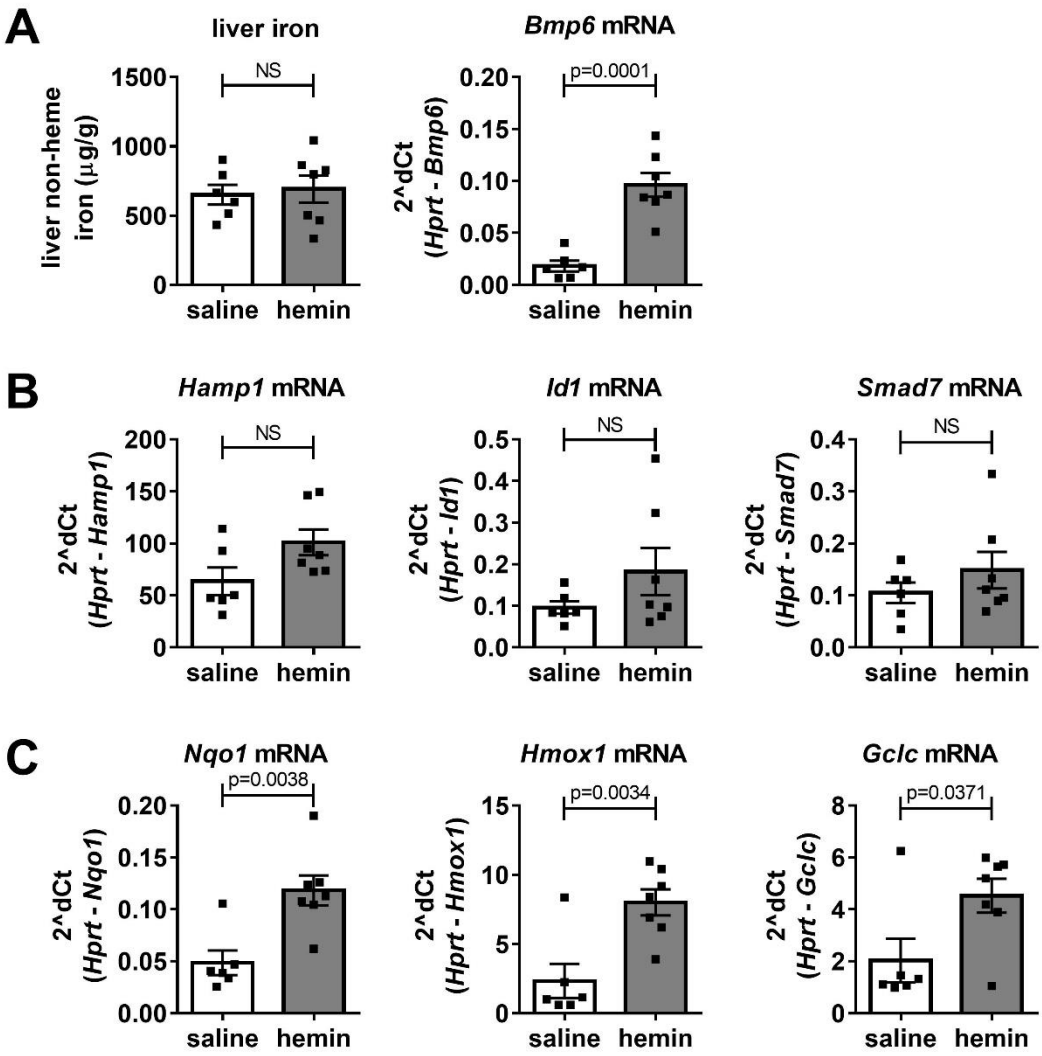


Figure 3.14: C57BL6 mice were intraperitoneally injected with 50µmol/kg hemin or saline, twice at 12 hours apart, and sacrificed 12 hours after the second injection. **(A)** Hemin did not alter liver non-heme iron content but upregulated *Bmp6* expression. **(B)** Expression of Bmp-target genes *Hamp1*, *Id1* and *Smad7* were marginally elevated in hemin-treated mice but not-significantly. **(C)** Expression of Nrf2-dependent antioxidant genes *Nqo1*, *Hmox1* and *Gclc* were also upregulated in response to hemin (n=6 to 8, t-test).

3.2.5 Effects of iron and hemin on the endogenous expression of *Bmp2* and *Bmp4*

Since BMP2 and BMP4 ligands can bind to hemojuvelin and upregulate the BMP signalling pathway to induce hepcidin expression (Babitt et al., 2006), and the expression of *Bmp2* in LSECs is necessary for hepcidin expression and iron homeostasis under resting conditions (Koch et al., 2017), we wanted to determine whether alterations in iron status affect endogenous *Bmp2* and *Bmp4* expression. Hence, we measured hepatic gene expression of *Bmp2* and *Bmp4* in mice in response to dietary iron loading, intraperitoneal FeDx, genetic deletion of hepcidin, and intraperitoneal hemin.

The expression of *Bmp2* was induced by dietary iron loading (consistent with Kautz et al., 2008) but not by injections with FeDx or hemin. Deletion of hepcidin in i*Hamp1*KO mice led to a marginal increase in *Bmp2* expression but that was not significantly different to tamoxifen-treated Cre-negative i*Hamp1*-control mice. *Bmp4* expression was downregulated in mice injected with FeDx, and unaltered in response to dietary iron loading, genetic deletion of hepcidin, or hemin injections (Figure 3.15). In contrast, *Bmp6* was consistently upregulated across our models of hepatic iron accumulation and hemin treatment as discussed previously. Thus, these data confirm that *Bmp6* expression is highly responsive to changes in iron status in comparison to *Bmp2* and *Bmp4*, although hepatic *Bmp2* expression may be increased to some extent by iron loading.

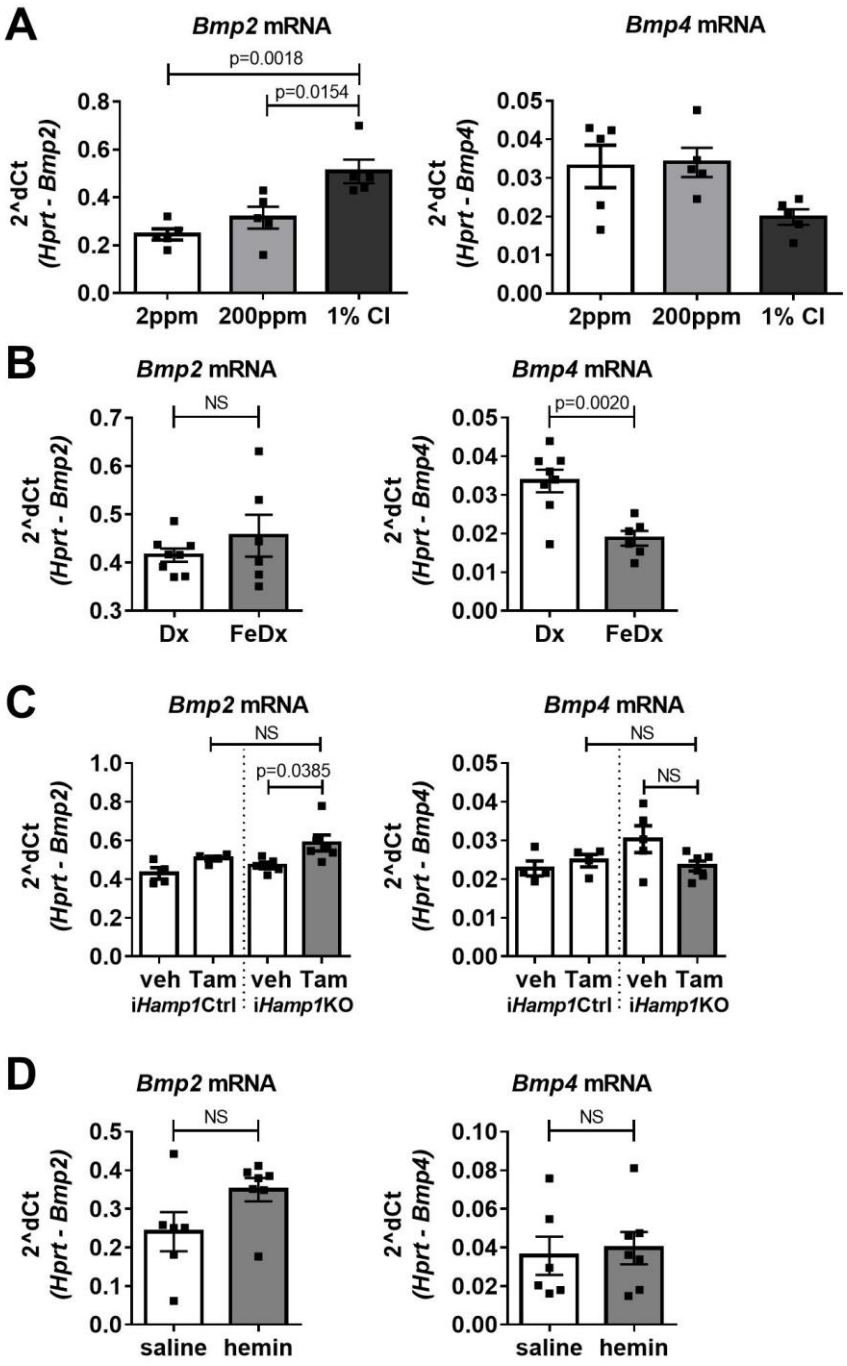


Figure 3.15: Liver gene expression of *Bmp2* and *Bmp4* in **(A)** C57BL6 mice fed 3 weeks of 200ppm iron or high iron diet containing 1% carbonyl iron (1% CI) (n=5, ANOVA), **(B)** C57BL6 mice intraperitoneally injected with dextran (Dx) or iron-dextran (FeDx) (n=6 to 8, t-test), **(C)** i*Hamp1*KO and i*Hamp1*Ctrl mice given vehicle (veh) or tamoxifen (Tam) daily for 4 days (n=4 to 6, t-test) and **(D)** C57BL6 mice given 2 intraperitoneal doses of hemin or saline control (n=6 to 8, t-test).

3.3 Discussion

This chapter documents several *ex vivo*, *in vitro* and *in vivo* models of iron accumulation and haem exposure and primarily investigates the effects of iron and haem on Nrf2 activity and *Bmp6* expression. Although there have been previous reports showing that iron activates the Nrf2 antioxidant response in mice (Moon et al., 2012), rats (Morales et al., 2014), and in *in vitro* cultures (Macco et al., 2013; Silva-Gomes et al., 2014), and that iron upregulates *Bmp6* gene expression (Corradini et al., 2009; Kautz et al., 2008; Ryan et al., 2010), these studies were conducted in separate biological systems of iron overloading. Thus, this is the first report to our knowledge demonstrating the concurrent activation of Nrf2 and upregulation of *Bmp6* expression in response to iron within one biological system. Moreover, the activation of Nrf2 and upregulation of *Bmp6* expression in parallel within the liver is generalizable across multiple *in vivo* models of liver iron overloading via (i) altering dietary iron content, (ii) intraperitoneal administration of iron, and (iii) genetic intervention of iron homeostasis by deleting hepcidin. More recently, LSECs were shown to be the main source of *Bmp6* in the liver, and have the greatest induction of *Bmp6* in comparison to hepatocytes and Kupffer cells in response to dietary iron loading. We purified LSECs from mice fed 4 weeks of normal or high iron diet and observed that Nrf2 activation occurs in parallel with *Bmp6* induction within this specific population of cells.

In a previously published microarray performed on livers of mice fed a low, normal or high iron diet (Kautz et al., 2008), the Nrf2 antioxidant response pathway was not picked up as a functional category that was overrepresented in response to dietary iron loading. However, we looked through the microarray data specifically for Nrf2-dependent genes and observed several of them in the list of genes that were induced in response to iron overload, including glutathione S-transferase, alpha 4 (*Gsta4*), UDP glucuronosyltransferase 1 family, polypeptide A6A (*Ugt1a6*), epoxide hydrolase 1, microsomal (*Ephx1*) and ferritin light chains (*Ftl1* and *Ftl2*) (Hu et al., 2006; Yeager et al., 2009). This provides corroborating evidence in support of our data that Nrf2 activation and *Bmp6* upregulation occurs simultaneously in response to iron accumulation.

In vitro, cell lines were treated with FeDx and tested for their ability to upregulate *Bmp6* gene expression in response to iron. An upregulation of *HMOX1* expression was observed in hepatoma-derived cells Huh7 and HepG2 in response to FeDx treatment, but *BMP6* expression was not robustly induced. FeDx also led to an increase in *HMOX1* expression, but a decrease in *BMP6* expression in HUVEC cells. Similarly, *Bmp6* was not convincingly induced in response to FeDx in MEF cells. Lastly, FeDx caused an upregulation of *Bmp6* and the classical Nrf2 target genes *Nqo1*, *Hmox1* and *Gclc* in L929 fibroblast cells. These experiments collectively suggest that iron is able to induce a general Nrf2 response in all the tested cell lines, which is in line with the fact that Nrf2 is ubiquitously expressed and acts as the main regulator of antioxidant response. However, of the tested cell lines, the induction of *Bmp6* expression was only observed in L929 cells. The lack of *BMP6* response to iron in hepatoma-derived cells was not unexpected, since the predominant subset of cells in the liver (hepatocytes) are not the major source of Bmp6 as discussed above.

The Nrf2/Bach1 axis can also be tilted in favour of Nrf2 activation and Bach1 derepression by haem. *In vivo*, intraperitoneal injection of hemin in mice caused an upregulation of hepatic *Bmp6* expression, alongside an induction in the ARE-regulated genes *Nqo1*, *Hmox1* and *Gclc*. The simultaneous upregulation of *Bmp6*, *Nqo1*, *Hmox1* and *Gclc* was also observed *in vitro* in L929 fibroblasts treated with hemin. Yet, intriguingly, the same cell lines that did not induce *Bmp6* expression in response to FeDx also failed to upregulate *Bmp6* in response to hemin.

The variability across different cell types in their ability to upregulate *Bmp6* in response to iron is striking. One plausible explanation could be that each cell type is unique and can have different levels of transcription regulators or repressive histone marks. Thus, the accessibility of the *Bmp6* promoter and enhancers to the transcriptional machinery may vary across different cell types and contribute to the differences in gene expression alterations to the same stimulus. Additionally, data in this Chapter showed that HUVEC cells have a higher baseline expression of *BMP6* than other tested cell lines, and is unable to upregulate *BMP6* in response to iron. However, unpublished data from our collaborator (Jodie Babitt, MGH Boston) demonstrates that iron chelation causes a

downregulation in *BMP6* expression. In the next Chapter, we also show that siRNA-mediated knockdown of *NRF2* suppresses *BMP6* expression. Thus, an alternative explanation could be that *Bmp6* expression is maximally expressed in certain cell lines such that treatment with iron cannot further induce its expression. The exact mechanism(s) underlying the variability in *Bmp6* response to iron across different cell lines is not further pursued within the thesis. However, it is worth noting that the variability in response is not unique to *Bmp6*. Instead, the control of ARE-regulated genes is generally complex and dependent on many factors, including the gene of interest, cell line and method of induction. It has been previously demonstrated that *Hmox1* is heavily Bach1-repressed as the knockdown of Bach1 in keratinocytes (HaCaT cell line) led to more than a 100-fold induction of *Hmox1*, while the other ARE-regulated genes tested for were either unaltered or upregulated up to 3-fold (Macleod et al., 2009). The authors also showed that *Nqo1* gene expression was unaltered upon knockdown of Bach1 in HaCaT cells; in contrast, we show in Chapter 4 that knockdown of Bach1 robustly increased *Nqo1* expression in L929, MEF and C2C12 cells, suggesting a cell line-dependent effect. Moreover, microarray analyses on livers from mice with hepatocyte-specific deletion of Keap1 (genetic activation model) and mice treated with a potent Nrf2 agonist CDDO-Imidazole (pharmacological activation model) showed that 196 genes were modulated only in the genetic activation model, 84 genes were modulated only in the pharmacological activation model, and 174 genes were modulated by both genetic and pharmacological activation (Yates et al., 2009), demonstrating that activating Nrf2 via different mechanisms causes different genes to be regulated.

Having achieved the first aim of this Chapter by demonstrating that iron and haem triggers the antioxidant response via altering the Nrf2/Bach1 axis and upregulates *Bmp6* in parallel in multiple models both *in vitro* and *in vivo*, the role of Nrf2 transcription factor in regulating *Bmp6* expression will be studied in the next Chapter. Additionally, the mechanism as to how iron activates Nrf2 will also be explored.

The second aim of this Chapter was to assess the effects of changes to iron status on the expression of *Bmp6* in comparison to expression of *Bmp2* and *Bmp4*, the former particularly because of its recently described role in hepcidin and iron regulation (Koch et al., 2017), and because soluble hemojuvelin blocks the induction of hepcidin by recombinant BMP2 and BMP4 *in vitro* (Babitt et al., 2007). In the microarray mentioned earlier on livers of mice fed a low, normal or high iron diet (Kautz et al., 2008), the authors highlighted that iron accumulation upregulates *Bmp2* expression while a reduction in liver iron content does not downregulate *Bmp2*. In contrast, *Bmp6* expression is altered in response to both a decrease and an increase in hepatic iron content. *Bmp4* was unaltered by dietary-induced changes in liver iron content. We performed dietary iron loading experiments in mice using rodent chow containing 2ppm iron, 200ppm iron and 1% CI and observed a dose-dependent increase in hepatic *Bmp2* and *Bmp6* expression, although the differences in gene expression between mice fed a 2ppm iron diet and mice fed a 200ppm iron diet were not statistically significant. Similar to the microarray data from Kautz, we did not observe significant changes in *Bmp4* expression. With the exception of the downregulation of *Bmp4* expression in response to intraperitoneal FeDx, *Bmp2* and *Bmp4* expression was unaltered in all other *in vivo* models of iron and hemin treatment documented in this thesis. In contrast, *Bmp6* was consistently upregulated across all our models of hepatic iron accumulation and hemin treatment. Thus, these data confirm that *Bmp6* expression is more sensitive to fluctuations in iron availability in comparison to *Bmp2* and *Bmp4*.

Chapter 4

Nrf2 regulates *Bmp6* expression in response to iron and haem

4.1 Background

4.1.1 *Bmp6* induction is associated with Nrf2 activation in response to iron

Bmp6 has been well-characterised as an essential signalling molecule involved in systemic iron homeostasis. Hepcidin expression is suppressed in *Bmp6*-knockout mice, and as a consequence, the mice are severely iron-loaded (Andriopoulos et al., 2009; Meynard et al., 2009). Downregulation of hepcidin and iron accumulation is also observed in mice with LSEC-specific deletion of *Bmp6* (Canali et al., 2017). Moreover, missense mutations in *BMP6* are associated with elevated serum ferritin and liver iron levels in humans (Daher et al., 2016). *Bmp6* has also been demonstrated as the critical endogenous responder to changes in hepatic iron content, as shown in Chapter 3 and also previously described by others (Kautz et al., 2008). Yet, how iron regulates the transcription of *Bmp6* is unknown. Thus, the first aim of this thesis is to identify an iron-sensing mechanism that regulates *Bmp6* expression in order to maintain systemic iron homeostasis. In Chapter 3, the upregulation of *Bmp6* expression and activation of Nrf2 concurrently in response to iron accumulation and hemin treatment was demonstrated in several *in vivo*, *ex vivo*, and *in vitro* models. This observation led us to hypothesize that the upregulation of *Bmp6* by iron is dependent on the transcriptional activator Nrf2.

4.1.2 Regulation of Nrf2 in response to physiological perturbations

The control of Nrf2 activity involves regulation at the transcriptional, post-transcriptional and post-translational level. Of these, the post-translational regulation of Nrf2 is the most extensively characterised.

Nrf2 protein is rapidly targeted for degradation at basal conditions and has a short half-life of less than 20 minutes (Itoh et al., 2003; Kobayashi et al., 2004c). The ubiquitin-mediated proteasomal degradation of Nrf2 is regulated by at least three different mechanisms involving (i) Keap1 and Cullin3 ubiquitin ligase, (ii) GSK3 and $SCF^{\beta\text{-}TrCP}$ ubiquitin ligase, and (iii) Hrd1 ubiquitin ligase. Firstly, Nrf2 associates with Keap1 through interactions between Neh2 domain of Nrf2 and Kelch domains and C-terminal region of Keap1. Keap1 functions as an adaptor that recruits the Cullin3

ubiquitin ligase and targets Nrf2 for ubiquitination and degradation by the 26S proteasome (Kobayashi et al., 2004c). The proteasomal degradation of Nrf2 is downregulated during oxidative stress as electrophilic agents modify the conformation of Keap1 by altering the disulphide bonds between thiol groups on Keap1, thus destabilising the Nrf2-Keap1-Cullin3 complex and preventing the ubiquitination of Nrf2 (described in Chapter 1). Nrf2 protein is also stabilised in conditions of elevated levels of nitric oxide •NO, such as the iNOS-dependent immune response mounted during bacterial infections, since •NO can associate directly with Keap1 at its cysteine 151 (C151) residue and destabilise the Nrf2-Keap1-Cullin3 complex (McMahon et al., 2010). In addition, the autophagosome cargo protein Sequesosome-1 (also known as p62) can compete with Nrf2 for binding with Keap1. In pathophysiological conditions of elevated p62 levels, such as in Hepatitis C virus-associated hepatocellular carcinoma, p62 binds to Keap1 and blocks the binding of Nrf2 to Keap1, thereby preventing ubiquitination and enhancing the stability of Nrf2 protein. This mechanism is thought to promote tumour survival and growth by upregulating genes encoding multidrug resistance proteins and enzymes involved in the biosynthesis of polysaccharides (Saito et al., 2016). The second mechanism regulating Nrf2 protein levels involves the $SCF^{\beta\text{-}TrCP}$ ubiquitin system. Nrf2 can be phosphorylated at its Neh6 domain by glycogen synthase kinase 3 (GSK3). The phosphorylated form is recognised by β-transducin repeats-containing proteins (β-TrCP), which serves as an adaptor for the S-phase kinase-associated protein 1 (Skp1) – Cullin – F-box (SCF) ubiquitin ligase and mediates the ubiquitination and degradation of Nrf2 (Rada et al., 2011). The physiological relevance of the regulation of Nrf2 by the $SCF^{\beta\text{-}TrCP}$ ubiquitin system is currently not well understood. Rada and colleagues proposed that an elevated GSK activity associated with neurodegenerative disorders, such as Parkinson's and Alzheimer's diseases, may account for the reduction in Nrf2 activity and thus higher levels of oxidative stress observed in these neurological diseases. Thirdly, the high mobility group (HMG)-CoA reductase degradation 1 (Hrd1) ubiquitin ligase regulates Nrf2 proteins by directly associating with the Neh4 and Neh5 domains of Nrf2. In human cirrhotic livers, *HRD1* is transcriptionally upregulated, which subsequently enhances the ubiquitination and degradation of NRF2 protein (Wu et al., 2014a).

Nrf2 can also be regulated at the transcriptional level. In particular, there are two ARE sequences located within 1000 base pairs upstream of the transcription start site of the *Nfe2l2* gene. Thus, the Nrf2 transcription factor is able to bind to the promoter region of *Nfe2l2* and positively autoregulate its own gene expression, which may consequentially allow the amplification of Nrf2 activity under stress conditions (Kwak et al., 2002). In addition, the aryl hydrocarbon receptor (AHR) is a ligand-activated transcription factor that may regulate the expression of Nrf2. The ligands of AHR include aromatic hydrocarbon-based environmental pollutants such as 2,3,7,8-tetrachlorodibenzo-p-dioxin (TCDD), and naturally occurring compounds including low-density lipoproteins and bilirubin. AHR binds to xenobiotic response elements (XRE) to induce the expression of genes encoding enzymes involved in metabolising xenobiotic compounds such as cytochrome P450 enzymes. AHR also binds to an XRE located within 1000 base pairs upstream and two XREs within 1000 base pairs downstream of the *Nfe2l2* transcription start site, thereby upregulating the gene expression of Nrf2 during xenobiotic-induced stress to enhance Nrf2-dependent cytoprotective mechanisms (Miao et al., 2005).

Post-transcriptionally, microRNA(miR)-mediated degradation of *Nfe2l2* mRNA have been described (reviewed by Kurinna and Werner, 2015). microRNAs with complementary nucleotide sequences are able to associate with *Nfe2l2* mRNA and recruit the RNA-induced silencing complex, causing the cleavage and degradation of *Nfe2l2* mRNA. For example, traumatic brain injury leads to an upregulation of miR-153 and miR-144 in the rat hippocampus, which bind to the 3' UTR of *Nfe2l2* mRNA and cause a reduction in Nrf2 mRNA and protein levels (Liu et al., 2014a).

4.1.3 Chapter Aims

In the previous chapter, we observed that the upregulation of *Bmp6* expression and activation of Nrf2 occurs simultaneously in response to iron accumulation and hemin treatment in several *in vivo*, *ex vivo*, and *in vitro* models. Thus, we hypothesize that the upregulation of *Bmp6* by iron is dependent on the transcriptional activator Nrf2. In this chapter, *in vivo* and *in vitro* experiments were set up to test this hypothesis.

In addition, the regulation of Nrf2 activity by various mechanisms at different levels have been documented in literature. Thus, we also investigated the molecular mechanism as to how iron activates Nrf2, and whether a blockade in this mechanism also affects the upregulation of *Bmp6* expression in response to iron.

Specifically, we aim to answer the following questions in this chapter:

(i) Is *Bmp6* an Nrf2-target gene?

(ii) Is the transcriptional upregulation of *Bmp6* in response to iron and haem dependent on Nrf2?

(iii) How does iron activate Nrf2?

4.1.4 Methodology

The methodology to study whether (i) *Bmp6* is an Nrf2-target gene, whether (ii) the transcriptional upregulation of *Bmp6* in response to iron and haem is dependent on Nrf2, and (iii) how iron activates Nrf2 is summarised in Figure 4.1.

In order to determine whether *Bmp6* is an Nrf2-target gene, publicly available Nrf2 ChIP-seq datasets were mapped onto the mouse genome on UCSC genome browser and queried to determine whether Nrf2 binds in proximity to the *Bmp6* promoter. The Nrf2 ChIP-seq datasets were generated from differentiated C2C12 myotube cells treated with the small molecule Nrf2 agonist CDDO-Imidazole (CDDO-Im) for 3 hours (Uruno et al., 2016) and from *Keap1*-knockout MEF cells (Malhotra et al., 2010). We subsequently validated the response of C2C12 and MEF cells to iron by treating them with ferric ammonium citrate (FAC) for 6 hours and measuring *Bmp6* expression.

Genetic interventions to alter the Nrf2/Bach1 axis *in vitro* was achieved through siRNA-mediated knockdown of Nrf2, Bach1 and Keap1 in L929, C2C12 and MEF cells. The knockdown efficiency was validated by quantifying the mRNA levels of the targeted genes, and detection of Nrf2, Bach1 or Keap1 proteins via Western blot. qRT-PCR was also performed to determine *Bmp6* gene expression levels 24 hours upon knockdown of Nrf2 and 48 hours after knockdown of Keap1, or Bach1. siRNA-mediated knockdown of NRF2 was performed in HUVEC and Huh7 cells, followed by quantification of *BMP6* expression.

Pharmacological activation of Nrf2 was also performed in L929 and LSECs by treating the cells with the small molecule Nrf2 agonist CDDO-Im, which binds to the BTB domain of Keap1 and disrupts the Keap1-Cullin3 interface either through steric hindrance or conformation change in Keap1 (Cleasby et al., 2014). *Bmp6* expression was quantified 2 and 4 hours post-treatment with CDDO-Im. Wildtype and *Nrf2*-knockout mice were also given a dose of CDDO-Im by oral gavage, and hepatic expression of *Bmp6* and other Nrf2-target genes was measured 6 hours post-treatment. In addition, phosphorylation of Nrf2 by GSK3 enhances the degradation of Nrf2 via the $SCF^{\beta\text{-TrCP}}$

ubiquitin system. Thus, L929 cells were treated with a GSK3 inhibitor (SB216763) to stabilise Nrf2 and qRT-PCR was performed to determine the gene expression of *Bmp6*.

Next, to investigate whether the induction of *Bmp6* in response to iron and hemin is Nrf2-dependent, L929, C2C12 and MEF cells were subjected to siRNA-mediated knockdown of Nrf2 for 24 hours, followed by treatment with 1mg/ml FeDx or 200µg/ml FAC for 6 hours. The induction of *Bmp6* by iron was compared between *Nrf2*-knockdown cells and control cells transfected with non-targeting control (NTC) siRNA. Additionally, *Nrf2*-knockout mice and wildtype littermates were subjected to hepatic iron accumulation by dietary iron loading and intraperitoneal administration of FeDx, or injected with hemin intraperitoneally. In the dietary iron loading model, 12-week old male mice were fed a high iron diet containing 2% CI or the 200ppm iron control diet for 2 weeks. In the FeDx model, 6-week old male and female mice were injected with 4mg FeDx intraperitoneally and sacrificed 24 hours later. In the hemin model, 6-week old male and female mice were injected with 2 doses of hemin (50µmol/kg body weight for each dose) 12 hours apart and culled 12 hours after the second dose of hemin. Additionally, in previously published data, when mice were fed a low iron diet (2ppm iron) for 2 weeks, followed by oral administration of 2mg/kg iron, hepatic *Bmp6* expression was modestly but significantly increased at 1 and 4 hours after oral iron administration with increase in serum transferrin saturation but no significant changes in liver iron content (Corradini et al., 2011b). Thus, we fed 5-week old wildtype and *Nrf2*-knockout male mice a 2ppm iron diet for 2 weeks, followed by oral gavage of water control or 2mg/kg iron in the form of ferrous sulphate. Hepatic gene expression of *Bmp6* and other Nrf2 target genes were quantified 6 hours post-iron treatment. The upregulation of *Bmp6* in response to dietary iron loading, intraperitoneal FeDx, intraperitoneal hemin and oral iron was compared between wildtype and *Nrf2*-knockout mice. In experiments where both males and females were used, data were analysed by stratifying the mice according to sex and statistical analysis was performed using 2-way ANOVA.

In this chapter, we also explored how iron activates Nrf2. Since Nrf2 can be regulated at the mRNA and protein levels, we quantified hepatic *Nfe2l2* mRNA in response to various forms of iron treatment by qRT-PCR. Changes in Nrf2 protein levels in response to iron has been demonstrated in Chapter 3. Additionally, oxidative stress levels were measured *in vivo* in response to iron. 7-week old wildtype male mice were fed a normal (200ppm iron) or a high iron diet (1% CI) for one week. Malondialdehyde, which is a product of lipid peroxidation, was quantified in the liver using the TBARS (thiobarbituric acid reactive substances) assay. To determine whether iron activates Nrf2 via the induction of oxidative stress, L929 cells were pre-treated with 500μM mitoTEMPO (a free radical scavenger) for one hour, followed by 1mg/ml FeDx for 6 hours. The classical Nrf2 target genes (*Nqo1* and *Hmox1*) and *Bmp6* expression was quantified by qRT-PCR. Additionally, 4-week old wildtype male mice were fed 2ppm iron diet for 3 weeks, then given 2mg/kg iron by oral gavage and treated with saline or 0.25mg mitoTEMPO intraperitoneally one hour after oral iron treatment. Mice were culled 6 hours after oral iron gavage, and hepatic gene expression was assayed by qRT-PCR. Lastly, the involvement of iNOS (encoded by *Nos2* gene) in the activation of Nrf2 in response to iron was investigated by measuring hepatic *Nos2* mRNA levels upon dietary iron loading, oral $FeSO_4$, intraperitoneal FeDx, and in i*Hamp1*-knockout mice. *Nos2*-knockout and wildtype littermates were also injected with 4mg FeDx intraperitoneally and hepatic gene expression was measured 6 hours post iron administration.

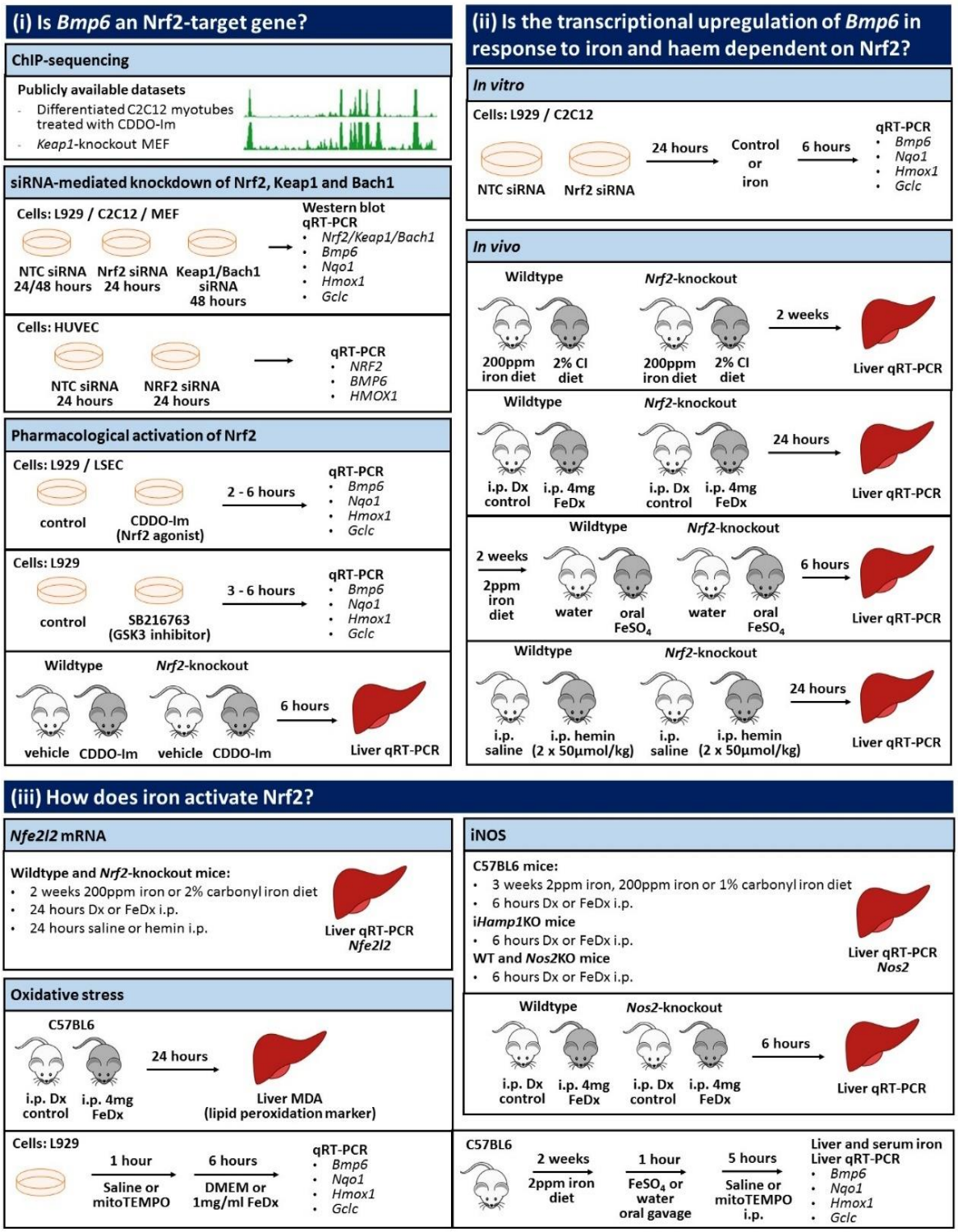


Figure 4.1: To investigate whether *Bmp6* is an Nrf2-target gene, publicly available Nrf2 ChIP-seq datasets were analysed, siRNA-mediated knockdown of Nrf2/NRF2, Keap1 and Bach1 were performed, and Nrf2 was pharmacologically activated with CDDO-Im or SB216763. To investigate whether Nrf2 is required for the upregulation of *Bmp6* by iron and haem, Nrf2 was knocked down, followed by iron treatment *in vitro*. *In vivo*, wildtype and *Nrf2*-knockout mice were administered iron and haem. Hepatic *Bmp6*, *Nqo1*, *Hmox1* and *Gclc* expression was quantified by qRT-PCR. To investigate how iron activates Nrf2, *Nfe2l2* mRNA and oxidative stress levels were quantified in response to iron and the effects of free radical scavenger mitoTEMPO was studied. The involvement of iNOS was also tested by measuring *Nos2* mRNA in response to iron and injecting wildtype and *Nos2*-knockout mice with FeDx.

4.2 Results

4.2.1 Nrf2 binds in proximity to the *Bmp6* promoter

4.2.1.1 Nrf2 ChIP-sequencing

Two publicly available Nrf2 ChIP-seq datasets were mapped onto the mouse mm9 genome build on UCSC genome browser. The two Nrf2 ChIP-seq datasets were generated from differentiated C2C12 myotube cells treated with 100nM CDDO-Im for 3 hours (Uruno et al., 2016, GEO accession number GSM2076704) using monoclonal antibodies against Nrf2 (Cell Signalling, D1Z9C) and from *Keap1*-knockout MEF cells (Malhotra et al., 2010, GEO accession number GSE87357) using monoclonal antibodies against Nrf2 (Epitomics Inc., CA). Publicly available ChIP-seq tracks of H3K4-monomethylation (H3K4me1) depicting enhancer regions, H3K4-trimethylation (H3K4me3) depicting promoter regions, and RNA polymerase II (Pol2) on MEF cells, as well as mammalian conservation based on multiple alignments of 30 vertebrate species were also mapped onto the mm9 mouse genome.

An Nrf2 ChIP-seq peak was observed 6kb downstream of the *Bmp6* promoter (in intron 1) in C2C12 cells, which overlaps with one of several Nrf2 ChIP-seq peaks in proximity to the *Bmp6* promoter in *Keap1*-knockout MEF cells. Binding of transcription factors to enhancers located within introns is not uncommon and have been observed for other genes; for example, the enhancer core region for murine immunoglobulin heavy chain is located in intron 2 of the gene (reviewed in Blackwood, 1998; Pennacchio et al., 2013). More importantly, the ChIP-seq peak 6kb downstream of the *Bmp6* promoter overlaps with an H3K4-monomethylation (H3K4me1) enhancer mark and RNA polymerase II binding region in MEF cells, is highly conserved in mammals, and contains an ARE consensus sequence TGCTGAGTCA (Yamamoto et al., 2006) (Figure 4.2). As a comparator, Nrf2 ChIP-seq peaks were observed at well-characterised AREs with the same TGCTGAGTCA consensus sequence at 9kb and 4kb upstream of the *Hmox1* promoter (Reichard et al., 2007) (Figure 4.3) in both C2C12 and *Keap1*-knockout MEF cells. The binding of Nrf2 to a conserved ARE site in close proximity to the *Bmp6* promoter in both C2C12 and MEF cells strongly suggests that *Bmp6* is under the transcriptional control of Nrf2.

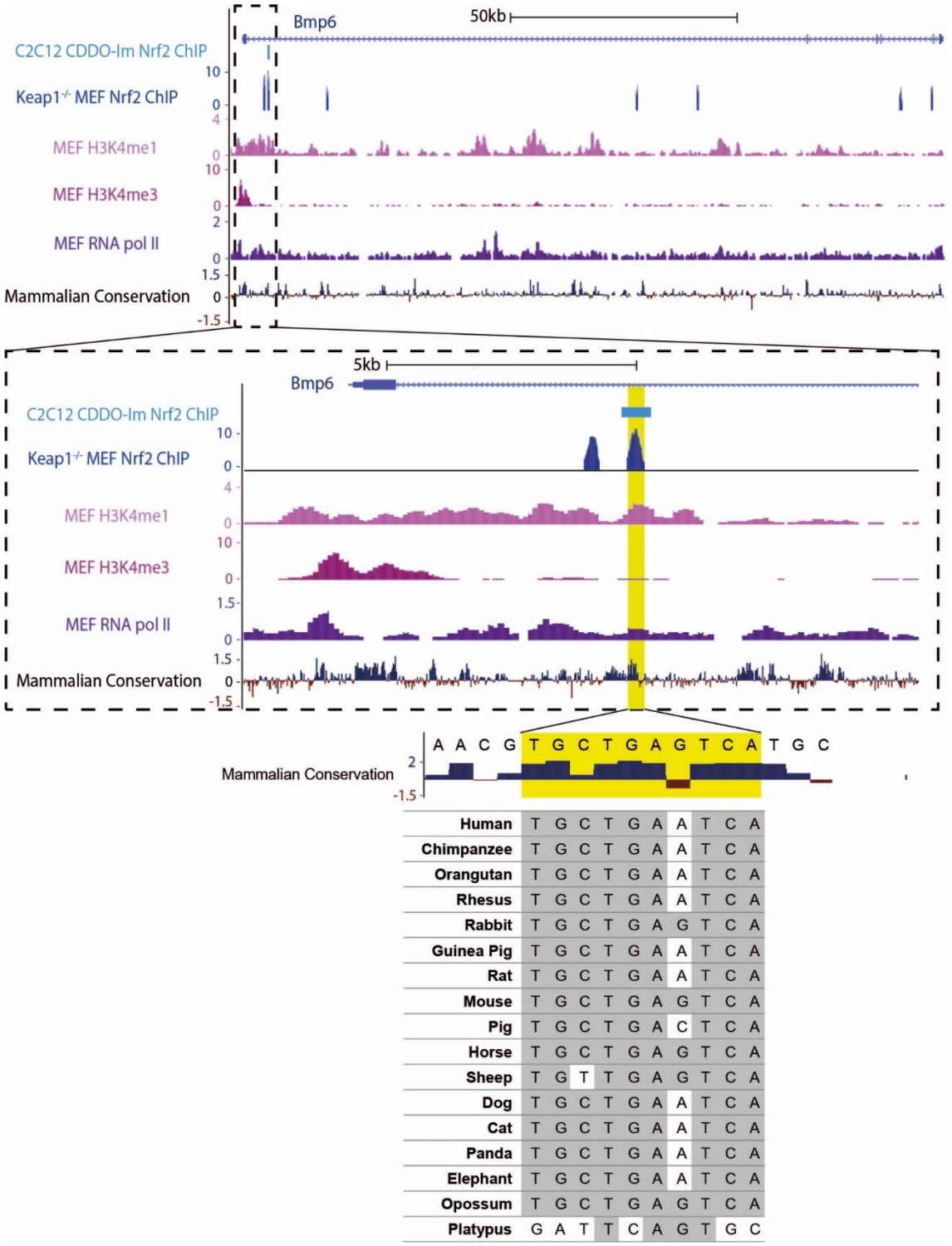


Figure 4.2: Publicly available Nrf2 ChIP-seq datasets from C2C12 cells treated with 100nM CDDO-Im for 3 hours and *Keap1*-knockout MEF cells were aligned to the mouse mm9 genome build on UCSC genome browser. H3K4me1 (enhancer mark), H3K4me3 (promoter mark), RNA polymerase II (RNA pol II) binding and mammalian conservation tracks were also aligned to the genome. The top panel shows a snapshot of the chromosome landscape around *Bmp6*, and the middle panel shows a zoomed in view of an enhancer region 6kb downstream of the *Bmp6* promoter, located within intron 1, that is bound by Nrf2. The ARE consensus sequence within the Nrf2 ChIP-seq peak is highlighted in yellow, and the conserved nucleotides in multiple mammalian species are highlighted in grey below.

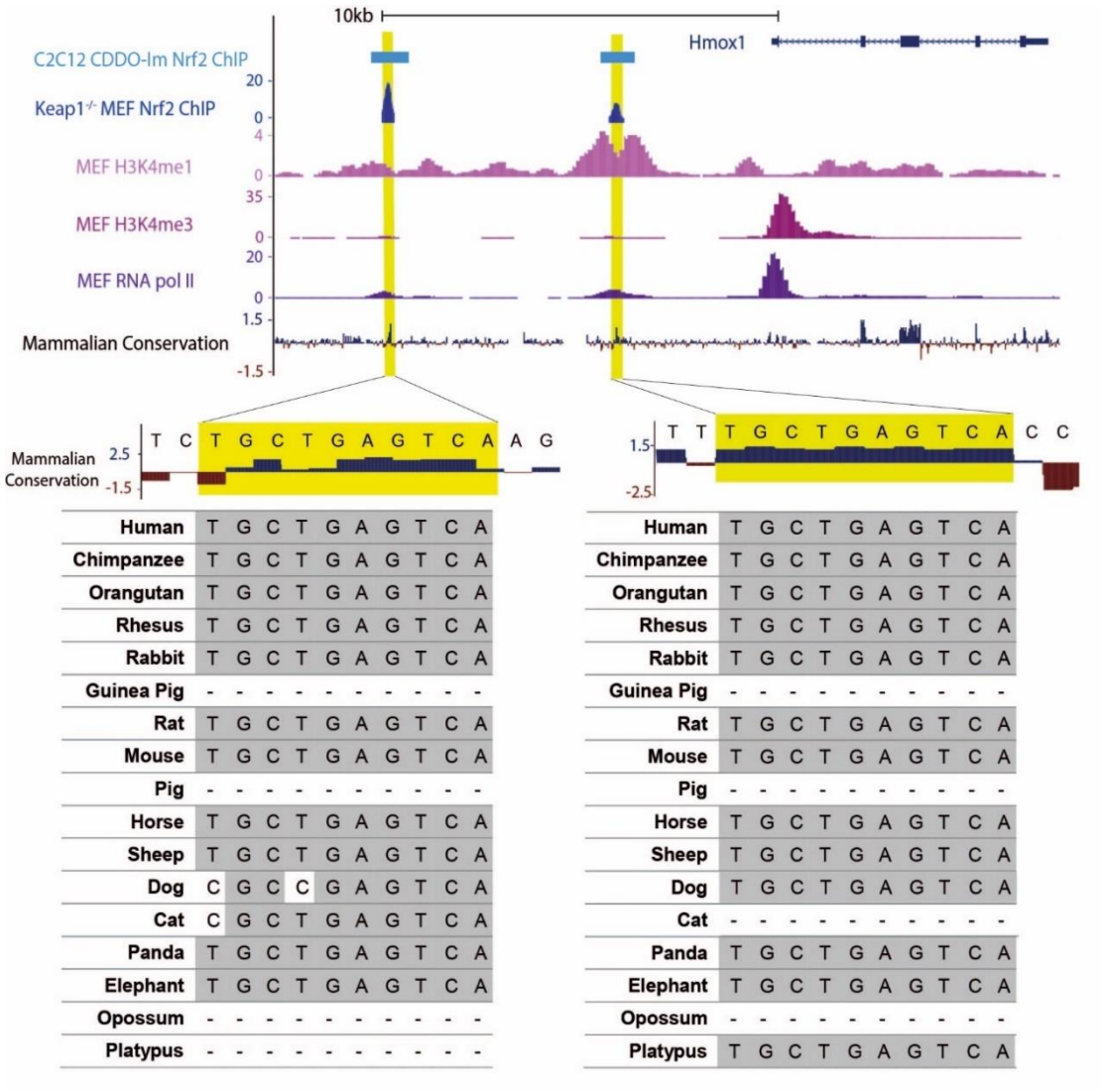


Figure 4.3: Publicly available Nrf2 ChIP-seq datasets from C2C12 cells treated with 100nM CDDO-Im for 3 hours and *Keap1*-knockout MEF cells were aligned to the mouse mm9 genome build on UCSC genome browser. H3K4me1 (enhancer mark), H3K4me3 (promoter mark), RNA polymerase II (RNA pol II) binding and mammalian conservation tracks were also aligned to the genome. The top panel shows a snapshot of the chromosome landscape around *Hmox1*. The ARE consensus sequences within the Nrf2 ChIP-seq peak located 10kb and 4kb upstream of the *Hmox1* promoter are highlighted in yellow, and the conserved nucleotides in mammalian species are highlighted in grey below, with dashes representing absence of the aligned region.

4.2.1.2 C2C12 and MEF induce *Bmp6* expression in response to ferric ammonium citrate

We subsequently investigated the response of C2C12 and MEF cells, which Nrf2 ChIP-seq experiments were performed on, to iron by treating them with 200µg/ml FAC for 6 hours. The expression of *Bmp6* was upregulated in parallel with *Nqo1*, *Hmox1* and *Gclc* in response to FAC in both C2C12 (Figure 4.4) and MEF cells (Figure 4.5). These data demonstrate that both C2C12 and

MEF cells are able to concurrently activate Nrf2 and enhance the transcription of *Bmp6* in response to iron, and thus validates the relevance of the ChIP-seq datasets described above.

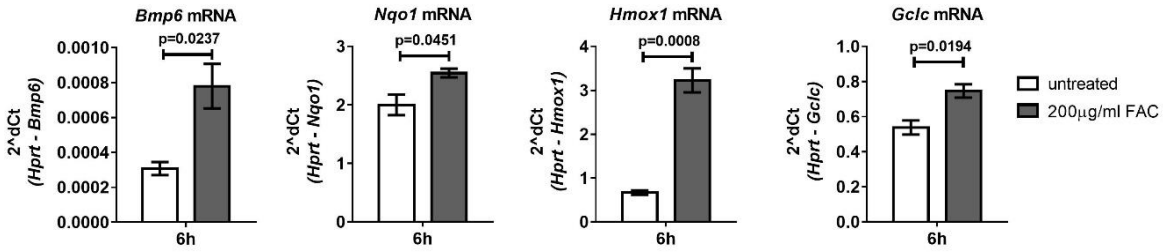


Figure 4.4: Expression of *Bmp6, Nqo1, Hmox1 and Gclc* was upregulated 6 hours post-treatment with 200µg/ml FAC in C2C12 cells (n=3, t-test).

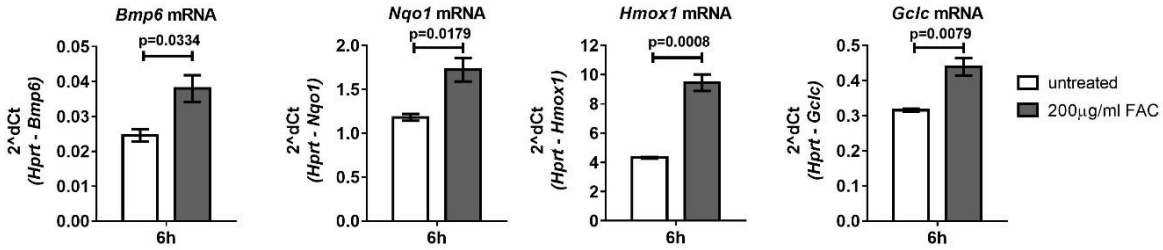


Figure 4.5: Expression of *Bmp6, Nqo1, Hmox1 and Gclc* was upregulated 6 hours post-treatment with 200µg/ml FAC in MEF cells (n=3, t-test).

4.2.2 Alterations in the Nrf2/Bach1 axis affects baseline *Bmp6* expression

4.2.2.1 siRNA-mediated knockdown of *Nrf2, Keap1* and *Bach1* alters *Bmp6* expression

Nrf2 activates the transcription of ARE-regulated genes during oxidative stress, and is sequestered in the cytoplasm by its inhibitory protein Keap1 at basal resting conditions. In contrast, Bach1 is a transcriptional repressor that blocks the expression of ARE-regulated genes. In order to investigate whether perturbations in the activating effect of Nrf2 and repressing effects of Bach1 and Keap1 alters *Bmp6* expression, siRNA-mediated knockdown of *Nrf2*, *Bach1* and *Keap1* were performed in L929, C2C12 and MEF cells.

24 hours after transfection with 100nM siRNA targeting *Nfe2l2*, Nrf2 protein and mRNA levels were reduced compared to cells transfected with 100nM NTC siRNA in L929 cells, confirming

efficient Nrf2 knockdown. At the same time, *Bmp6* and *Nqo1* mRNA were also downregulated, while *Hmox1* and *Gclc* mRNA were unaltered (Figure 4.6). Knockdown of Keap1 was achieved by transfecting L929 cells with 100nM siRNA targeting *Keap1* for 48 hours and confirmed by measuring Nrf2 protein via Western blot and *Keap1* mRNA via qRT-PCR. Knockdown of Keap1 increased Nrf2 protein levels as expected, and led to an upregulation of *Nqo1* and *Gclc* expression but did not alter *Bmp6* and *Hmox1* expression significantly (Figure 4.7). Knockdown of Bach1 was performed by transfecting L929 cells with 100nM siRNA targeting *Bach1* for 48 hours. Knockdown of Bach1 was confirmed by demonstrating a reduction in Bach1 protein and mRNA by Western blot and qRT-PCR, respectively, and led to an upregulation of *Bmp6* expression, as well as derepression of the classical Nrf2 target genes *Nqo1*, *Hmox1* and *Gclc* (Figure 4.8).

In C2C12 cells, gene expression of *Bmp6*, *Nqo1* and *Gclc* was suppressed upon knockdown of Nrf2 (Figure 4.9) and induced upon knockdown of Keap1 (Figure 4.10); knockdown efficiencies were validated by Western blot of Nrf2 protein. Knockdown of Bach1 reduced Bach1 protein and mRNA levels and led to an upregulation of *Bmp6*, *Hmox1* and *Gclc* (Figure 4.11).

In MEF cells, knockdown of Nrf2 did not lead to detectable reduction in Nrf2 protein levels by Western blot, possibly due to the low Nrf2 protein levels at baseline. Nevertheless, Nrf2 mRNA level was reduced and expression of *Bmp6*, *Nqo1*, *Hmox1* and *Gclc* was downregulated (Figure 4.12). Conversely, the expression of *Bmp6*, *Nqo1*, *Hmox1* and *Gclc* were all upregulated upon knockdown of Keap1 (Figure 4.13) and of Bach1 (Figure 4.14).

The siRNA-mediated gene knockdown experiments collectively show that knockdown of Nrf2 decreases the expression of ARE-regulated genes, while knockdown of Keap1 or Bach1 increases the expression of ARE-regulated genes in general, although the sensitivity of each gene to changes in Nrf2, Keap1 or Bach1 levels are different. For example, Macleod and colleagues showed that *Hmox1* is heavily Bach1-repressed, since knockdown of Bach1 in keratinocytes causes an increase in *Hmox1* expression by more than 100-fold (Macleod et al., 2009). Moreover, data in

Chapter 3 demonstrated that hemin-induced Bach1 degradation increases *Hmox1* expression massively. Here, siRNA-mediated knockdown of Bach1 also led to a robust induction of *Hmox1* expression by more than 100-fold, which is starkly greater than the upregulation of *Nqo1*, *Gclc* and *Bmp6* (between 2- and 5-fold). Moreover, *Nqo1* expression was downregulated upon Nrf2-knockdown and upregulated in response to Keap1-knockdown; in comparison, *Gclc* was responsive to Keap1-knockdown but not Nrf2-knockdown.

The complexity of the Nrf2/Keap1/Bach1 system in regulating ARE-driven gene expression is further demonstrated by the different responses in each cell type. For example, knockdown of Bach1 induced *Nqo1* expression in L929 and MEF but not in C2C12 cells. Additionally, *Hmox1* expression was upregulated upon knockdown of Keap1 in MEF cells, but not L929 or C2C12. Similarly, *Bmp6* expression was upregulated upon knockdown of Keap1 in C2C12 and MEF cells, but not in L929 cells. While the gene expression responses varied across different cells, the general trend is consistent with *Bmp6* being an ARE-driven gene, since its expression is downregulated upon knockdown of Nrf2 and upregulated upon Bach1-knockdown in all three cell lines tested.

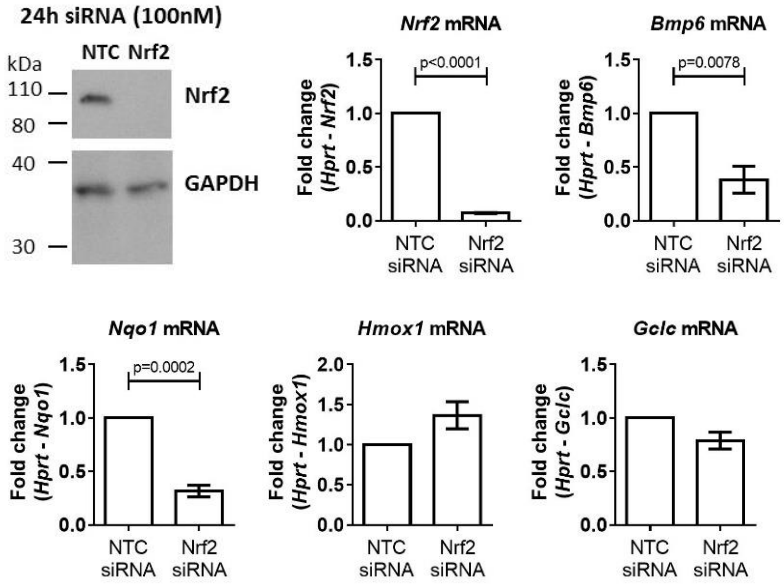


Figure 4.6: siRNA-mediated knockdown of Nrf2 in L929 cells caused a reduction in Nrf2 protein and mRNA levels, a downregulation in *Bmp6* and *Nqo1* expression, and no significant changes to *Hmox1* and *Gclc* expression (n=5, paired t-test).

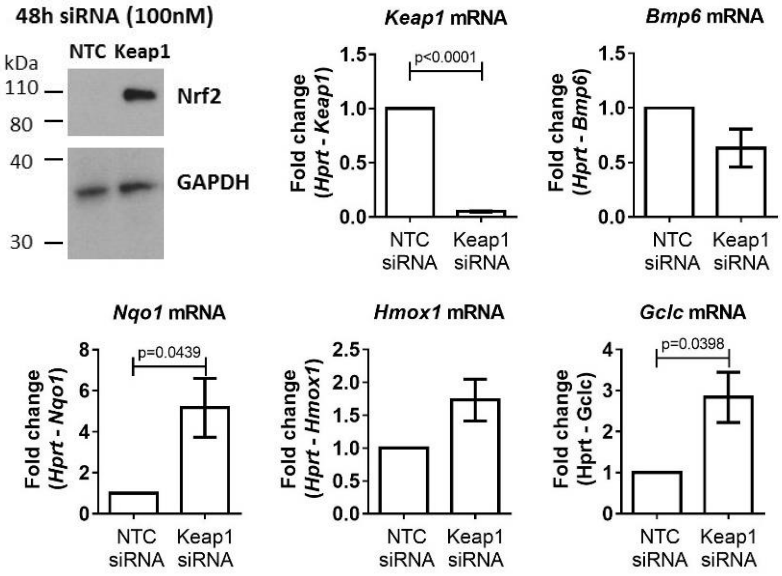


Figure 4.7: siRNA-mediated knockdown of Keap1 caused a reduction in Keap1 mRNA levels and increase in Nrf2 protein levels, an upregulation in *Nqo1* and *Gclc* expression, and no significant changes to *Bmp6* and *Hmox1* expression in L929 cells (n=5, paired t-test).

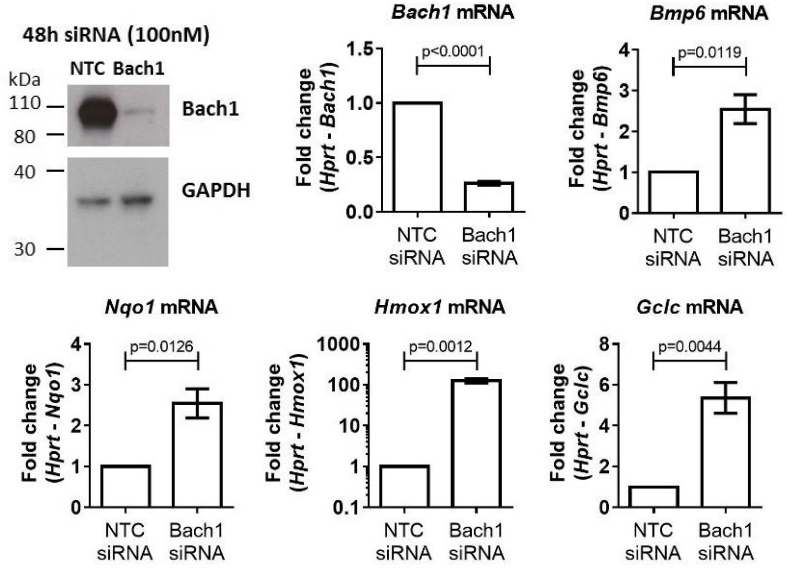


Figure 4.8: siRNA-mediated knockdown of Bach1 caused a reduction in Bach1 protein and mRNA levels, and an upregulation in *Bmp6*, *Nqo1*, *Hmox1* and *Gclc* expression in L929 cells (n=5, paired t-test).

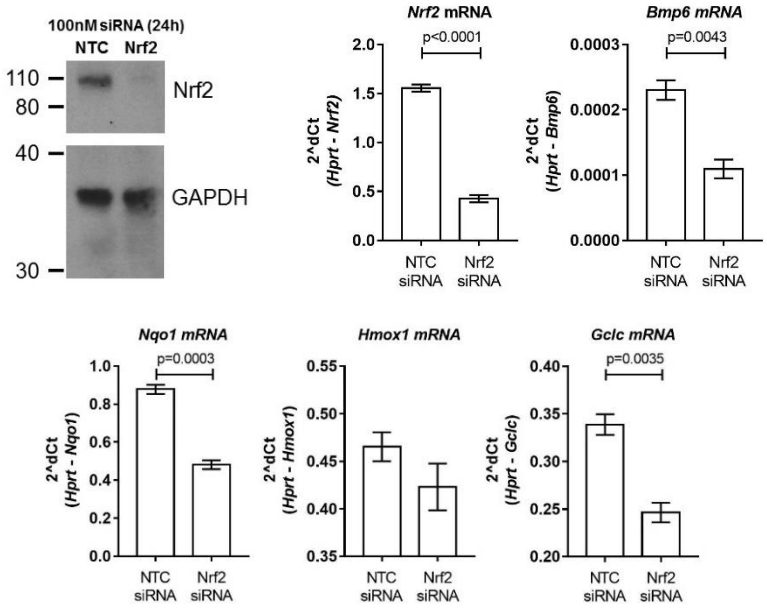


Figure 4.9: siRNA-mediated knockdown of Nrf2 in C2C12 cells caused a reduction in Nrf2 protein and mRNA levels, and a downregulation in *Bmp6*, *Nqo1* and *Gclc* expression (n=3, t-test).

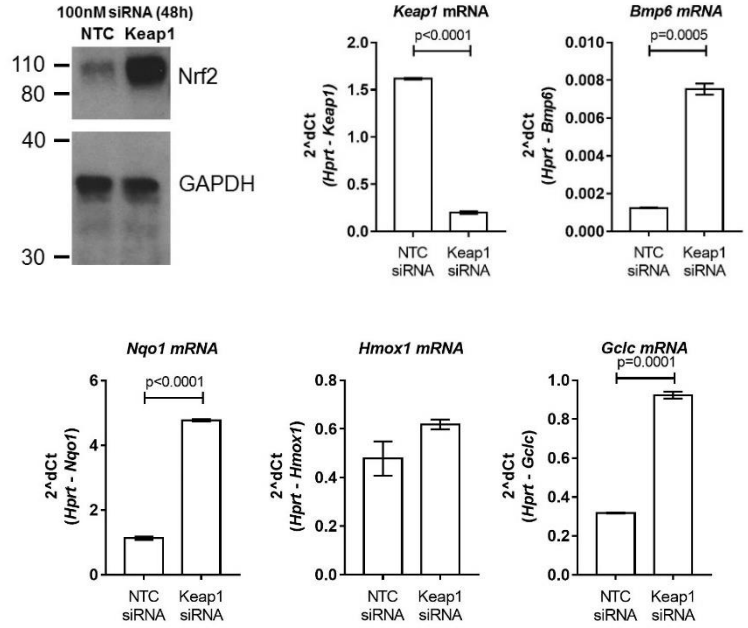


Figure 4.10: siRNA-mediated knockdown of Keap1 in C2C12 cells caused a reduction in Keap1 mRNA levels, increase in Nrf2 protein levels, and upregulation in *Bmp6*, *Nqo1* and *Gclc* expression (n=3, t-test).

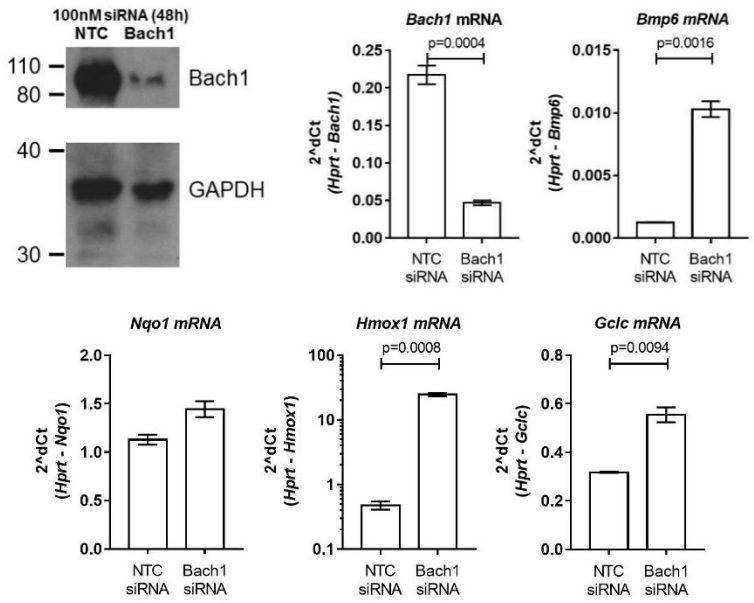


Figure 4.11: siRNA-mediated knockdown of Bach1 in C2C12 cells reduced Bach1 protein and mRNA levels, and led to derepression of *Bmp6*, *Hmox1* and *Gclc* expression (n=3, t-test).

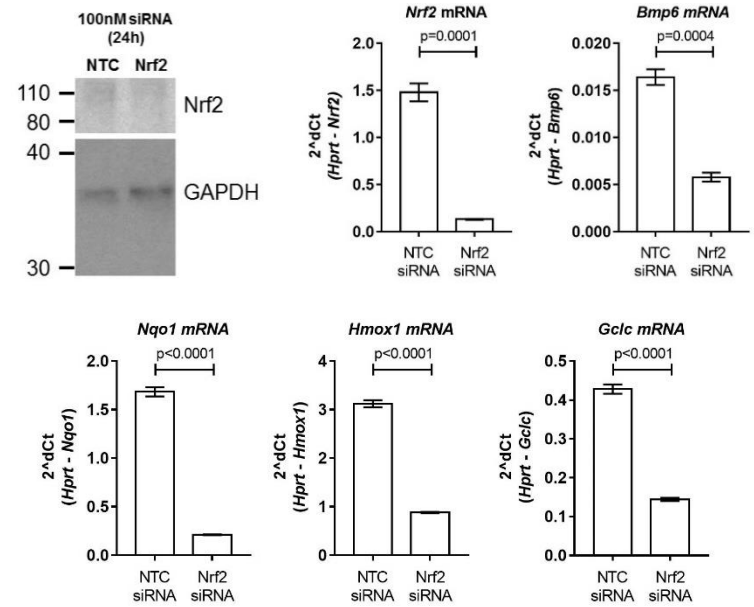


Figure 4.12: siRNA-mediated knockdown of Nrf2 in MEF cells caused a downregulation in expression of *Bmp6* and well-characterised Nrf2 target genes *Nqo1*, *Hmox1* and *Gclc* (n=3, t-test).

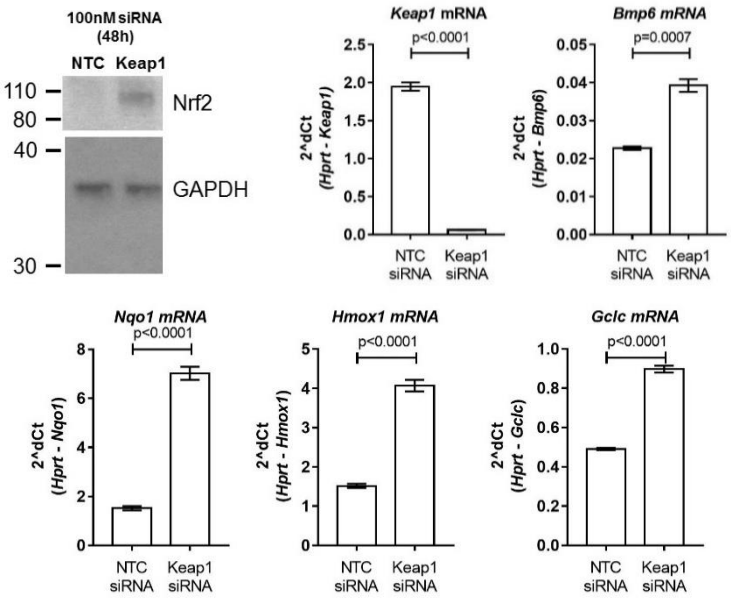


Figure 4.13: siRNA-mediated knockdown of Keap1 in MEF cells increased Nrf2 protein levels and caused an upregulation in *Bmp6*, *Nqo1*, *Hmox1* and *Gclc* expression (n=3, t-test).

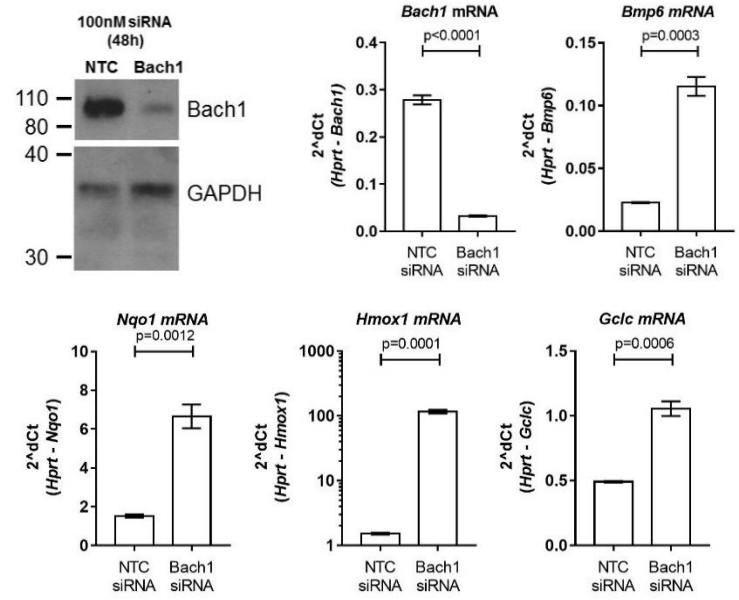


Figure 4.14: siRNA-mediated knockdown of Bach1 in MEF cells decreased Bach1 protein and mRNA, and caused an upregulation in *Bmp6*, *Nqo1*, *Hmox1* and *Gclc* expression (n=3, t-test).

Human HUVEC cells do not induce *Bmp6* in response to iron (Figure3.3C), but unpublished data from our collaborator (Jodie Babitt, MGH) show that *Bmp6* expression can be suppressed by chelating iron in HUVEC cells. We tested whether siRNA-mediated knockdown of NRF2 also

suppresses *BMP6* expression in HUVEC cells. HUVEC cells were transfected with 100nM of siRNA targeting NRF2 or control NTC siRNA, and qRT-PCR was performed 24 hours post-transfection to quantify *BMP6* and *HMOX1* gene expression, and of *NRF2* mRNA as confirmation of knockdown. Indeed, knockdown of NRF2 led to a downregulation of both *BMP6* and *HMOX1* expression (Figure 4.15), in agreement with our hypothesis that *BMP6* is an NRF2-dependent gene.

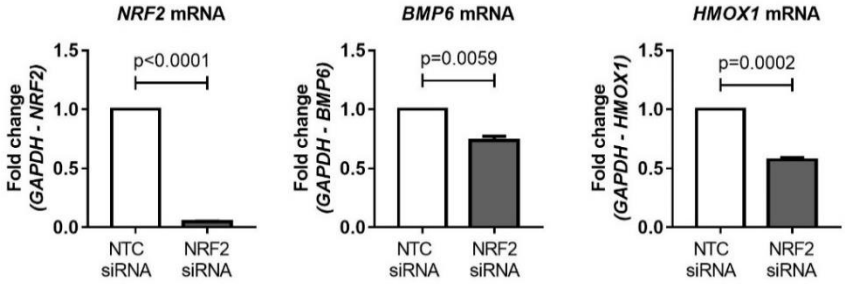


Figure 4.15: *BMP6* and *HMOX1* expression were downregulated upon siRNA-mediated knockdown of NRF2 in HUVEC cells (n=4, paired t-test).

4.2.2.2 Small molecule Nrf2 agonists upregulate *Bmp6* expression *in vitro*

CDDO-Im stabilises Nrf2 by disrupting interactions between Keap1 and Cullin3 ubiquitin ligase (Cleasby et al., 2014). The effects of Nrf2 activation by CDDO-Im was tested in primary LSEC cells (by Chia-Yu Wang and Jodie Babitt). Treatment of LSEC cells with 100nM CDDO-Im for 6 hours led to a robust upregulation of *Bmp6* in parallel with induction of *Nqo1*, *Hmox1* and *Gclc* (Figure 4.16).

L929 cells were treated with two small molecule Nrf2 agonists, CDDO-Im and SB216763, to pharmacologically activate Nrf2. At 2 hours and 4 hours post-treatment with 10nM, 100nM or 1000nM CDDO-Im, expression of *Bmp6*, *Nqo1*, *Hmox1* and *Gclc* was quantified by qRT-PCR. CDDO-Im led to a significant increase in *Nqo1* expression at 2 hours post-treatment, while *Bmp6* and *Hmox1* expression was significantly upregulated at 4 hours post-treatment. The expression of *Gclc* was unexpectedly suppressed by CDDO-Im in L929 cells (Figure 4.17). SB216763 inhibits GSK3 kinase, thereby blocking the phosphorylation and recognition of Nrf2 by the $SCF^{\beta\text{-}TrCP}$ ubiquitin system. *Bmp6* and *Hmox1* expression were significantly upregulated 6 hours post-treatment with SB216763, alongside a trend towards induction of *Nqo1* and *Gclc* expression (Figure 4.18).

The activation of Nrf2 by CDDO-Im enhanced *Bmp6* expression in primary LSECs, which are the most physiological relevant cells that regulate *Bmp6* expression in response to iron. Moreover, pharmacological activation of Nrf2 by two agonists acting via different molecular mechanisms, CDDO-Im and SB216763, consistently increased *Bmp6* expression in L929, an *in vitro* model which we have characterised to be responsive to iron by inducing *Bmp6* expression.

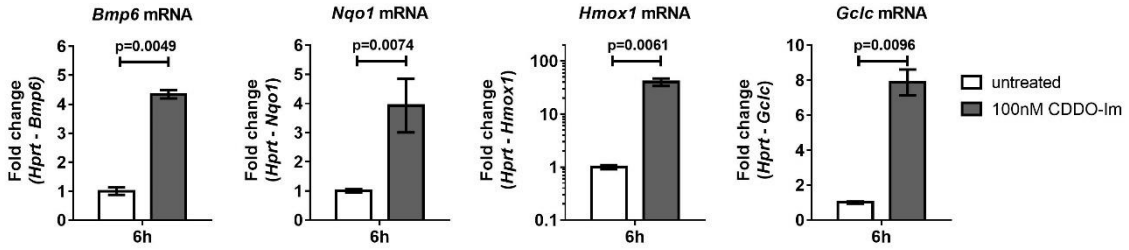


Figure 4.16: LSEC cells were treated 100nM CDDO-Im for 6 hours. Gene expression of *Bmp6*, *Nqo1*, *Hmox1* and *Gclc* were robustly upregulated in response to CDDO-Im (n=3, t-test).

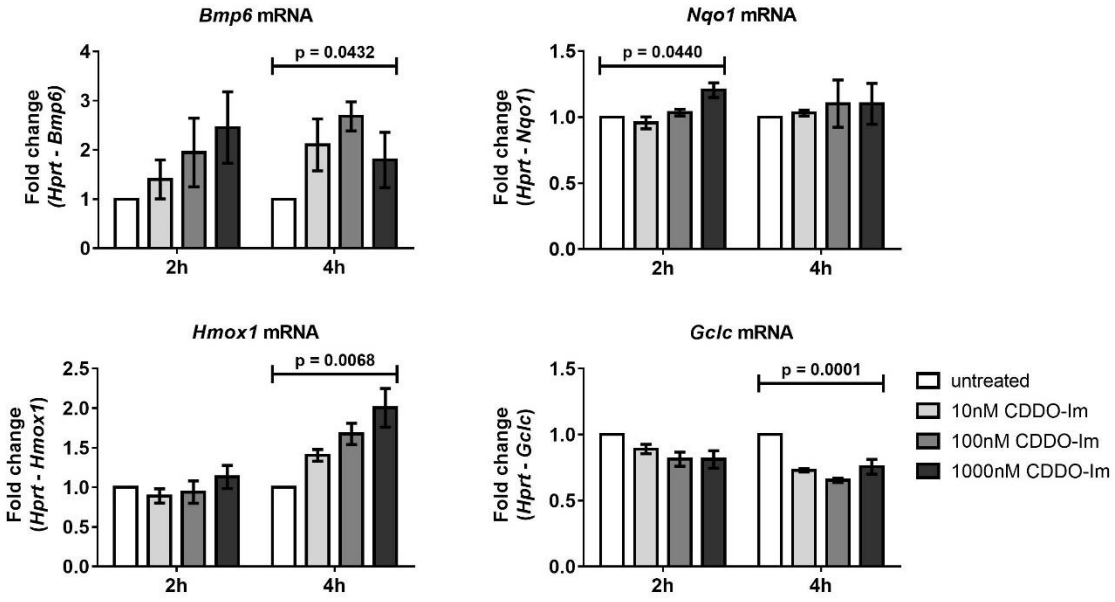


Figure 4.17: L929 cells were treated with titrating concentrations of CDDO-Im for 2 or 4 hours. *Nqo1* expression, and *Bmp6* and *Hmox1* expression and were induced at 2 hours and 4 hours respectively, while *Gclc* expression was downregulated at 4 hours post-treatment (n=3, one-way ANOVA).

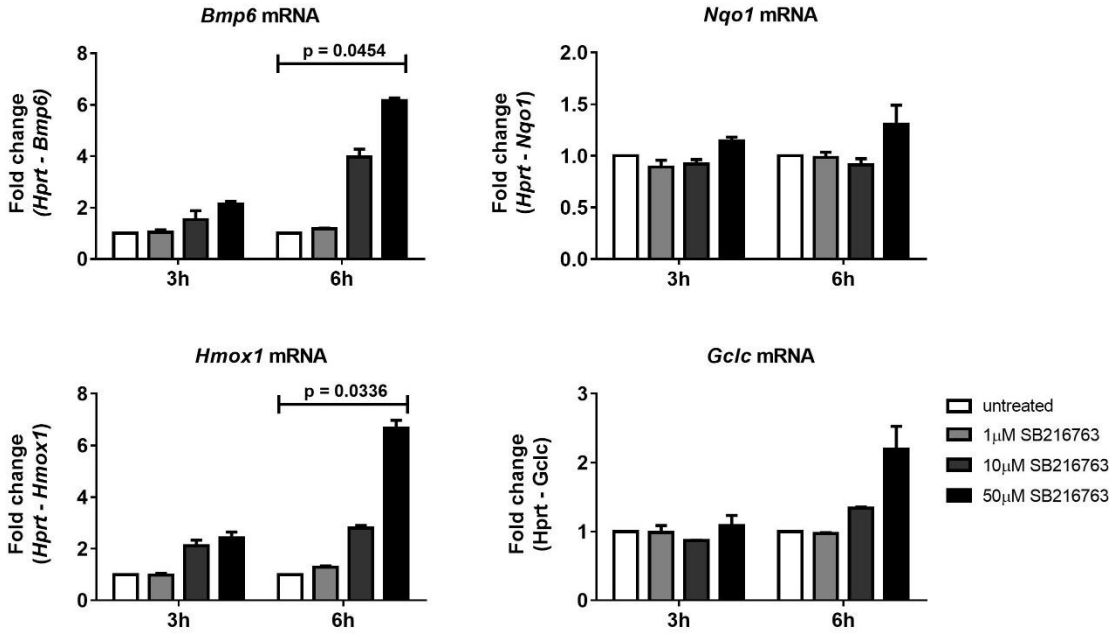


Figure 4.18: L929 cells were treated with titrating concentrations of SB216763 for 3 or 6 hours. SB216763 treatment led to an upregulation of *Bmp6* and *Hmox1* expression and a trend towards increasing *Nqo1* and *Gclc* expression after 6 hours (n=2, one-way ANOVA).

4.2.2.3 CDDO-Im upregulates *Bmp6* expression in an Nrf2-dependent manner *in vivo*

Next, we tested whether the induction of *Bmp6* expression by CDDO-Im could be reproduced *in vivo*, and to confirm the involvement of Nrf2. 6-week old wildtype and *Nrf2*-knockout mice were given 30μmol/kg CDDO-Im orally, and livers were harvested 6 hours post-treatment for qRT-PCR. Indeed, *Bmp6* was upregulated in parallel with the other classical Nrf2-target genes (*Nqo1*, *Hmox1* and *Gclc*) in the liver of wildtype mice treated with CDDO-Im by more than 4-fold, but not in *Nrf2*-knockout mice, demonstrating that CDDO-Im causes Nrf2-dependent transcriptional induction of *Bmp6 in vivo* (Figure 4.19). In addition, the hepatic expression of ferritin genes *Fth1* and *Ftl1*, which are also Nrf2-responsive genes, were quantified. *Fth1* and *Ftl1* were significantly, albeit marginally, upregulated by CDDO-Im in an Nrf2-dependent manner (Figure 4.19).

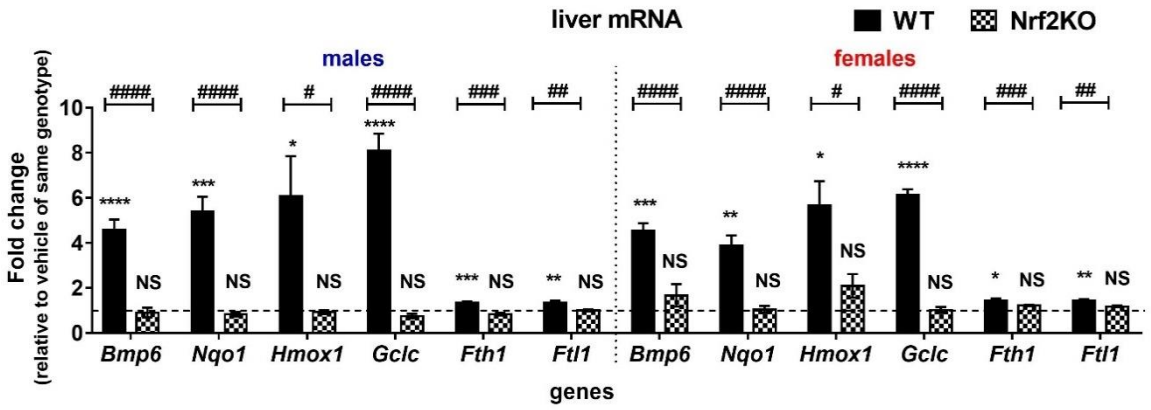


Figure 4.19: Wildtype (WT) and *Nrf2*-knockout (Nrf2KO) mice were given 30µmol/kg CDDO-Im or vehicle control by oral gavage. qRT-PCR was performed on the livers 6 hours post-treatment. CDDO-Im upregulated *Bmp6*, *Nqo1*, *Hmox1*, *Gclc*, *Fth1* and *Ftl1* in an Nrf2-dependent manner. Data is expressed as a fold change of gene expression in mice treated with CDDO-Im compared to vehicle-treated mice of the same genotype and sex. Solid bars represent wildtype mice, chequered bars represent *Nrf2*-knockout mice. Left panel = males, right panel = females (n=3 to 5; t-test for fold change relative to vehicle: * p<0.05, ** p<0.01, *** p<0.001, **** p<0.0001; 2-way ANOVA for comparison of effects between wildtype and *Nrf2*-knockout mice by stratifying on sex and genotype: # p<0.05, ## p<0.01, ### p<0.001, #### p<0.0001).

The data so far in this chapter show (i) Nrf2 binds a well-conserved ARE sequence in intron 1 of *Bmp6*, in C2C12 and MEF cells; (ii) in these cells, expression of *Bmp6* and classical Nrf2 target genes are increased by exposure to iron; (iii) perturbation of the Nrf2/Keap1/Bach1 regulatory axis in multiple cell types by siRNA-mediated knockdown alters *Bmp6* expression; (iv) small molecule agonists of the Nrf2 system increase *Bmp6* expression *in vitro* and *in vivo*. These data collectively show that the Nrf2 system regulates *Bmp6* expression.

4.2.3 Nrf2 controls the upregulation of *Bmp6* in response to iron

Next, we test the hypothesis that the upregulation of *Bmp6* by iron is Nrf2-dependent.

4.2.3.1 siRNA-mediated knockdown of *Nrf2* blocks the induction of *Bmp6* by iron

L929 cells were knocked down for Nrf2 for 24 hours, followed by treatment with 1mg/ml FeDx for 6 hours. qRT-PCR was performed to quantify gene expression of *Nrf2* to confirm knockdown, and of *Bmp6, Nqo1* and *Hmox1*. The upregulation of *Nqo1* in response to FeDx was completely abrogated in *Nrf2*-knocked down cells. Knockdown of Nrf2 also led to a trend towards a reduction in *Hmox1* induction by FeDx. Moreover, knockdown of Nrf2 blocked the upregulation of

Bmp6 expression by FeDx (Figure 4.20). Next, C2C12 cells were knocked down for Nrf2 for 24 hours, then treated with 200µg/ml FAC for 6 hours. Knockdown of Nrf2 was confirmed by qRT-PCR, although the degree of Nrf2 knockdown based on mRNA levels was less efficient in C2C12 cells (20% of NTC) compared to L929 cells (7% of NTC). The upregulation of *Bmp6*, *Nqo1* and *Hmox1* expression by FAC was blunted by the knockdown of Nrf2 (Figure 4.21). Similarly, in MEF cells, the upregulation of *Nqo1* expression in response to FAC was abrogated by the knockdown of Nrf2, and the upregulation of *Bmp6* and *Hmox1* was blunted (Figure 4.22).

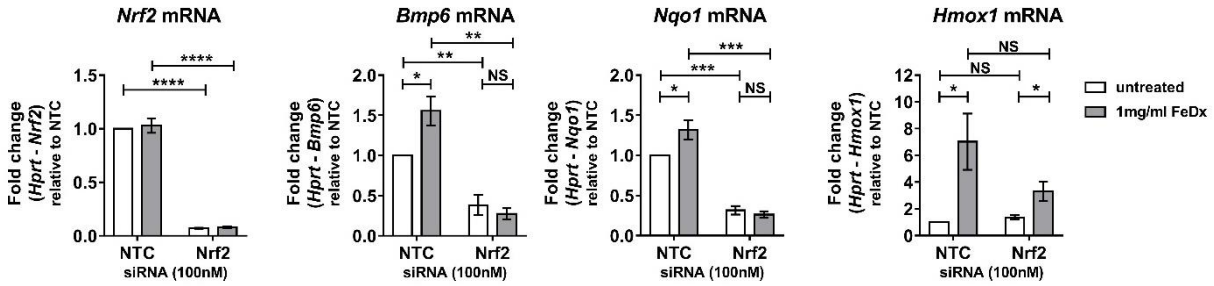


Figure 4.20: L929 cells were treated with 1mg/ml FeDx for 6 hours at 24 hours after siRNA-mediated knockdown of Nrf2. The upregulation of *Bmp6* and *Nqo1* by FeDx was completely blocked by the knockdown of Nrf2, while the induction of *Hmox1* by FeDx is marginally and insignificantly blunted (n=5, paired t-test: * p<0.05, ** p<0.01, *** p<0.001, **** p<0.0001).

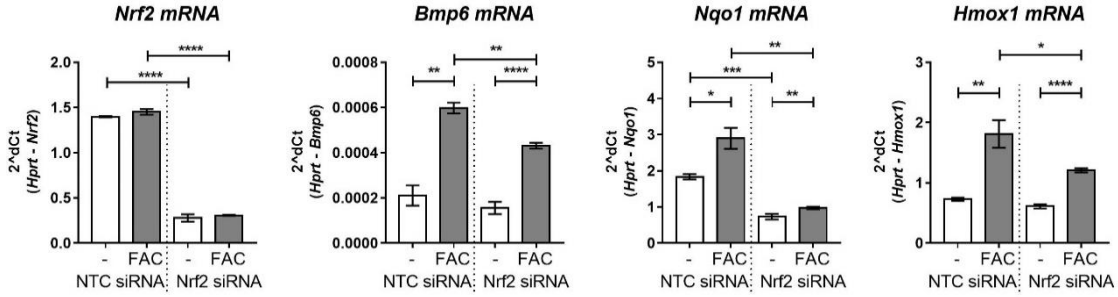


Figure 4.21: C2C12 cells were knocked down for Nrf2 for 24 hours, followed by treatment with 200µg/ml FAC for 6 hours. Knockdown of Nrf2 blunted the upregulation of *Bmp6*, *Nqo1* and *Hmox1* by FAC (n=3, t-test: * p<0.05, ** p<0.01, *** p<0.001, **** p<0.0001).

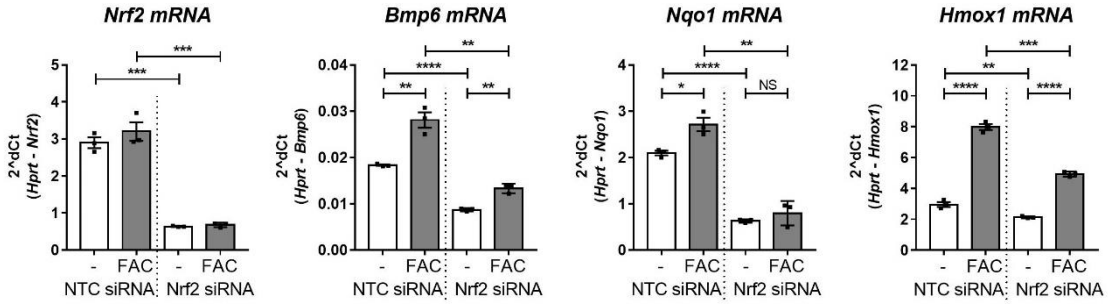


Figure 4.22: MEF cells were knocked down for Nrf2 for 24 hours, followed by treatment with 200µg/ml FAC for 6 hours. Knockdown of Nrf2 blocked the upregulation of *Nqo1* and blunted the upregulation of *Bmp6* and *Hmox1* by FAC (n=3, t-test: * $p<0.05$, ** $p<0.01$, *** $p<0.001$, **** $p<0.0001$).

Next, Nrf2 knockdown was performed in L929 cells, followed by treatment with 2µM or 10µM hemin for 6 hours. Knockdown of Nrf2 completely blocked the upregulation of *Nqo1* by hemin, suggesting that Nrf2 is required to transcriptionally activate *Nqo1* upon hemin-mediated Bach1 degradation and derepression. In contrast, the induction of *Hmox1* by hemin was unaltered by knockdown of Nrf2. It has been previously shown that siRNA-mediated knockdown of Bach1 increases *Hmox1* expression, while a double knockdown of Bach1 and Nrf2 still led to enhanced *Hmox1* expression, suggesting that Bach1 derepression by hemin can allow other transcription factors in addition to Nrf2 to induce gene expression (Macleod et al., 2009). We also observed that Nrf2 knockdown led to a trend towards suppression of *Bmp6* induction by 2µM hemin, but did not block the upregulation of *Bmp6* by a higher concentration of hemin at 10µM. This suggests that hemin-mediated Bach1 degradation can cause derepression of *Bmp6*, allowing Nrf2 as well as other transcription factors to transcriptionally activate *Bmp6* (Figure 4.23).

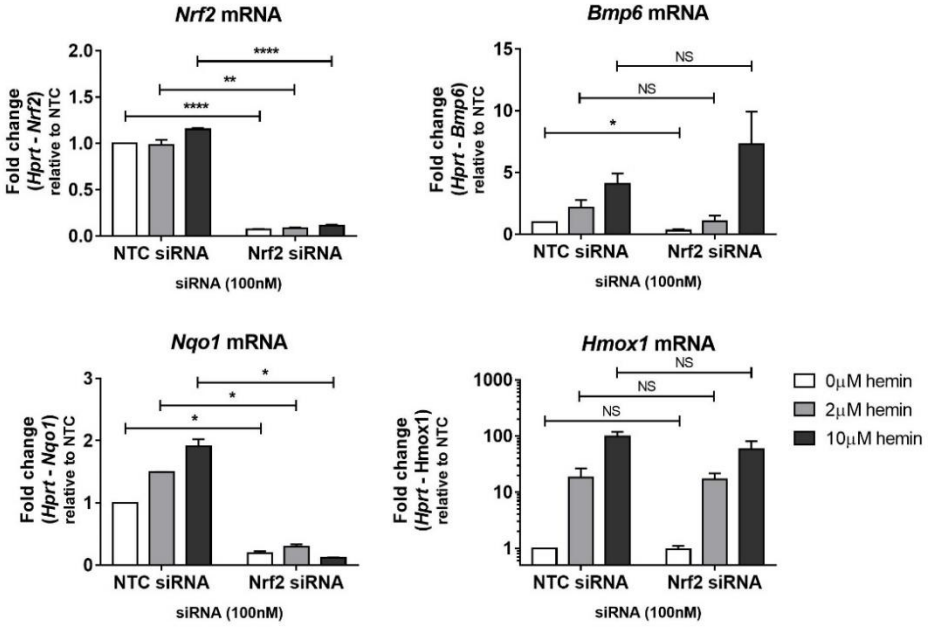


Figure 4.23: 24 hours after siRNA-mediated knockdown of Nrf2, L929 cells were treated with 2μM or 10μM hemin for 6 hours. The upregulation of *Nqo1* by hemin was completely blocked by the knockdown of Nrf2, while the upregulation of *Bmp6* and *Hmox1* by hemin was not significantly altered (n=3, paired t-test: * $p<0.05$, ** $p<0.01$, *** $p<0.001$, **** $p<0.0001$).

4.2.3.2 Induction of *Bmp6* by iron and hemin is blunted in *Nrf2*-knockout mice

In order to determine whether Nrf2 is required for the upregulation of *Bmp6* by iron *in vivo*, 12-week old male *Nrf2*-knockout and wildtype littermate mice were given a control 200ppm iron diet or a high iron diet (2% CI) for 2 weeks, and qRT-PCR gene expression analysis was performed on the livers. Dietary iron loading led to upregulation of *Bmp6, Nqo1* and *Hmox1* gene expression in wildtype mice. Contrary to previous observations where *Gclc* and *Bmp2* expression were elevated upon dietary iron loading in wildtype mice given 3 weeks of 1% CI diet (Figure 3.8C and Figure 3.15A), *Bmp2* was not induced and *Gclc* was surprisingly suppressed by iron accumulation in this model (Figure 4.24). Notably, *Nrf2*-knockout mice failed to upregulate hepatic *Bmp6* in response to dietary iron loading, in support of our hypothesis that iron enhances the expression of *Bmp6* via Nrf2. Additionally, the upregulation of *Nqo1* was also blunted and the upregulation of *Hmox1* was blocked in iron-loaded *Nrf2*-knockout mice (Figure 4.24).

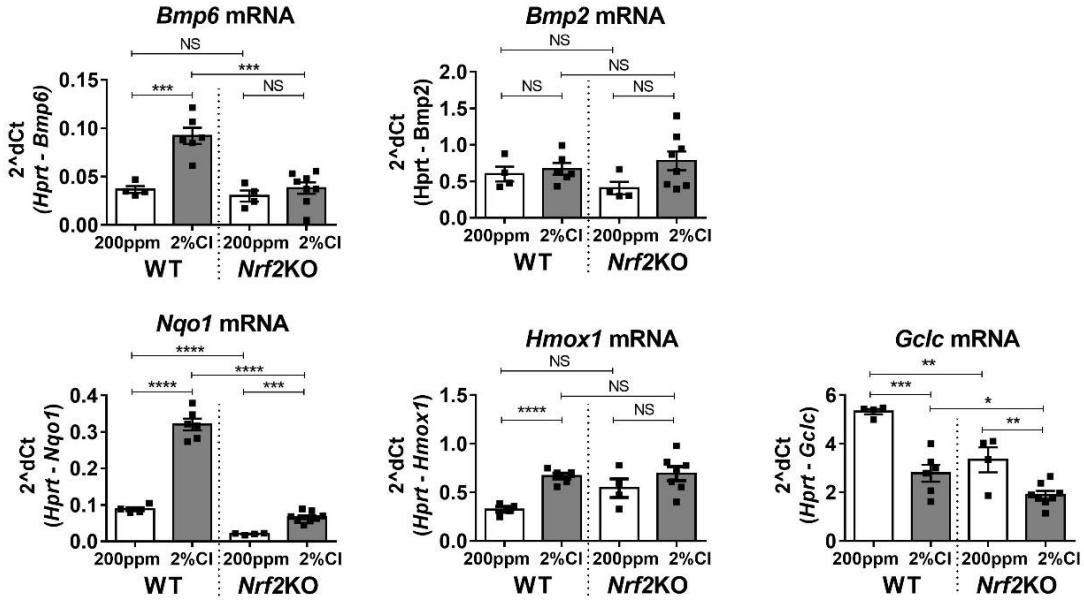


Figure 4.24: Wildtype (WT) and *Nrf2*-knockout (*Nrf2*KO) mice were fed diet containing 200ppm iron or 2% carbonyl iron (2% CI) for 2 weeks. Hepatic gene expression was quantified by qRT-PCR. The upregulation of *Bmp6*, *Nqo1* and *Hmox1* in response to dietary iron loading is blocked in *Nrf2*-knockout mice (n=4 to 8; t-test: * $p<0.05$, ** $p<0.01$, *** $p<0.001$, **** $p<0.0001$).

In another *in vivo* model, 6- to 7-week old male and female *Nrf2*-homozygous knockout, heterozygous knockout and wildtype littermate mice were injected intraperitoneally with 4mg FeDx or Dx control and culled 24 hours later. Hepatic gene expression was quantified by qRT-PCR. Intraperitoneal administration of FeDx led to iron accumulation in the liver in all mice (Figure 4.25A). *Bmp6*, *Nqo1*, *Hmox1* and *Gclc* gene expression were upregulated in response to FeDx in wildtype mice. The induction of *Bmp6*, *Nqo1* and *Gclc* was blunted in *Nrf2*-heterozygous and homozygous knockout mice; the blockage in upregulation of gene expression was observed to be stronger in homozygous knockouts than heterozygous knockouts (Figure 4.25B, C, E). The induction of *Hmox1* by FeDx is not significantly different across all genotypes (Figure 4.25D). Although the absolute gene expression levels (2^{dCt} relative to housekeeping gene *Hprt*) differ between males and females, the trends in effects of Nrf2 deficiency on gene expression response to FeDx were similar between males (blue) and females (red). Thus, the fold change in gene expression between Dx and FeDx groups of the same sex and genotype was calculated and 2-way ANOVA was performed by stratifying on sex and genotype for statistical analysis of whether the genotype (WT, heterozygous and homozygous knockout) affects the fold change in gene expression in response to iron. The

statistical analysis (right panel in Figure 4.25) demonstrates that the loss of Nrf2 significantly affects the ability of the liver to upregulate *Bmp6*, *Nqo1* and *Gclc* expression, but not *Hmox1*, in response to FeDx. Thus, the data is in agreement with our hypothesis that Nrf2 is required for the induction of *Bmp6* in response to iron.

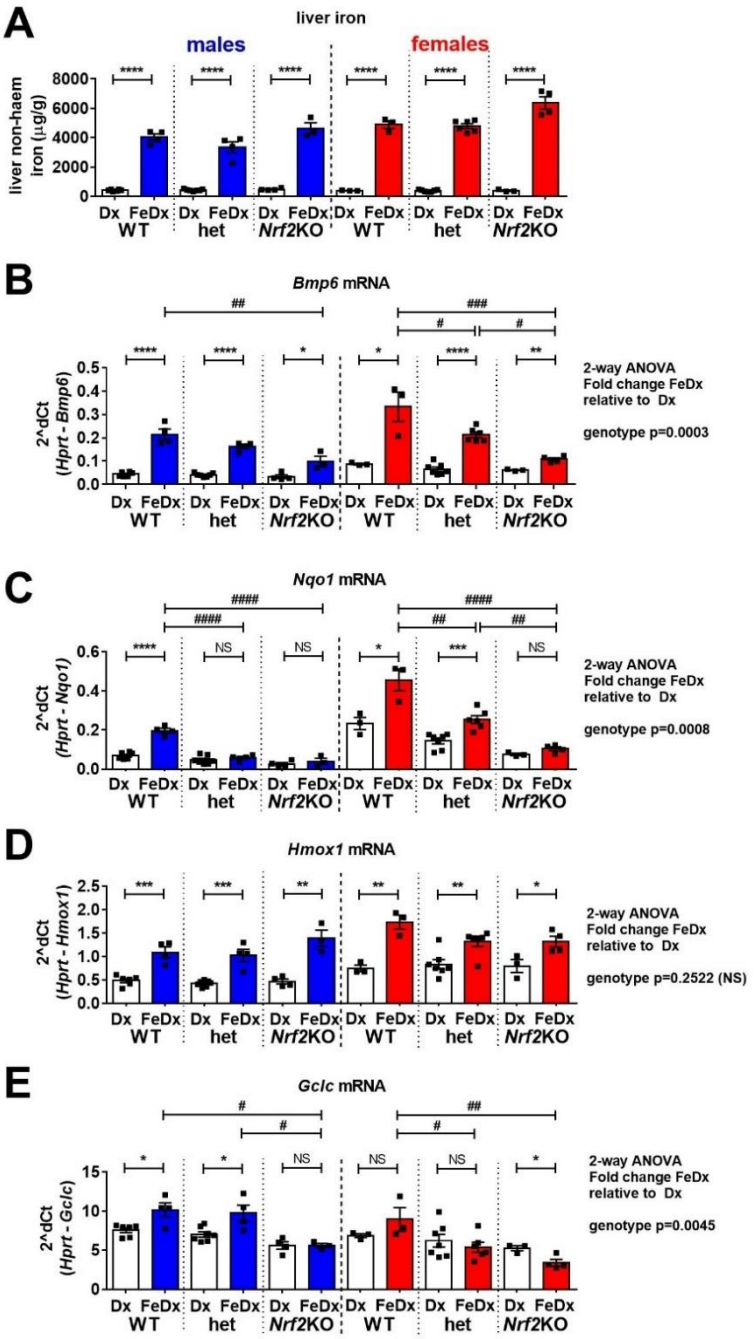


Figure 4.25: Wildtype (WT), heterozygous (het) and homozygous *Nrf2*-knockout (*Nrf2*KO) mice injected with 4mg FeDx or Dx control intraperitoneally. 24 hours post-injection, **(A)** liver non-haem iron and **(B-E)** liver gene expression was quantified. Nrf2 deficiency led to a blunting in the upregulation of *Bmp6*, *Nqo1* and *Gclc* in response to FeDx (n=3 to 7; t-test between Dx and FeDx: * $p<0.05$, ** $p<0.01$, *** $p<0.001$, **** $p<0.0001$; 2-way ANOVA between WT FeDx, het FeDx and *Nrf2*KO FeDx: # $p<0.05$, ## $p<0.01$, ### $p<0.001$, #### $p<0.0001$; right panel: 2-way ANOVA on fold change gene expression to compare effects across genotypes by stratifying on sex and genotype).

In a third *in vivo* model, 5-week old male *Nrf2*-knockout and wildtype littermate mice were fed a 2ppm low iron diet for 2 weeks, followed by oral gavage of 2mg iron per kg body weight in the form of ferrous sulphate or water control. The mice were culled 6 hours after oral iron administration. Serum and liver iron concentration was measured and hepatic gene expression was quantified. Acute oral iron administration did not alter liver iron content (Figure 4.26A), but raised serum iron levels significantly in wildtype mice, and marginally but not significantly in *Nrf2*-knockout mice (Figure 4.26B). The oral administration of $FeSO_4$ also increased hepatic *Bmp6*, *Nqo1* and *Gclc* expression in wildtype but not *Nrf2*-knockout mice (Figure 4.26C, E, G). This observation is also supportive of the hypothesis that the upregulation of *Bmp6* by iron requires Nrf2. *Bmp2* and *Hmox1* expression were unaltered by oral administration of $FeSO_4$ (Figure 4.26D, F).

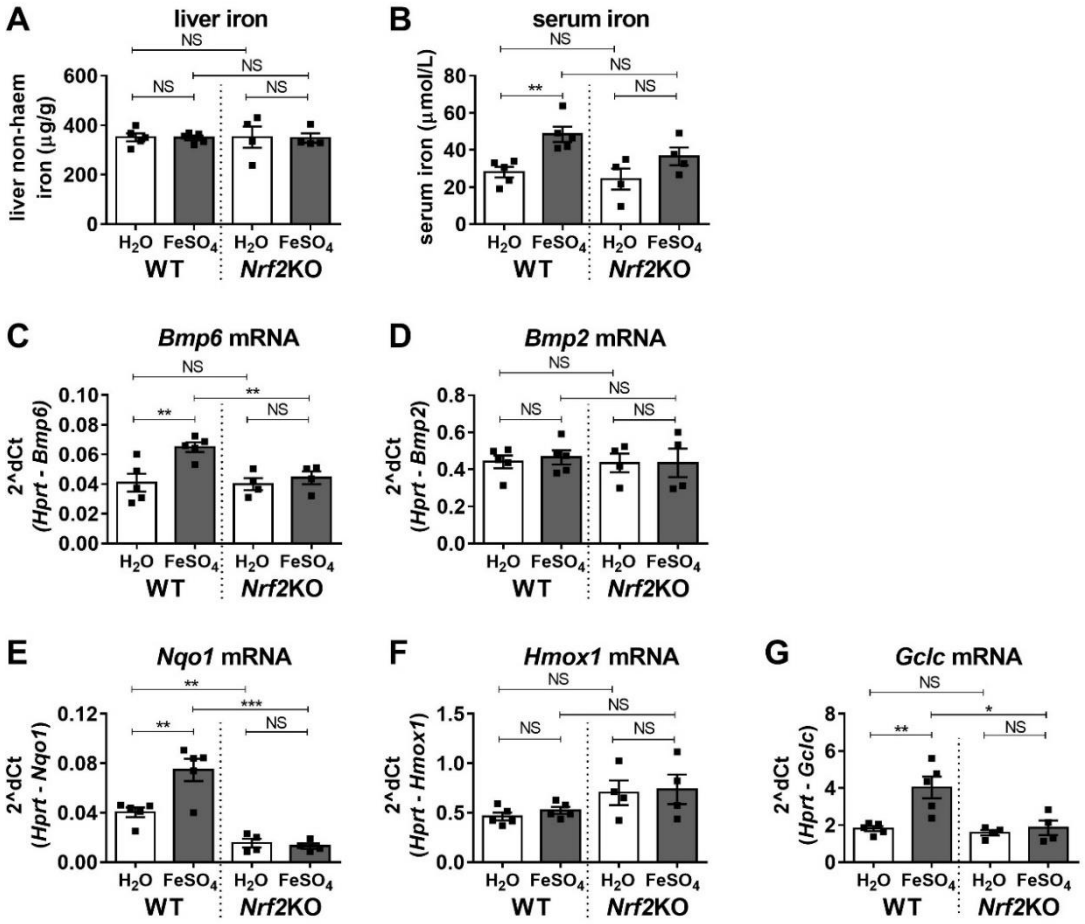


Figure 4.26: Wildtype (WT) and *Nrf2*-knockout (*Nrf2*KO) mice were fed 2 weeks of low iron diet, followed by oral gavage of 2mg/kg iron in the form of $FeSO_4$. **(A)** Liver non-haem iron, **(B)** serum iron and **(C-G)** liver gene expression was quantified 6 hours after iron gavage. Unlike wildtype mice, *Nrf2*KO mice failed to upregulate *Bmp6*, *Nqo1* and *Gclc* in response to $FeSO_4$ (n=4 to 5; t-test: * $p<0.05$, ** $p<0.01$, *** $p<0.001$).

We previously showed that hemin caused an upregulation of *Bmp6* in the livers of C57BL6 mice without altering liver non-haem iron concentration (Figure 3.14), and the upregulation of *Bmp6* is likely mediated by Bach1 degradation and/or Nrf2 activation, since hemin reduces Bach1 protein levels and induce Nrf2 nuclear accumulation *in vitro* (Figure 3.12). To test this hypothesis, 6-week old male and female *Nrf2*-homozygous knockout, heterozygous knockout and wildtype littermate mice were injected intraperitoneally with 2 doses of hemin (50µmol/kg body weight for each dose) 12 hours apart and culled 12 hours after the second dose of hemin.

The upregulation of *Bmp6* and *Hmox1* by hemin was blunted in *Nrf2*-heterozygous and homozygous knockout mice, with a stronger effect in homozygous knockouts than heterozygous knockouts (Figure 4.27A, C). Lack of Nrf2 completely prevented upregulation of *Bmp6* by hemin, while upregulation of *Hmox1* by hemin was decreased, but still significant, in the absence of Nrf2, indicating that even without Nrf2 activation, loss of repression by Bach1 due to haem-induced degradation is sufficient to drive some *Hmox1* upregulation. In this experiment, hemin did not induce the expression of *Nqo1* even in wildtype mice. However, the expression of *Nqo1* was lower in mice deficient in Nrf2 (Figure 4.27B). 2-way ANOVA was performed on fold change in gene expression by stratifying on sex and genotype (WT, heterozygous and homozygous knockout); the statistical analysis (right panel in Figure 4.27) demonstrates that the loss of Nrf2 significantly blocks the ability of the liver to upregulate *Bmp6* and *Hmox1* expression in response to hemin. Thus, the data supports our hypothesis that Nrf2 is required for the induction of *Bmp6* by hemin.

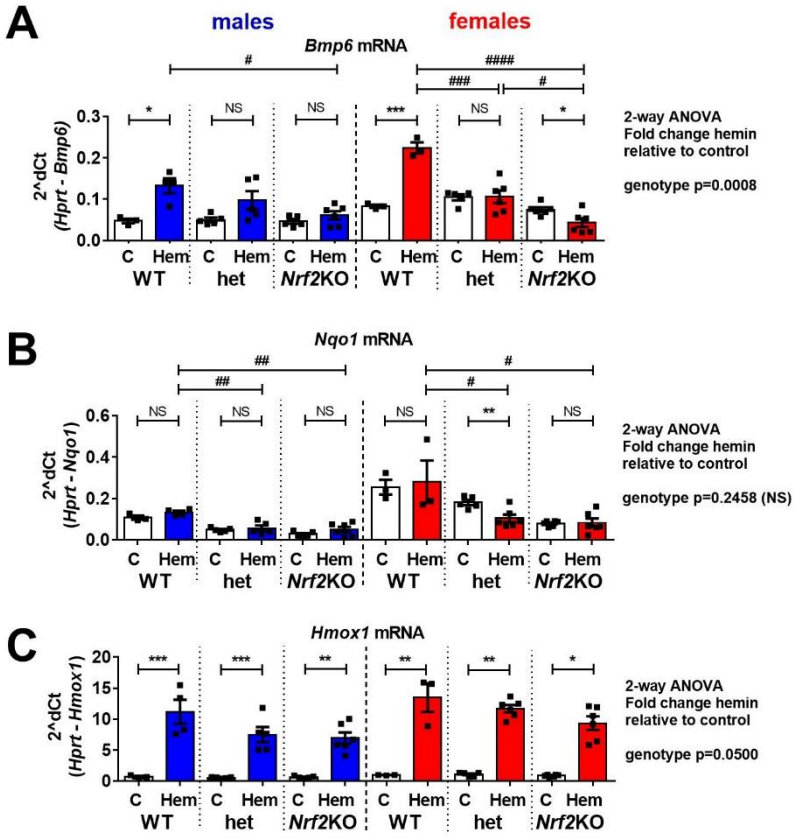


Figure 4.27: Wildtype (WT), heterozygous *Nrf2*-knockout (het) and homozygous *Nrf2*-knockout (*Nrf2*KO) mice were injected with 2 doses of hemin (50µmol/kg per dose, 12 hours apart) or saline intraperitoneally. 12 hours after the last injection, hepatic gene expression of **(A)** *Bmp6*, **(B)** *Nqo1* and **(C)** *Hmox1* was quantified by qRT-PCR. Nrf2 deficiency led to a blunting in the upregulation of *Bmp6* and *Hmox1* in response to hemin (n=3 to 6; t-test between hemin and saline: * $p<0.05$, ** $p<0.01$, *** $p<0.001$, **** $p<0.0001$; 2-way ANOVA between WT hemin, het hemin and *Nrf2*KO hemin: # $p<0.05$, ## $p<0.01$, ### $p<0.001$, #### $p<0.0001$; right panel: 2-way ANOVA on fold change gene expression to compare effects across genotypes by stratifying on sex and genotype).

4.2.4 Mechanism of Nrf2 activation by iron

4.2.4.1 Nrf2 mRNA is not consistently upregulated in response to iron and hemin

The stabilisation and nuclear accumulation of Nrf2 protein in response to iron and hemin has been demonstrated in Chapter 3 (Figure 3.7B, Figure 3.12B). However, Nrf2 can also be regulated at the mRNA level via transcriptional control by itself (Kwak et al., 2002) or the AHR transcription factor (Miao et al., 2005), or by miRNA-mediated mRNA degradation (Kurinna and Werner, 2015). To investigate whether the iron treatments we used altered Nrf2 mRNA levels, hepatic *Nfe2l2* mRNA was quantified in response to intraperitoneal FeDx, intraperitoneal hemin or 2 weeks of dietary iron loading. The data demonstrates that *Nfe2l2* mRNA level was significantly higher in WT and *Nrf2*-

heterozygous knockout male mice in response to FeDx; this trend was however not observed in female mice injected with FeDx (Figure 4.28A). Moreover, *Nfe2l2* mRNA level was unaltered in male and female mice in response to hemin (Figure 4.28B). Dietary iron loading did not alter *Nfe2l2* mRNA level (Figure 4.28C). The data collectively suggest that the activation of Nrf2 by iron and hemin is unlikely to occur solely at the transcriptional level, but instead works via protein stabilisation of Nrf2.

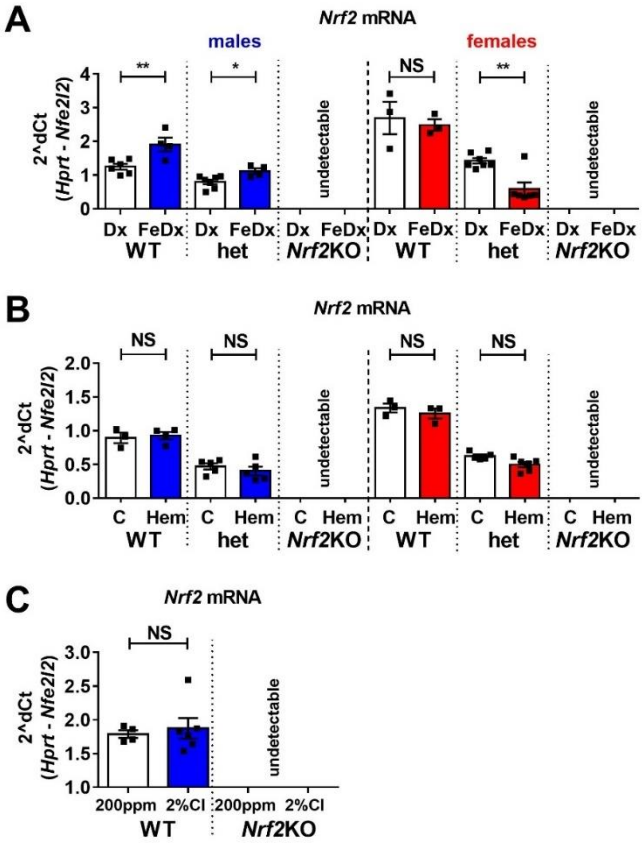


Figure 4.28: Hepatic *Nfe2l2* mRNA was quantified in mice **(A)** 24 hours post-intraperitoneal injection of 4mg FeDx or Dx control, **(B)** 24 hours post-intraperitoneal injection of 2 doses of hemin (50µmol/kg) and **(C)** fed a 200ppm iron or 2% CI diet for 2 weeks (t-test: * p<0.05, ** p<0.01, *** p<0.001, **** p<0.0001).

4.2.4.2 Iron activates Nrf2 and upregulates *Bmp6* via induction of oxidative stress

To determine whether the activation of Nrf2 by iron could occur via oxidative stress, we first measured oxidative stress levels in mice fed a 200ppm or 1% CI diet for a week. One week of dietary iron loading increased hepatic non-haem iron content and hepatic malondialdehyde concentration (Figure 4.29), which is a product of lipid peroxidation and serves as a marker of oxidative stress. This demonstrates that iron accumulation elevates oxidative stress levels.

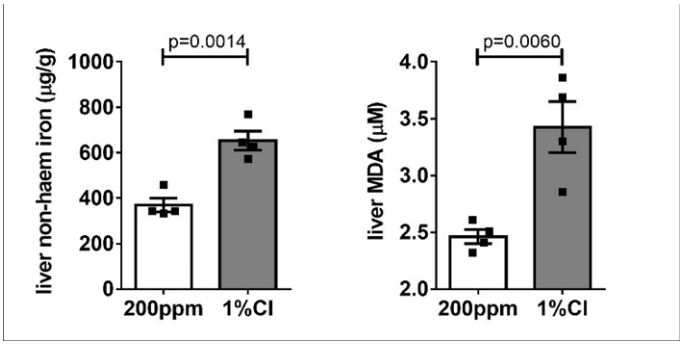


Figure 4.29: C57BL6 mice were fed diets containing 200ppm or 1% CI for a week. Mice fed a high iron diet had higher levels of non-haem iron and malondialdehyde (MDA) in the liver (n=4, t-test).

Next, we investigated whether oxidative stress is required for the upregulation of Nrf2 target genes in response to iron. mitoTEMPO acts as an antioxidant by scavenging free radicals by reacting with and neutralising superoxide and other free radicals (Dikalova et al., 2010). L929 cells were pre-treated with mitoTEMPO for one hour, then exposed to 1mg/ml FeDx for 6 hours. Pre-treatment with mitoTEMPO caused a block in the upregulation of *Bmp6* and a trend towards blunting in *Nqo1* induction in response to FeDx; the upregulation of *Hmox1* by FeDx was unaltered by mitoTEMPO (Figure 4.30).

We also tested the effect of mitoTEMPO *in vivo.* Wildtype mice were fed a 2ppm iron diet for 3 weeks, then gavaged with 2mg/kg iron ($FeSO_4$) or water control, and injected with saline control or 0.25mg mitoTEMPO intraperitoneally one hour after oral iron treatment. Liver non-haem iron content was unaltered while serum iron was raised in mice gavaged with iron (Figure 4.31), similarly to previous observations (Figure 4.26). In mice treated with mitoTEMPO, the upregulation of *Bmp6* and *Hmox1* in the liver in response to iron was completely blocked; the upregulation of *Gclc* was marginally blunted, albeit not significantly. However, the induction of *Nqo1* was not altered by mitoTEMPO (Figure 4.31). Collectively, although the effects of mitoTEMPO on the upregulation of *Bmp6* and other Nrf2 target genes appear modest, the data suggest that the activation of Nrf2 by iron may in part involve iron-induced formation of free radicals and oxidative stress, since the neutralisation of superoxide and other free radicals using mitoTEMPO caused a trend towards suppression of Nrf2 target genes. Both *in vitro* and *in vivo,* the upregulation of *Bmp6* by iron was

also blocked by mitoTEMPO, which is coherent with our previous data demonstrating that *Bmp6* is induced by iron in an Nrf2-dependent manner, and suggests *Bmp6* expression is responsive to iron-induced oxidative stress, not only iron accumulation *per se*.

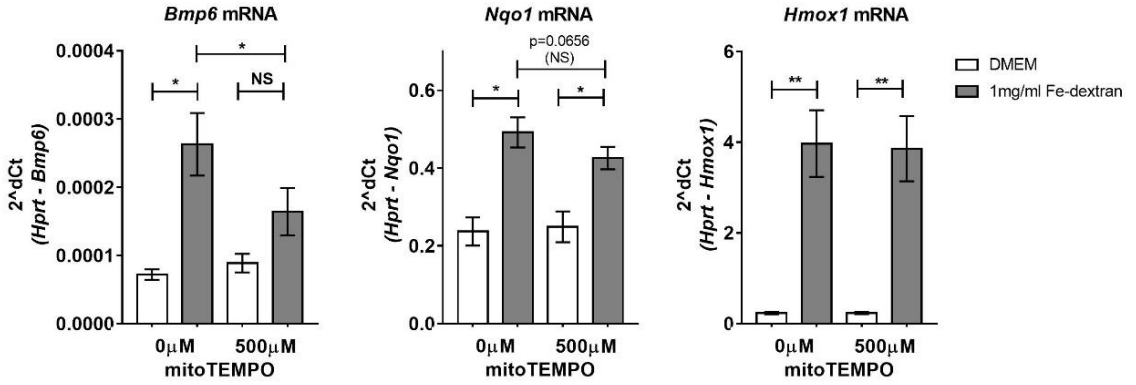


Figure 4.30: Pre-treatment of L929 cells with 500μM mitoTEMPO one hour prior to FeDx treatment blocked *Bmp6* induction by iron. The upregulation of *Nqo1* and *Hmox1* was not significantly altered (n=5, paired t-test: * p<0.05, ** p<0.01).

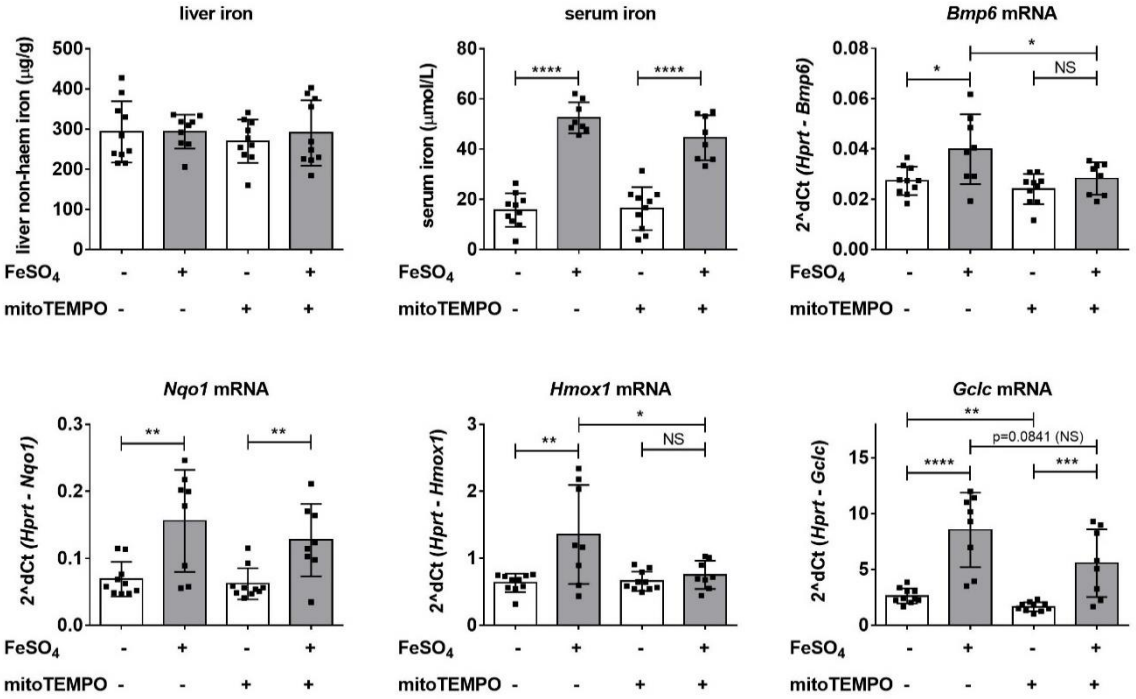


Figure 4.31: 4-week old wildtype male mice were fed 2ppm iron diet for 2 weeks, then gavaged with 2mg/kg iron ($FeSO_4$) or water control, and intraperitoneally injected with 500μM mitoTEMPO or saline control 1 hour after gavage. Mice were culled 6 hours post-gavage. Liver non-haem iron was unaltered, while serum iron was raised in response to iron gavage. Hepatic gene expression analysis showed a block in *Bmp6* and *Hmox1* induction in mice treated with mitoTEMPO (n=8 to10; t-test: * p<0.05, ** p<0.01, *** p<0.001, **** p<0.0001).

4.2.4.3 Activation of Nrf2 by iron is independent of inducible nitric oxide synthase

Nitric oxide •NO can associate directly with Keap1 at its C151 residue and destabilises the Nrf2-Keap1-Cullin3 complex, thus stabilising Nrf2 protein (McMahon et al., 2010). In macrophages, infection with *Salmonella typhimurium* causes an iNOS-dependent elevation of •NO levels, which in turn activates Nrf2. This consequentially increases the expression of ferroportin, an Nrf2-dependent gene, and causes iron efflux. This mechanism is thought to be protective to the host by reducing iron availability to the bacteria (Nairz et al., 2013).

To investigate whether iNOS is involved in the activation of Nrf2 by iron, hepatic *Nos2* mRNA was quantified in mice in response to dietary iron loading, oral $FeSO_4$ or intraperitoneal injection of FeDx, and in i*Hamp1*-knockout mice. *Nos2* mRNA was not significantly different among mice fed 3 weeks of diet containing either 2ppm iron, 200ppm iron or 1% CI (Figure 4.32A). *Nos2* expression was significantly elevated in i*Hamp1*KO (Cre positive) and i*Hamp1*Ctrl (Cre negative) mice injected with 1mg tamoxifen intraperitoneally daily for 4 consecutive days compared to vehicle-treated mice. However, *Nos2* mRNA levels were not different between tamoxifen-treated i*Hamp1*KO and i*Hamp1*Ctrl, suggesting that the upregulation of *Nos2* is tamoxifen-driven rather than iron-induced (Figure 4.32B). Oral gavage of 2mg/kg iron in the form of $FeSO_4$ did not alter *Nos2* expression in wildtype and *Nrf2*-knockout mice (fed 2 weeks of 2ppm iron diet prior to iron gavage) (Figure 4.32C). However, we did observe a mild upregulation in *Nos2* expression in mice 6 hours post-intraperitoneal administration of FeDx (Figure 4.32D).

To follow up on the observation that intraperitoneal FeDx increases *Nos2* expression, *Nos2*-knockout and wildtype littermate mice were intraperitoneally injected with FeDx and hepatic liver iron and gene expression were measured 6 hours post FeDx administration. Liver non-haem iron was elevated in mice injected with FeDx. FeDx also upregulated *Bmp6*, *Hmox1* and *Gclc* expression in both wildtype and *Nos2*-knockout mice; *Nqo1* expression was not upregulated by 6 hours after FeDx treatment (Figure 4.33).

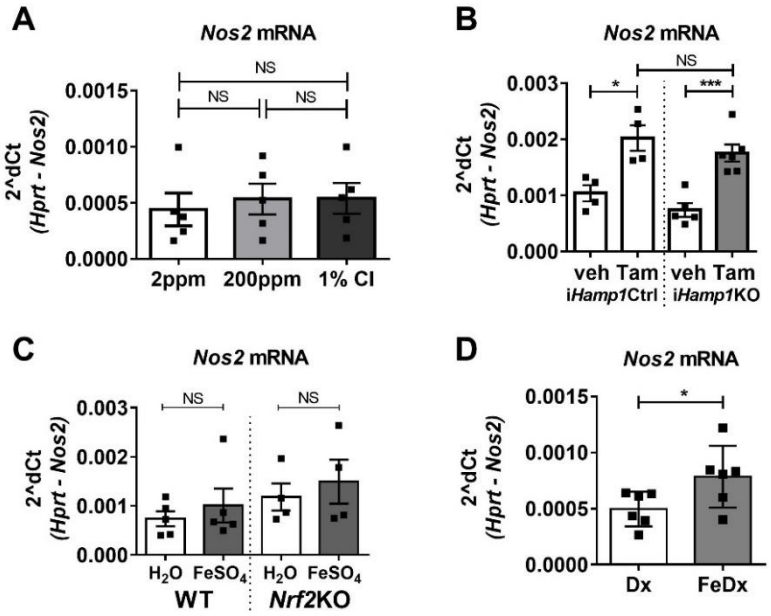


Figure 4.32: Hepatic *Nos2* mRNA was quantified by qRT-PCR in response to iron. **(A)** 3-week old male C57BL6 mice were fed diets containing 2ppm iron, 200ppm iron or 1% CI for 3 weeks (n=5, ANOVA). **(B)** i*Hamp1*KO and i*Hamp1*Ctrl mice were injected with vehicle (veh) or 1mg tamoxifen (Tam) daily for 4 days (n=4 to 6, t-test). **(C)** Wildtype (WT) and *Nrf2*-knockout (*Nrf2*KO) mice were fed 2 weeks of 2ppm iron diet, followed by oral gavage of 2mg/kg iron ($FeSO_4$) and culled 6 hours post-gavage (n=4 to 5, t-test). **(D)** 6-week old male C57BL6 mice were injected with 4mg FeDx or Dx control intraperitoneally and culled 6 hours post-injection (n=6, t-test). * p<0.05, *** p<0.001.

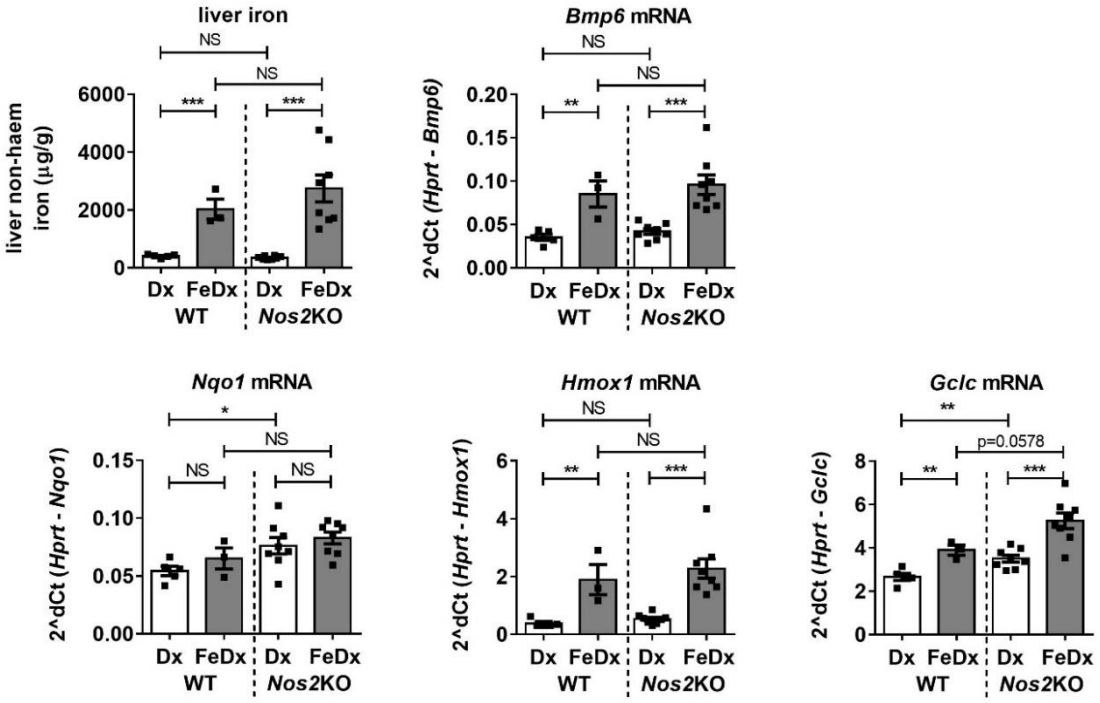


Figure 4.33: 6- to 8-week old male wildtype (WT) and *Nos2*-knockout (*Nos2*KO) mice were injected with 4mg FeDx or Dx control intraperitoneally and culled 6 hours post-injection. Liver non-haem iron and gene expression were quantified. Both WT and *Nos2*KO mice are able to upregulate *Bmp6*, *Hmox1* and *Gclc* expression in response to FeDx (n=3 to 8, t-test: * p<0.05, ** p<0.01, *** p<0.001).

In summary, the data suggest that the activation of Nrf2 in response to iron is not iNOS-dependent, since *Nos2* mRNA is not altered in response to dietary iron loading, hepcidin deletion and oral $FeSO_4$. Additionally, although intraperitoneal FeDx upregulates *Nos2* expression, *Nos2*-knockout mice upregulate *Bmp6*, *Hmox1* and *Gclc* expression in response to FeDx in a manner similar to wildtype mice.

4.3 Discussion

The central aim of this thesis is to identify the molecular mechanism linking iron overload to the transcriptional control of *Bmp6*. Since iron induces oxidative stress due to its redox-active nature, and cells combat oxidative stress by activating Nrf2 transcription factor, which positively controls the expression of a battery of cytoprotective and antioxidant genes, we hypothesized that *Bmp6* may be an Nrf2 target gene that is transcriptionally activated in response to iron-induced oxidative stress.

Firstly, we demonstrated that *Bmp6* is under the transcriptional control of Nrf2 by several approaches. Analysis of published Nrf2 ChIP-seq data from C2C12 cells treated with Nrf2 agonist and Keap1-deficient MEF cells show binding of Nrf2 to an ARE in proximity to the *Bmp6* promoter. This ARE is highly conserved in mammals suggesting its function is important. To test whether *Bmp6* expression is altered by manipulation of the Nrf2 system, we performed siRNA-mediated knockdown of Nrf2 in C2C12 and MEF cells and observed a downregulation in *Bmp6* expression. Knockdown of Nrf2 in L929 cells, the *in vitro* model established in Chapter 3, also led to a suppression in *Bmp6* expression. Conversely, *Bmp6* expression was derepressed upon knockdown of Bach1 in C2C12, MEF and L929 cells, and knockdown of Keap1 showed that *Bmp6* expression was upregulated in C2C12 and MEF cells although it was unaltered in L929 cells. Moreover, pharmacological activation of Nrf2 using either CDDO-Im or SB216763 enhanced *Bmp6* expression both *in vitro* and *in vivo*. Previously published work demonstrated a 6.24-fold induction of *Bmp6* expression in the liver 6 hours after oral gavage of CDDO-Im in wildtype mice (Yates et al., 2009). This study was, however, only performed on wildtype mice. To account for the possibility of Nrf2-independent effects exerted by CDDO-Im, we treated *Nrf2*-knockout and wildtype littermates with CDDO-Im using a similar regimen as Yates, and showed that the upregulation of *Bmp6* in response to CDDO-Im is indeed Nrf2-dependent, since the effects were only observed in wildtype and not *Nrf2*-knockout mice. In addition, we also looked at hepatic gene expression in wildtype mice 3 hours after oral administration of CDDO-Im and observed a robust upregulation of *Bmp6* expression in parallel with other Nrf2 target genes *Nqo1, Hmox1, Gclc, Fth1* and *Ftl1* (Supplementary Figure 2). This acute response within a short period of time suggests a direct effect of Nrf2 on the transcriptional

control of *Bmp6*. Yates and colleagues also demonstrated that conditional knockout of Keap1 in the liver in Albumin-Cre:*Keap1*$^{(flox/-)}$ did not alter hepatic *Bmp6* expression. *In vivo*, the key cell type that makes *Bmp6* to control iron homeostasis is likely the LSECs (Canali et al., 2017). Our collaborators found that CDDO-Im induced *Bmp6* mRNA, as well as *Nqo1*, *Hmox1* and *Gclc*, consistent with Nrf2 activation driving *Bmp6* expression in this cell type.

In contrast to LSECs, the expression of *Bmp6* by hepatocytes is low, and furthermore does not appear to be under the control of Nrf2. We looked at hepatic gene expression profiles of mice expressing constitutively active Nrf2 (caNrf2) in hepatocytes in collaboration with Sabine Werner and Ulrike Köhler (ETH, Zürich). caNrf2 mice express a construct of Nrf2 lacking the Neh2 domain involved in Keap1-binding under the control of a cytomegalovirus enhancer and ß-actin promoter (Köhler et al., 2014). A transcription/translation STOP cassette flanked by loxP sites between the promoter and caNrf2 gene sequence allows the expression of caNrf2 specifically in hepatocytes when the Cre recombinase under the control of the albumin promoter excises the STOP cassette (AlbCre-caNrf2 mice). AlbCre-caNrf2 mice have elevated hepatic *Nqo1*, *Fth1* and *Slc40a1* expression compared to AlbCre mice. However, hepatic *Hmox1* and *Bmp6* expression was not different between AlbCre-caNrf2 mice and AlbCre mice (Supplementary Table 1). In addition, Yates and colleagues demonstrated that conditional knockout of Keap1 in hepatocytes in Albumin-Cre:*Keap1*$^{(flox/-)}$ did not alter hepatic *Bmp6* expression. In fact, only 174 genes were modulated by both Keap1-deficiency and CDDO-Im, while 196 and 84 genes were modulated specifically in response to Keap1-deficiency and CDDO-Im, respectively (Yates et al., 2009).

There is clearly some complexity in the regulation of ARE/Nrf2-driven genes, where the effects are dependent on multiple factors including the mechanism of Nrf2 activation, cell type involved, and the gene of interest being studied. For example the results of siRNA experiments in C2C12 cells indicate that *Hmox1* is primarily repressed by Bach1 and its expression is not strongly affected by knockdown of Nrf2 or Keap1, whereas *Nqo1* expression is predominantly controlled by Nrf2 and Keap1 but not Bach1; *Bmp6* expression is regulated by all three factors in the system.

However, this scheme is not precisely reproduced in all cell types tested. Nevertheless, the data in the first section of Chapter 4 collectively provide strong evidences pointing towards *Bmp6* as an Nrf2/ARE-regulated gene including, importantly, in LSECs.

Building up on these observations, we next investigated whether the upregulation of *Bmp6* expression by iron occurs in an Nrf2-dependent manner. siRNA-mediated knockdown of Nrf2 completely blocked *Bmp6* induction by FeDx in L929 cells, and blunted the *Bmp6* response to FAC in C2C12 cells. Similarly, *in vivo*, mice lacking Nrf2 cannot upregulate *Bmp6* in response to chronic dietary iron loading over 2 weeks and acute oral iron gavage for 6 hours. The upregulation of *Bmp6* by intraperitoneal FeDx was blunted, although not completely blocked, in the absence of Nrf2. Hence, it is apparent that Nrf2 is necessary to trigger a *Bmp6* response during conditions of elevated iron status, especially in response to iron accumulation by the oral route. *Bmp6* can seemingly be induced via Nrf2-independent mechanisms since *Nrf2*-knockout mice are able to mount a small *Bmp6* response upon intraperitoneal FeDx treatment, although the upregulation of *Bmp6* is significantly blunted compared to wildtype mice. Nevertheless, this data represents the first report characterising the molecular mechanism involved in the upregulation of *Bmp6* expression by iron accumulation.

The role of Nrf2 in regulating *Bmp6* expression in response to haem was also studied. Unlike their wildtype littermates, *Nrf2*-knockout mice were unable to upregulate *Bmp6* in response to intraperitoneally-administered hemin, once again suggesting the crucial role of Nrf2 in controlling *Bmp6* transcription. *In vitro*, knockdown of Nrf2 completely blocks the upregulation of *Nqo1* by haem, while the induction of *Hmox1* was unaltered. This observation was not unexpected since derepression of Bach1 allows Nrf2-independent regulation of *Hmox1* expression (Macleod et al., 2009), and this can be mediated via haem-induced degradation of Bach1. The induction of *Bmp6* by hemin was not abrogated upon the knockdown of Nrf2 *in vitro*, similar to observations on *Hmox1*. This suggests that while we have characterised *Bmp6* to be under the transcriptional control of Nrf2 and ARE enhancers, *Bmp6* may also be regulated by other transcription factors that are able to operate when the suppressive factor Bach1 is degraded by haem and in the absence of Nrf2.

In the last section of this Chapter, we show that hepatic oxidative stress level is elevated in response to liver iron accumulation, in line with previous studies (Jomova and Valko, 2011; Koskenkorva-Frank et al., 2013). Combatting oxidative stress using the free radical scavenger mitoTEMPO blunts the induction of *Bmp6* by iron both *in vivo* and *in vitro*; the upregulation of *Hmox1* in response to oral iron was also blocked by mitoTEMPO *in vivo*. We noted that mitoTEMPO only had a modest effect on preventing iron-induced Nrf2 activation as expression of other Nrf2 target genes *Nqo1* and *Gclc* was only partially inhibited. A plausible explanation for this is that mitoTEMPO neutralises free radicals but not iron, which is the source catalysing the formation of free radicals. Thus, the single dose of mitoTEMPO may be insufficient to neutralise the free radicals being constantly generated over 6 hours, the time point used for both *in vitro* and *in vivo* experiments.

In a literature search for effects of other antioxidants on *Bmp6* expression, we came across microarray data of wildtype and *Nrf2*-knockout mice treated with butylated hydroxyanisole (BHA) (Nair et al., 2006). BHA is a phenolic compound with antioxidant properties as it is able to donate a hydrogen atom to oxygen radicals and stabilise its oxidised form via the inherent resonance of its benzene ring, and by enhancing the synthesis of glutathione in the liver (Festjens et al., 2006). However, BHA has also been demonstrated to be an activator of Nrf2, as its metabolite tert-butylbenzoquinone binds to cysteine residues of Keap1 and blocks its inhibitory function on Nrf2 (Abiko et al., 2011). Nair and colleagues showed that oral administration of BHA led to a downregulation of hepatic *Bmp6* expression but an upregulation of hepatic *Hmox1* and *Gclc* expression by 3 hours, and a delayed induction of *Nqo1* expression at 12 hours. The contrasting effect of BHA on *Bmp6* and the other known Nrf2-target genes is intriguing; *Bmp6* might be more sensitive to the antioxidant effects of BHA while *Nqo1*, *Hmox1* and *Gclc* might be more sensitive to the Nrf2-activating effects of BHA.

Interestingly, opposing effects of Nrf2 on gene expression has been previously shown. The Nrf2 agonist sulforaphane caused an Nrf2-dependent upregulation of interleukin-6 (*Il6*) expression

(Wruck et al., 2011), while another Nrf2 agonist diethyl maleate caused an Nrf2-dependent downregulation of *Il6* expression (Kobayashi et al., 2016). In the latter case, binding of Nrf2 to an ARE enhancer region in proximity to *Il6* blocked the recruitment of RNA polymerase II at the transcriptional start site of *Il6*. Hence, there appears to be much about regulation of gene expression by Nrf2 that remains to be fully understood.

Bmp6 is expressed in multiple tissues, including but not limited to the liver, heart, duodenum, osteoblasts and osteoclasts (Canali et al., 2017; Kautz et al., 2011; McCullough et al., 2007). Global genetic deletion of *Bmp6* in mice causes bone deformities such as sternum ossification (Solloway et al., 1998), impaired growth plate function leading to formation of smaller long bones (Perry et al., 2008) and iron overload (Meynard et al., 2009). However, our studies on the role of Nrf2 in controlling *Bmp6* expression are focused on the liver, since the liver is the main iron storage organ and main source of the iron regulatory hormone hepcidin. While knockdown of Nrf2 decreases *Bmp6* expression *in vitro* in L929, C2C12 and MEF cells, hepatic *Bmp6* expression is not different between wildtype and *Nrf2*-knockout mice on a standard 200ppm iron diet. This highlights that alternative mechanisms other than Nrf2 may be facilitating the maintenance of basal *Bmp6* expression in the liver in order to maintain a normal physiological state. In line with this, Nrf2 has a very short half-life at resting conditions (Itoh et al., 2003; Kobayashi et al., 2004a) and is stabilised and activated under stress conditions, suggesting that its role in maintaining basal gene expression levels could be minimal. In contrast, iron-loaded *Nrf2*-knockout mice are unable to upregulate *Bmp6* expression in the liver, demonstrating that Nrf2 is a molecular sensor of toxic iron and is activated in response to iron accumulation to enhance *Bmp6* synthesis.

In summary, we showed that *Bmp6* is under the transcriptional control of the Nrf2/Keap1/Bach1 system likely via a conserved ARE enhancer in intron 1. Iron accumulation induces oxidative stress, which consequentially activates the Nrf2 antioxidant response pathway and upregulates the expression of *Bmp6* in an Nrf2-dependent manner. In the next Chapter, we investigate the impact of a deficient *Bmp6* response on hepcidin and iron physiology in *Nrf2*-knockout mice.

Chapter 5

Regulation of iron homeostasis and haemochromatosis by Nrf2

5.1 Background

5.1.1 Disruption of hepcidin synthesis causes dysregulation of iron homeostasis and iron disorders

Systemic iron homeostasis is regulated by controlling dietary iron absorption through duodenal enterocytes and iron recycling from senescent erythrocytes by splenic red pulp macrophages. The regulation of systemic iron homeostasis is mediated by the iron hormone hepcidin (encoded by *HAMP* gene in humans and *Hamp1* in mice). Elevation in tissue or serum iron levels upregulate hepcidin synthesis by hepatocytes via the Bmp/Smad signalling pathway. Bmp6 is a non-redundant endogenous regulator of hepcidin in response to hepatic tissue iron accumulation, since dietary iron loading upregulates the expression of *Bmp6* (Kautz et al., 2008, also see Chapter 3), and *Bmp6*-deficient mice have suppressed hepcidin expression and experience massive iron accumulation (Andriopoulos et al., 2009; Canali et al., 2017; Meynard et al., 2009). Mutations in BMP6 have also been associated with reduced hepcidin synthesis and iron overload in humans (Daher et al., 2016). Increased serum iron levels also upregulated the Bmp/Smad signalling pathway, but without major induction of *Bmp6* expression (Corradini et al., 2011b). Instead, the interaction of HFE and Tfr2 in response to elevated serum iron has been proposed to stabilise the Bmp/Smad signalling pathway, thus enhancing hepcidin expression (Gao et al., 2009). Hepcidin is then secreted into the circulation, binds to ferroportin on enterocytes and macrophages and induces the degradation of ferroportin (Nemeth et al., 2004a), thus, forming a negative feedback loop by restricting dietary iron absorption by enterocytes and iron recycling by macrophages.

Since hepcidin plays a critical role in controlling iron homeostasis, mutations in hepcidin can cause dysregulation of iron homeostasis and lead to haemochromatosis, the iron overload disease (Roetto et al., 2003, 2004). Additionally, haemochromatosis can also be caused by mutations in the iron export protein ferroportin rendering ferroportin resistant to hepcidin (Drakesmith et al., 2005; Sham et al., 2009), and in molecules involved in regulating hepcidin synthesis via the Bmp/Smad signalling in the liver, including TfR2 (Camaschella et al., 2000), HJV (Niederkofler et al., 2005; Papanikolaou et al., 2004) and HFE. Notably, the most common cause of hereditary

haemochromatosis is the HFE C282Y substitution (c.845G>A (p.Cys282Tyr)), where 9 in 10 haemochromatosis patients in the United Kingdom are homozygous for this mutation, and 1.9% of the world population carries the mutant allele (Merryweather-Clarke et al., 1997); the clinical penetrance of the mutation is still being assessed (Beutler et al., 2002; Gallego et al., 2015; Grosse et al., 2017). Haemochromatosis predisposes patients to liver cirrhosis, diabetes, cardiovascular diseases and infections by siderophilic microorganisms (Jomova and Valko, 2011; Pietrangelo, 2015).

5.1.2 Hepcidin as a therapeutic target for ameliorating HFE-haemochromatosis

Despite the prevalence of haemochromatosis and its contribution to other disease states, treatment options are somewhat limited, therefore urging the need for research in developing new therapeutic strategies for haemochromatosis. Removal of excess iron by phlebotomy remains the main therapeutic strategy for haemochromatosis. While phlebotomy is effective for most patients, it drastically reduces the quality of life as the treatment is lifelong and are occasionally associated with side effects including soreness in arms, extreme fatigue, dizziness and heart palpitations (Adams and Barton, 2010; Assi and Baz, 2014). Furthermore, the necessity to attend outpatient clinics for blood removal places a time and financial burden on both patient and health services that could potentially be avoided if other treatment strategies were available. Since hepcidin plays a central role in regulating iron homeostasis, therapeutic approaches targeting hepcidin to ameliorate haemochromatosis and other iron disorders are currently under development.

One strategy proposes the use of hepcidin mimetics called minihepcidins, which are small peptides consisting of 7 to 9 amino acids and were designed based on the ferroportin-binding region of hepcidin (Preza et al., 2011). Minihepcidins retain the ability to induce ferroportin degradation, and chronic administration of minihepcidins in hepcidin-knockout mice reduced serum and liver iron content (Ramos et al., 2012), highlighting the potential of minihepcidins in treating iron overload disorders.

An alternative approach is to stimulate endogenous hepcidin synthesis. The first method targets the transmembrane protease serine 6 (*Tmprss6*), a protease that downregulates the Bmp/Smad signalling pathway and hepcidin expression by cleaving the Bmp co-receptor Hjv (Silvestri et al., 2008). Suppression of *Tmprss6* expression using antisense oligonucleotides (Guo et al., 2013) or siRNAs (Schmidt et al., 2013) raised hepcidin expression and reduced serum and liver iron content in *Hfe*-knockout haemochromatosis mice. Additionally, a single supraphysiological dose of exogenous recombinant BMP6 increased hepcidin expression by 6 hours; repeated administration of recombinant BMP6 over 10 days reduced serum iron and caused iron retention in the spleen and duodenum in *Hfe*-knockout mice (Corradini et al., 2010). These demonstrate that targeting the Bmp/Smad signalling pathway to induce endogenous hepcidin production is a promising approach to ameliorating iron-overloading diseases.

5.1.3 Chapter Aims

In the previous Chapter, we demonstrated that iron accumulation upregulates *Bmp6* expression via the Nrf2 transcription factor. Since *Bmp6* is a critical regulator of hepcidin and systemic iron homeostasis, we first aimed to study whether the inability to upregulate *Bmp6* due to Nrf2 deficiency disrupts hepcidin expression and iron physiology, in wildtype and *Hfe*-knockout mice. Second, we assessed whether genetic variation associated with the *NRF2* locus in humans could influence iron status in haemochromatosis patients. Third, we aimed to investigate whether pharmacological induction of Nrf2 could ameliorate iron loading in mouse models of haemochromatosis, potentially via induction of *Bmp6* and hepcidin.

5.1.4 Methodology

To investigate the effects of Nrf2 deficiency on iron-induced upregulation of hepcidin, *Nrf2*-knockout mice and wildtype littermates were subjected to hepatic iron accumulation by intraperitoneal administration of FeDx and dietary iron loading. In the FeDx model, 6-week old mice were injected with 4mg FeDx intraperitoneally and sacrificed 24 hours later (same mice as in Chapter 4 Figure 4.25). In the dietary iron loading models, 12-week old mice were fed a high iron diet

containing 2% CI or the 200ppm iron control diet for 2 weeks (same mice as in Chapter 4 Figure 4.24). Additionally, wildtype and *Nrf2*-knockout mice were fed a diet containing 1% CI for 1 week or 4 weeks. Hepatic *Hamp1* expression was quantified by qRT-PCR and compared between wildtype and *Nrf2*-knockout mice. To determine whether hepcidin could be a direct target of Nrf2, we performed siRNA-mediated knockdown of *Nrf2*, *Bach1* and *Keap1* in C2C12 and MEF cells, and knockdown of NRF2 in HepG2 cells. qRT-PCR was performed to determine *Hamp1* or *HAMP* gene expression levels 24 hours upon knockdown of *Nrf2*/*NRF2* and 48 hours after knockdown of *Keap1* or *Bach1*. Hepatic expression of *Hamp1* was also quantified in wildtype and *Nrf2*-knockout mice 6 hours post-treatment with Nrf2 agonist CDDO-Im, and in mice expressing constitutively active Nrf2 in hepatocytes (AlbCre-caNrf2, data from Prof. Sabine Werner and Ulrike Köhler, ETH Zürich (Köhler et al., 2014)). Furthermore, in the two dietary iron loading models described above, hepatic iron content was quantified colourimetrically following reaction with a chromogen reagent containing bathophenanthrolinedisulphonic acid and thioglycolic acid and/or by Perls' staining of tissue sections. Liver damage was also assessed by quantifying hepatic malondialdehyde (product of lipid peroxidation) levels and gene expression of fibrosis markers collagen type I alpha 1 (*Col1a1*) (Friedman, 2008; Koilan et al., 2010) and transgelin (*Tagln*) (Bracht et al., 2015; Mölleken et al., 2009).

Next, to study the role of Nrf2 in haemochromatosis, *Nrf2*-knockout and *Hfe*-knockout mice were crossbred to generate double-heterozygous ($Hfe^{+/-}$ and $Nrf2^{+/-}$) mice, which were then interbred to generate *Hfe*/*Nrf2*-double knockout mice. *Hfe*-knockout mice have elevated serum and tissue iron but a block in Bmp/Smad signalling and inadequate hepcidin synthesis, and serve as a model of haemochromatosis (Corradini et al., 2009; Kautz et al., 2009). Hepatic gene expression of *Nqo1*, *Bmp6* and *Hamp1*, and tissue iron for liver, heart and pancreas were measured in female wildtype, *Nrf2*-knockout, *Hfe*-knockout and *Hfe*/*Nrf2*-double knockout mice at 6-, 12-, 18- and 24-months of age.

In humans, we investigated the effect of a single nucleotide polymorphism (SNP) Rs35652124 located within the promoter region of *NRF2* that was previously reported to affect NRF2 expression (Morales-Marin et al., 2015) on haemochromatosis. Rs35652124 SNP was aligned to publicly available DNase hypersensitivity and histone modification ChIP-seq tracks from HepG2 and human primary hepatocytes on the UCSC genome browser. Sasquatch analysis was also performed to predict the impact of the SNP on DNase footprinting potential by querying 7-nucleotide fragments in a repository of tissue-specific DNase hypersensitivity sites throughout the whole genome and calculating the cut probability of the fragments within a 250-base pair window (Schwessinger et al., 2017). The association of Rs35652124 SNP with iron parameters in hereditary haemochromatosis (HH) patients was assessed in collaboration with Graça Porto and Tiago Duarte. The study was performed on 42 patients regularly followed at the HH clinics of the Hematology Service at *Centro Hospitalar do Porto* (CHP). All subjects were male patients diagnosed after the age of 30 with HFE-related HH (defined as the occurrence of increased body iron stores and homozygosity for the C282Y HFE variant or compound heterozygosity for C282Y/138*, where 138* encodes a STOP codon at position 138 such that a compound heterozygous for C282Y/138* is phenotypically similar to homozygous C282Y (Mendes et al., 2009)). None of the individuals presented associated viral, alcoholic or other chronic inflammatory disease. Serum ferritin and transferrin saturation values were determined at the time of diagnosis, and total body iron stores (TBIS) was calculated by the amount of iron removed by intensive therapeutic phlebotomies until reaching a serum ferritin value of 50ng/ml. For SNP genotyping, a 284bp fragment of the NRF2 promoter was amplified using the Type-it® Microsatellite PCR Kit (Qiagen) with the primers 5'-GCGTGGTGGCTGCGCTTT-3' and 5'-CCGTGCCACTGCCAACTGC-3'. The amplification conditions were: denaturation at 95°C for 5min and 40 cycles of 95°C for 30sec, annealing at 63°C for 30sec, and extension at 72°C for 30sec with a final extension at 60ºC for 30min. For sequencing, the PCR fragment was amplified using BigDye® Terminator v1.1 Cycle Sequencing Kit (Applied Biosystems). Samples were injected in the ABI 3130xl Genetic Analyzer (Applied Biosystems) and the final product was precipitated in DyeEx 96 well plates (Qiagen). The Rs35652124 SNP was determined using ProSeq3 software. All patients provided written informed consent for the use of their stored DNA samples and clinical

information for the present research. All patient data were anonymized and confidentiality was maintained during the whole process according to Helsinki Declaration and Portuguese Law. The study received ethical approval by the CHP Ethics committee.

Lastly, to investigate whether pharmacological activation of Nrf2 could alter the *Bmp6*/hepcidin axis and ameliorate iron accumulation in haemochromatosis, 8-week old female *Hfe*-knockout mice were given 10 doses of the small molecule Nrf2 activator CDDO-Im by oral gavage over 3 weeks. Liver gene expression was analysed by qRT-PCR. Serum hepcidin protein was also quantified by ELISA. Iron status was assessed by quantifying liver, spleen and serum iron, and hepatic lipid peroxidation was measured by TBARS assay. In addition, 22-week old female *Hamp1*-knockout mice were also treated with 10 doses of CDDO-Im over 3 weeks, followed by hepatic gene expression analysis and hepatic iron quantification to determine whether the rescue of iron accumulation by Nrf2 activation acts via hepcidin.

The methodology described above is summarised in Figure 5.1.

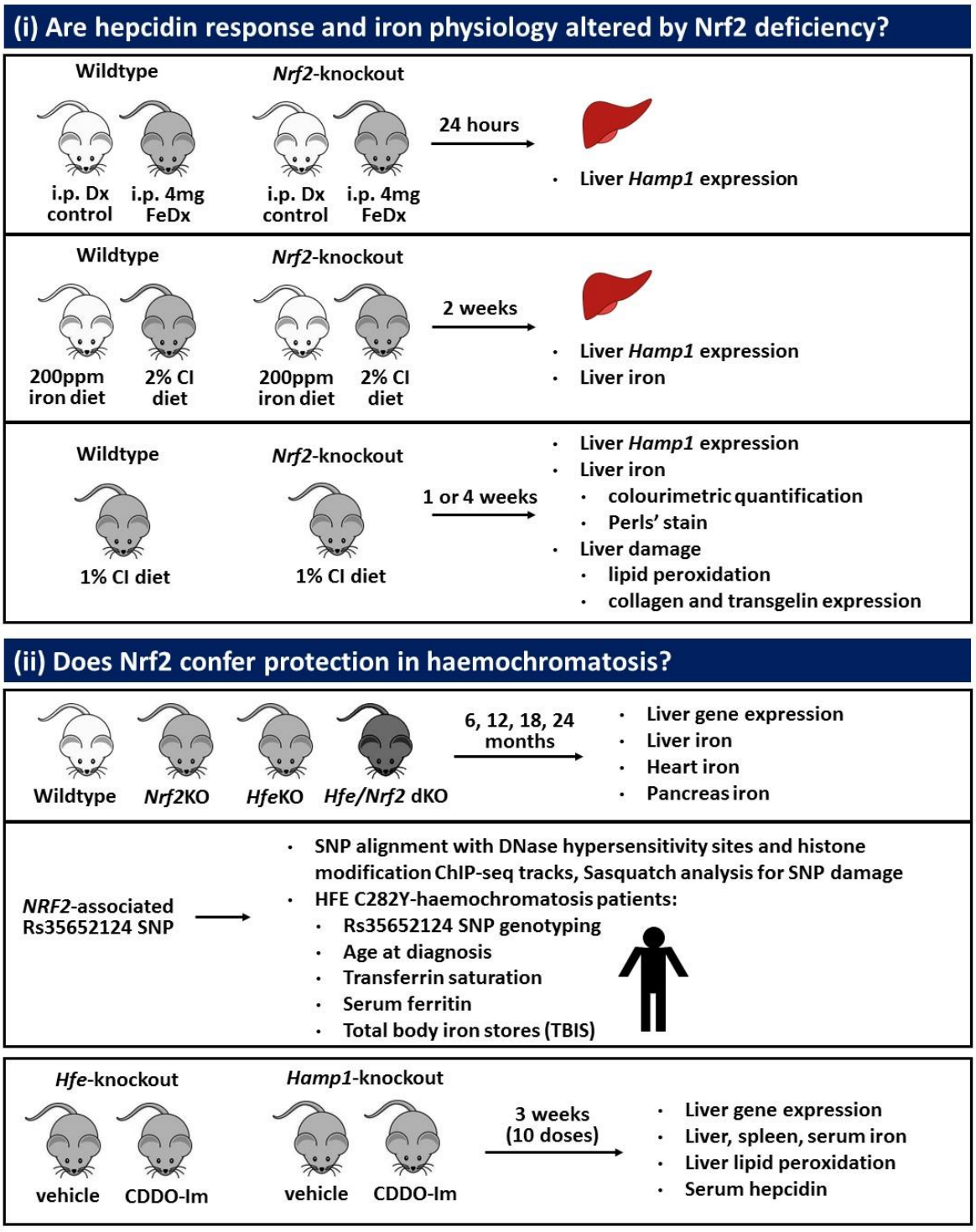


Figure 5.1: Hepcidin induction, iron status and liver damage was assessed in wildtype and *Nrf2*-knockout mice in response to intraperitoneal FeDx and dietary iron loading. The role of Nrf2 in haemochromatosis was studied by generating *Hfe*/*Nrf2*-double knockout mice. Liver gene expression, and tissue iron for liver, heart and pancreas were measured at 6-month intervals up till 24-month of age. *NRF2*-associated Rs35652124 SNP was aligned with DNase hypersensitivity and histone modification ChIP-seq and analysed by Sasquatch tool. The genotype of Rs35652124 SNP was correlated to clinical characteristics in HFE-haemochromatosis patients. *Hfe*-knockout mice were given the small molecule Nrf2 activator CDDO-Imidazole for 10 doses over 3 weeks. Liver gene expression was analysed by qRT-PCR. Serum hepcidin was quantified by ELISA. Iron status was assessed by quantifying liver, spleen and serum iron. Liver lipid peroxidation was measured by TBARS assay.

5.2 Results

5.2.1 *Nrf2*-knockout mice have dampened iron-induced hepcidin response, enhanced iron accumulation and more oxidative damage

In the previous chapter, *Nrf2*-homozygous knockout, heterozygous knockout and wildtype littermate mice were injected intraperitoneally with 4mg FeDx, which raised hepatic iron content after 24 hours. The upregulation of *Bmp6* expression in response to intraperitoneal FeDx was blunted in *Nrf2*-deficient mice (Figure 4.25). Since *Bmp6* controls hepcidin synthesis, hepatic *Hamp1* expression was also quantified by qRT-PCR to determine whether the block in upregulation of *Bmp6* consequentially blunted hepcidin induction. Indeed, the upregulation of hepcidin in response to intraperitoneal FeDx was dampened in *Nrf2*-heterozygous and homozygous knockout mice (Figure 5.2).

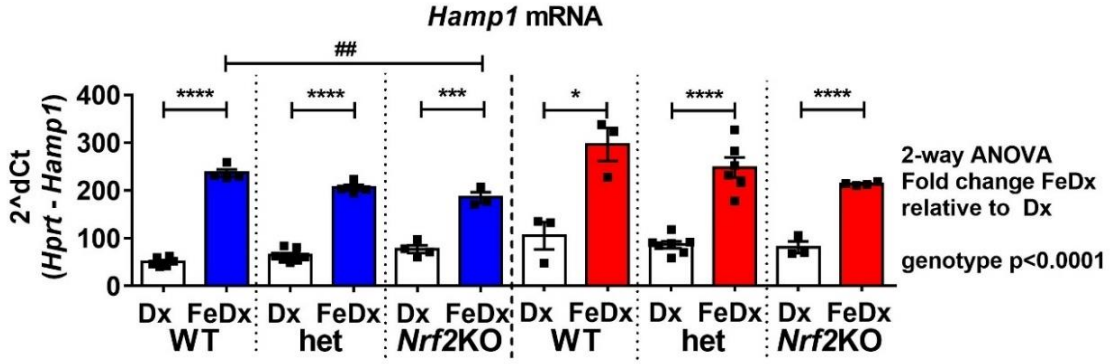


Figure 5.2: Wildtype (WT), heterozygous *Nrf2*-knockout (het) and homozygous *Nrf2*-knockout (*Nrf2*KO) mice were injected with 4mg FeDx or Dx intraperitoneally (blue = males, red = females). 24 hours post-injection, liver hepcidin gene expression was quantified. Nrf2 deficiency dampened the upregulation of *Hamp1* by FeDx (n=3 to 6; t-test between Dx and FeDx: * $p<0.05$, *** $p<0.001$, **** $p<0.0001$; 2-way ANOVA between WT FeDx, het FeDx and *Nrf2*KO FeDx: ## $p<0.01$; right panel: 2-way ANOVA on fold change gene expression stratified on sex and genotype).

In the *in vivo* model where 12-week old *Nrf2*-knockout and wildtype littermate mice were given a control 200ppm iron or high iron (2% CI) diet for 2 weeks, the upregulation of hepatic *Bmp6* expression by dietary iron loading was completely abrogated in *Nrf2*-knockout mice (Figure 4.24). Thus, we quantified hepatic *Hamp1*, *Id1* and *Smad7* expression to study the effect of the loss of *Bmp6* induction on downstream Bmp/Smad signalling. Liver Bmp/Smad signalling appears likely to be inhibited in *Nrf2*-knockout mice, as evident from the lack of *Id1* and *Smad7* induction. *Hamp1* was

upregulated by dietary iron loading in both wildtype and *Nrf2*-knockout mice; notably, the absolute gene expression of *Hamp1* was marginally lower in iron-loaded *Nrf2*-knockout mice than wildtype mice, albeit statistically not significant (Figure 5.3A). However, when fold change calculation was performed relative to mice fed 200ppm iron diet within each genotype, *Bmp6* induction was completely abrogated and *Hamp1* induction was significantly blunted, by about 25%, in *Nrf2*-knockout mice (Figure 5.3B). Additionally, *Nrf2*-knockout mice accumulated more iron in the liver than wildtype mice on the high iron diet, suggesting that the blunted hepcidin response conferred less protection against iron loading in *Nrf2*-knockout mice (Figure 5.3C). This data indicates that the Nrf2-dependent iron-induced upregulation of *Bmp6* makes a non-redundant contribution (albeit minor, about a quarter of total) to the increased hepcidin synthesis that occurs in response to iron challenge.

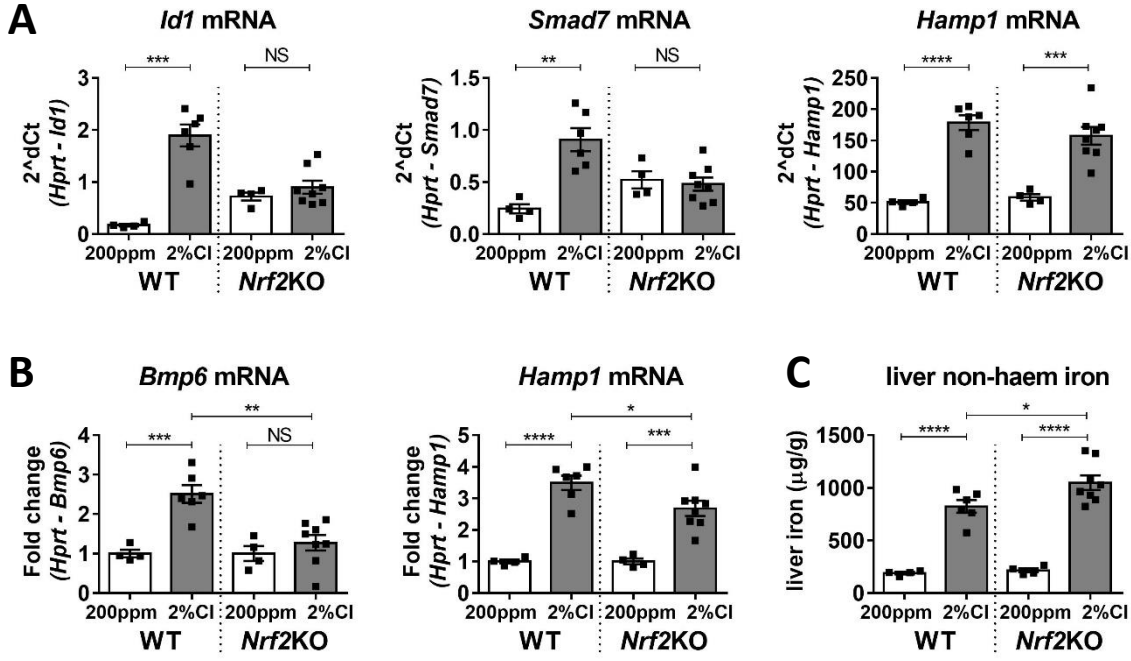


Figure 5.3: Wildtype (WT) and *Nrf2*-knockout (*Nrf2*KO) mice were fed diet containing 200ppm iron or 2% carbonyl iron (2% CI) for 2 weeks. **(A)** Hepatic gene expression of Bmp/Smad signalling pathway target genes was quantified by qRT-PCR. **(B)** Hepatic *Bmp6* and *Hamp1* expression expressed as fold change relative to mice fed 200ppm iron diet within each genotype. **(C)** Liver non-haem iron was quantified (n=4 to 8; t-test: * p<0.05, ** p<0.01, *** p<0.001, **** p<0.0001).

The iron phenotype in *Nrf2*-knockout mice was further investigated by feeding wildtype and *Nrf2*-knockout 7-week old mice 1% CI diet for 1 week, and 4-week old mice 1% CI diet for 4 weeks. Hepatic iron content increased in both wildtype and *Nrf2*-knockout mice proportional to the amount of time they were fed a high iron diet, but *Nrf2*-knockout mice accumulated iron more rapidly than wildtype mice, as evident by higher liver iron content after 4 weeks of dietary iron loading (Figure 5.4A). This iron phenotype was further confirmed by Perls' stain of liver sections after 4 weeks of dietary iron loading, which demonstrated more iron deposition in *Nrf2*-knockout mice (Figure 5.5). Furthermore, hepatic MDA was significantly elevated in *Nrf2*-knockout mice after 4 weeks of dietary iron loading, but not in wildtype mice (Figure 5.4B). Liver fibrosis markers *Col1a1* and *Tagln* were also higher in *Nrf2*-knockout mice (Figure 5.4C). These data suggest that *Nrf2*-knockout mice, likely due to defective *Bmp6* and hepcidin response, are less protected against iron loading. Moreover, the elevated oxidative stress and liver damage markers in *Nrf2*-knockout mice could be a combined effect of raised iron status and lack of a protective Nrf2-driven antioxidant response.

The lack of protection against iron-induced oxidative stress due to Nrf2 deficiency was further demonstrated by histological analysis of liver sections. More necroinflammatory foci were observed in *Nrf2*-knockout mice than wildtype mice 30 days post-injection with 4mg FeDx (Supplementary Figure 3). This suggests that the same amount of iron causes more tissue damage in the absence of Nrf2, highlighting the crucial role of Nrf2 in detoxifying iron-induced oxidative stress.

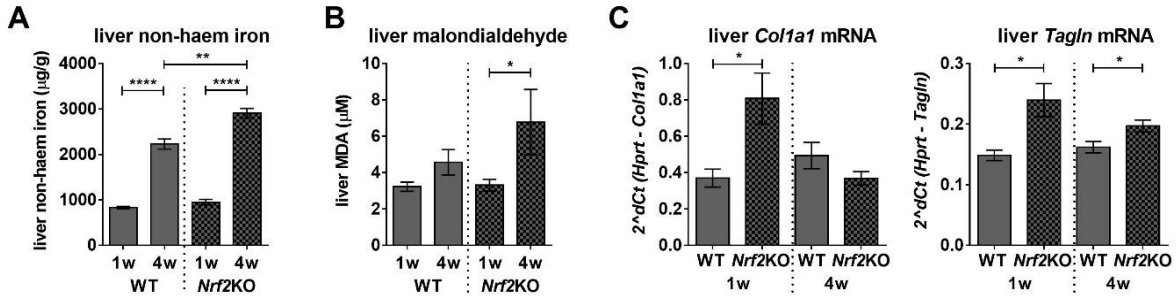


Figure 5.4: Wildtype (WT) and *Nrf2*-knockout (*Nrf2*KO) mice were fed 1% carbonyl iron diet for 1 or 4 weeks. **(A)** Liver non-haem iron and **(B)** malondialdehyde content were quantified. **(C)** Hepatic *Col1a1* and *Tagln* expression was quantified (n=5 to 8; t-test: * $p<0.05$, ** $p<0.01$, *** $p<0.001$, **** $p<0.0001$).

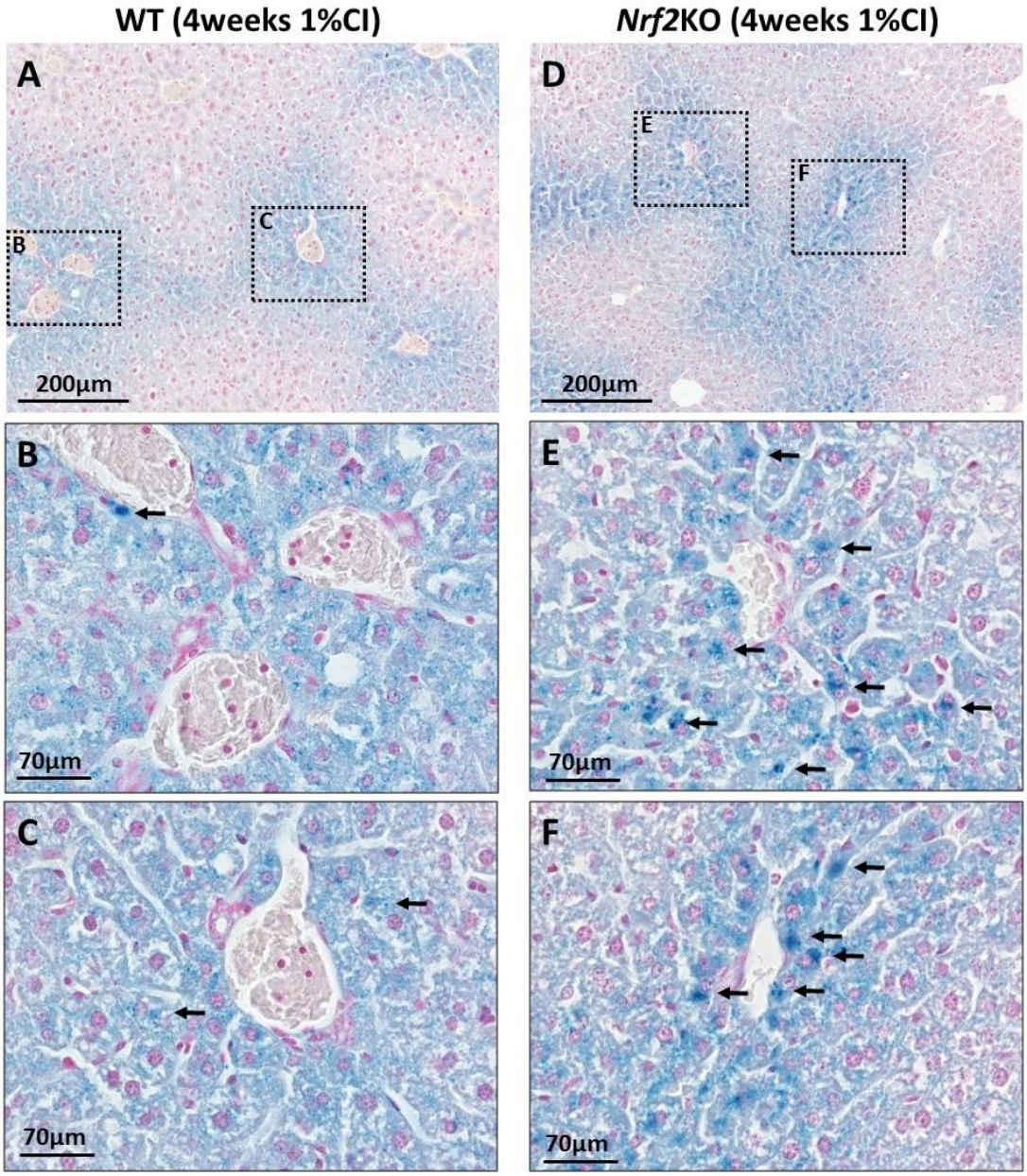


Figure 5.5: Perls' stain of liver sections from **(A-C)** wildtype and **(D-F)** *Nrf2*-knockout mice fed 4 weeks of 1% carbonyl iron diet. More iron deposition (arrows) was observed in *Nrf2*-knockout mice.

5.2.2 Hepcidin is not a direct target of Nrf2

Previously, Bayele and colleagues suggested that hepcidin could be an Nrf2 target gene, whereby administration of phytoestrogens to human HepG2 cells *in vitro* and to rats *in vivo* increased hepcidin expression. A putative hepcidin ARE was identified 1.7kb upstream of the *HAMP* promoter

by looking for consensus ARE sequences with low stringency (nTGACnnnGC). In HepG2 cells expressing luciferase under the control of the putative hepcidin ARE, overexpression of Nrf2 increased luciferase activity. The putative *HAMP* ARE was immunoprecipitated in HepG2 cells by a ChIP-PCR assay using polyclonal Nrf2 antibodies (Bayele et al., 2015). However, the authors did not account for possible NRF2-independent effects exerted by phytoestrogens on hepcidin transcription. Moreover, the putative *HAMP* ARE is not conserved in mouse *Hamp1*; the antibodies used in the ChIP-PCR assay were also not well-validated. Thus, we sought to further clarify whether the blunted hepcidin response due to Nrf2 deficiency could be an effect of direct transcriptional control of hepcidin expression by Nrf2.

Hepcidin expression was quantified in MEF and C2C12 cells upon siRNA-mediated knockdown of Nrf2, Keap1 or Bach1 (validated in Figure 4.9 – 4.14). Alterations in the Nrf2/Keap1/Bach1 system did not change hepcidin expression in MEF cells (Figure 5.6A); knockdown of Nrf2 in C2C12 did not alter hepcidin expression either (Figure 5.6B), while hepcidin expression was undetectable by qRT-PCR in C2C12 cells 48 hours post-transfection with NTC, Keap1 and Bach1 siRNA. Furthermore, siRNA-mediated knockdown of NRF2 in human hepatoma-derived cells HepG2 (same cell line used by Bayele et al., 2015) downregulated *BMP6* and *NQO1* expression, but increased *HAMP* expression instead (Figure 5.7).

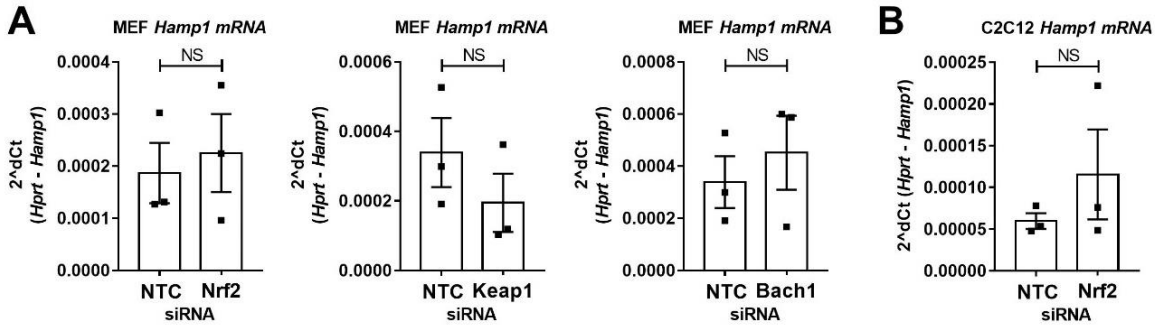


Figure 5.6: (A) siRNA-mediated knockdown of Nrf2 (24 hours), Keap1 (48 hours) and Bach1 (48 hours) were performed in MEF cells. **(B)** siRNA-mediated knockdown of Nrf2 (24 hours) was performed in C2C12 cells. *Hamp1* mRNA was quantified by qRT-PCR (n=3, t-test)

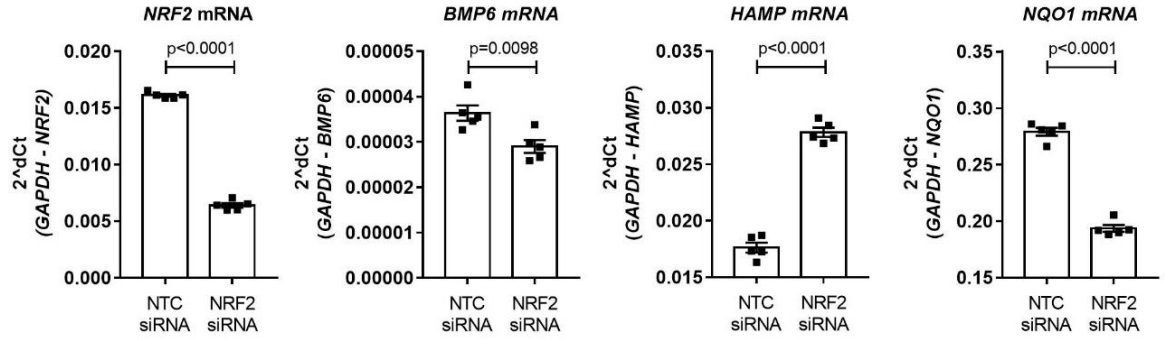


Figure 5.7: siRNA-mediated knockdown of NRF2 was performed HepG2 cells. qRT-PCR was performed after 24 hours to quantify *NRF2, BMP6, HAMP* and *NQO1* mRNA (n=5, t-test).

In vivo, the Nrf2 agonist CDDO-Im robustly upregulated the expression of *Bmp6* and other well-characterised Nrf2 target genes by 6 hours post-treatment (Figure 4.19). However, in the same experiment, hepatic *Hamp1* expression was not significantly altered in response to Nrf2 activation by CDDO-Im at this time point (Figure 5.8). In addition, hepatic gene expression profiles show that hepcidin expression, unlike several other canonical Nrf2 target genes, was not different between mice expressing constitutively active Nrf2 in hepatocytes (AlbCre-caNrf2) and control AlbCre mice (Supplementary Table 1, data from Sabine Werner and Ulrike Köhler, ETH Zürich, and derived from mice described in Köhler et al., 2014(Köhler et al., 2014)).

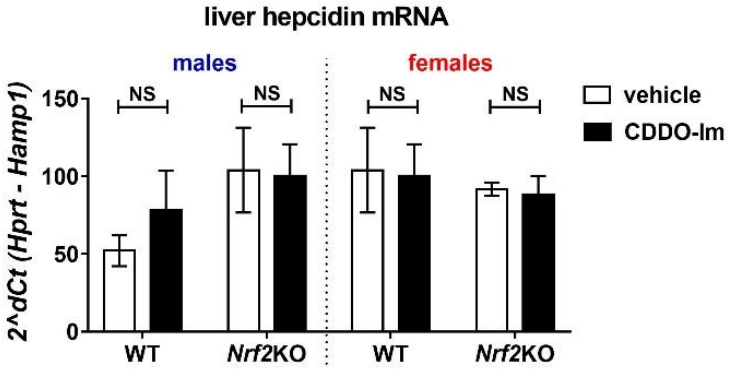
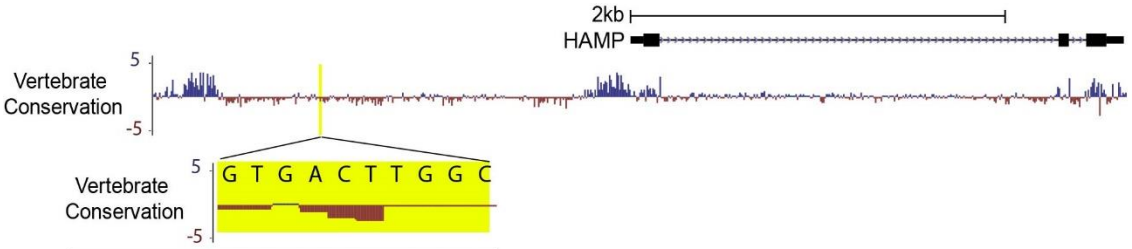


Figure 5.8: Wildtype (WT) and *Nrf2*-knockout (*Nrf2*KO) mice were given 30µmol/kg CDDO-Im or vehicle control by oral gavage. qRT-PCR was performed on the livers 6 hours post-treatment to measure hepcidin gene expression (n=3 to 5, t-test).

In addition, we queried the putative ARE identified by Bayele and colleagues 1.7kb upstream of the *HAMP* promoter on the UCSC Genome Browser and observed poor conservation of this region (Figure 5.9). Notably, the ARE sequence was absent not only in mice, but also in rats, suggesting that Bayele's observation where phytoestrogens induced hepcidin transcription in the rat liver was independent of the putative ARE. The ARE is present in humans and non-human primates, and so could theoretically regulate *HAMP* expression in these species. However, as shown above in Figures 5.6 and 5.7, we cannot find experimental evidence to support this concept.



Human	G	T	G	A	C	T	T	G	G	C
Chimpanzee	G	T	G	A	C	T	T	G	G	C
Orangutan	G	T	G	A	C	T	G	G	G	C
Rhesus	G	T	G	A	C	T	G	G	G	C
Rabbit	-	-	-	-	-	-	-	-	-	-
Guinea Pig	G	C	A	G	C	A	G	G	G	G
Rat	-	-	-	-	-	-	-	-	-	-
Mouse	-	-	-	-	-	-	-	-	-	-
Pig	-	-	-	G	A	C	A	G	G	C
Horse	G	T	G	A	T	-	G	G	G	T
Sheep	-	-	-	G	T	A	G	C	A	T
Dog	A	T	G	C	C	A	G	A	G	C
Cat	C	T	G	C	C	G	G	A	G	T
Panda	A	G	G	C	C	A	G	A	G	C
Elephant	-	-	-	-	-	-	-	-	-	-
Opossum	-	-	-	-	-	-	-	-	-	-
Platypus	-	-	-	-	-	-	-	-	-	-

Figure 5.9: Vertebrate conservation was aligned to the human hg19 build on UCSC Genome Browser. The putative ARE upstream of *HAMP* identified by Bayele is highlighted in yellow, and the conserved nucleotides in multiple mammalian species are highlighted in grey below.

Hence, the data collectively suggest that hepcidin is not under the transcriptional control of Nrf2. Rather, the blunted hepcidin response to iron accumulation in *Nrf2*-knockout mice is likely to be an effect of suppressed Bmp/Smad signalling, which is also evident from the lack of upregulation of other Bmp/Smad signalling pathway target genes *Id1* and *Smad7* (Figure 5.3A), due to a lack of *Bmp6* induction.

5.2.3 Nrf2 deficiency worsens haemochromatosis

Having shown that the lack of Nrf2 prevents the upregulation of the *Bmp6*-hepcidin axis in response to iron loading and causes more severe iron accumulation, we next investigated the role of Nrf2 in haemochromatosis. In previous studies, the loss of Nrf2 increases the susceptibility of primary hepatocytes to iron-induced toxicity and cell death *in vitro*, and caused more severe liver necrosis in *Nrf2*-knockout mice in response to a high iron diet (Silva-Gomes et al., 2014). More recently, work from the same group demonstrated that Nrf2 deficiency induces necroinflammation and promotes liver fibrosis in *Hfe*-knockout haemochromatosis mice (Duarte et al., 2017).

In collaboration with Tiago Duarte, we studied the effects of the loss of Nrf2 on hepatic *Bmp6* and hepcidin expression and accumulation of iron in tissues in the *Hfe*-knockout haemochromatosis mouse model. Female wildtype, *Nrf2*-knockout, *Hfe*-knockout and *Hfe*/*Nrf2*-double knockout mice were fed standard rodent chow containing 480ppm iron and sacrificed at 6-, 12-, 18- and 24-month of age. Hepatic gene expression of *Nqo1*, *Bmp6* and *Hamp1* was quantified by qRT-PCR, and 2-way ANOVA stratified by age was performed between mice of different genotype. *Bmp6* expression was significantly lower in *Nrf2*-knockout mice compared to wildtype mice, as well as in *Hfe*/*Nrf2*-double knockout mice compared to *Hfe*-knockout mice; the trend was similar for *Nqo1* expression, which is in agreement with our previous data demonstrating that *Bmp6* is transcriptionally regulated by Nrf2. Moreover, *Hamp1* expression was significantly lower in *Nrf2*-knockout mice compared to wildtype mice, suggesting dysregulation of hepcidin production in Nrf2 deficiency (Figure 5.10A). In addition, we observed suppressed *Hamp1* expression, elevated hepatic iron content and *Bmp6* expression, but with no alteration in cardiac and pancreatic iron content in *Hfe*-knockout mice compared to wildtype mice, similar to that documented by others (Corradini et al., 2009; Kautz et al., 2009; Subramaniam et al., 2012). Interestingly, *Hfe*/*Nrf2*-double knockout mice have marginally elevated (statistically not significant) hepatic iron and significantly higher cardiac and pancreatic iron content compared to *Hfe*-knockout mice, which is also evident from Perls' stain of tissue sections (Figure 5.10B), suggesting that the loss of Nrf2 worsens the iron overloading phenotype in Hfe-haemochromatosis.

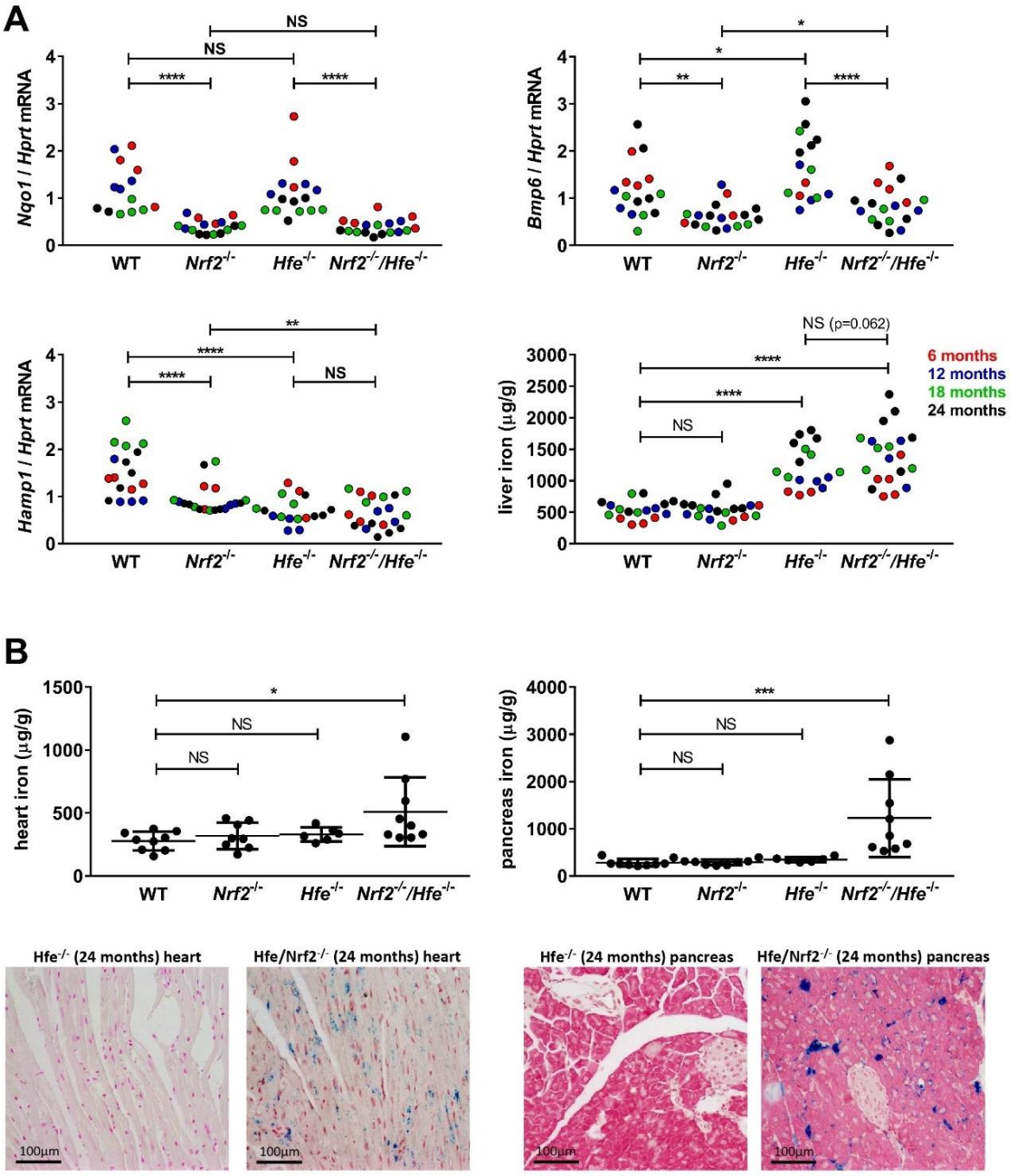


Figure 5.10: Wildtype (WT), *Nrf2*$^{-/-}$, *Hfe*$^{-/-}$ and *Hfe*/*Nrf2*$^{-/-}$ female mice were fed a standard diet and culled at 6-(red), 12-(blue), 18-(green) or 24-(black) month of age. **(A)** Hepatic gene expression of *Nqo1*, *Bmp6* and *Hamp1*, and hepatic non-haem iron was quantified. **(B)** Cardiac and pancreatic non-haem iron was quantified in 24-month old female mice. Perls' staining for iron deposition was performed on heart and pancreas tissue sections of 24-month old *Hfe*$^{-/-}$ and *Hfe*/*Nrf2*$^{-/-}$ mice. Asterisks: 2-way ANOVA performed between each genotype, stratified by age.

Subsequently, we were motivated to investigate whether genetic variation associated with *NRF2* in humans might impact on disease phenotype in haemochromatosis patients. We assessed the effect of an *NRF2*-associated SNP (rs35652124). The rs35652124 SNP is located within the myeloid zinc finger 1 (MZF1) transcription factor binding motif in the promoter region of *NRF2*, where a change from a C allele to a T allele was previously predicted to disrupt MZF1 binding and suppress NRF2 activity by downregulating *NRF2* mRNA expression (also referred to as -653A/G, with an A or G allele on the complementary strand) (Marzec et al., 2007; Morales-Marin et al., 2015). We aligned rs35652124 SNP on the hg19 human genome build on UCSC genome browser, together with DNase hypersensitivity, ChIP-seq peaks of RNA polymerase II binding, H3K4-trimethylation (H3K4me3), H3K4-monomethylation (H3K4me1) and H3K27-acetylation (H3K27ac) from HepG2 cells, and DNase hypersensitivity from human hepatocytes. The data demonstrate that rs35652124 SNP is located within an active regulatory region since it is located within accessible chromatin regions in HepG2 and human primary hepatocytes, as demonstrated by DNase hypersensitivity peaks, and overlaps with RNA polymerase II binding, H3K4me3 promoter mark, H3K4me1 enhancer mark and H3K27ac which distinguishes the enhancer as being active as opposed to being poised (Shlyueva et al., 2014) in HepG2 cells (Figure 5.11A).

Furthermore, using the Sasquatch bioinformatics tool, the following sequences containing the rs35652124 SNP were queried against a repository of DNase hypersensitivity sites in the human liver, with the SNP of interest shown in bold: AACGCCC**C**CCTCTGA (C allele) and AACGCCC**T**CCTCTGA (T allele). Sasquatch analysis predicts the impact of sequence variation on DNase footprinting potential by querying 7-nucleotide fragments in the repository of DNase hypersensitivity sites throughout the whole genome and calculates the cut probability of the fragments within a 250-base pair window. A snapshot of one of the 7-nucleotide fragments is shown in (Figure 5.11B), where stronger binding by transcription factors leads to a bigger dip in cut frequency. A damage score of the SNP allele is then calculated based on changes in cut probability. The Sasquatch analysis predicts that the T allele increases DNase hypersensitivity in human liver as compared to the C allele with a damage score of 1.867 (a damage score >1 indicates a significant

loss of protection from DNase). This suggests that a T allele at the rs35652124 SNP would be associated with less transcription factor binding in the liver and thus a reduction in *NRF2* expression, which is consistent with predictions and observations in previous reports (Marzec et al., 2007; Morales-Marin et al., 2015).

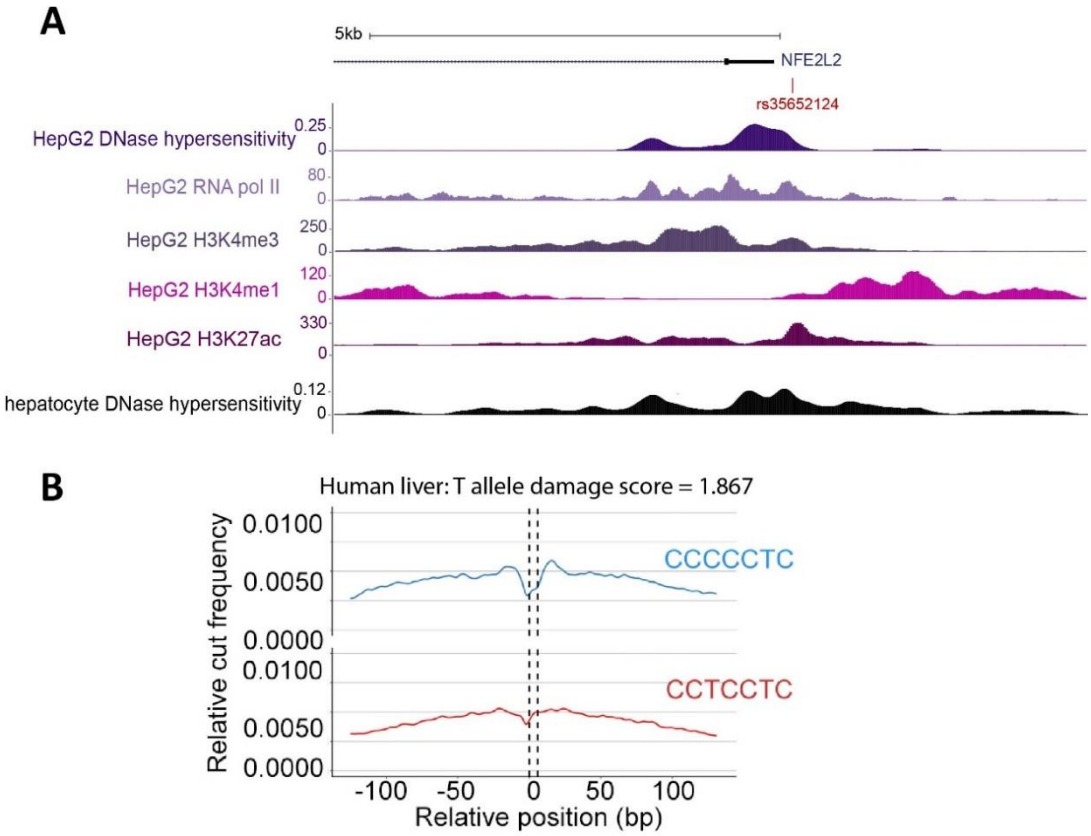


Figure 5.11: (A) rs35652124 SNP, HepG2 DNase hypersensitivity, RNA polymerase II binding, H3K4-trimethylation (H3K4me3), H3K4-monomethylation (H3K4me1) and H3K27-acetylation (H3K27ac) ChIP-seq peaks and human primary hepatocyte DNase hypersensitivity tracks were aligned on the hg19 human genome build on UCSC genome browser. **(B)** The impact of a change from C allele (blue line) to T allele (red line) in rs35652124 SNP was predicted by Sasquatch analysis against a repository of DNase hypersensitivity site in the human liver.

Next, we investigated whether NRF2 could contribute to disease burden in hereditary haemochromatosis in humans by assessing the effect of the rs35652124 SNP on iron parameters in HFE C282Y patients. In collaboration with Graça Porto and Tiago Duarte, we examined a cohort of male HFE-linked hereditary haemochromatosis patients genotyped for the rs35652124 SNP allele. HFE patients who are TT homozygotes for the rs35652124 SNP were diagnosed at a similar age compared to grouped CT or CC patients. Homozygosity for the T allele was associated with equivalent transferrin saturation but higher serum ferritin at diagnosis indicative of increased iron

levels (Figure 5.12A) , and TT patients were found to have significantly higher total body iron stores (TBIS, calculated by phlebotomies required to normalize ferritin levels) (Figure 5.12B). We also found that TBIS correlated with increasing age in both the CT + CC patients group and in the TT patients, suggesting the TT genotype defines patients who are prone to load with iron from an earlier age (red line Figure 5.12C).

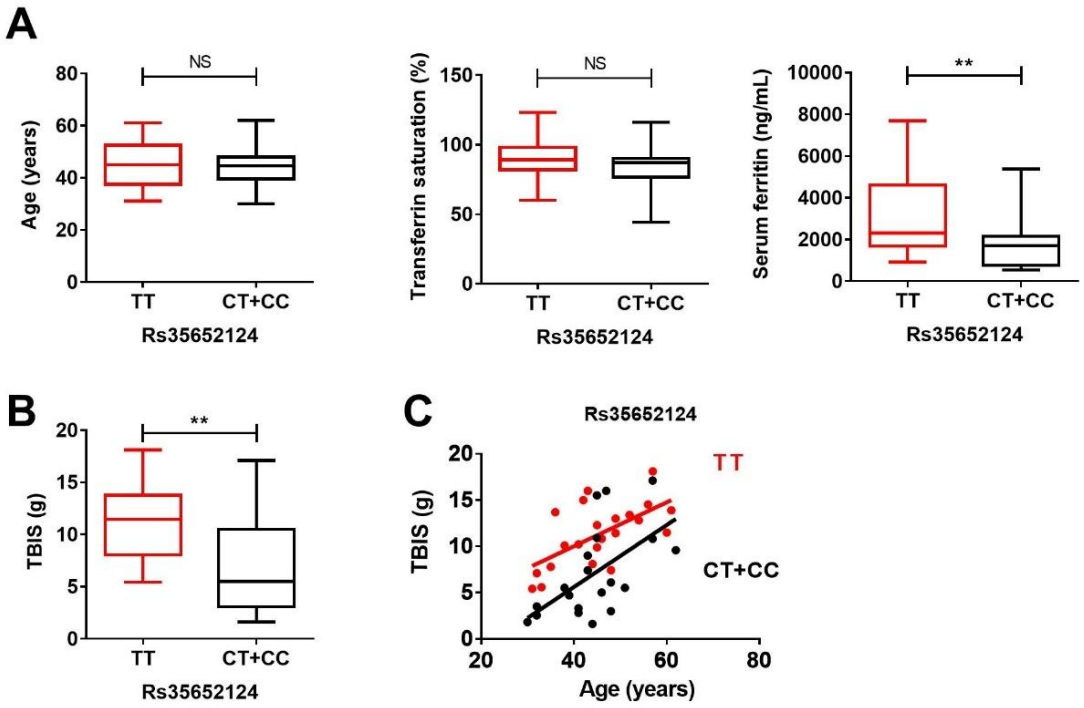


Figure 5.12: Male patients homozygous for the HFE C282Y mutation were genotyped for the rs35652124 SNP (n=42). **(A)** Age at diagnosis for HFE-HH were recorded, serum transferrin saturation and serum ferritin at diagnosis were quantified. Data represented as box plots showing 25th, 50th and 75th percentile. Asterisks: Mann-Whitney test (**p<0.01, NS = not significant). **(B)** Relationship between TBIS and age at diagnosis in HFE-HH patients homozygous for T allele at SNP rs35652124 (red, n=22, R^2=0.3905, deviation of slope from zero p=0.0019), or grouped CT and CC genotypes (black, n=20, R^2= 0. 0.3318, deviation of slope from zero: p=0.0079). TBIS were calculated based on amount of iron removed by intensive phlebotomy until serum ferritin reached a value of 50ng/ml. Asterisks: Mann-Whitney test (**p<0.01).

The data collectively demonstrates that a T allele at the rs35652124 SNP is predicted to reduce transcription factor binding to *NRF2* regulatory elements and suppress *NRF2* expression, and homozygosity for the T allele is associated with elevated iron parameters in HFE HH patients. The data in mice and humans suggest that Nrf2 deficiency may worsen disease burden in haemochromatosis.

5.2.4 Pharmacological Nrf2 activation protects *Hfe*-knockout haemochromatosis mice against iron loading

As a result of the data above, we hypothesized that pharmacological induction of Nrf2 activity could protect against iron accumulation and disease progression in mouse models of haemochromatosis. Previously, using wildtype and *Nrf2*-knockout mice, we demonstrated that the Nrf2 activator CDDO-Im upregulated hepatic *Bmp6* expression in an Nrf2-dependent manner (Figure 4.19).

To explore the effects of Nrf2 activation in haemochromatosis, we treated 12-week and 15-week old female *Hfe*-knockout mice with a single dose of CDDO-Im or vehicle control for 6 hours. 2-way ANOVA was performed by stratifying on age of mice to determine the effects of acute CDDO-Im treatment on hepatic gene expression and serum iron content. The classical Nrf2 target genes *Nqo1*, *Hmox1* and *Gclc* were upregulated by CDDO-Im administration (Figure 5.13A), in parallel with enhancement of *Bmp6* expression (Figure 5.13B). Hepatic *Hamp1* expression was also increased in mice treated with CDDO-Im, alongside a reduction in serum iron content, which is likely an effect of hepcidin-mediated ferroportin degradation thereby restricting iron absorption and/or recycling (Figure 5.13B). However, expression of the other Bmp/Smad signalling target genes *Id1*, *Smad6*, *Smad7* and *Atoh8* were not significantly altered (Figure 5.13C).

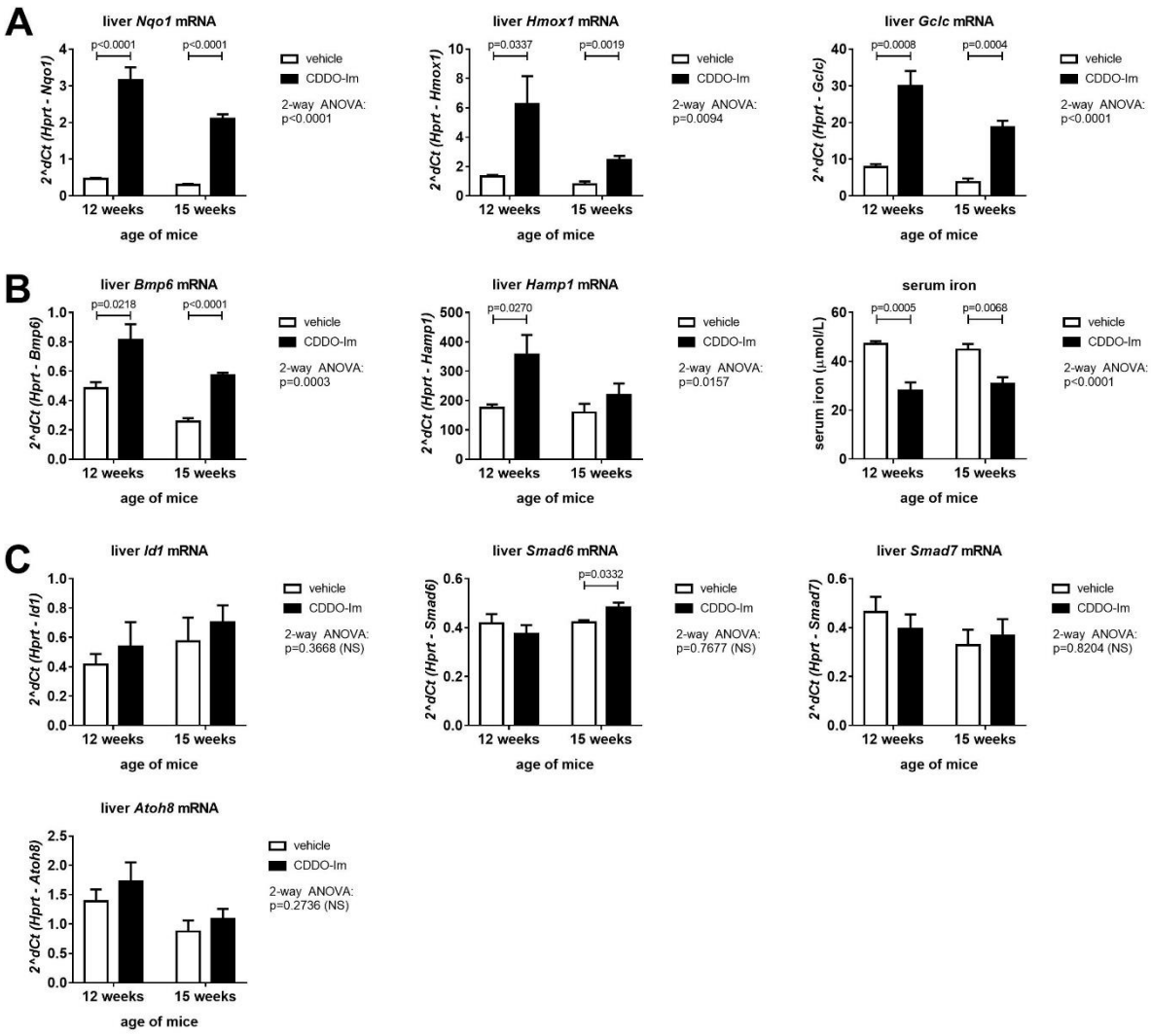


Figure 5.13: 12-week (n=5) and 15-week old (n=4) female *Hfe*-knockout mice were treated with CDDO-Im or vehicle control for 6 hours. (A) Hepatic gene expression of classical Nrf2 target genes *Nqo1*, *Hmox1* and *Gclc* were quantified by qRT-PCR. (B) Hepatic gene expression of *Bmp6*, *Hamp1*, and serum iron content were measured. (C) Expression of Bmp/Smad signalling pathway target genes *Id1*, *Smad6*, *Smad7* and *Atoh8* were also quantified. t-test was performed between age-matched mice treated with vehicle or CDDO-Im; right panel: 2-way ANOVA was performed by stratifying on age (NS = not significant).

Subsequently, to investigate whether pharmacological manipulation of Nrf2 activity improves disease burden in iron overload disorders, we gave 8-week old female *Hfe*-knockout mice 10 doses of CDDO-Im (30µmol/kg) or vehicle control orally over 3 weeks. Administration of CDDO-Im to *Hfe*-knockout mice increased Nrf2 protein levels in the liver as measured by Western blot (Figure 5.14A). Induction of Nrf2 activity was also evident from the upregulation of *Nqo1*, *Hmox1* and *Gclc* gene expression in the liver; *Bmp6* expression was also induced in mice treated with CDDO-Im

(Figure 5.14A). In addition, while absolute levels of hepatic *Hamp1* gene expression and serum hepcidin levels were not significantly altered, chronic CDDO-Im treatment decreased the accumulation of hepatic iron in *Hfe*-knockout mice compared to vehicle-treated mice; in fact, 11-week old *Hfe*-knockout mice treated with CDDO-Im for 3 weeks did not have significantly more hepatic iron than 8-week old *Hfe*-knockout mice, whereas vehicle-treated 11-week old *Hfe*-knockout mice accumulated approximately 30% more hepatic iron. Moreover, serum iron levels were also suppressed in mice treated with CDDO-Im compared to vehicle-treated mice (Figure 5.14B), such that serum hepcidin was significantly elevated in proportion to serum iron in mice treated with CDDO-Im relative to controls (Figure 5.14C). The ratio of serum hepcidin to liver iron, *Hamp1* mRNA to serum iron, and *Hamp1* mRNA to liver iron were also marginally increased albeit non-significantly (Figure 5.14C). A trend towards reduction in splenic iron content was also observed in mice given CDDO-Im (Figure 5.14B). Perls' staining was performed on liver sections, which further confirmed that CDDO-Im treatment reduced hepatic iron accumulation in *Hfe*-knockout mice (Figure 5.14D). These suggest that pharmacological Nrf2 activation upregulates the Bmp6/hepcidin axis to block iron absorption, thus resulting in a decrease in systemic iron loading. Additionally, chronic administration of CDDO-Im also led to an upregulation of *Fth1* and trend towards increase in *Ftl1* expression in the liver (Figure 5.14E), which were previously described to be transcriptionally regulated by Nrf2 (Tsuji et al., 2000; Wasserman and Fahl, 1997). This may allow cells to synthesize more ferritin protein to store intracellular iron in a safe, redox-inactive state. Hence, the reduction in systemic iron accumulation mediated by the Bmp6/hepcidin axis, and the increase in intracellular iron storage capacity by ferritin, might cooperatively reduce oxidative stress levels. The other antioxidant responses known to be stimulated by Nrf2, such as glutathione synthesis, may also be beneficial in this context. Consistent with this idea, we observed a significant reduction in the lipid peroxidation marker malondialdehyde in the livers of mice treated with CDDO-Im (Figure 5.14F).

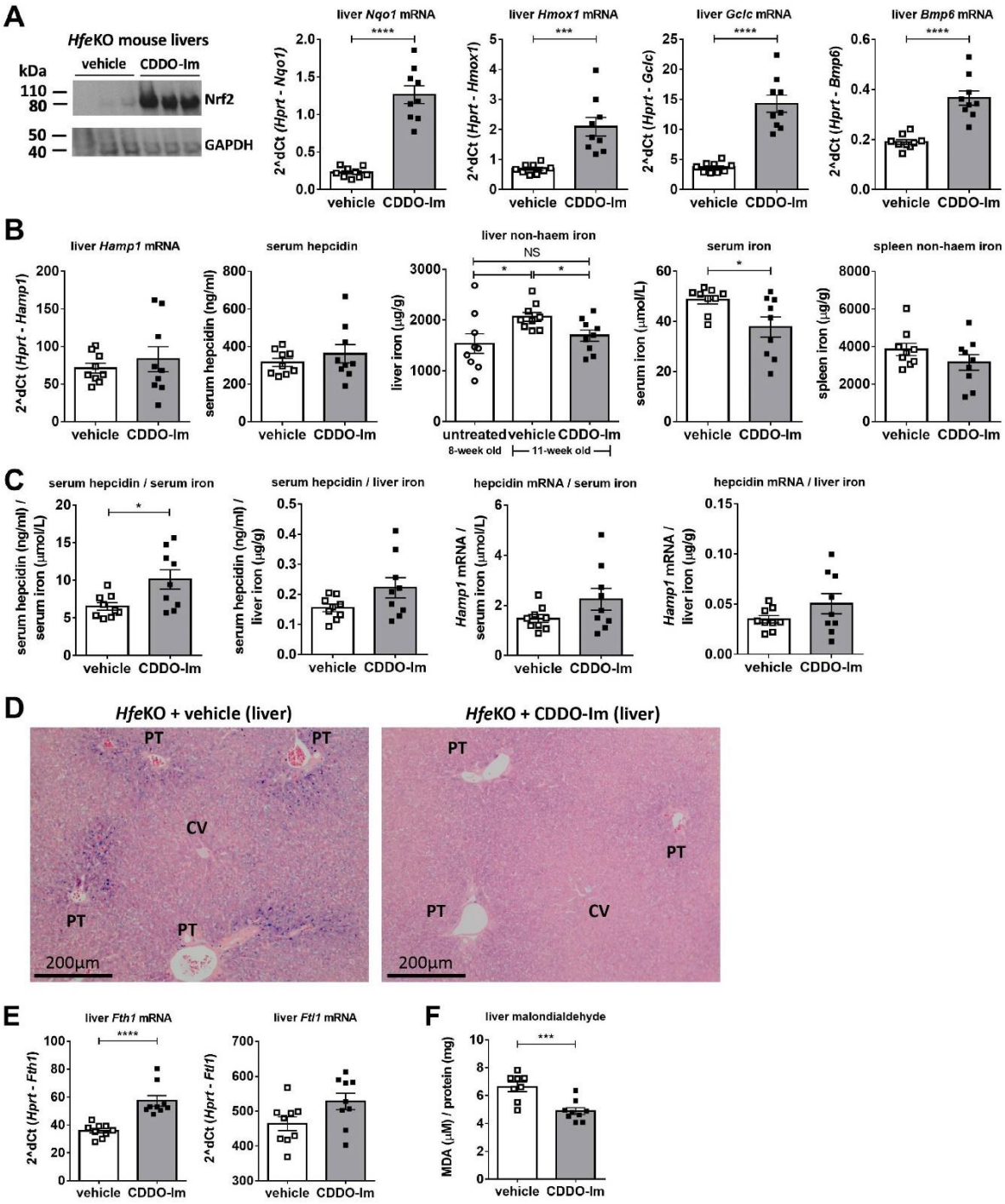


Figure 5.14: 8-week old female *Hfe*-knockout mice were treated with the Nrf2 activator CDDO-Im or vehicle control for 10 doses over 3 weeks. **(A)** Nrf2 activation by CDDO-Im was assessed by Western blot detection of Nrf2 protein in the liver, and quantification of hepatic gene expression of *Nqo1*, *Hmox1*, *Gclc* and *Bmp6* by qRT-PCR. **(B)** Quantification of hepatic *Hamp1* expression by qRT-PCR, serum hepcidin by ELISA, liver iron, serum iron and spleen iron were performed. **(C)** Hepcidin to iron ratios were calculated. **(D)** Perls' stain of liver sections. **(E)** Quantification of hepatic *Fth1* and *Ftl1* expression by qRT-PCR. **(F)** Liver MDA was quantified by TBARS assay. Asterisks: n=9, t-test, * $p<0.05$, *** $p<0.001$, **** $p<0.0001$.

We also quantified the expression of other Bmp/Smad signalling target genes *Id1*, *Smad6*, *Smad7* and *Atoh8* in response to chronic CDDO-Im administration in *Hfe*-knockout. Similar to the trend observed for *Hamp1*, the absolute gene expression levels of *Id1*, *Smad6*, *Smad7* and *Atoh8* was not significantly altered (Figure 5.15A), but the ratio of *Smad6* and *Smad7* expression to serum iron was raised in mice treated with CDDO-Im (Figure 5.15B). The lack of robust absolute Bmp/Smad signalling induction may be contributed by two opposing signalling mechanisms, where upregulation of *Bmp6* due to elevated Nrf2 activity is predicted to induce Bmp/Smad signalling, while the reduction in liver and serum iron is predicted to suppress Bmp/Smad signalling. Thus, we aimed to further clarify the molecular mechanism in the alleviation of iron accumulation in Hfe-haemochromatosis by CDDO-Im.

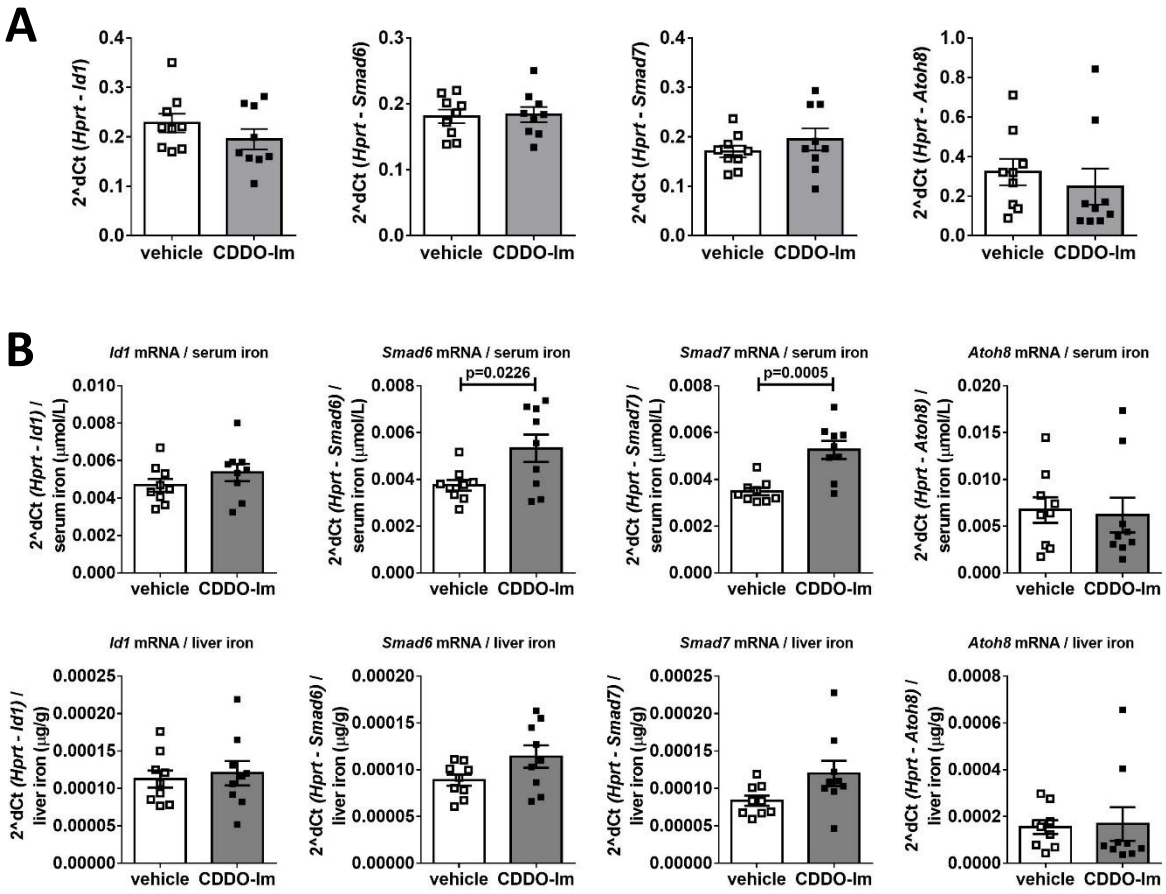


Figure 5.15: 8-week old female *Hfe*-knockout mice were treated with CDDO-Im or vehicle control for 10 doses over 3 weeks. **(A)** Target genes downstream of Bmp/Smad signalling pathway *Id1*, *Smad6*, *Smad7* and *Atoh8* were quantified in the liver by qRT-PCR. **(B)** Ratios of gene expression to serum iron or liver iron were calculated (n=9, t-test).

22-week old female *Hamp1*-knockout mice were administered 10 doses of 30µmol/kg CDDO-Im over 3 weeks. Nrf2 activation was evident from upregulation of *Nqo1*, *Gclc* and *Bmp6* expression (Figure 5.16A). Despite increased hepatic expression of *Bmp6*, CDDO-Im did not cause a reduction in liver iron accumulation, serum iron and oxidative stress levels in hepcidin-null mice (Figure 5.16B), unlike that observed in *Hfe*-knockout mice. This suggests that the inhibition of systemic iron accumulation by CDDO-Im in *Hfe*-knockout haemochromatosis mice requires hepcidin. Since hepcidin is not a direct target of Nrf2, this effect is likely mediated via *Bmp6*.

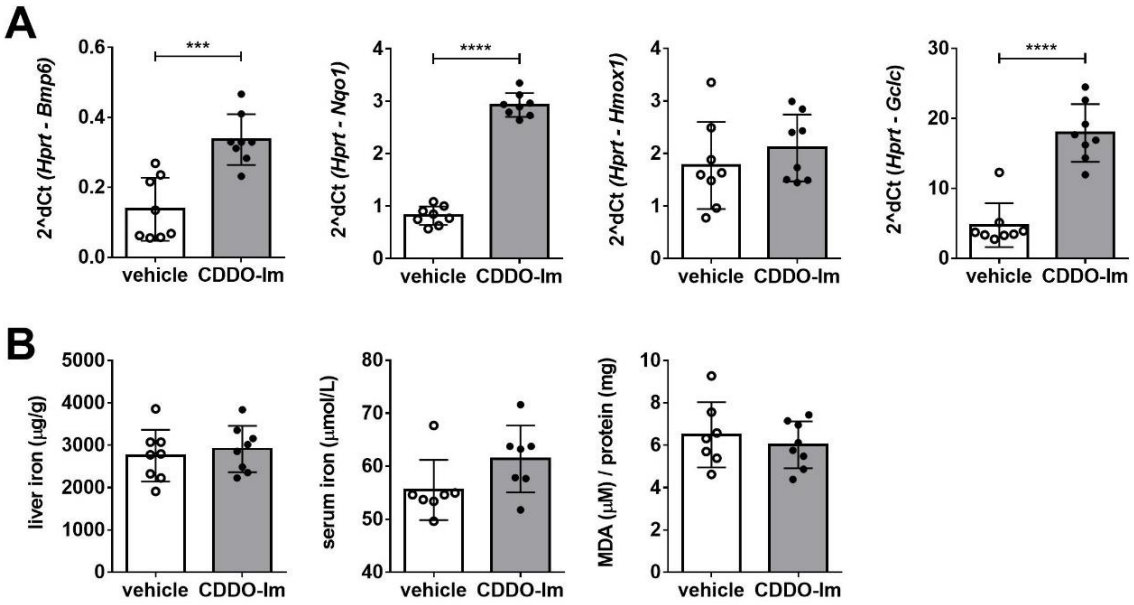


Figure 5.16: 22-week old female *Hamp1*-knockout mice were treated with CDDO-Im or vehicle control for 10 doses over 3 weeks. **(A)** Hepatic gene expression of *Nqo1*, *Hmox1*, *Gclc* and *Bmp6* was quantified by qRT-PCR. **(B)** Liver iron, serum iron and liver MDA levels were quantified. Asterisks: n=8, t-test, *** p<0.001, **** p<0.0001.

Next, we assessed changes in the expression of the iron export protein ferroportin (encoded by *Slc40a1*), which was previously described as an Nrf2-target gene in the context of haem-mediated Bach1 degradation and enhanced iron recycling by red pulp macrophages via ferroportin (Haldar et al., 2014; Marro et al., 2010) and in response to *Salmonella typhimurium* infection as a protective mechanism in peritoneal exudate macrophages (Nairz et al., 2013).

In the liver, *Slc40a1* expression is upregulated by 6 hours post-administration of CDDO-Im, and remains upregulated in response to chronic CDDO-Im administration for 3 weeks in *Hfe*-

knockout mice (Figure 5.17A). Likewise, hepatic *Slc40a1* expression was upregulated in response to chronic administration of CDDO-Im in *Hamp1*-knockout mice (Figure 5.17B). However, because a reduction in liver non-haem iron content in response to chronic CDDO-Im administration was only observed in *Hfe*-knockout mice and not in *Hamp1*-knockout mice, this indicates that the block in hepatic iron accumulation in the former case is unlikely due to enhanced ferroportin expression and export of iron from the liver. This is further supported by the observation of reduced serum iron in *Hfe*-knockout mice given CDDO-Im, since tissue iron export would be expected to increase serum iron instead.

Since we and others have observed transcriptional activation of *Slc40a1* by Nrf2 in the liver and in macrophages, we explored whether CDDO-Im administration alters iron absorption at the duodenum. The prediction would be that if CDDO-Im activates Nrf2 and upregulates *Slc40a1* expression, iron absorption would be enhanced leading to elevated tissue and serum iron levels (which is opposite to our actual observations (Figure 5.14)). We quantified *Slc40a1* expression in duodenal enterocytes 3 hours after oral administration of CDDO-Im in 6-week old C57BL6 male mice. CDDO-Im did not change the expression of *Slc40a1*; *Tfrc* expression was also not different between CDDO-Im and vehicle-treated mice suggesting that enterocyte intracellular iron content is unaltered (Figure 5.18). These demonstrate that iron absorption is unlikely to be altered/enhanced by administration of CDDO-Im acting directly on duodenal enterocytes.

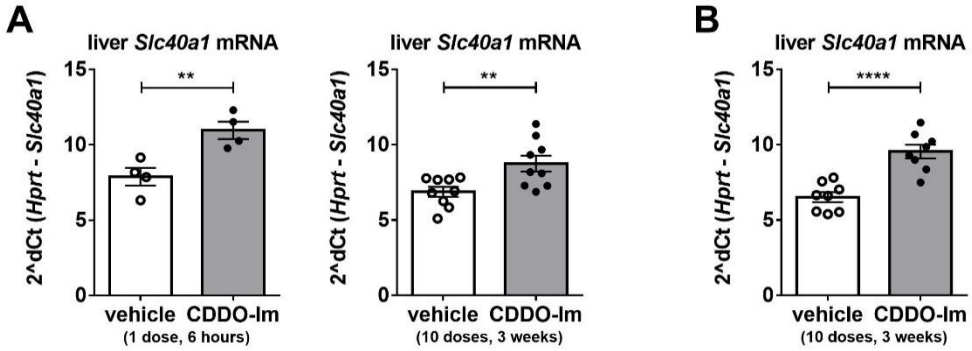


Figure 5.17: Hepatic gene expression of *Slc40a1* in **(A)** 15-week old female *Hfe*-knockout mice 6 hours post-administration of a single dose of CDDO-Im or vehicle control (left, n=4), 8-week old female *Hfe*-knockout mice given 10 doses of CDDO-Im or vehicle over 3 weeks (right, n=9) and in **(B)** 22-week old female *Hamp1*-knockout mice given 10 doses of CDDO-Im or vehicle over 3 weeks (n=8). Asterisks: t-test, ** p<0.01, **** p<0.0001.

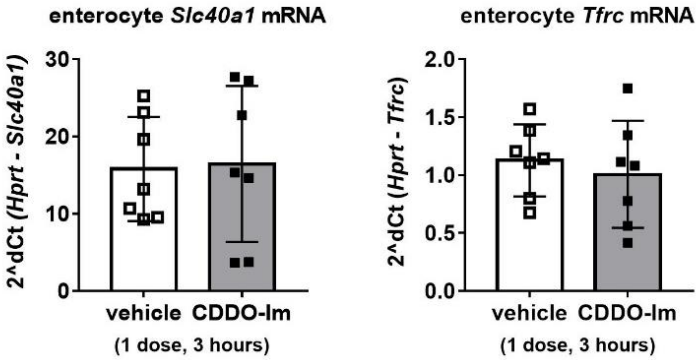


Figure 5.18: Gene expression of *Slc40a1* and *Tfrc* was measured in duodenal enterocytes 3 hours after the administration of a single dose of CDDO-Im.

In conclusion, we demonstrate that Nrf2 plays an essential role linking cellular health to a balanced systemic iron status by sensing iron accumulation and upregulating the *Bmp6*-hepcidin axis as a homeostatic feedback, thus constraining the toxic effects of iron-induced oxidative stress. Pharmacological activation of Nrf2 imparts beneficial effects by preventing the over-accumulation of iron in the body, which is likely mediated by upregulation of the *Bmp6*-hepcidin axis. Moreover, Nrf2 activation promotes antioxidative properties and may increase iron storage capacity via induction of *Nqo1*, *Gclc*, *Fth1* and *Ftl1*, thus alleviating oxidative stress and reducing tissue damage. This highlights the potential of targeting the Nrf2-Bmp6-hepcidin pathway to develop new therapeutic manipulations for iron overload disorders.

5.3 Discussion

In the previous Chapter, we show that iron upregulates *Bmp6* transcription in an Nrf2-dependent manner. In this Chapter, as a follow up, we demonstrate that iron-induced Bmp/Smad signalling appears to be blocked in the absence of Nrf2, since *Nrf2*-knockout mice failed to induce *Smad7* and *Id1* expression in response to a high iron diet. As such, *Nrf2*-knockout mice cannot efficiently increase hepcidin synthesis in response to iron. Consequentially, *Nrf2*-knockout mice accumulate iron more rapidly than wildtype littermates and furthermore have elevated oxidative stress and fibrosis markers.

We also demonstrated that hepcidin is unlikely to be under the direct transcriptional regulation

by Nrf2. Our findings contradict a previous report which claimed that hepcidin is transcriptionally controlled by NRF2, whereby phytoestrogens increase NRF2 activity and *HAMP* expression in HepG2 *in vitro* and rat liver *in vivo* (Bayele et al., 2015). The authors, however, did not control for NRF2-independent effects of phytoestrogens by comparing wildtype and NRF2-deficient systems. Moreover, the ChIP-PCR assays were performed using polyclonal Nrf2 antibodies (Santa Cruz) that gave multiple non-specific bands on our Western blots (Supplementary Figure 4), suggesting the observations may be experimental artefacts. The putative ARE is not well-conserved and absent in rats and mice, suggesting that induction of hepcidin expression by phytoestrogens is unlikely mediated by Nrf2 binding to ARE, but may be mediated by mechanisms independent of Nrf2. Instead, we demonstrated Nrf2-dependent upregulation of *Bmp6*, but not *Hamp1*, in wildtype and not *Nrf2*-knockout mice using a potent and selective Nrf2 agonist that directly binds Keap1 and blocks its interactions with Nrf2 (Cleasby et al., 2014). Moreover, hepatic *Hamp1* expression was unaltered in mice expressing constitutively active Nrf2 in hepatocytes (AlbCre-caNrf2), and siRNA-mediated manipulation of the Nrf2/Keap1/Bach1 system did not change *Hamp1* or *HAMP* expression. Thus, the blunted hepcidin response and iron overload phenotype we observe in our *Nrf2*-knockout mice is more likely a consequence of lack of *Bmp6* induction and a blunting of the Bmp/Smad signalling pathway rather than due to a direct effect of Nrf2 on hepcidin.

The role of Nrf2 in the context of Hfe-linked haemochromatosis was also explored in this Chapter. *Hfe*-knockout mice have inappropriately low levels of hepcidin synthesis, causing hepatic iron overload. Deletion of Nrf2 in *Hfe*-knockout mice caused iron loading in the heart and pancreas, a phenotype that is not observed in Nrf2-expressing *Hfe*-knockout mice. In contrast, hereditary haemochromatosis patients often show iron overload in both hepatic and extrahepatic tissues including the heart, pancreas and kidney. The exact mechanism(s) leading to iron accumulation in these extrahepatic tissues remains to be further investigated. Plausible hypotheses include (i) elevated systemic iron levels due to defective Nrf2-Bmp6-hepcidin signalling surpassing the liver's iron storage capacity, resulting in deposition of iron in other tissues, and (ii) a decrease of ARE-driven ferroportin expression leading to increased iron retention within the tissues.

We also demonstrated in a cohort of *HFE* C282Y hereditary haemochromatosis patients that a SNP in the *NRF2* promoter predicted to reduce transcription factor binding and *NRF2* expression is associated with elevated serum ferritin levels at diagnosis and total body iron stores. However, we appreciate that this study's findings might be limited by the small sample size (n=42) and require study in other hereditary haemochromatosis cohorts. In other studies, exome sequencing identified a SNP in *GNPAT* (glyceronephosphate O-acyltransferase) gene rs11558492 that is associated with severe iron overload in *HFE* C282Y haemochromatosis patients from the United States, Canada and Australia; the authors proposed that the effects may be hepcidin-dependent, since siRNA-mediated knockdown of *GNPAT* in HepGc/C3A cells reduced hepcidin expression by 17-fold (Mclaren et al., 2015). The rs11558492 SNP was also found to be associated with more severe iron accumulation in a group of *HFE* C282Y patients from France (Besson-Fournier et al., 2016). However, the same SNP was not associated with severity of iron overload in other cohorts of *HFE* C282Y patients from Canada (Levstik et al., 2016) or from Italy (Greni et al., 2017). These studies highlight the need to assess the effect of SNPs on disease burden in different populations. Thus, the reproducibility of our observations of *NRF2* SNP rs35652124 on iron accumulation should be investigated in other patient cohorts to further validate the conclusions. It would also be interesting to study whether the *NRF2* SNP is associated with other clinical phenotypes of haemochromatosis, such as liver cirrhosis, diabetes and cardiomyopathy. These may inform clinicians on whether co-screening for *HFE* C282Y mutation and *NRF2* SNP in certain populations can aid identification of high-risk patients and better management of haemochromatosis.

Having shown that Nrf2 affects iron loading in haemochromatosis, we investigated whether pharmacological activation of Nrf2 alleviates iron accumulation by administering CDDO-Im to *Hfe*-knockout mice for 3 weeks. Nrf2 activation robustly increased *Bmp6* expression, raised hepcidin levels in proportion to iron content, and prevented systemic iron accumulation as evident from reduced hepatic and serum iron levels, as well as a non-significant decrease in spleen iron. We attempted to detect enterocyte ferroportin protein levels by Western blot. In a preliminary experiment to validate the antibodies (Novus Biologics, NBP1-21502), C57BL6 mice were fed diets containing

either 2ppm or 200ppm iron for 4 weeks. Unfortunately, no bands were observed at the predicted molecular weight of ferroportin (62kDa). There was also no observable difference in the most distinct band at 80kDa between iron deficient and iron replete mice (Supplementary Figure 5), imposing a technical limitation of detecting enterocyte ferroportin levels. Instead, we treated *Hamp1*-knockout mice with CDDO-Im to determine whether the inhibition of systemic iron accumulation by Nrf2 activation requires hepcidin. We noted that the *Hamp1*-knockout mice used were older than *Hfe*-knockout mice due to availability of mice from breeding. Nevertheless, in the sex-matched *Hamp1*-knockout mice given the same routine of CDDO-Im treatment as *Hfe*-knockout mice, hepatic and serum iron content were unaltered. Therefore, the data suggest that the inhibition of systemic iron accumulation by CDDO-Im in *Hfe*-knockout haemochromatosis mice is likely mediated by upregulation of the *Bmp6*-hepcidin axis.

We propose several other approaches that can be taken to investigate and confirm that Nrf2 regulates iron homeostasis and alleviates iron overload via upregulating *Bmp6*, which in turn induces hepcidin synthesis. For example, we hypothesise that co-administration of CDDO-Im and anti-BMP6 antibodies would not alleviate iron overload in *Hfe*-knockout mice, akin to that observed in *Hamp1*-knockout mice. Additionally, *Bmp6*-knockout mice experience iron overload due to defective hepcidin synthesis; severe iron accumulation is also observed in transgenic mice expressing hepcidin-resistant ferroportin (Fpn^{C326S}) due to dysregulated iron absorption and recycling. We expect that administration of CDDO-Im would not block iron accumulation in *Bmp6*-knockout mice and Fpn^{C326S} transgenic mice. However, chronic pharmacological activation of Nrf2 might reduce oxidative stress-associated tissue damage in *Bmp6*-knockout mice and Fpn^{C326S} transgenic mice through better storage of intracellular iron and enhanced oxidative capacity. In addition, we observed that hepatic *Bmp6* expression was not upregulated in mice expressing constitutively active Nrf2 in hepatocytes. However, endothelial cells are the predominant source of Bmp6 in the liver, where LSEC-specific deletion of *Bmp6* resulted in hepcidin deficiency and severe iron overload (Canali et al., 2017). Thus, it would be interesting to generate mice expressing constitutively active Nrf2 in LSECs and determine whether these mice have higher hepcidin expression and display symptoms of

anaemia.

The targeting of the *Bmp6*/hepcidin axis as a therapeutic strategy against iron overloading disorders using minihepcidin (Ramos et al., 2012) and supraphysiological doses of exogenous BMP6 protein (Corradini et al., 2010) have been described previously. Administration of minihepcidin at a low dose for 6 weeks improved haemoglobin and erythrocyte cell numbers in a thalassaemic mouse model, while higher doses of minihepcidin led to exacerbation of anaemia due to severe iron restriction (Casu et al., 2016). Hence, the effects of Nrf2-mediated suppression of iron accumulation on iron availability for erythropoiesis remains an interesting topic to be investigated. This could inform us about the possibility of activating Nrf2 as a therapeutic strategy for iron-overloading anaemia diseases such as thalassaemia. In other studies, administration of minihepcidin to *Hamp1*-knockout mice or recombinant BMP6 protein to *Hfe*-knockout mice for 2 weeks caused splenic iron retention, likely an effect of hepcidin-induced ferroportin degradation in the splenic red pulp macrophages. In contrary, Nrf2 activation by CDDO-Im led to a trend towards reduction in splenic iron content after 3 weeks, possibly due to opposing effects of Nrf2-driven ferroportin gene transcription and upregulation of the Nrf2-Bmp6-hepcidin axis inducing ferroportin protein degradation. As such, whether Nrf2 activation has an added advantage of reducing oxidative stress and tissue damage in the spleen could be further explored. Additionally, CDDO-Im reduced oxidative stress-associated liver tissue damage, likely by upregulating multiple other Nrf2 target genes encoding proteins with antioxidant and cytoprotective functions, including *Gclc* that encodes the rate limiting enzyme for glutathione synthesis and ferritin genes for safe intracellular iron storage. Hence, pharmacological activation of Nrf2 may be more beneficial in improving the disease burden of iron-overload disorders by providing multiple levels of protection via (i) suppressing systemic iron accumulation and (ii) increasing the antioxidant capacity to reduce tissue damage.

In another study, activation of Nrf2 by genetic ablation of *Keap1* or administration of CDDO-Im reduced inflammation and tissue damage in a murine model of sickle cell disease. Although Nrf2 activation did not rescue haemolysis or alter the rate of stress erythropoiesis, it reduced plasma haem

level, liver necrosis and expression of pro-inflammatory cytokines such as interleukin-6 and interleukin-1ß (Keleku-Lukwete et al., 2015). This highlights the potential of pharmacological Nrf2 activation in alleviating other haematological disorders by preventing accumulation of toxic haem and exerting cytoprotective and anti-inflammatory effects.

The ease of administrating CDDO-Im via the oral route might lead to better patient compliance as opposed to injections of minihepcidin or recombinant BMP6. Furthermore, CDDO-Methyl, an analogue of CDDO-Im, is currently under phase II and III clinical trials for pulmonary hypertension and chronic kidney disease, highlighting approval of this class of drug for clinical use in the near future.

Alternative approaches independent of the *Bmp6*/hepcidin axis have been used for the treatment of iron overloading diseases. The iron chelators deferoxamine, deferiprone and deferasirox enhance the removal of iron from the body via faecal and/or urinary excretion, and are approved for the management of iron overload associated with blood transfusion, including in transfusion-dependent ß-thalassaemia. However, iron chelation therapy is often poorly tolerated due to adverse side effects including irritation of the gut and skin, leading to poorer patient compliance (Poggiali et al., 2012). In addition, alleviating iron accumulation via sequestration of iron-bound siderophores and subsequent excretion of iron have also been investigated. Lipocalin-2, also known as Neutrophil Gelatinase Associated Lipocalin (NGAL), interacts with siderophores that have a high affinity for iron. These include Enterochelin, which is produced by Gram negative bacteria, as well as catechol metabolites of amino acids and dietary polyphenols in mammals. In the former case, sequestration of Enterochelin-iron complex by lipocalin-2 restricts bacterial growth by reducing iron availability (Flo et al., 2004). More recently, Barasch and colleagues engineered a mutant form of lipocalin-2 harbouring a substitution of cysteine to serine on amino acid residue 87 (C87S). C87S lipocalin-2 retained its siderophore-iron complex binding capacity and avoided megalin-mediated reabsorption at the kidney, thereby enhancing urinary iron excretion in mice in response to FeDx injection, blood transfusion, and in *Hfe*-knockout mice. Moreover, daily administration of C87S lipocalin-2 daily

over 4 days reduced hepatic iron content in *Hfe*-knockout mice (Barasch et al., 2016), demonstrating the potential of enhancing iron excretion in alleviating iron overload disorders. The combined approach of iron chelation and excretion to achieve physiologically normal iron levels, followed by maintenance of normal iron levels via regulation of the hepcidin-ferroportin axis using minihepcidins, recombinant BMP6 or Nrf2 agonists to prevent excessive iron absorption may be an interesting concept to explore in future.

Chapter 6

Summary and future perspectives

6.1 Summary

The redox-active nature of iron is contributed by its ability to exist in two oxidation states in a biological system. This allows iron in red blood cells to interact with and deliver oxygen to tissues throughout the body. By facilitating oxidation and reduction processes, iron also serves as a cofactor for many enzymes. For example, iron stabilises the tyrosyl radical in ribonucleotide reductases that catalyse the formation of deoxyriboucleotides for DNA replication, and also facilitates the transfer of electrons down the electron transport chain in mitochondria for energy production. For the same reason, iron is toxic when present in excessive amounts that surpass the body's ability to chaperone and store it in a safe redox-inactive manner as it can react with biological molecules and alter their structures and hence function. As such, the amount of iron within an organism is tightly regulated by the liver-produced hormone hepcidin under healthy conditions. Unfortunately, disorders of iron ranging from iron deficiencies to iron overload are common, therefore warranting the need to better understand iron homeostasis.

Each day, our body absorbs iron through duodenal enterocytes and loses iron through sweat, urine and shedding of epithelial cells. Unlike iron absorption, iron excretion is not regulated. Thus, excess iron that is absorbed and not used for erythropoiesis or for enzymatic reactions in other tissues is stored, primarily in the liver. Accumulation of iron in the liver upregulates hepatic *Bmp6* expression (Kautz et al., 2008), which in turn activates the Bmp/Smad signalling pathway and induces the transcription and synthesis of hepcidin (Casanovas et al., 2009). The crucial role of Bmp6 in maintaining iron homeostasis is evident from iron overloading phenotypes in *Bmp6*-knockout mice (Andriopoulos et al., 2009; Canali et al., 2017; Meynard et al., 2009) and humans carrying BMP6 mutations (Daher et al., 2016). However, the molecular mechanism as to how iron upregulates *Bmp6* expression remains an important unanswered question in the field. Although the IRP/IRE system has been shown to regulate the mRNA levels of multiple genes involved in cellular iron homeostasis, *Bmp6* is not regulated by the IRP/IRE system due to the lack of IREs on its mRNA (Sanchez et al., 2011). Therefore, the primary aim of this thesis was to identify an alternative iron-sensing mechanism that controls hepatic *Bmp6* expression, and thus maintains systemic iron homeostasis.

Since excess iron causes oxidative stress, we hypothesized that Nrf2, the transcription factor that coordinates antioxidant response, acts as a molecular sensor for iron-induced oxidative stress and regulates the transcription of *Bmp6* and consequentially hepcidin production in order to convert the toxic signal into a mechanism to decrease systemic iron. In Chapter 3, we demonstrate that Nrf2 activation and transcriptional upregulation of *Bmp6* occurs concurrently in several models of iron accumulation both *in vitro* and *in vivo*, hinting towards a link between Nrf2 and *Bmp6*. The hypothesis that Nrf2 regulates *Bmp6* transcription was further confirmed in Chapter 4 in a series of bioinformatics analyses and experiments showing (i) direct binding of Nrf2 to a conserved ARE at an active regulatory region in intron 1 of the *Bmp6* gene, (ii) suppression of basal *Bmp6* expression upon siRNA-mediated knockdown of Nrf2 and induction of basal *Bmp6* expression upon knockdown of Bach1 or Keap1 *in vitro*, (iii) upregulation of *Bmp6* expression upon pharmacological activation of Nrf2 *in vitro* and *in vivo*, (iv) concurrent blocking of iron-induced Nrf2 activation and *Bmp6* upregulation by antioxidant mitoTEMPO and (v) blunting or complete abrogation of *Bmp6* induction in response to iron upon *Nrf2*-knockdown *in vitro* and *Nrf2*-knockout *in vivo*. Thus, this is the first report documenting that Nrf2 and iron-induced pro-oxidants are required for the induction of *Bmp6* expression in response to iron.

Subsequently, in Chapter 5, we show that the induction of hepcidin in response to iron overload is impaired in *Nrf2*-deficient mice as a consequence of the block in upregulation of *Bmp6*. As a result, *Nrf2*-knockout mice are less protected against dietary iron loading and accumulate more hepatic iron than wildtype mice over time. The toxicity of iron overload in *Nrf2*-knockout mice was further demonstrated by elevated oxidative stress evident from lipid peroxidation levels in the liver (Figure 6.1A). Moreover, work from our collaborators demonstrated that the lack of Nrf2 induces more necroinflammation compared to wildtype mice in response to the same amount of intraperitoneal iron (Supplementary Figure 3), and promotes necroinflammation and liver fibrosis in *Hfe*-knockout haemochromatosis mice (Duarte et al., 2017), further highlighting the crucial role of Nrf2 in protection against iron toxicity.

The role of Nrf2 was also investigated in the context of haemochromatosis. We observed a trend towards an increase in hepatic iron content in *Hfe*/*Nrf2* double knockout mice compared to *Hfe*-knockout mice and significantly more iron accumulation in non-hepatic tissues in *Hfe*/*Nrf2* double knockout mice. Furthermore, in a cohort of age- and sex-matched Portuguese *HFE*-C282Y patients, we show that an *NRF2* SNP predicted to reduce NRF2 activity is associated with increased serum ferritin at diagnosis and total body iron stores, supporting the notion that the loss of Nrf2 worsens the iron loading phenotype in haemochromatosis (Figure 6.1B).

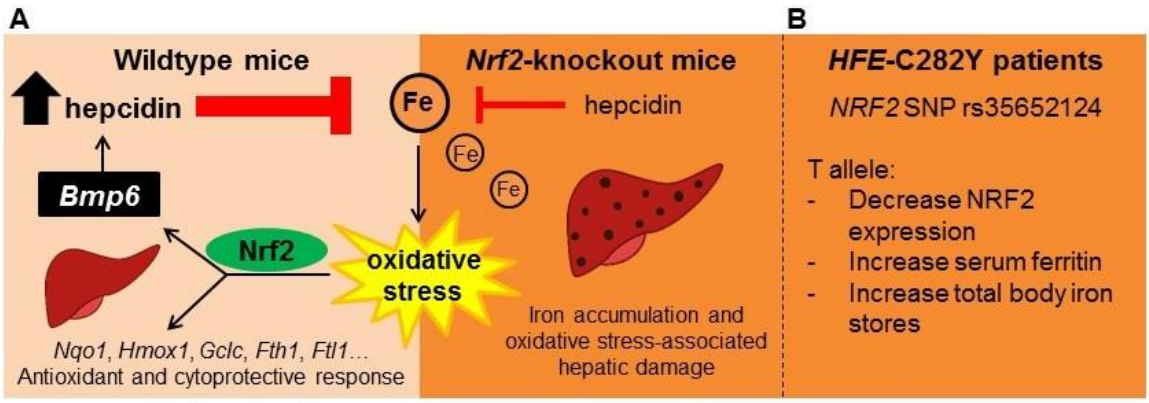


Figure 6.1: (A) Nrf2 is activated by iron-induced oxidative stress, which upregulates *Bmp6* and subsequently increases hepcidin synthesis as a homeostatic feedback to block further iron uptake. Nrf2 also upregulates a battery of genes encoding proteins with antioxidant and cytoprotective functions, maintaining cellular health. *Nrf2*-knockout mice accumulate more iron due to defective Bmp6/hepcidin signalling and have elevated oxidative stress, resulting in liver tissue damage. **(B)** In *HFE*-C282Y haemochromatosis patients, homozygosity for the T allele for rs35652124 SNP in the *NRF2* promoter is predicted to reduce *NRF2* expression and is associated with increased iron parameters.

Lastly, we explored the therapeutic potential of an Nrf2 agonist in alleviating iron overloading disorders. Administration of a potent and selective Nrf2 agonist CDDO-Im to *Hfe*-knockout mice enhanced the Bmp6/hepcidin axis as evident by acute and sustained increase in *Bmp6* expression and elevated hepcidin levels in proportion to iron status over time, thereby preventing hepatic iron overload and decreasing oxidative damage (Figure 6.2). Furthermore, CDDO-Im did not rescue the iron phenotype in *Hamp1*-knockout mice, suggesting Nrf2 protects against iron accumulation in a hepcidin-dependent manner.

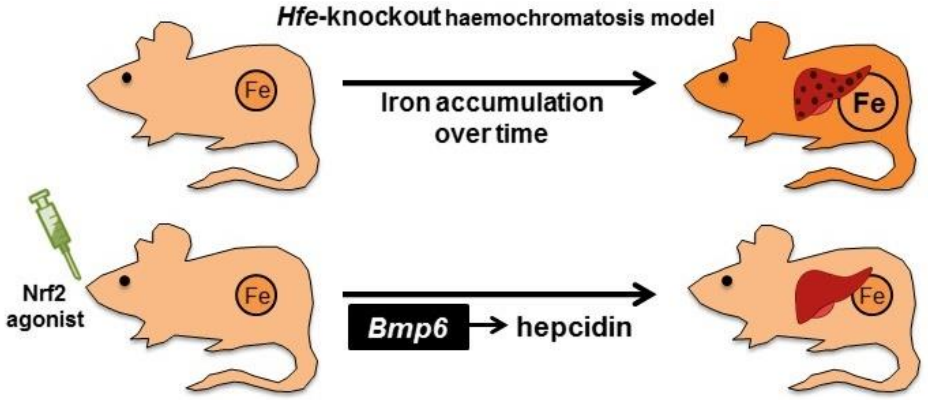


Figure 6.2: *Hfe*-knockout mice accumulate iron over time; pharmacological activation of Nrf2 increased *Bmp6* expression and hepcidin levels relative to iron status, restricting further iron uptake and protecting against oxidative damage.

6.2 Future perspectives

6.2.1 Therapeutic potential of Nrf2 activation in iron overload disorders

Our collaborators previously demonstrated that Nrf2 is protective against iron-induced hepatocyte cell death and liver tissue damage in response to dietary iron loading (Silva-Gomes et al., 2014) and in *Hfe*-knockout mice (Duarte et al., 2017). In this thesis, we characterised a novel role of Nrf2 in iron homeostasis via regulating *Bmp6* transcription which subsequently controls hepcidin synthesis and systemic iron homeostasis. Thus, our work collectively highlight Nrf2's dual roles in guarding the liver against iron-associated damage by (i) inducing enzymes involved in the antioxidant and cytoprotective response and (ii) preventing excessive systemic iron accumulation, which is the source of oxidative stress. As such, adopting Nrf2-mediated therapeutic strategies against iron overload disorders may confer better outcomes as compared to solely altering Bmp/Smad signalling or hepcidin levels.

The effect of Nrf2 activation on other iron overload disorders remains an exciting topic to be investigated. The complexity of alleviating iron accumulation in thalassaemia stems from the need to restrict iron absorption yet maintain sufficient iron availability for erythropoiesis. Interestingly, a moderate degree of hepcidin-mediated iron restriction counter-intuitively improved anaemia in murine ß-thalassaemia, likely due to decreased oxidative stress and longer half-life of red blood cells (Casu et al., 2016; Guo et al., 2013). With the dosing regimen of CDDO-Im used in this thesis, we

observed a milder effect on serum iron reduction compared to high-dosing regimens of minihepcidins used by others (Casu et al., 2016; Ramos et al., 2012); the milder effect could be beneficial for maintaining adequate iron availability yet alleviating iron accumulation. Whether pharmacological activation of Nrf2 would affect erythropoiesis in thalassaemia can be formally tested by measuring haematological parameters such as haemoglobin level, erythrocyte count and reticulocyte count upon administration of Nrf2 agonists at different doses. Constitutive activation of Nrf2 by genetic deletion of Keap1 was not associated with altered erythropoiesis in a mouse model of sickle cell disease (Keleku-Lukwete et al., 2015). However, this disorder does not cause the same degree of hepcidin suppression and iron overload as is evident in ß-thalassaemia. It is possible that decreased iron absorption and increased protection against oxidative stress mediated by Nrf2 activation could be particularly beneficial in the context of ß-thalassaemia. On a related note, it would be interesting to test whether the SNP in the human *NRF2* promoter, which we found to modify iron status in haemochromatosis, is also a modifier of iron levels, anaemia and disease progression in thalassaemia.

6.2.2 The role of Nrf2 and Bach1 in non-hepatic tissues in regulating iron homeostasis

In vitro experiments using the murine macrophage cell line RAW264.7 demonstrated that the transcription of ferroportin is regulated by an ARE 7kb upstream of the *Slc40a1* promoter. *Slc40a1* mRNA was upregulated upon siRNA-mediated knockdown of Bach1, hemin-induced Bach1 degradation and treatment with the Nrf2 activator sulforaphane (Marro et al., 2010). Nrf2 activator diethyl maleate also increased *Slc40a1* expression in human peripheral blood-derived macrophages. Furthermore, *ex vivo* experiments using peritoneal macrophages isolated from wildtype and *Nrf2*-knockout mice showed Nrf2-dependent upregulation of *Slc40a1* expression by sulforaphane and diethyl maleate; the upregulation of *Slc40a1* by diethyl maleate subsequently leads to iron efflux from macrophages (Harada et al., 2011). However, the role of iron- and haem-mediated changes in *Slc40a1* expression driven by Nrf2 activity and downstream effects on systemic iron homeostasis has not been characterised *in vivo*. For example, the expression of ARE-regulated genes *Hmox1* and *Slc40a1* and the efficiency of splenic red pulp macrophages in recycling iron from erythrocytes at resting state and in response to haemolysis could be compared in wildtype and *Nrf2*-knockout mice.

Additionally, it would be interesting to understand the role of Nrf2 and Bach1 in dietary iron absorption as either haem or non-haem iron by duodenal enterocytes. Previously, deletion of *Fth1* in intestinal cells resulted in less iron retention in enterocytes and elevation of hepatic and serum iron levels mice (Vanoaica et al., 2010). Conversely, deletion of *Slc40a1* in intestinal cells blocked iron export from enterocytes and led to iron deficiency (Donovan et al., 2005). Thus, whether *Fth1* and *Slc40a1* expression is altered in enterocytes of *Nrf2*-knockout mice, and whether that affects dietary iron absorption could be investigated. Furthermore, haem is not detected in the plasma of healthy individuals, suggesting that iron is released from dietary haem by haem oxygenase 1 in enterocytes before entering our circulation (reviewed in Ponka et al., 2017). Thus, it would be interesting to investigate whether Nrf2 deficiency reduces *Hmox1* expression in enterocytes and subsequently affects dietary haem iron absorption, or whether haem-mediated Bach1 degradation is sufficient to upregulate *Hmox1* expression even in the absence of Nrf2 in enterocytes. Conversely, whether pharmacological activation of Nrf2 facilitates haem iron absorption could be explored.

The transport of iron across the placenta during pregnancy is also an important process to supply adequate iron for foetal growth and establishment of iron stores at birth to sustain growth in early infancy. This process is mediated by the uptake of transferrin-bound iron via transferrin receptor by placental syncytiotrophoblasts and basolateral export via ferroportin to the foetal stroma. Notably, global deletion of ferroportin is embryonic lethal in mice while deletion of ferroportin in all tissues except the extraembryonic visceral endoderm and placenta (*Meox2-Cre Fpn*$^{flox/flox}$ mice) led to viable mice, suggesting that ferroportin expression at the maternal-foetal interface is required for iron supply and development of the foetus (Donovan et al., 2005). Vascularisation of the placenta is also important for facilitating the transfer of iron, other nutrients, respiratory gases and wastes across the maternal-foetal interface. Oxidative stress levels in the placenta rises during the course of pregnancy due to oxygenation of the placenta and increased mitochondrial activity for energy production (reviewed in Myatt and Cui, 2004; Pereira et al., 2015). However, the role of Nrf2 in protection against oxidative stress and in the regulation of iron transport across the placenta during

pregnancy is not well understood. Elevated oxidative stress levels have been associated with pregnancy complications such as preeclampsia and intrauterine growth retardation (Steegers et al., 2010). Consistent with this, upregulation of Nrf2 expression has been observed in extravillous trophoblasts isolated from preeclampsia pregnancies (Kweider et al., 2012), suggestive of an antioxidative response mounted in preeclampsia. However, in a murine model of preeclampsia, reduction of oxidative stress by overactivation of Nrf2 via genetic ablation of Keap1 or CDDO-Im administration worsened the outcomes of preeclampsia as demonstrated by reductions in placenta vascularisation and embryo size, and increase in embryo lethality. Conversely, genetic deletion of Nrf2 in the preeclampsia murine model improved size and survival rate of the foetuses (Nezu et al., 2017). Nezu and colleagues' findings hint towards oxidative stress having physiological roles for maintaining placental angiogenesis and vascularisation, which is beneficial in the case of preeclampsia in this mouse model. Overall however, the role of Nrf2 in pregnancy in humans, particularly for placenta vascularisation and iron transport, is not yet well understood, and is an opportunity for further investigation.

6.2.3 The role of Nrf2 in microbial infections

Alterations in Nrf2 activity in response to infections by various microbial pathogens have been demonstrated. As discussed in Chapter 4, infection of macrophages by *Salmonella typhimurium* increases $^{\bullet}$NO levels and activates Nrf2, thereby upregulating ferroportin expression and iron efflux from the macrophage to reduce iron availability for bacterial growth (Nairz et al., 2013). Nrf2 also confers protection against influenza virus infection by limiting inflammation and lung tissue damage (Yageta et al., 2011).

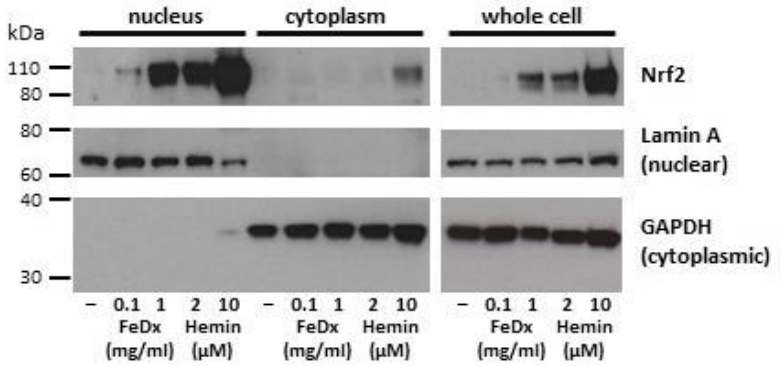
The Nrf2 response to Hepatitis C virus (HCV) is less well understood, with contradicting reports suggesting either activation or inhibition of Nrf2 activity upon HCV infection. Nuclear localisation of Nrf2 and its obligatory heterodimerisation partners the small Maf proteins was blocked in Huh7.5 cells electroporated with HCV replicons capable of replication compared to cells electroporated with replication-deficient HCV constructs; as a consequence, Nrf2 activity was

downregulated in cells harbouring replicative HCV constructs (Carvajal-Yepes et al., 2011). In a later study, the same group demonstrated that expression and phosphorylation of the autophagosome cargo protein p62 was enhanced in cells harbouring HCV replicon. Phospho-p62 binds to Keap1 and releases Nrf2 from inhibition by Keap1. In addition, phospho-p62 also mediates the induction of autophagy, which is hijacked by HCV to release new virus progenies (Medvedev et al., 2017). However, other studies demonstrated enhanced Nrf2 nuclear localisation and activity upon HCV infection in Huh7 (Burdette et al., 2010) and Huh7.5.1 (Jiang et al., 2015) cells. Jiang and colleagues also showed that inhibition of Nrf2 potentiated HCV-induced apoptosis while expression of constitutively active Nrf2 rescued HCV-induced apoptosis. Nevertheless, these studies collectively suggest that Nrf2 activation may be beneficial for the host by limiting HCV virus propagation and by conferring protection against tissue damage, which could be validated in animal models in future. In addition, our lab (Armitage et al., 2014) and others (Miura et al., 2008) have reported the suppression of hepcidin expression during chronic HCV infection and in *in vitro* models, respectively. Whether the suppression of hepcidin expression is caused in part by downregulation of the Nrf2-*Bmp6* axis could be further investigated.

6.3 Final statement

This thesis demonstrates the novel role of Nrf2 in regulating systemic iron homeostasis via regulating *Bmp6* and hence hepcidin production by the liver, and highlights the therapeutic potential of pharmacological Nrf2 activation in alleviating iron overloading in *Hfe*-linked haemochromatosis. Nrf2's role in duodenal enterocytes and splenic red pulp macrophages and its effects on systemic iron homeostasis remain to be characterised, and might suggest new treatment strategies for disorders of both iron overload and iron deficiency.

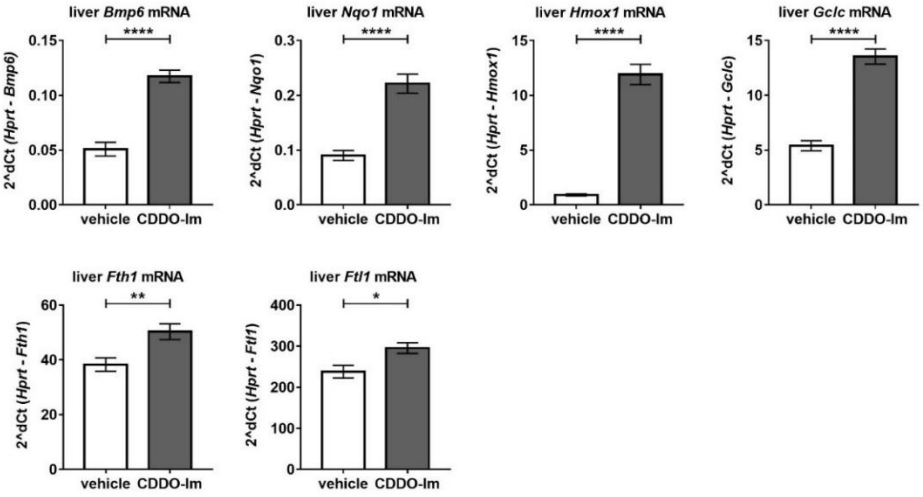
Supplementary Data



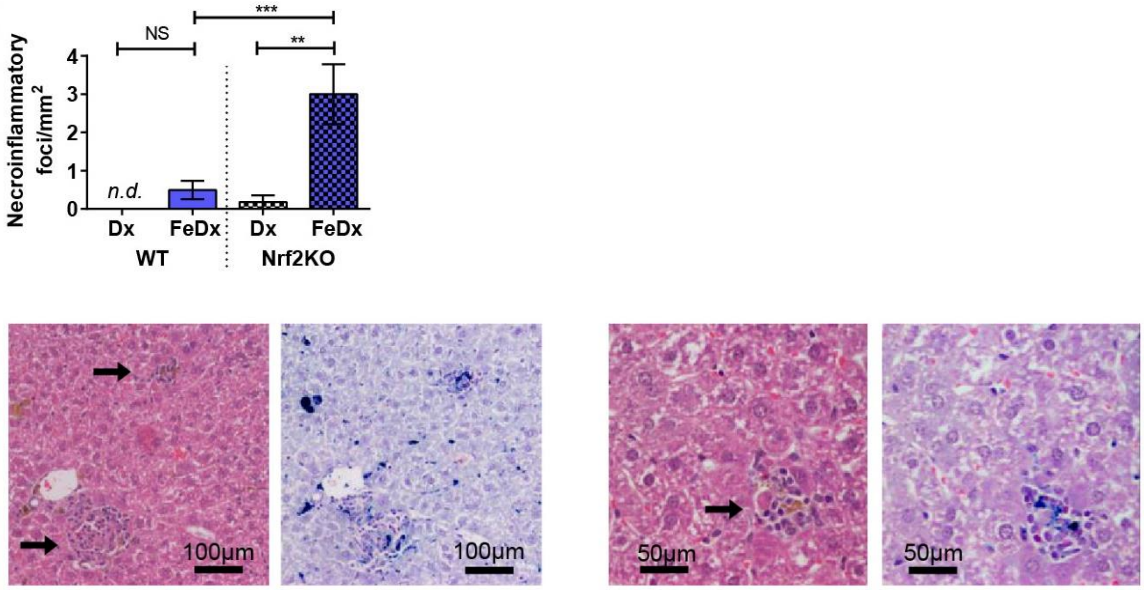
Supplementary Figure 1: Unedited Western blot image for Nrf2 protein detection in nuclear, cytoplasmic and whole cell lysates of L929 cells 6 hours after treatment with 0.1mg/ml FeDx, 1mg/ml FeDx, 2µM hemin or 10µM hemin.

Supplementary Table 1: Fold change in hepatic gene expression in mice expressing constitutively active Nrf2 in hepatocytes (AlbCre-caNrf2) compared to AlbCre mice. Mann-Whitney's U test: *p<0.05.

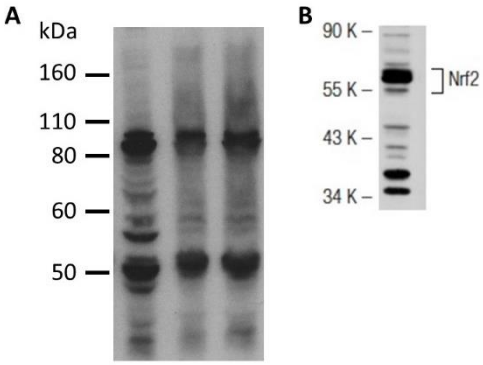
	Fold change	
Gene	**AlbCre**	**AlbCre-caNrf2**
Nqo1	1	12 *
Hmox1	1	1
Bmp2	1	1
Bmp4	1	0.8 *
Bmp6	1	0.9
Hamp1	1	0.9
Fth1	1	1.2 *
Slc40a1	1	1.3 *



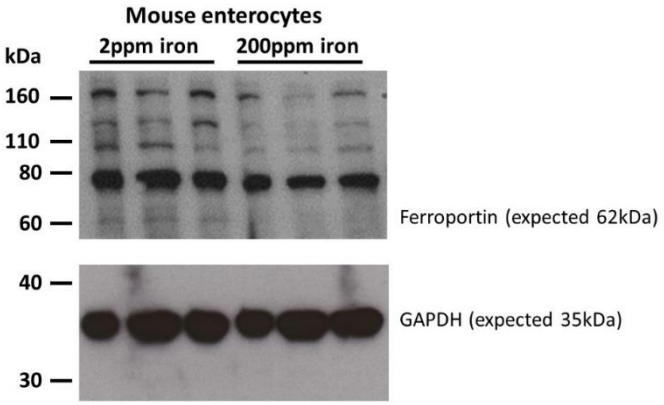
Supplementary Figure 2: Hepatic gene expression of 6-week old male C57BL6 mice 3 hours post oral administration of 30µmol/kg CDDO-Im or vehicle control was quantified by qRT-PCR. Asterisks: n=7, t-test, * $p<0.05$, ** $p<0.01$, **** $p<0.0001$.



Supplementary Figure 3: *Nrf2*-knockout and wildtype mice were given a single intraperitoneal injection of 4mg FeDx or Dx control. Iron-induced necroinflammatory foci was quantified in the liver 30 days post-injection by staining liver sections with Haemotoxylin and Eosin (first and third image) or Perls' Prussian blue (second and fourth image). Representative necroinflammatory foci in *Nrf2*-knockout mouse livers at 30 days post-FeDx injection containing hepatocyte apoptotic bodies and iron pigment in histiocytes are shown (arrows).



Supplementary Figure 4: Western blot detection of Nrf2 proteins using polyclonal Nrf2 antibodies (Santa Cruz, sc-722). **(A)** From left to right: liver lysates of mice fed diets containing 1% CI, 200ppm or 2ppm iron for 2 weeks. **(B)** Whole cell lysate from Jurkat cells (adapted from Santa Cruz datasheet).



Supplementary Figure 5: Western blot detection of ferroportin proteins in mouse duodenal enterocytes using polyclonal ferroportin antibodies (Novus Biologics, NBP1-21502). C57BL6 mice were fed diets containing either 2ppm or 200ppm iron for 4 weeks. No bands were observed at the predicted molecular weight of ferroportin (62kDa).

References

Abiko, Y., Miura, T., Phuc, B.H., Shinkai, Y., and Kumagai, Y. (2011). Participation of covalent modification of Keap1 in the activation of Nrf2 by tert-butylbenzoquinone, an electrophilic metabolite of butylated hydroxyanisole. Toxicol. Appl. Pharmacol. *255*, 32–39.

Adams, P.C., and Barton, J.C. (2010). How I treat hemochromatosis. Blood *116*, 317–325.

Andriopoulos, B., Corradini, E., Xia, Y., Faasse, S.A., Chen, S., Grgurevic, L., Knutson, M.D., Pietrangelo, A., Vukicevic, S., Lin, H.Y., et al. (2009). BMP6 is a key endogenous regulator of hepcidin expression and iron metabolism. Nat. Genet. *41*, 482–487.

Arezes, J., Jung, G., Gabayan, V., Valore, E., Ruchala, P., Gulig, P.A., Ganz, T., Nemeth, E., and Bulut, Y. (2015). Hepcidin-induced hypoferremia is a critical host defense mechanism against the siderophilic bacterium vibrio vulnificus. Cell Host Microbe *17*, 47–57.

Armitage, A.E., Eddowes, L.A., Gileadi, U., Cole, S., Spottiswoode, N., Selvakumar, T.A., Ho, L.P., Townsend, A.R.M., and Drakesmith, H. (2011). Hepcidin regulation by innate immune and infectious stimuli. Blood *118*, 4129–4139.

Armitage, A.E., Stacey, A.R., Giannoulatou, E., Marshall, E., Sturges, P., Chatha, K., Smith, N.M.G., Huang, X., Xu, X., Pasricha, S.-R., et al. (2014). Distinct patterns of hepcidin and iron regulation during HIV-1, HBV, and HCV infections. Proc. Natl. Acad. Sci. *111*, 12187–12192.

Armitage, A.E., Lim, P.J., Frost, J.N., Pasricha, S.-R., Soilleux, E.J., Evans, E., Morovat, A., Santos, A., Diaz, R., Biggs, D., et al. (2016). Induced Disruption of the Iron-Regulatory Hormone Hepcidin Inhibits Acute Inflammatory Hypoferraemia. J. Innate Immun. *8*, 517–528.

Assi, T.B., and Baz, E. (2014). Current applications of therapeutic phlebotomy. Int. J. Infect. Dis. *12*, s75-83.

Babitt, J.L., Huang, F.W., Wrighting, D.M., Xia, Y., Sidis, Y., Samad, T.A., Campagna, J.A., Chung, R.T., Schneyer, A.L., Woolf, C.J., et al. (2006). Bone morphogenetic protein signaling by hemojuvelin regulates hepcidin expression. Nat. Genet. *38*, 531–539.

Babitt, J.L., Huang, F.W., Xia, Y., Sidis, Y., Andrews, N.C., and Lin, H.Y. (2007). Modulation of bone morphogenetic protein signaling in vivo regulates systemic iron balance. J. Clin. Invest. *117*, 1933–1939.

Bai, X., Chen, Y., Hou, X., Huang, M., and Jin, J. (2016). Emerging role of NRF2 in chemoresistance by regulating drug-metabolizing enzymes and efflux transporters. Drug Metab. Rev. *48*, 541–567.

Barasch, J., Hollmen, M., Deng, R., Hod, E.A., Rupert, P.B., Abergel, R.J., Allred, B.E., Xu, K., Darrah, S.F., Tekabe, Y., et al. (2016). Disposal of iron by a mutant form of lipocalin 2. Nat. Commun. *7*, 12973.

Barton, J.C. (2007). Optimal management strategies for chronic iron overload. Drugs *67*, 685–700.

Bayele, H.K., Balesaria, S., and Srai, S.K.S. (2015). Phytoestrogens modulate hepcidin expression by Nrf2: Implications for dietary control of iron absorption. Free Radic. Biol. Med. *89*, 1192–1202.

Beguin, Y., Huebers, H.A., Weber, G., Eng, M., Finch Seattle, C.A., and Likge, W. (1989). Hepatocyte iron release in rats. J. Lab. Clin. Med. *113*, 346–354.

Bennett, M.J., Lebrón, J.A., and Bjorkman, P.J. (2000). Crystal structure of the hereditary haemochromatosis protein HFE complexed with transferrin receptor. Nature *403*, 46–53.

Besson-Fournier, C., Martinez, M., Vinel, J.-P., Aguilar-Martinez, P., Coppin, H., and Roth, M.-P. (2016). Further support for the association of GNPAT variant rs11558492 with severe iron overload in hemochromatosis. Hepatology *63*, 2054–2055.

Beutler, E., Felitti, V.J., Koziol, J.A., Ho, N.J., and Gelbart, T. (2002). Penetrance of 845G→A (C282Y) HFE hereditary haemochromatosis mutation in the USA. Lancet *359*, 211–218.

Biswas, M., and Chan, J.Y. (2010). Role of Nrf1 in antioxidant response element-mediated gene expression and beyond. Toxicol. Appl. Pharmacol. *244*, 16–20.

Blackwood, E.M. (1998). Going the Distance: A Current View of Enhancer Action. Science (80-.). *281*, 60–63.

Le Blanc, S., Garrick, M.D., and Arredondo, M. (2012). Heme carrier protein 1 transports heme and is involved in heme-Fe metabolism. AJP Cell Physiol. *302*, C1780–C1785.

Bogdan, C. (2015). Nitric oxide synthase in innate and adaptive immunity: an update. Trends Immunol. *36*, 161–178.

Bolondi, G., Garuti, C., Corradini, E., Zoller, H., Vogel, W., Finkenstedt, A., Babitt, J.L., Lin, H.Y., and Pietrangelo, A. (2010). Altered hepatic BMP signaling pathway in human HFE hemochromatosis. Blood Cells, Mol. Dis. *45*, 308–312.

Bracht, T., Schweinsberg, V., Trippler, M., Kohl, M., Ahrens, M., Padden, J., Naboulsi, W., Barkovits, K., Megger, D.A., Eisenacher, M., et al. (2015). Analysis of disease-associated protein expression using quantitative proteomics-fibulin-5 is expressed in association with hepatic fibrosis. J. Proteome Res. *14*, 2278–2286.

Bridle, K.R., Frazer, D.M., Wilkins, S.J., Dixon, J.L., Purdie, D.M., Crawford, D.H.G., Subramaniam, V.N., Powell, L.W., Anderson, G.J., and Ramm, G.A. (2003). Disrupted hepcidin regulation in HFE-associated haemochromatosis and the liver as a regulator of body iron homoeostasis. Lancet *361*, 669–673.

Burdette, D., Olivarez, M., and Waris, G. (2010). Activation of transcription factor Nrf2 by hepatitis C virus induces the cell-survival pathway. J. Gen. Virol. *91*, 681–690.

Burton, N.C., Kensler, T.W., and Guilarte, T.R. (2006). In vivo modulation of the Parkinsonian phenotype by Nrf2. Neurotoxicology *27*, 1094–1100.

Camaschella, C., Roetto, a, Calì, a, De Gobbi, M., Garozzo, G., Carella, M., Majorano, N., Totaro, a, and Gasparini, P. (2000). The gene TFR2 is mutated in a new type of haemochromatosis mapping to 7q22. Nat. Genet. *25*, 14–15.

Canali, S., Zumbrennen-Bullough, K.B., Core, A.B., Wang, C.-Y., Nairz, M., Bouley, R., Swirski, F.K., and Babitt, J.L. (2017). Endothelial cells produce bone morphogenetic protein 6 required for iron homeostasis in mice. Blood *129*, 405–414.

Carvajal-Yepes, M., Himmelsbach, K., Schaedler, S., Ploen, D., Krause, J., Ludwig, L., Weiss, T., Klingel, K., and Hildt, E. (2011). Hepatitis C virus impairs the induction of cytoprotective Nrf2 target genes by delocalization of small maf proteins. J. Biol. Chem. *286*, 8941–8951.

Casanovas, G., Mleczko-Sanecka, K., Altamura, S., Hentze, M.W., and Muckenthaler, M.U. (2009). Bone morphogenetic protein (BMP)-responsive elements located in the proximal and distal hepcidin promoter are critical for its response to HJV/BMP/SMAD. J. Mol. Med. *87*, 471–480.

Casanovas, G., Spasić, M.V., Casu, C., Rivella, S., Strelau, J., Unsicker, K., and Muckenthaler, M.U. (2013). The murine growth differentiation factor 15 is not essential for systemic iron homeostasis in phlebotomized mice. Haematologica *98*, 444–447.

Casu, C., Oikonomidou, P.R., Chen, H., Nandi, V., Ginzburg, Y., Prasad, P., Fleming, R.E., Shah, Y.M., Valore, E. V., Nemeth, E., et al. (2016). Minihepcidin peptides as disease modifiers in mice affected by β-thalassemia and polycythemia vera. Blood *128*, 265–276.

Chan, J.Y., Kwong, M., Lu, R., Chang, J., Wang, B., Yen, T.S.B., and Kan, Y.W. (1998). Targeted disruption of the ubiquitous CNC-bZIP transcription factor, Nrf-1, results in anemia and embryonic lethality in mice. EMBO J. *17*, 1779–1787.

Chan, J.Y., Kwong, M., Lo, M., Emerson, R., and Kuypers, F.A. (2001a). Reduced oxidative-stress response in red blood cells from p45NFE2-deficient mice. Blood *97*, 2151–2158.

Chan, K., Lu, R., Chang, J.C., and Kan, Y.W. (1996). NRF2, a member of the NFE2 family of transcription factors, is not essential for murine erythropoiesis, growth, and development. Proc. Natl. Acad. Sci. U. S. A. *93*, 13943–13948.

Chan, K., Han, X.D., and Kan, Y.W. (2001b). An important function of Nrf2 in combating oxidative stress: detoxification of acetaminophen. Proc. Natl. Acad. Sci. U. S. A. *98*, 4611–4616.

Chen, J., Chloupková, M., Gao, J., Chapman-Arvedson, T.L., and Enns, C.A. (2007). HFE modulates transferrin receptor 2 levels in hepatoma cells via interactions that differ from transferrin receptor 1-HFE interactions. J. Biol. Chem. *282*, 36862–36870.

Chen, Q.X., Song, S.W., Chen, Q.H., Zeng, C.L., Zheng, X., Wang, J.L., and Fang, X.M. (2014). Silencing airway epithelial cell-derived hepcidin exacerbates sepsis induced acute lung injury. Crit. Care *18*, 470.

Chevillard, G., Nouhi, Z., Anna, D., Paquet, M., and Blank, V. (2010). Nrf3-deficient mice are not protected against acute lung and adipose tissue damages induced by butylated hydroxytoluene. FEBS Lett. *584*, 923–928.

Cho, J.M., Manandhar, S., Lee, H.R., Park, H.M., and Kwak, M.K. (2008). Role of the Nrf2-antioxidant system in cytotoxicity mediated by anticancer cisplatin: Implication to cancer cell resistance. Cancer Lett. *260*, 96–108.

Cleasby, A., Yon, J., Day, P.J., Richardson, C., Tickle, I.J., Williams, P.A., Callahan, J.F., Carr, R., Concha, N., Kerns, J.K., et al. (2014). Structure of the BTB domain of Keap1 and its interaction with the triterpenoid antagonist CDDO. PLoS One *9*, e98896.

Corradini, E., Garuti, C., Montosi, G., Ventura, P., Andriopoulos, B., Lin, H.Y., Pietrangelo, A., and Babitt, J.L. (2009). Bone morphogenetic protein signaling is impaired in an HFE knockout mouse model of hemochromatosis. Gastroenterology *137*, 1489–1497.

Corradini, E., Schmidt, P.J., Meynard, D., Garuti, C., Montosi, G., Chen, S., Vukicevic, S., Pietrangelo, A., Lin, H.Y., and Babitt, J.L. (2010). BMP6 treatment compensates for the molecular defect and ameliorates hemochromatosis in Hfe knockout mice. Gastroenterology *139*, 1721–1729.

Corradini, E., Rozier, M., Meynard, D., Odhiambo, A., Lin, H.Y., Feng, Q., Migas, M.C., Britton, R.S., Babitt, J.L., and Fleming, R.E. (2011a). Iron regulation of hepcidin despite attenuated Smad1,5,8 signaling in mice without transferrin receptor 2 or Hfe. Gastroenterology *141*, 1907–1914.

Corradini, E., Meynard, D., Wu, Q., Chen, S., Ventura, P., Pietrangelo, A., and Babitt, J.L. (2011b). Serum and liver iron differently regulate the bone morphogenetic protein 6 (BMP6)-SMAD signaling pathway in mice. Hepatology *54*, 273–284.

Cullinan, S.B., Gordan, J.D., Jin, J., Harper, J.W., and Diehl, J.A. (2004). The Keap1-BTB protein is an adaptor that bridges Nrf2 to a Cul3-based E3 ligase: oxidative stress sensing by a Cul3-Keap1 ligase. Mol. Cell. Biol. *24*, 8477–8486.

D'Alessio, F., Hentze, M.W., and Muckenthaler, M.U. (2012). The hemochromatosis proteins HFE, TfR2, and HJV form a membrane-associated protein complex for hepcidin regulation. J. Hepatol. *57*, 1052–1060.

Daher, R., Kannengiesser, C., Houamel, D., Lefebvre, T., Bardou-Jacquet, E., Ducrot, N., de Kerguenec, C., Jouanolle, A.-M., Robreau, A.-M., Oudin, C., et al. (2016). Heterozygous Mutations in BMP6 Pro-peptide Lead to Inappropriate Hepcidin Synthesis and Moderate Iron Overload in Humans. Gastroenterology *150*, 672–683.

DeNicola, G.M., Karreth, F.A., Humpton, T.J., Gopinathan, A., Wei, C., Frese, K., Mangal, D., Yu, K.H., Yeo, C.J., Calhoun, E.S., et al. (2011). Oncogene-induced Nrf2 transcription promotes ROS detoxification and tumorigenesis. Nature *475*, 106–109.

Derjuga, A., Gourley, T.S., Holm, T.M., Heng, H.H.Q., Shivdasani, R.A., Ahmed, R., Andrews, N.C., and Blank, V. (2004). Complexity of CNC Transcription Factors As Revealed by Gene Targeting of the Nrf3 Locus. Mol. Cell. Biol. *24*, 3286–3294.

Devireddy, L.R., Hart, D.O., Goetz, D.H., and Green, M.R. (2010). A mammalian siderophore synthesized by an enzyme with a bacterial homolog involved in enterobactin production. Cell *141*, 1006–1017.

Dikalova, A.E., Bikineyeva, A.T., Budzyn, K., Nazarewicz, R.R., McCann, L., Lewis, W., Harrison, D.G., and Dikalov, S.I. (2010). Therapeutic targeting of mitochondrial superoxide in hypertension. Circ. Res. *107*, 106–116.

Dinkova-Kostova, A.T., Kostov, R. V, and Canning, P. (2017). Keap1, the cysteine-based mammalian intracellular sensor for electrophiles and oxidants. Arch. Biochem. Biophys. *617*, 84–93.

Donovan, A., Lima, C.A., Pinkus, J.L., Pinkus, G.S., Zon, L.I., Robine, S., and Andrews, N.C. (2005). The iron exporter ferroportin/Slc40a1 is essential for iron homeostasis. Cell Metab. *1*, 191–200.

Drakesmith, H., and Prentice, A.M. (2012). Hepcidin and the iron-infection axis. Science *338*, 768–772.

Drakesmith, H., Schimanski, L.M., Ormerod, E., Merryweather-Clarke, A.T., Viprakasit, V., Edwards, J.P., Sweetland, E., Bastin, J.M., Cowley, D., Chinthammitr, Y., et al. (2005). Resistance to hepcidin is conferred by hemochromatosis-associated mutations of ferroportin. Blood *106*, 1092–1097.

Duarte, T.L., Caldas, C., Santos, A.G., Silva-Gomes, S., Santos-Gonçalves, A., Martins, M.J., Porto, G., and Lopes, J.M. (2017). Genetic disruption of NRF2 promotes the development of necroinflammation and liver

fibrosis in a mouse model of HFE-hereditary hemochromatosis. Redox Biol. *11*, 157–169.

Enns, C.A., Ahmed, R., Wang, J., Ueno, A., Worthen, C., Tsukamoto, H., and Zhang, A.S. (2013). Increased Iron Loading Induces Bmp6 Expression in the Non-Parenchymal Cells of the Liver Independent of the BMP-Signaling Pathway. PLoS One *8*, e60534.

Falize, L., Guillygomarc'h, A., Perrin, M., Lainé, F., Guyader, D., Brissot, P., Turlin, B., and Deugnier, Y. (2006). Reversibility of hepatic fibrosis in treated genetic hemochromatosis: A study of 36 cases. Hepatology *44*, 472–477.

Feder, J.N., Gnirke, A., Thomas, W., Tsuchihashi, Z., Ruddy, D.A., Basava, A., Dormishian, F., Domingo, R., Ellis, M.C., Fullan, A., et al. (1996). A novel MHC class I–like gene is mutated in patients with hereditary haemochromatosis. Nat. Genet. *13*, 399–408.

Fernandes, A., Preza, G.C., Phung, Y., De Domenico, I., Kaplan, J., Ganz, T., and Nemeth, E. (2009). The molecular basis of hepcidin-resistant hereditary hemochromatosis. Blood *114*, 437–443.

Festjens, N., Kalai, M., Smet, J., Meeus, A., Van Coster, R., Saelens, X., and Vandenabeele, P. (2006). Butylated hydroxyanisole is more than a reactive oxygen species scavenger. Cell Death Differ. *13*, 166–169.

Flo, T.H., Smith, K.D., Sato, S., Rodriguez, D.J., Holmes, M.A., Strong, R.K., Akira, S., and Aderem, A. (2004). Lipocalin 2 mediates an innate immune response to bacterial infection by sequestrating iron. Nature *432*, 917–921.

Fortes, G.B., Alves, L.S., De Oliveira, R., Dutra, F.F., Rodrigues, D., Fernandez, P.L., Souto-Padron, T., De Rosa, M.J., Kelliher, M., Golenbock, D., et al. (2012). Heme induces programmed necrosis on macrophages through autocrine TNF and ROS production. Blood *119*, 2368–2375.

Friedman, S.L. (2008). Mechanisms of Hepatic Fibrogenesis. Gastroenterology *134*, 1655–1669.

Gallego, C.J., Burt, A., Sundaresan, A.S., Ye, Z., Shaw, C., Crosslin, D.R., Crane, P.K., Fullerton, S.M., Hansen, K., Carrell, D., et al. (2015). Penetrance of Hemochromatosis in HFE Genotypes Resulting in p.Cys282Tyr and p.[Cys282Tyr];[His63Asp] in the eMERGE Network. Am. J. Hum. Genet. *97*, 512–520.

Ganz, T. (2012). Macrophages and systemic iron homeostasis. J. Innate Immun. *4*, 446–453.

Ganz, T. (2013). Systemic iron homeostasis. Physiol. Rev. *93*, 1721–1741.

Gao, A.M., Ke, Z.P., Shi, F., Sun, G.C., and Chen, H. (2013). Chrysin enhances sensitivity of BEL-7402/ADM cells to doxorubicin by suppressing PI3K/Akt/Nrf2 and ERK/Nrf2 pathway. Chem. Biol. Interact. *206*, 100–108.

Gao, J., Chen, J., Kramer, M., Tsukamoto, H., Zhang, A.S., and Enns, C.A. (2009). Interaction of the Hereditary Hemochromatosis Protein HFE with Transferrin Receptor 2 Is Required for Transferrin-Induced Hepcidin Expression. Cell Metab. *9*, 217–227.

Gozzelino, R., Jeney, V., and Soares, M.P. (2010). Mechanisms of cell protection by heme oxygenase-1. Annu. Rev. Pharmacol. Toxicol. *50*, 323–354.

Graça-Souza, A. V., Arruda, M.A.B., De Freitas, M.S., Barja-Fidalgo, C., and Oliveira, P.L. (2002). Neutrophil activation by heme: Implications for inflammatory processes. Blood *99*, 4160–4165.

Greni, F., Valenti, L., Mariani, R., Pelloni, I., Rametta, R., Busti, F., Ravasi, G., Girelli, D., Fargion, S., Galimberti, S., et al. (2017). GNPAT rs11558492 is not a Major Modifier of Iron Status: Study of Italian Hemochromatosis Patients and Blood Donors. Ann. Hepatol. *16*, 451–456.

Grosse, S.D., Gurrin, L.C., Bertalli, N.A., and Allen, K.J. (2017). Clinical penetrance in hereditary hemochromatosis: estimates of the cumulative incidence of severe liver disease among HFE C282Y homozygotes. Genet. Med.

Gunshin, H., Mackenzie, B., Berger, U. V., Gunshin, Y., Romero, M.F., Boron, W.F., Nussberger, S., Gollan, J.L., and Hediger, M.A. (1997). Cloning and characterization of a mammalian proton-coupled metal-ion transporter. Nature *388*, 482–488.

Guo, S., Casu, C., Gardenghi, S., Booten, S., Aghajan, M., Peralta, R., Watt, A., Freier, S., Monia, B.P., and Rivella, S. (2013). Reducing TMPRSS6 ameliorates hemochromatosis and β-thalassemia in mice. J. Clin. Invest. *123*, 1531–1541.

Guyader, D., Jacquelinet, C., Moirand, R., Turlin, B., Mendler, M.H., Chaperon, J., David, V., Brissot, P., Adams, P., and Deugnier, Y. (1998). Noninvasive prediction of fibrosis in C282Y homozygous

hemochromatosis. Gastroenterology *115*, 929–936.

Haldar, M., Kohyama, M., So, A.Y.L., Kc, W., Wu, X., Briseño, C.G., Satpathy, A.T., Kretzer, N.M., Arase, H., Rajasekaran, N.S., et al. (2014). Heme-mediated SPI-C induction promotes monocyte differentiation into iron-recycling macrophages. Cell *156*, 1223–1234.

Harada, N., Kanayama, M., Maruyama, A., Yoshida, A., Tazumi, K., Hosoya, T., Mimura, J., Toki, T., Maher, J.M., Yamamoto, M., et al. (2011). Nrf2 regulates ferroportin 1-mediated iron efflux and counteracts lipopolysaccharide-induced ferroportin 1 mRNA suppression in macrophages. Arch. Biochem. Biophys. *508*, 101–109.

Harris, Z.L., Durley, A.P., Man, T.K., and Gitlin, J.D. (1999). Targeted gene disruption reveals an essential role for ceruloplasmin in cellular iron efflux. Proc. Natl. Acad. Sci. U. S. A. *96*, 10812–10817.

Hentze, M.W., Muckenthaler, M.U., Galy, B., and Camaschella, C. (2010). Two to Tango: Regulation of Mammalian Iron Metabolism. Cell *142*, 24–38.

Hu, X., Roberts, J.R., Apopa, P.L., Kan, Y.W., and Ma, Q. (2006). Accelerated Ovarian Failure Induced by 4-Vinyl Cyclohexene Diepoxide in Nrf2 Null Mice. Mol. Cell. Biol. *26*, 940–954.

Igarashi, K., and Watanabe-Matsui, M. (2013). Wearing red for signaling: the heme-bach axis in heme metabolism, oxidative stress response and iron immunology. Tohoku J. Exp. Med. 229–253.

Iida, K., Itoh, K., Kumagai, Y., Oyasu, R., Hattori, K., Kawai, K., Shimazui, T., Akaza, H., and Yamamoto, M. (2004). Nrf2 is essential for the chemopreventive efficacy of oltipraz against urinary bladder carcinogenesis. Cancer Res. *64*, 6424–6431.

Itoh, K., Igarashi, K., Hayashi, N., Nishizawa, M., and Yamamoto, M. (1995). Cloning and characterization of a novel erythroid cell-derived CNC family transcription factor heterodimerizing with the small Maf family proteins. Mol. Cell. Biol. *15*, 4184–4193.

Itoh, K., Chiba, T., Takahashi, S., Ishii, T., Igarashi, K., Katoh, Y., Oyake, T., Hayashi, N., Satoh, K., Hatayama, I., et al. (1997). An Nrf2/small Maf heterodimer mediates the induction of phase II detoxifying enzyme genes through antioxidant response elements. Biochem. Biophys. Res. Commun. *236*, 313–322.

Itoh, K., Wakabayashi, N., Katoh, Y., Ishii, T., O'Connor, T., and Yamamoto, M. (2003). Keap1 regulates both cytoplasmic-nuclear shuttling and degradation of Nrf2 in response to electrophiles. Genes to Cells *8*, 379–391.

Jastroch, M., Divakaruni, A.S., Mookerjee, S., Treberg, J.R., and Brand, M.D. (2010). Mitochondrial proton and electron leaks. Essays Biochem. *47*, 53–67.

Jiang, T., Chen, N., Zhao, F., Wang, X.J., Kong, B., Zheng, W., and Zhang, D.D. (2010). High levels of Nrf2 determine chemoresistance in type II endometrial cancer. Cancer Res. *70*, 5486–5496.

Jiang, Y., Bao, H., Ge, Y., Tang, W., Cheng, D., Luo, K., Gong, G., and Gong, R. (2015). Therapeutic targeting of GSK3β enhances the Nrf2 antioxidant response and confers hepatic cytoprotection in hepatitis C. Gut *64*, 168–179.

Jomova, K., and Valko, M. (2011). Advances in metal-induced oxidative stress and human disease. Toxicology *283*, 65–87.

Jones, E., Pasricha, S.R., Allen, A., Evans, P., Fisher, C.A., Wray, K., Premawardhena, A., Bandara, D., Perera, A., Webster, C., et al. (2015). Hepcidin is suppressed by erythropoiesis in hemoglobin E β-thalassemia and β-thalassemia trait. Blood *125*, 873–880.

Katoh, Y., Itoh, K., Yoshida, E., Miyagishi, M., Fukamizu, A., and Yamamoto, M. (2001). Two domains of Nrf2 cooperatively bind CBP, a CREB binding protein, and synergistically activate transcription. Genes to Cells *6*, 857–868.

Kautz, L., Meynard, D., Monnier, A., Darnaud, V., Bouvet, R., Wang, R.H., Deng, C., Vaulont, S., Mosser, J., Coppin, H., et al. (2008). Iron regulates phosphorylation of Smad1/5/8 and gene expression of Bmp6, Smad7, Id1, and Atoh8 in the mouse liver. Blood *112*, 1503–1509.

Kautz, L., Meynard, D., Besson-Fournier, C., Darnaud, V., Al Saati, T., Coppin, H., and Roth, M.P. (2009). BMP/Smad signaling is not enhanced in Hfe-deficient mice despite increased Bmp6 expression. Blood *114*, 2515–2520.

Kautz, L., Besson-Fournier, C., Meynard, D., Latour, C., Roth, M.P., and Coppin, H. (2011). Iron overload

induces BMP6 expression in the liver but not in the duodenum. Haematologica *96*, 199–203.

Kautz, L., Jung, G., Valore, E. V, Rivella, S., Nemeth, E., and Ganz, T. (2014). Identification of erythroferrone as an erythroid regulator of iron metabolism. Nat. Genet. *46*, 678–684.

Kautz, L., Jung, G., Du, X., Gabayan, V., Chapman, J., Nasoff, M., Nemeth, E., and Ganz, T. (2015). Erythroferrone contributes to hepcidin suppression and iron overload in a mouse model of β-thalassemia. Blood *126*, 2031–2037.

Kawabata, H., Germain, R.S., Vuong, P.T., Nakamaki, T., Said, J.W., and Koeffler, H.P. (2000). Transferrin receptor 2-alpha supports cell growth both in iron-chelated cultured cells and in vivo. J. Biol. Chem. *275*, 16618–16625.

Kawabata, H., Germain, R.S., Ikezoe, T., Tong, X., Green, E.M., Gombart, A.F., and Koeffler, H.P. (2001). Regulation of expression of murine transferrin receptor 2. Blood *98*, 1949–1954.

Kawabata, H., Fleming, R.E., Gui, D., Moon, S.Y., Saitoh, T., O'Kelly, J., Umehara, Y., Wano, Y., Said, J.W., and Koeffler, H.P. (2005). Expression of hepcidin is down-regulated in TfR2 mutant mice manifesting a phenotype of hereditary hemochromatosis. Blood *105*, 376–381.

Keel, S.B., Doty, R.T., Yang, Z., Quigley, J.G., Chen, J., Knoblaugh, S., Kingsley, P.D., De Domenico, I., Vaughn, M.B., Kaplan, J., et al. (2008). A heme export protein is required for red blood cell differentiation and iron homeostasis. Science (80-.). *319*, 825–828.

Keleku-Lukwete, N., Suzuki, M., Otsuki, A., Tsuchida, K., Katayama, S., Hayashi, M., Naganuma, E., Moriguchi, T., Tanabe, O., Engel, J.D., et al. (2015). Amelioration of inflammation and tissue damage in sickle cell model mice by Nrf2 activation. Proc. Natl. Acad. Sci. *112*, 12169–12174.

Khan, F.A., Fisher, M.A., and Khakoo, R.A. (2007). Association of hemochromatosis with infectious diseases: expanding spectrum. Int. J. Infect. Dis. *11*, 482–487.

Khor, T.O., Huang, M.T., Prawan, A., Liu, Y., Hao, X., Yu, S., Cheung, W.K.L., Chan, J.Y., Reddy, B.S., Yang, C.S., et al. (2008). Increased susceptibility of Nrf2 knockout mice to colitis-associated colorectal cancer. Cancer Prev. Res. *1*, 187–191.

Kidane, T.Z., Sauble, E., and Linder, M.C. (2006). Release of iron from ferritin requires lysosomal activity. Am. J. Physiol. Cell Physiol. *291*, C445-455.

Kim, S.K., Yang, J.W., Kim, M.R., Roh, S.H., Kim, H.G., Lee, K.Y., Jeong, H.G., and Kang, K.W. (2008). Increased expression of Nrf2/ARE-dependent anti-oxidant proteins in tamoxifen-resistant breast cancer cells. Free Radic. Biol. Med. *45*, 537–546.

Kobayashi, A., Ito, E., Toki, T., Kogame, K., Takahashi, S., Igarashi, K., Hayashi, N., and Yamamoto, M. (1999). Molecular cloning and functional characterization of a new Cap'n' collar family transcription factor Nrf3. J. Biol. Chem. *274*, 6443–6452.

Kobayashi, A., Kang, M.-I., Okawa, H., Ohtsuji, M., Zenke, Y., Chiba, T., Igarashi, K., and Yamamoto, M. (2004a). Oxidative Stress Sensor Keap1 Functions as an Adaptor for Cul3-Based E3 Ligase To Regulate Proteasomal Degradation of Nrf2. Mol. Cell. Biol. *24*, 7130–7139.

Kobayashi, A., Ohta, T., and Yamamoto, M. (2004b). Unique Function of the Nrf2-Keap1 Pathway in the Inducible Expression of Antioxidant and Detoxifying Enzymes. Methods Enzymol. *378*, 273–286.

Kobayashi, A., Kang, M.-I., Okawa, H., Ohtsuji, M., Zenke, Y., Chiba, T., Igarashi, K., and Yamamoto, M. (2004c). Oxidative stress sensor Keap1 functions as an adaptor for Cul3-based E3 ligase to regulate proteasomal degradation of Nrf2. Mol. Cell. Biol. *24*, 7130–7139.

Kobayashi, E.H., Suzuki, T., Funayama, R., Nagashima, T., Hayashi, M., Sekine, H., Tanaka, N., Moriguchi, T., Motohashi, H., Nakayama, K., et al. (2016). Nrf2 suppresses macrophage inflammatory response by blocking proinflammatory cytokine transcription. Nat. Commun. *7*, 11624.

Koch, P.S., Olsavszky, V., Ulbrich, F., Sticht, C., Demory, A., Leibing, T., Henzler, T., Meyer, M., Zierow, J., Schneider, S., et al. (2017). Angiocrine Bmp2 signaling in murine liver controls normal iron homeostasis. Blood *129*, 415–419.

Köhler, U.A., Kurinna, S., Schwitter, D., Marti, A., Schäfer, M., Hellerbrand, C., Speicher, T., and Werner, S. (2014). Activated Nrf2 impairs liver regeneration in mice by activation of genes involved in cell-cycle control and apoptosis. Hepatology *60*, 670–678.

Koilan, S., Hamilton, D., Baburyan, N., Padala, M.K., Weber, K.T., and Guntaka, R. V (2010). Prevention of liver fibrosis by triple helix-forming oligodeoxyribonucleotides targeted to the promoter region of type I collagen gene. Oligonucleotides *20*, 231–237.

Koskenkorva-Frank, T.S., Weiss, G., Koppenol, W.H., and Burckhardt, S. (2013). The complex interplay of iron metabolism, reactive oxygen species, and reactive nitrogen species: Insights into the potential of various iron therapies to induce oxidative and nitrosative stress. Free Radic. Biol. Med. *65*, 1174–1194.

Krause, A., Neitz, S., Mägert, H.-J., Schulz, A., Forssmann, W.-G., Schulz-Knappe, P., and Adermann, K. (2000). LEAP-1, a novel highly disulfide-bonded human peptide, exhibits antimicrobial activity. FEBS Lett. *480*, 147–150.

Kurinna, S., and Werner, S. (2015). NRF2 and microRNAs: new but awaited relations. Biochem. Soc. Trans. *43*, 595–601.

Kwak, M.-K., Itoh, K., Yamamoto, M., and Kensler, T.W. (2002). Enhanced expression of the transcription factor Nrf2 by cancer chemopreventive agents: role of antioxidant response element-like sequences in the nrf2 promoter. Mol. Cell. Biol. *22*, 2883–2892.

Kweider, N., Huppertz, B., Wruck, C.J., Beckmann, R., Rath, W., Pufe, T., and Kadyrov, M. (2012). A Role for Nrf2 in Redox Signalling of the Invasive Extravillous Trophoblast in Severe Early Onset IUGR Associated with Preeclampsia. PLoS One *7*, e47055.

Kwong, M., Kan, Y.W., and Chan, J.Y. (1999). The CNC basic leucine zipper factor, Nrf1, is essential for cell survival in response to oxidative stress-inducing agents. Role for Nrf1 in gamma-gcs(l) and gss expression in mouse fibroblasts. J. Biol. Chem. *274*, 37491–37498.

Lakhal-Littleton, S., Wolna, M., Carr, C.A., Miller, J.J.J., Christian, H.C., Ball, V., Santos, A., Diaz, R., Biggs, D., Stillion, R., et al. (2015). Cardiac ferroportin regulates cellular iron homeostasis and is important for cardiac function. PNAS *112*, 3164–3169.

Lakhal-Littleton, S., Wolna, M., Chung, Y.J., Christian, H.C., Heather, L.C., Brescia, M., Ball, V., Diaz, R., Santos, A., Biggs, D., et al. (2016). An essential cell-autonomous role for hepcidin in cardiac iron homeostasis. Elife *5*, e19804.

Lecine, P., Villeval, J.-L., Vyas, P., Swencki, B., Xu, Y., and Shivdasani, R.A. (1998). Mice Lacking Transcription Factor NF-E2 Provide In Vivo Validation of the Proplatelet Model of Thrombocytopoiesis and Show a Platelet Production Defect That Is Intrinsic to Megakaryocytes. Blood *92*, 1608–1616.

Leung, L., Kwong, M., Hou, S., Lee, C., and Chan, J.Y. (2003). Deficiency of the Nrf1 and Nrf2 transcription factors results in early embryonic lethality and severe oxidative stress. J. Biol. Chem. *278*, 48021–48029.

Levstik, A., Stuart, A., and Adams, P.C. (2016). GNPAT variant (D519G) is not associated with an elevated serum ferritin or iron removed by phlebotomy in patients referred for C282Y-linked hemochromatosis. Ann. Hepatol. *15*, 907–910.

Linker, R.A., Lee, D.H., Ryan, S., Van Dam, A.M., Conrad, R., Bista, P., Zeng, W., Hronowsky, X., Buko, A., Chollate, S., et al. (2011). Fumaric acid esters exert neuroprotective effects in neuroinflammation via activation of the Nrf2 antioxidant pathway. Brain *134*, 678–692.

Liu, L., Sun, T., Liu, Z., Chen, X., Zhao, L., Qu, G., and Li, Q. (2014a). Traumatic brain injury dysregulates microRNAs to modulate cell signaling in rat hippocampus. PLoS One *9*, e103948.

Liu, Z., Ciocea, A., and Devireddy, L. (2014b). Endogenous siderophore 2,5-dihydroxybenzoic acid deficiency promotes anemia and splenic iron overload in mice. Mol. Cell. Biol. *34*, 2533–2546.

Macco, R., Pelizzoni, I., Consonni, A., Vitali, I., Giacalone, G., Martinelli Boneschi, F., Codazzi, F., Grohovaz, F., and Zacchetti, D. (2013). Astrocytes acquire resistance to iron-dependent oxidative stress upon proinflammatory activation. J. Neuroinflammation *10*, 130.

Macleod, a. K., Mcmahon, M., Plummer, S.M., Higgins, L.G., Penning, T.M., Igarashi, K., and Hayes, J.D. (2009). Characterization of the cancer chemopreventive NRF2-dependent gene battery in human keratinocytes: Demonstration that the KEAP1-NRF2 pathway, and not the BACH1-NRF2 pathway, controls cytoprotection against electrophiles as well as redox-cycling compounds. Carcinogenesis *30*, 1571–1580.

Malhotra, D., Portales-Casamar, E., Singh, A., Srivastava, S., Arenillas, D., Happel, C., Shyr, C., Wakabayashi, N., Kensler, T.W., Wasserman, W.W., et al. (2010). Global mapping of binding sites for Nrf2 identifies novel targets in cell survival response through ChIP-Seq profiling and network analysis. Nucleic

Acids Res. *38*, 5718–5734.

Mancias, J.D., Wang, X., Gygi, S.P., Harper, J.W., and Kimmelman, A.C. (2014). Quantitative proteomics identifies NCOA4 as the cargo receptor mediating ferritinophagy. Nature *509*, 105–109.

Mancias, J.D., Vaites, L.P., Nissim, S., Biancur, D.E., Kim, A.J., Wang, X., Liu, Y., Goessling, W., Kimmelman, A.C., and Harper, J.W. (2015). Ferritinophagy via NCOA4 is required for erythropoiesis and is regulated by iron dependent HERC2-mediated proteolysis. Elife *4*, e10308.

Marro, S., Chiabrando, D., Messana, E., Stolte, J., Turco, E., Tolosano, E., and Muckenthaler, M.U. (2010). Heme controls ferroportin1 (FPN1) transcription involving Bach1, Nrf2 and a MARE/ARE sequence motif at position -7007 of the FPN1 promoter. Haematologica *95*, 1261–1268.

Marzec, J.M., Christie, J.D., Reddy, S.P., Jedlicka, A.E., Vuong, H., Lanken, P.N., Aplenc, R., Yamamoto, T., Yamamoto, M., Cho, H.-Y., et al. (2007). Functional polymorphisms in the transcription factor NRF2 in humans increase the risk of acute lung injury. FASEB J. *21*, 2237–2246.

Mastrogiannaki, M., Matak, P., Mathieu, J.R.R., Delga, S., Mayeux, P., Vaulont, S., and Peyssonnaux, C. (2012). Hepatic hypoxia-inducible factor-2 down-regulates hepcidin expression in mice through an erythropoietin-mediated increase in erythropoiesis. Haematologica *97*, 827–834.

McCullough, K.A., Waits, C.A., Garimella, R., Tague, S.E., Sipe, J.B., and Anderson, H.C. (2007). Immunohistochemical localization of bone morphogenetic proteins (BMPs) 2, 4, 6, and 7 during induced heterotopic bone formation. J. Orthop. Res. *25*, 465–472.

McKie, A.T., Marciani, P., Rolfs, A., Brennan, K., Wehr, K., Barrow, D., Miret, S., Bomford, A., Peters, T.J., Farzaneh, F., et al. (2000). A Novel Duodenal Iron-Regulated Transporter, IREG1, Implicated in the Basolateral Transfer of Iron to the Circulation. Mol. Cell *5*, 299–309.

McKie, A.T., Barrow, D., Latunde-Dada, G.O., Rolfs, A., Sager, G., Mudaly, E., Mudaly, M., Richardson, C., Barlow, D., Bomford, A., et al. (2001). An Iron-Regulated Ferric Reductase Associated with the Absorption of Dietary Iron. Science (80-.). *291*, 1755–1759.

Mclaren, C.E., Emond, M.J., Subramaniam, V.N., Phatak, P.D., Barton, J.C., Adams, P.C., Goh, J.B., Mcdonald, C.J., Powell, L.W., Gurrin, L.C., et al. (2015). Exome sequencing in HFE C282Y homozygous men with extreme phenotypes identifies a GNPAT variant associated with severe iron overload. Hepatology *62*, 429–439.

McMahon, M., Lamont, D.J., Beattie, K.A., and Hayes, J.D. (2010). Keap1 perceives stress via three sensors for the endogenous signaling molecules nitric oxide, zinc, and alkenals. Proc. Natl. Acad. Sci. U. S. A. *107*, 18838–18843.

Medvedev, R., Ploen, D., Spengler, C., Elgner, F., Ren, H., Bunten, S., and Hildt, E. (2017). HCV-induced oxidative stress by inhibition of Nrf2 triggers autophagy and favors release of viral particles. Free Radic. Biol. Med. *110*, 300–315.

Mendes, A.I., Ferro, A., Martins, R., Picanço, I., Gomes, S., Cerqueira, R., Correia, M., Nunes, A.R., Esteves, J., Fleming, R., et al. (2009). Non-classical hereditary hemochromatosis in Portugal: Novel mutations identified in iron metabolism-related genes. Ann. Hematol. *88*, 229–234.

Merryweather-Clarke, A.T., Pointon, J.J., Shearman, J.D., and Robson, K.J. (1997). Global prevalence of putative haemochromatosis mutations. J. Med. Genet. *34*, 275–278.

Meynard, D., Kautz, L., Darnaud, V., Canonne-Hergaux, F., Coppin, H., and Roth, M.-P. (2009). Lack of the bone morphogenetic protein BMP6 induces massive iron overload. Nat. Genet. *41*, 478–481.

Miao, W., Hu, L., Scrivens, P.J., and Batist, G. (2005). Transcriptional regulation of NF-E2 p45-related factor (NRF2) expression by the aryl hydrocarbon receptor-xenobiotic response element signaling pathway: Direct cross-talk between phase I and II drug-metabolizing enzymes. J. Biol. Chem. *280*, 20340–20348.

Miura, K., Taura, K., Kodama, Y., Schnabl, B., and Brenner, D.A. (2008). Hepatitis C virus-induced oxidative stress suppresses hepcidin expression through increased histone deacetylase activity. Hepatology *48*, 1420–1429.

Moi, P., Chant, K., Asunis, I., Cao, A., Kant, Y.W., and Kan, Y.W. (1994). Isolation of NF-E2-related factor 2 (Nrf2), a NF-E2-like basic leucine zipper transcriptional activator that binds to the tandem NF-E2/AP1 repeat of the f-globin locus control region. Genetics *91*, 9926–9930.

Mölleken, C., Sitek, B., Henkel, C., Poschmann, G., Sipos, B., Wiese, S., Warscheid, B., Broelsch, C.,

Reiser, M., Friedman, S.L., et al. (2009). Detection of novel biomarkers of liver cirrhosis by proteomic analysis. Hepatology *49*, 1257–1266.

Moon, M.S., McDevitt, E.I., Zhu, J., Stanley, B., Krzeminski, J., Amin, S., Aliaga, C., Miller, T.G., and Isom, H.C. (2012). Elevated hepatic iron activates NF-E2-related factor 2-regulated pathway in a dietary iron overload mouse model. Toxicol. Sci. *129*, 74–85.

Morales, P., Vargas, R., Videla, L. a, and Fernández, V. (2014). Nrf2 activation in the liver of rats subjected to a preconditioning sub-chronic iron protocol. Food Funct. *5*, 243–250.

Morales-Marin, M.E., Cordova, E.J., Centeno, F., Martínez-Hernández, A., Méndez-García, A., Molina, B., Frías, S., and Orozco, L. (2015). NFE2L2 Gene Variants and Arsenic Susceptibility: A Lymphoblastoid Model. J. Toxicol. Environ. Health. A *78*, 628–634.

Muckenthaler, M.U., Galy, B., and Hentze, M.W. (2008). Systemic iron homeostasis and the iron-responsive element/iron-regulatory protein (IRE/IRP) regulatory network. Annu. Rev. Nutr. *28*, 197–213.

Myatt, L., and Cui, X. (2004). Oxidative stress in the placenta. Histochem. Cell Biol. *122*, 369–382.

Nair, S., Xu, C., Shen, G., Hebbar, V., Gopalakrishnan, A., Hu, R., Jain, M.R., Lin, W., Keum, Y.S., Liew, C., et al. (2006). Pharmacogenomics of phenolic antioxidant butylated hydroxyanisole (BHA) in the small intestine and liver of Nrf2 knockout and C57BL/6J mice. Pharm. Res. *23*, 2621–2637.

Nairz, M., Schleicher, U., Schroll, A., Sonnweber, T., Theurl, I., Ludwiczek, S., Talasz, H., Brandacher, G., Moser, P.L., Muckenthaler, M.U., et al. (2013). Nitric oxide-mediated regulation of ferroportin-1 controls macrophage iron homeostasis and immune function in Salmonella infection. J. Exp. Med. *210*, 855–873.

Nandal, A., Ruiz, J.C., Subramanian, P., Ghimire-Rijal, S., Sinnamon, R.A., Stemmler, T.L., Bruick, R.K., and Philpott, C.C. (2011). Activation of the HIF prolyl hydroxylase by the iron chaperones PCBP1 and PCBP2. Cell Metab. *14*, 647–657.

Nemeth, E., Tuttle, M.S., Powelson, J., Vaughn, M.B., Donovan, A., Ward, D.M., Ganz, T., and Kaplan, J. (2004a). Hepcidin regulates cellular iron efflux by binding to ferroportin and inducing its internalization. Science *306*, 2090–2093.

Nemeth, E., Rivera, S., Gabayan, V., Keller, C., Taudorf, S., Pedersen, B.K., and Ganz, T. (2004b). IL-6 mediates hypoferremia of inflammation by inducing the synthesis of the iron regulatory hormone hepcidin. J. Clin. Invest. *113*, 1271–1276.

Neves, J., Leitz, D., Kraut, S., Brandenberger, C., Agrawal, R., Weissmann, N., Mühlfeld, C., Mall, M.A., Altamura, S., and Muckenthaler, M.U. (2017). Disruption of the Hepcidin/Ferroportin Regulatory System Causes Pulmonary Iron Overload and Restrictive Lung Disease. EBioMedicine *20*, 230–239.

Nezu, M., Souma, T., Yu, L., Sekine, H., Takahashi, N., Wei, A.Z.-S., Ito, S., Fukamizu, A., Zsengeller, Z.K., Nakamura, T., et al. (2017). Nrf2 inactivation enhances placental angiogenesis in a preeclampsia mouse model and improves maternal and fetal outcomes. Sci. Signal. *10*, 5711.

Niederau, C., Strohmeyer, G., and Stremmel, W. (1994). Epidemiology, clinical spectrum and prognosis of hemochromatosis. Adv. Exp. Med. Biol. *356*, 293–302.

Niederkofler, V., Salie, R., and Arber, S. (2005). Hemojuvelin is essential for dietary iron sensing, and its mutation leads to severe iron overload. J. Clin. Invest. *115*, 2180–2186.

Nioi, P., Nguyen, T., Sherratt, P.J., and Pickett, C.B. (2005). The carboxy-terminal Neh3 domain of Nrf2 is required for transcriptional activation. Mol. Cell. Biol. *25*, 10895–10906.

No, J.H., Kim, Y.-B., and Song, Y.S. (2014). Targeting Nrf2 Signaling to Combat Chemoresistance. J. Cancer Prev. *19*, 111–117.

Ogawa, K., Sun, J., Taketani, S., Nakajima, O., Nishitani, C., Sassa, S., Hayashi, N., Yamamoto, M., Shibahara, S., Fujita, H., et al. (2001). Heme mediates derepression of Maf recognition element through direct binding to transcription repressor Bach1. EMBO J. *20*, 2835–2843.

Ohgami, R.S., Campagna, D.R., Greer, E.L., Antiochos, B., McDonald, A., Chen, J., Sharp, J.J., Fujiwara, Y., Barker, J.E., and Fleming, M.D. (2005). Identification of a ferrireductase required for efficient transferrin-dependent iron uptake in erythroid cells. Nat. Genet. *37*, 1264–1269.

Ohkoshi, A., Suzuki, T., Ono, M., Kobayashi, T., and Yamamoto, M. (2013). Roles of keap1-Nrf2 system in upper aerodigestive tract carcinogenesis. Cancer Prev. Res. *6*, 149–159.

Okada, K., Warabi, E., Sugimoto, H., Horie, M., Tokushige, K., Ueda, T., Harada, N., Taguchi, K., Hashimoto, E., Itoh, K., et al. (2012). Nrf2 inhibits hepatic iron accumulation and counteracts oxidative stress-induced liver injury in nutritional steatohepatitis. J. Gastroenterol. *47*, 924–935.

Origa, R., Galanello, R., Ganz, T., Giagu, N., Maccioni, L., Faa, G., and Nemeth, E. (2007). Liver iron concentrations and urinary hepcidin in beta-thalassemia. Haematologica *92*, 583–588.

Oyake, T., Itoh, K., Motohashi, H., Hayashi, N., Hoshino, H., Nishizawa, M., Yamamoto, M., and Igarashi, K. (1996). Bach proteins belong to a novel family of BTB-basic leucine zipper transcription factors that interact with MafK and regulate transcription through the NF-E2 site. Mol. Cell. Biol. *16*, 6083–6095.

Pak, M., Lopez, M.A., Gabayan, V., Ganz, T., and Rivera, S. (2006). Suppression of hepcidin during anemia requires erythropoietic activity. Blood *108*, 3730–3735.

Papanikolaou, G., Samuels, M.E., Ludwig, E.H., MacDonald, M.L.E., Franchini, P.L., Dubé, M.-P., Andres, L., MacFarlane, J., Sakellaropoulos, N., Politou, M., et al. (2004). Mutations in HFE2 cause iron overload in chromosome 1q–linked juvenile hemochromatosis. Nat. Genet. *36*, 77–82.

Park, C.H., Valore, E. V., Waring, A.J., and Ganz, T. (2001). Hepcidin, a Urinary Antimicrobial Peptide Synthesized in the Liver. J. Biol. Chem. *276*, 7806–7810.

Pennacchio, L.A., Bickmore, W., Dean, A., Nobrega, M.A., and Bejerano, G. (2013). Enhancers: five essential questions. Nat. Rev. Genet. *14*, 288–295.

Pereira, R.D., De Long, N.E., Wang, R.C., Yazdi, F.T., Holloway, A.C., and Raha, S. (2015). Angiogenesis in the placenta: The role of reactive oxygen species signaling. Biomed Res. Int. 814543.

Perry, M.J., McDougall, K.E., Hou, S. chen, and Tobias, J.H. (2008). Impaired growth plate function in bmp-6 null mice. Bone *42*, 216–225.

Peyssonnaux, C., Zinkernagel, A.S., Schuepbach, R.A., Rankin, E., Vaulont, S., Haase, V.H., Nizet, V., and Johnson, R.S. (2007). Regulation of iron homeostasis by the hypoxia-inducible transcription factors (HIFs). J. Clin. Invest. *117*, 1926–1932.

Pietrangelo, A. (2015). Genetics, Genetic Testing, and Management of Hemochromatosis: 15 Years since Hepcidin. Gastroenterology *149*, 1240–1251.

Pigeon, C., Ilyin, G., Courselaud, B., Leroyer, P., Turlin, B., Brissot, P., and Loréal, O. (2001). A New Mouse Liver-specific Gene, Encoding a Protein Homologous to Human Antimicrobial Peptide Hepcidin, Is Overexpressed during Iron Overload. J. Biol. Chem. *276*, 7811–7819.

Piubelli, C., Castagna, A., Marchi, G., Rizzi, M., Busti, F., Badar, S., Marchetti, M., De Gobbi, M., Roetto, A., Xumerle, L., et al. (2017). Identification of New BMP6 Pro-Peptide Mutations in Patients with Iron Overload. Am. J. Hematol. *92*, 562–568.

Poggiali, E., Cassinerio, E., Zanaboni, L., and Cappellini, M.D. (2012). An update on iron chelation therapy. Blood Transfus. *10*, 411–422.

Ponka, P., Sheftel, A.D., English, A.M., Scott Bohle, D., and Garcia-Santos, D. (2017). Do Mammalian Cells Really Need to Export and Import Heme? Trends Biochem. Sci. *42*, 395–406.

Porto, G., Brissot, P., Swinkels, D.W., Zoller, H., Kamarainen, O., Patton, S., Alonso, I., Morris, M., and Keeney, S. (2016). EMQN best practice guidelines for the molecular genetic diagnosis of hereditary hemochromatosis (HH). Eur. J. Hum. Genet. *24*, 479–495.

Preza, G.C., Ruchala, P., Pinon, R., Ramos, E., Qiao, B., Peralta, M.A., Sharma, S., Waring, A., Ganz, T., and Nemeth, E. (2011). Minihepcidins are rationally designed small peptides that mimic hepcidin activity in mice and may be useful for the treatment of iron overload. J. Clin. Invest. *121*, 4880–4888.

Qiu, A., Jansen, M., Sakaris, A., Min, S.H., Chattopadhyay, S., Tsai, E., Sandoval, C., Zhao, R., Akabas, M.H., and Goldman, I.D. (2006). Identification of an Intestinal Folate Transporter and the Molecular Basis for Hereditary Folate Malabsorption. Cell *127*, 917–928.

Rada, P., Rojo, A.I., Chowdhry, S., McMahon, M., Hayes, J.D., and Cuadrado, A. (2011). SCF/{beta}-TrCP promotes glycogen synthase kinase 3-dependent degradation of the Nrf2 transcription factor in a Keap1-independent manner. Mol. Cell. Biol. *31*, 1121–1133.

Ramey, G., Deschemin, J.C., Durel, B., Canonne-Hergaux, F., Nicolas, G., and Vaulont, S. (2010). Hepcidin targets ferroportin for degradation in hepatocytes. Haematologica *95*, 501–504.

Ramos, E., Ruchala, P., Goodnough, J.B., Kautz, L., Preza, G.C., Nemeth, E., and Ganz, T. (2012). Minihepcidins prevent iron overload in a hepcidin-deficient mouse model of severe hemochromatosis. Blood *120*, 3829–3836.

Ramos-Gomez, M., Kwak, M.K., Dolan, P.M., Itoh, K., Yamamoto, M., Talalay, P., and Kensler, T.W. (2001). Sensitivity to carcinogenesis is increased and chemoprotective efficacy of enzyme inducers is lost in nrf2 transcription factor-deficient mice. Proc. Natl. Acad. Sci. U. S. A. *98*, 3410–3415.

Reichard, J.F., Motz, G.T., and Puga, A. (2007). Heme oxygenase-1 induction by NRF2 requires inactivation of the transcriptional repressor BACH1. Nucleic Acids Res. *35*, 7074–7086.

Richardson, D.R., Lane, D.J.R., Becker, E.M., Huang, M.L.-H., Whitnall, M., Rahmanto, Y.S., Sheftel, A.D., and Ponka, P. (2010). Mitochondrial iron trafficking and the integration of iron metabolism between the mitochondrion and cytosol. Proc. Natl. Acad. Sci. U. S. A. *107*, 10775–10782.

Roetto, A., Papanikolaou, G., Politou, M., Alberti, F., Girelli, D., Christakis, J., Loukopoulos, D., and Camaschella, C. (2003). Mutant antimicrobial peptide hepcidin is associated with severe juvenile hemochromatosis. Nat Genet *33*, 21–22.

Roetto, A., Daraio, F., Porporato, P., Caruso, R., Cox, T.M., Cazzola, M., Gasparini, P., Piperno, A., and Camaschella, C. (2004). Sceening hepcidin for mutations in juvenile hemochromatosis: Identification of a new mutation (C70R). Blood *103*, 2407–2409.

Ryan, J.D., Ryan, E., Fabre, A., Lawless, M.W., and Crowe, J. (2010). Defective bone morphogenic protein signaling underlies hepcidin deficiency in HFE hereditary hemochromatosis. Hepatology *52*, 1266–1273.

Saito, T., Ichimura, Y., Taguchi, K., Suzuki, T., Mizushima, T., Takagi, K., Hirose, Y., Nagahashi, M., Iso, T., Fukutomi, T., et al. (2016). p62/Sqstm1 promotes malignancy of HCV-positive hepatocellular carcinoma through Nrf2-dependent metabolic reprogramming. Nat. Commun. *7*, 12030.

Salahudeen, A.A., Thompson, J.W., Ruiz, J.C., Ma, H.-W., Kinch, L.N., Li, Q., Grishin, N. V, and Bruick, R.K. (2009). An E3 ligase possessing an iron-responsive hemerythrin domain is a regulator of iron homeostasis. Science (80-.). *326*, 722–726.

Salojin, K. V., Cabrera, R.M., Sun, W., Chang, W.C., Lin, C., Duncan, L., Platt, K.A., Read, R., Vogel, P., Liu, Q., et al. (2011). A mouse model of hereditary folate malabsorption: Deletion of the PCFT gene leads to systemic folate deficiency. Blood *117*, 4895–4904.

Sanchez, M., Galy, B., Schwanhaeusser, B., Blake, J., Bähr-Ivacevic, T., Benes, V., Selbach, M., Muckenthaler, M.U., and Hentze, M.W. (2011). Iron regulatory protein-1 and -2: transcriptome-wide definition of binding mRNAs and shaping of the cellular proteome by iron regulatory proteins. Blood *118*, e168-179.

Satoh, H., Moriguchi, T., Takai, J., Ebina, M., and Yamamoto, M. (2013). Nrf2 prevents initiation but accelerates progression through the kras signaling pathway during lung carcinogenesis. Cancer Res. *73*, 4158–4168.

Schäfer, M., Farwanah, H., Willrodt, A.-H., Huebner, A.J., Sandhoff, K., Roop, D., Hohl, D., Bloch, W., and Werner, S. (2012). Nrf2 links epidermal barrier function with antioxidant defense. EMBO Mol. Med. *4*, 364–379.

Schmidt, P.J., Toran, P.T., Giannetti, A.M., Bjorkman, P.J., and Andrews, N.C. (2008). The Transferrin Receptor Modulates Hfe-Dependent Regulation of Hepcidin Expression. Cell Metab. *7*, 205–214.

Schmidt, P.J., Toudjarska, I., Sendamarai, A.K., Racie, T., Milstein, S., Bettencourt, B.R., Hettinger, J., Bumcrot, D., and Fleming, M.D. (2013). An RNAi therapeutic targeting Tmprss6 decreases iron overload in Hfe -/- mice and ameliorates anemia and iron overload in murine β-thalassemia intermedia. Blood *121*, 1200–1208.

Schwessinger, R., Suciu, M.C., McGowan, S.J., Telenius, J., Taylor, S., Higgs, D.R., and Hughes, J.R. (2017). Sasquatch: Predicting the impact of regulatory SNPs on transcription factor binding from cell- and tissue-specific DNase footprints. Genome Res. *27*, 1730–1742.

Sham, R.L., Phatak, P.D., West, C., Lee, P., Andrews, C., and Beutler, E. (2005). Autosomal dominant hereditary hemochromatosis associated with a novel ferroportin mutation and unique clinical features. Blood Cells, Mol. Dis. *34*, 157–161.

Sham, R.L., Phatak, P.D., Nemeth, E., and Ganz, T. (2009). Hereditary hemochromatosis due to resistance to hepcidin: high hepcidin concentrations in a family with C326S ferroportin mutation. Blood *114*, 493–494.

Shayeghi, M., Latunde-Dada, G.O., Oakhill, J.S., Laftah, A.H., Takeuchi, K., Halliday, N., Khan, Y., Warley, A., McCann, F.E., Hider, R.C., et al. (2005). Identification of an intestinal heme transporter. Cell *122*, 789–801.

Shi, H., Bencze, K.Z., Stemmler, T.L., and Philpott, C.C. (2008). A cytosolic iron chaperone that delivers iron to ferritin. Science *320*, 1207–1210.

Shimoyama, Y., Mitsuda, Y., Hamajima, N., and Niwa, T. (2014). Polymorphisms of Nrf2 , an Antioxidative Gene , Are Associated With Blood Pressure in Japanese. Nagoya J. Med. Sci. *76*, 113–120.

Shivdasani, R. a (1996). The role of transcription factor NF-E2 in megakaryocyte maturation and platelet production. Stem Cells *14*, 112–115.

Shlyueva, D., Stampfel, G., and Stark, A. (2014). Transcriptional enhancers: from properties to genome-wide predictions. Nat. Rev. Genet. *15*, 272–286.

Sidwell, T., and Kallies, A. (2016). Bach2 is required for B cell and T cell memory differentiation. Nat. Immunol. *17*, 744–745.

Silva-Gomes, S., Santos, A.G., Caldas, C., Silva, C.M., Neves, J. V., Lopes, J., Carneiro, F., Rodrigues, P.N., and Duarte, T.L. (2014). Transcription factor NRF2 protects mice against dietary iron-induced liver injury by preventing hepatocytic cell death. J. Hepatol. *60*, 354–361.

Silvestri, L., Pagani, A., Nai, A., De Domenico, I., Kaplan, J., and Camaschella, C. (2008). The Serine Protease Matriptase-2 (TMPRSS6) Inhibits Hepcidin Activation by Cleaving Membrane Hemojuvelin. Cell Metab. *8*, 502–511.

Solis, L.M., Behrens, C., Dong, W., Suraokar, M., Ozburn, N.C., Moran, C.A., Corvalan, A.H., Biswal, S., Swisher, S.G., Bekele, B.N., et al. (2010). Nrf2 and Keap1 abnormalities in non-small cell lung carcinoma and association with clinicopathologic features. Clin. Cancer Res. *16*, 3743–3753.

Solloway, M.J., Dudley, A.T., Bikoff, E.K., Lyons, K.M., Hogan, B.L.M., and Robertson, E.J. (1998). Mice lacking Bmp6 function. Dev. Genet. *22*, 321–339.

Sonnweber, T., Nachbaur, D., Schroll, A., Nairz, M., Seifert, M., Demetz, E., Haschka, D., Mitterstiller, A.-M., Kleinsasser, A., Burtscher, M., et al. (2014). Hypoxia induced downregulation of hepcidin is mediated by platelet derived growth factor BB. Gut *63*, 1951–1959.

Steegers, E.A., von Dadelszen, P., Duvekot, J.J., and Pijnenborg, R. (2010). Pre-eclampsia. Lancet *376*, 631–644.

Subramaniam, V.N., McDonald, C.J., Ostini, L., Lusby, P.E., Wockner, L.F., Ramm, G.A., and Wallace, D.F. (2012). Hepatic iron deposition does not predict extrahepatic iron loading in mouse models of hereditary hemochromatosis. Am. J. Pathol. *181*, 1173–1179.

Suzuki, T., and Yamamoto, M. (2015). Molecular basis of the Keap1-Nrf2 system. Free Radic. Biol. Med. *88*, 93–100.

Suzuki, H., Tashiro, S., Hira, S., Sun, J., Yamazaki, C., Zenke, Y., Ikeda-Saito, M., Yoshida, M., and Igarashi, K. (2004). Heme regulates gene expression by triggering Crm1-dependent nuclear export of Bach1. EMBO J. *23*, 2544–2553.

Suzuki, T., Shibata, T., Takaya, K., Shiraishi, K., Kohno, T., Kunitoh, H., Tsuta, K., Furuta, K., Goto, K., Hosoda, F., et al. (2013). Regulatory nexus of synthesis and degradation deciphers cellular Nrf2 expression levels. Mol. Cell. Biol. *33*, 2402–2412.

Tahara, T., Sun, J., Nakanishi, K., Yamamoto, M., Mori, H., Saito, T., Fujita, H., Igarashi, K., and Taketani, S. (2004a). Heme positively regulates the expression of beta-globin at the locus control region via the transcriptional factor Bach1 in erythroid cells. J. Biol. Chem. *279*, 5480–5487.

Tahara, T., Sun, J., Igarashi, K., and Taketani, S. (2004b). Heme-dependent up-regulation of the alpha-globin gene expression by transcriptional repressor Bach1 in erythroid cells. Biochem. Biophys. Res. Commun. *324*, 77–85.

Talbot, N.P., Lakhal, S., Smith, T.G., Privat, C., Nickol, A.H., Rivera-Ch, M., León-Velarde, F., Dorrington, K.L., Mole, D.R., and Robbins, P.A. (2012). Regulation of hepcidin expression at high altitude. Blood *119*, 857–860.

Tang, X., Wang, H., Fan, L., Wu, X., Xin, A., Ren, H., and Wang, X.J. (2011). Luteolin inhibits Nrf2 leading

to negative regulation of the Nrf2/ARE pathway and sensitization of human lung carcinoma A549 cells to therapeutic drugs. Free Radic. Biol. Med. *50*, 1599–1609.

Tanno, T., Bhanu, N. V, Oneal, P.A., Goh, S.-H., Staker, P., Lee, Y.T., Moroney, J.W., Reed, C.H., Luban, N.L.C., Wang, R.-H., et al. (2007). High levels of GDF15 in thalassemia suppress expression of the iron regulatory protein hepcidin. Nat. Med. *13*, 1096–1101.

Tanno, T., Porayette, P., Sripichai, O., Noh, S.J., Byrnes, C., Bhupatiraju, A., Lee, Y.T., Goodnough, J.B., Harandi, O., Ganz, T., et al. (2009). Identification of TWSG1 as a second novel erythroid regulator of hepcidin expression in murine and human cells. Blood *114*, 181–186.

Thangasamy, A., Rogge, J., Krishnegowda, N.K., Freeman, J.W., and Ammanamanchi, S. (2011). Novel function of transcription factor Nrf2 as an inhibitor of RON tyrosine kinase receptor-mediated cancer cell invasion. J. Biol. Chem. *286*, 32115–32122.

Thimmulappa, R.K., Lee, H., Rangasamy, T., Reddy, S.P., Yamamoto, M., Kensler, T.W., and Biswal, S. (2006). Nrf2 is a critical regulator of the innate immune response and survival during experimental sepsis. J. Clin. Invest. *116*, 984–995.

Tong, K.I., Katoh, Y., Kusunoki, H., Itoh, K., Tanaka, T., and Yamamoto, M. (2006). Keap1 recruits Neh2 through binding to ETGE and DLG motifs: characterization of the two-site molecular recognition model. Mol. Cell. Biol. *26*, 2887–2900.

Touret, N., Furuya, W., Forbes, J., Gros, P., and Grinstein, S. (2003). Dynamic Traffic through the Recycling Compartment Couples the Metal Transporter Nramp2 (DMT1) with the Transferrin Receptor. J. Biol. Chem. *278*, 25548–25557.

Truksa, J., Lee, P., and Beutler, E. (2009). Two BMPresponsive elements, STAT, and bZIP/HNF4/COUP motifs of the hepcidin promoter are critical for BMP, SMAD1, and HJV responsiveness. Blood *113*, 688–695.

Tsuji, Y., Ayaki, H., Whitman, S.P., Morrow, C.S., Torti, S. V, and Torti, F.M. (2000). Coordinate transcriptional and translational regulation of ferritin in response to oxidative stress. Mol. Cell. Biol. *20*, 5818–5827.

Uruno, A., Yagishita, Y., Katsuoka, F., Kitajima, Y., Nunomiya, A., Nagatomi, R., Pi, J., Biswal, S.S., and Yamamoto, M. (2016). Nrf2-Mediated Regulation of Skeletal Muscle Glycogen Metabolism. Mol. Cell. Biol. *36*, 1655–1672.

Vanoaica, L., Darshan, D., Richman, L., Schümann, K., and Kühn, L.C. (2010). Intestinal ferritin H is required for an accurate control of iron absorption. Cell Metab. *12*, 273–282.

Vashisht, A.A., Zumbrennen, K.B., Huang, X., Powers, D.N., Durazo, A., Sun, D., Bhaskaran, N., Persson, A., Uhlen, M., Sangfelt, O., et al. (2009). Control of iron homeostasis by an iron-regulated ubiquitin ligase. Science *326*, 718–721.

Verga Falzacappa, M.V., Spasic, M.V., Kessler, R., Stolte, J., Hentze, M.W., and Muckenthaler, M.U. (2007). STAT3 mediates hepatic hepcidin expression and its inflammatory stimulation. Blood *109*, 353–358.

Verga Falzacappa, M.V., Casanovas, G., Hentze, M.W., and Muckenthaler, M.U. (2008). A bone morphogenetic protein (BMP)-responsive element in the hepcidin promoter controls HFE2-mediated hepatic hepcidin expression and its response to IL-6 in cultured cells. J. Mol. Med. *86*, 531–540.

Viprakasit, V., Merryweather-Clarke, A.T., Chinthammitr, Y., Schimanski, L., Drakesmith, H., Srichairatanakool, S., Limwongse, C., Townsend, A., and Robson, K.J.H. (2004). Molecular Diagnosis of the First Ferroportin Mutation (C326Y) in the Far East Causing a Dominant Form of Inherited Iron Overload. Blood *104*, 3204.

Vokurka, M., Krijt, J., Šulc, K., and Nečas, E. (2006). Hepcidin mRNA levels in mouse liver respond to inhibition of erythropoiesis. Physiol. Res. *55*, 667–674.

Vulpe, C.D., Kuo, Y.-M., Murphy, T.L., Cowley, L., Askwith, C., Libina, N., Gitschier, J., and Anderson, G.J. (1999). Hephaestin, a ceruloplasmin homologue implicated in intestinal iron transport, is defective in the sla mouse. Nat. Genet. *21*, 195–199.

Wang, R.H., Li, C., Xu, X., Zheng, Y., Xiao, C., Zerfas, P., Cooperman, S., Eckhaus, M., Rouault, T., Mishra, L., et al. (2005). A role of SMAD4 in iron metabolism through the positive regulation of hepcidin expression. Cell Metab. *2*, 399–409.

Wasserman, W.W., and Fahl, W.E. (1997). Functional antioxidant responsive elements. Proc. Natl. Acad. Sci. U. S. A. *94*, 5361–5366.

Weinberg, E.D. (1999). Iron loading and disease surveillance. Emerg. Infect. Dis. *5*, 346–352.

West, A.P., Giannetti, A.M., Herr, A.B., Bennett, M.J., Nangiana, J.S., Pierce, J.R., Weiner, L.P., Snow, P.M., and Bjorkman, P.J. (2001). Mutational analysis of the transferrin receptor reveals overlapping HFE and transferrin binding sites. J. Mol. Biol. *313*, 385–397.

Wood, M.J., Crawford, D.H.G., Wockner, L.F., Powell, L.W., and Ramm, G.A. (2017). Serum ferritin concentration predicts hepatic fibrosis better than hepatic iron concentration in human HFE-Haemochromatosis. Liver Int. Off. J. Int. Assoc. Study Liver *37*, 1382–1388.

Wray, K., Allen, A., Evans, E., Fisher, C., Premawardhena, A., Perera, L., Rodrigo, R., Goonathilaka, G., Ramees, L., Webster, C., et al. (2017). Hepcidin detects iron deficiency in Sri Lankan adolescents with a high burden of hemoglobinopathy: A diagnostic test accuracy study. Am. J. Hematol. *92*, 196–203.

Wruck, C.J., Streetz, K., Pavic, G., Götz, M.E., Tohidnezhad, M., Brandenburg, L.O., Varoga, D., Eickelberg, O., Herdegen, T., Trautwein, C., et al. (2011). Nrf2 induces interleukin-6 (IL-6) expression via an antioxidant response element within the IL-6 promoter. J. Biol. Chem. *286*, 4493–4499.

Wu, T., Zhao, F., Gao, B., Tan, C., Yagishita, N., Nakajima, T., Wong, P.K., Chapman, E., Fang, D., and Zhang, D.D. (2014a). Hrd1 suppresses Nrf2-mediated cellular protection during liver cirrhosis. Genes Dev. *28*, 708–722.

Wu, X.G., Wang, Y., Wu, Q., Cheng, W.H., Liu, W., Zhao, Y., Mayeur, C., Schmidt, P.J., Yu, P.B., Wang, F., et al. (2014b). HFE interacts with the BMP type I receptor ALK3 to regulate hepcidin expression. Blood *124*, 1335–1343.

Yageta, Y., Ishii, Y., Morishima, Y., Masuko, H., Ano, S., Yamadori, T., Itoh, K., Takeuchi, K., Yamamoto, M., and Hizawa, N. (2011). Role of Nrf2 in host defense against influenza virus in cigarette smoke-exposed mice. J. Virol. *85*, 4679–4690.

Yamamoto, T., Kyo, M., Kamiya, T., Tanaka, T., Engel, J.D., Motohashi, H., and Yamamoto, M. (2006). Predictive base substitution rules that determine the binding and transcriptional specificity of Maf recognition elements. Genes to Cells *11*, 575–591.

Yates, M.S., Tauchi, M., Katsuoka, F., Flanders, K.C., Liby, K.T., Honda, T., Gribble, G.W., Johnson, D.A., Johnson, J.A., Burton, N.C., et al. (2007). Pharmacodynamic characterization of chemopreventive triterpenoids as exceptionally potent inducers of Nrf2-regulated genes. Mol. Cancer Ther. *6*, 154–162.

Yates, M.S., Tran, Q.T., Dolan, P.M., Osburn, W.O., Shin, S., McCulloch, C.C., Silkworth, J.B., Taguchi, K., Yamamoto, M., Williams, C.R., et al. (2009). Genetic versus chemoprotective activation of Nrf2 signaling: Overlapping yet distinct gene expression profiles between Keap1 knockout and triterpenoid-treated mice. Carcinogenesis *30*, 1024–1031.

Yeager, R.L., Reisman, S.A., Aleksunes, L.M., and Klaassen, C.D. (2009). Introducing the "TCDD-inducible AhR-Nrf2 gene battery." Toxicol. Sci. *111*, 238–246.

Zenke-Kawasaki, Y., Dohi, Y., Katoh, Y., Ikura, T., Ikura, M., Asahara, T., Tokunaga, F., Iwai, K., and Igarashi, K. (2007). Heme induces ubiquitination and degradation of the transcription factor Bach1. Mol. Cell. Biol. *27*, 6962–6971.

Zhang, D.D., and Hannink, M. (2003). Distinct cysteine residues in Keap1 are required for Keap1-dependent ubiquitination of Nrf2 and for stabilization of Nrf2 by chemopreventive agents and oxidative stress. Mol. Cell. Biol. *23*, 8137–8151.

Zhang, Y., Mikhael, M., Xu, D., Li, Y., Soe-Lin, S., Ning, B., Li, W., Nie, G., Zhao, Y., and Ponka, P. (2010). Lysosomal proteolysis is the primary degradation pathway for cytosolic ferritin and cytosolic ferritin degradation is necessary for iron exit. Antioxid. Redox Signal. *13*, 999–1009.

Zhang, Z., Zhang, F., Guo, X., An, P., Tao, Y., and Wang, F. (2012). Ferroportin1 in hepatocytes and macrophages is required for the efficient mobilization of body iron stores in mice. Hepatology *56*, 961–971.

Zhao, Y., Vanhoutte, P.M., and Leung, S.W.S. (2015). Vascular nitric oxide: Beyond eNOS. J. Pharmacol. Sci. *129*, 83–94.

Zipper, L.M., and Timothy Mulcahy, R. (2002). The Keap1 BTB/POZ dimerization function is required to sequester Nrf2 in cytoplasm. J. Biol. Chem. *277*, 36544–36552.